INFORMATION TO USERS

This manuscript has been reproduced from the microfilm master. UMI films the text directly from the original or copy submitted. Thus, some thesis and dissertation copies are in typewriter face, while others may be from any type of computer printer.

The quality of this reproduction is dependent upon the quality of the copy submitted. Broken or indistinct print, colored or poor quality illustrations and photographs, print bleedthrough, substandard margins, and improper alignment can adversely affect reproduction.

In the unlikely event that the author did not send UMI a complete manuscript and there are missing pages, these will be noted. Also, if unauthorized copyright material had to be removed, a note will indicate the deletion.

Oversize materials (e.g., maps, drawings, charts) are reproduced by sectioning the original, beginning at the upper left-hand corner and continuing from left to right in equal sections with small overlaps. Each original is also photographed in one exposure and is included in reduced form at the back of the book.

Photographs included in the original manuscript have been reproduced xerographically in this copy. Higher quality 6" x 9" black and white photographic prints are available for any photographs or illustrations appearing in this copy for an additional charge. Contact UMI directly to order.

UMI

A Bell & Howell Information Company
300 North Zeeb Road, Ann Arbor MI 48106-1346 USA
313/761-4700 800/521-0600

LAND SURFACE PROCESS/RADIOBRIGHTNESS MODELS FOR NORTHERN PRAIRIE

by

Yuei-An Liou

A dissertation submitted in partial fulfillment
of the requirements for the degree of
Doctor of Philosophy
(Electrical Engineering and Atmospheric, Oceanic and Space Sciences)
in The University of Michigan
1996

Doctoral Committee:
Professor Anthony W. England, Co-Chair
Professor William R. Kuhn, Co-Chair
Professor Henry N. Pollack
Professor John F. Vesecky

UMI Number: 9635554

Copyright 1996 by
Liou, Yuei-An

All rights reserved.

UMI Microform 9635554
Copyright 1996, by UMI Company. All rights reserved.

This microform edition is protected against unauthorized
copying under Title 17, United States Code.

UMI
300 North Zeeb Road
Ann Arbor, MI 48103

© Yuei-An Liou 1996
All Rights Reserved

To my mother, Mu-Tang Chang, my father, Ching-Chu, my wife, Shu-Yi, my daughter, Alicia, and my family.

ACKNOWLEDGEMENTS

I thank my advisor, Prof. Anthony W. England, for his constant supervision, assistance, encouragement, and friendship during my graduate studies. Mere words can never describe my gratitude to him.

My graduate studies would not be complete without the support, help, and advice of the many professors and the many current and former fellow graduate students both with the Radiation Lab, Department of Electrical Engineering and Computer Science and with the Department of Atmospheric, Oceanic and Space Science (AOSS). I thank my committee members for their insightful comments and suggestions. In particular, I thank Prof. Bill Kuhn for his generous help when I enrolled in the Ph.D. Graduate Program in Electrical Engineering and AOSS. I also thank Dr. Richard Austin, Mr. Richard Carnes, Mr. Jui-Ching Cheng, Dr. Chen-Yu Chi, Mr. Tsen-Chieh Chiu, Mr. Craig Dobson, Mr. Mark Fischman, Ms. Natasha Flyer, Mr. Ed Kim, Dr. John Galantowicz, Ms. Jasmeet Judge, Dr. John Kendra, Dr. Joe Landry, Mr. Eric Li, Mr. Yi-Cheng Lin, Mr. Paul Siqueira, Dr. Jim Stiles, and Dr. Dong-Liang Wu for their technical advice and assistance, and friendship.

Finally, I would like to thank my wife, Shu-Yi, who has been my lasting support spiritually, and who has given me the joy and happiness of being a father of a lovely daughter, Alicia.

TABLE OF CONTENTS

LIST OF TABLES

LIST OF FIGURES

LIST OF APPENDICES

CHAPTER 1
INTRODUCTION

1.1 Overview

In this dissertation, I use four numerical models to examine the sensitivity of radiobrightness to soil moisture in bare and grass-covered prairie soils. These models are: an Annual Thermal/Radiobrightness (AT/R) model for freezing soils (Chapter 2); a one-dimensional Hydrology/Radiobrightness (1dH/R) model for bare, unfrozen soils (a 1dHbu/R model — Chapter 3); a 1dH/R model for bare, freezing soils (a 1dHb/R model — Chapter 4); and a 1dH/R model for a prairie grassland (Chapter 5). Each successive model involves increasing complexity. I present a chapter on each model describing the added complexity and its consequences. The FORTRAN computer codes for the AT/R model and a 1dH/R model of mixed bare and grass-covered soils are included in Appendices A and B, respectively.

1.2 Background

1.2.1 Soil Moisture

Moisture plays a crucial role in the land-atmosphere energy balance because it governs the partitioning of energy and water through evaporation and transpiration at the lower boundary of the atmosphere. Considerable effort has been made to understand the effects of soil moisture on atmospheric circulation. For example,

Namias [83] was among the first to address the influence of anomalous soil moisture conditions on the atmosphere. Because he and others found that seasonal anomalies of soil wetness had a significant effect on the atmospheric seasonal cycles, models of energy and moisture transfer in soil and vegetation that lead to estimates of land-air energy fluxes must be accurate if the predictions of atmospheric circulation models are to be reliable.

Energy and moisture transfer in soil were successfully described by Philip and de Vries [92] and de Vries [23]. In their theory, energy and moisture movement are coupled through temperature gradients, liquid water concentration gradients, pressure gradients, and gravity. The theory has been used by Milly and Eagleson [79, 80], Milly [77, 78], Abdel-Hadi and Mitchell [1], Shah et al [107], Thomas [114], Ewen and Thomas [34], and Thomas and King [115]. Its weaknesses are relatively well understood by the soil science community, and it continues to be the best theory available.

Freezing soils exhibit a very different coupled transfer of energy and moisture from that of non-freezing soils. The differences are associated with the following four respects: 1) liquid water and ice co-exist over a wide range of temperatures below the freezing depression point (FDP) [127, 4, 36, 116, 90, 12]; 2) liquid water content becomes the iterative solution of highly nonlinear, coupled temperature-suction and water-retention equations; 3) temperature-moisture content curves for repeatedly freezing and thawing soils exhibit hysteresis [64, 50]; and 4) ice lensing and frost heaving occur as liquid water is drawn to the freezing front [5, 42, 16, 63].

In vegetated areas, moisture available to the atmosphere is from both the wetted foliage through evaporation and the dry foliage through transpiration [25, 106, 130]. Transpired water is affected by the incoming solar radiation, air vapor pressure deficit,

soil moisture (matric head), and air temperature [86]. Among these factors, soil moisture determines the maximum rate of water that can be extracted from the root zone. In this manner, soil moisture regulates the exchanges of energy and moisture fluxes at the land-air interface.

1.2.2 Biophysically-Based Models

Many researchers over the past few years have attempted to develop biophysically-based models that predict vertical moisture and temperature profiles of soil and vegetation as well as surface fluxes. Two of the most comprehensive ones are BATS [25] and the Simple Biosphere model (SiB) [106]. They possess three common features. First, both are designed for use in general circulation models (GCMs). Second, they consider a broad range of soil textures whose thermal and hydraulic properties are specifically prescribed. Third, land cover is modeled biophysically and realistically to compute the albedo, drag, and energy partitioning characteristics of the associated vegetated surface.

The two models were applied in a variety of studies related to weather and climate. First, Dickinson and Henderson-Sellers [26] incorporated the BATS model into the NCAR Community Climate Model (CCM) to study the effects of tropical deforestation on climate. They replaced the Amazon tropical forest in South America with impoverished grassland and ran a 13-month simulation. The results were compared with those obtained from the original CCM. They found that reduced sensible heat exchange and less interception and evaporation from the canopy caused runoff to increase and surface temperatures to rise by 3 to 5 K. This had a detrimental impact on the survival of the remaining forest and on attempts at cultivation in deforested areas. Second, Sato et al [103] implemented SiB in a modified version of the

National Meteorological Center's global spectral GCM (SiB-GCM). Their motivation was to investigate the effect of replacing the conventional bucket hydrology model of Manabe [75] with SiB of Sellers et al [106] and Dorman and Sellers [28]. The study showed that the SiB-GCM produced a more realistic partitioning of energy at the land surface than the conventional GCM.

In summary, it has been recognized that the inclusion of more biophysically realistic parameterizations of land surface processes leads to better GCM performance [26, 103]. The degree of parameterization should be carefully balanced between computational economy and model performance.

1.2.3 Passive Microwave Remote Sensing

Satellites that are designed for frequent coverage of the land surface are particularly useful in inferring land-surface parameters and fluxes. In particular, microwave frequencies are sensitive to soil moisture through the dominant influence of liquid water upon microwave emissivity in bare or sparsely vegetated soils [19, 87, 88, 3]. Dense vegetation becomes the physical link between the soil and the atmosphere and absorption and scattering of microwave energy in a dense canopy can dramatically decrease the sensitivity of radiobrightness to soil moisture, especially at higher microwave frequencies. In general, lower-frequencies are preferred for their sensitivity to soil moisture with L-band being the best [105].

Microwave frequencies are sensitive to the state and amount of soil moisture because of a significant contrast in the relative dielectric permittivity between liquid water and ice as described by the Debye relaxation equation [119]. The relaxation frequency of liquid water lies in the microwave band, while that of ice lies in the kilohertz band. Since moisture content and state dominate soil dielectric properties

(i.e., the radiometric behaviors of frozen and thawed soils are very different), it is possible to classify frozen and thawed soils using radiobrightness. For example, a combination of the 37 GHz radiobrightness and the 10.7 to 37 GHz spectral gradient from the Scanning Multichannel Microwave Radiometer (SMMR) has been used to map the freeze/thaw boundaries in the upper Midwest of the United States for the fall of 1984 [131, 132].

1.3 Format and Research Questions of the Thesis

The overall objective of the thesis is to link the moisture stored in bare and grass-covered prairie soils to radiobrightness. Because radiobrightness is sensitive only to moisture in the upper few centimeters of soil [33], the linkage to relevant moisture stored in the upper meter of soil requires a model of moisture transport in the soil, i.e., 1dH models. The thesis is organized according to increasing complexity of these models.

Chapter 2 introduces the AT/R model. The AT module focuses upon physical treatments of soil to track energy transfer for estimates of the temporal soil temperature profile. Thermal properties such as apparent volumetric heat capacity [6] and thermal conductivity [24] are functions of temperature — particularly at freezing temperatures in moist soils. These temperature dependences render the heat flow equation highly nonlinear, especially as free water freezes or thaws and as phase boundaries propagate. The depressed freezing point (DFP) is determined using the approach of Andersland et al [6]. I solved the one-dimensional heat flow equation using the finite element scheme of England [29] which tracks isotherms within the soil.

Results from the AT module are linked to an R module for predictions of annual

radiobrightnesses. Wet soils are sufficiently absorptive of microwaves that effective emission depths are usually less than a few centimeters. This permits a first-order approximation to the radiobrightnesses of bare, quasi-specular, wet soils [29, 69]. At temperatures above the DFP, soil dielectric properties are estimated from a four-component mixture of soil solids, air, free water, and bound water [27, 119]. Below the DFP, ice becomes a 5th component. Fresnel coefficients are used to estimate reflectivities. To demonstrate the significance of seasonal weather forcing upon thermal and radiobrightness signatures, I compare the predictions from the AT/R model with those of an equivalent diurnal thermal/radiobrightness model.

The 1dHbu/R model for bare, unfrozen soils is described in Chapter 3. Unlike the AT/R model, energy and moisture transport are coupled through theory of Philip and de Vries [92, 23]. A finite difference scheme is used to solve these coupled equations to obtain the temperature and moisture profiles in the soil. At the upper boundary of the soil column, the Newton-Raphson method [94] is applied to match energy and moisture fluxes. At the lower boundary, constant energy fluxes are obtained from the AT module results. The hydraulic conductivity of the moist soil follows the Mualem model [82]. The corresponding water-retention relation follows the two-parameter junction model of Rossi and Nimmo [102]. I also incorporate improved models for the vapor diffusion coefficients [61] and the tortuosity factor for the diffusion of gases in soil [66].

The thermal module is linked to an R module as in the AT/R model. I simulate a 60-day dry-down of bare, unfrozen soils in summer to examine the relative influence of moisture movement on radiobrightness. I also re-examine the Radiobrightness Thermal Inertia (RTI) [31] measure of soil moisture for bare soil. RTI relates soil moisture to the diurnal variation in radiobrightness through the increase in thermal

inertia and the decrease in emissivity with increasing moisture content.

Chapter 4 concerns the 1dHb/R model for bare, freezing soils. The 1dHb module is an improved version of the 1dHbu module that accounts for soil freezing and thawing. Using the 1dHb/R model, I ran a 90-day, northern latitude, fall/winter, drydown simulation to examine the influence of water transport on the soil temperature, moisture, and radiobrightness signatures of bare, freezing soils.

Chapter 5 concerns the 1dH/R model for prairie grassland. The 1dH module simulates the land surface processes and estimates the temporal temperature and moisture profiles in the soil and canopy for a prairie grassland. The treatment of the soil is similar to that in the 1dHb and 1dHbu modules except that I also account for the influence of transpiration on the coupled energy and moisture transfer within the root zone. The grass canopy is regarded as a one-layer biophysical medium with dynamic energy and moisture exchanges with the soil and with the atmosphere. The grass cover may vary from 0 % to 100 %. Sensible heat transfer is determined using the bulk aerodynamic approach [117]. The aerodynamic resistance is given by Chehbouni et al [18]. Latent heat transfer by evaporation from bare soil or wet foliage is modeled in a fashion similar to the sensible heat transfer. Latent heat transfer due to transpiration is treated using the approach of Verseghy et al [123]. In this approach, the latent heat transfer is affected by foliage temperature, water potential, insolation, soil temperature, and moisture content/state. The Newton-Raphson method is applied to match the boundary energy and moisture fluxes at the soil-canopy interface. Thatch is included as an insulting layer that is subject only to radiation exchange with the overlying canopy and the underlying soil.

Temperature and moisture profiles from the 1dH module are incorporated into the R module to estimate radiobrightness. The R module and its associated dielectric

properties are similar to the radiative transfer model of England and Galantowicz [32]. The total model brightness is comprised of the soil brightness attenuated by one trip through the canopy, the downwelling canopy brightness reflected by the soil and attenuated by one trip through the canopy, the upwelling canopy brightness, and the sky brightness reflected by the soil and attenuated by two trips through the canopy. The relative permittivity of the wet canopy is approximated by the dual-dispersion model of Ulaby and El-Rayes [120]. The optical thickness of the grass layer is from England and Galantowicz [32].

Predictions from the 1dH/R model are compared with observations from the First Radiobrightness Energy Balance Experiment (REBEX-1) on prairie grassland near Sioux Falls, South Dakota, during the fall and winter of 1992-1993 [39]. The comparisons include soil heat flux at 2 cm depth, soil temperatures at 2, 4, 8, 16, 32, and 64 cm depths, canopy temperature, and horizontally polarized radiobrightnesses at 19 and 37 GHz.

Upon verifying the 1dH/R model, I ran the model for a 60-day dry-down simulation for a 100 % vegetation-covered prairie in summer to study the sensitivity of radiobrightness to soil moisture. The utility of the RTI measure of soil moisture in vegetated fields is also examined.

Chapter 6 is a summary that includes the major contributions of the thesis and recommendations for future research.

CHAPTER 2

The Annual Thermal/Radiobrightness (AT/R) MODEL

Abstract — We have developed physically based, diurnal and annual models for freezing/thawing moist soils subject to annual insolation, radiant heating and cooling, and sensible and latent heat exchanges with the atmosphere. Both models have the same weather forcing, numerical scheme, and soil constitutive properties. We find that surface temperature differences over a diurnal cycle between the annual and diurnal models are as much as -5 Kelvins in March, -7 Kelvins in June, -4 Kelvins in September, and 5 Kelvins in December for 38 % (by volume fraction) moist soil. This difference occurs because the annual model includes the history of energy fluxes at the surface of the soil.

The annual model is linked to microwave emission models for predictions of temporal radiobrightness signatures. The model predicts a relatively weak decrease in diurnal differences in soil temperature with increased moisture content, but a significant decrease in diurnal differences in radiobrightness. It also exhibits notable perturbations in radiobrightness when soils freeze and thaw. The moisture dependent, day-to-night radiobrightness difference is enhanced by as much as -42 Kelvins at 19.35

GHz horizontal polarization for frozen soil if daytime thawing occurs.

2.1 INTRODUCTION

Land surface processes strongly influence the dynamics of the atmosphere over a wide range of space and time scales through exchanges of momentum, moisture, and energy. Soil surface temperature and moisture are key parameters in that they are products of the energy balance between the land and atmosphere. They are also diagnostic parameters in that they govern infrared and microwave emission. Reliably modeling soil surface temperature and moisture are crucial to simulate land-atmosphere interactions and to study radiometric signatures of bare or sparsely vegetated soil.

The focus of this paper is upon the radiobrightness of moist agricultural soils in northern prairie during periods when they are bare of vegetation. Such conditions exist over significant periods of a year for many fields in the northern Great Plains and on the steppes of Asia. None of these fields will fill a resolution cell of a satellite sensor such as the Special Sensor Microwave/Imagers (SSM/I) which have spatial resolutions of 69 × 43 km at 19.35 GHz, 37 × 28 km at 37.0 GHz, and 15 × 13 km at 85.5 GHz [49].

One strategy for synthesizing an expected radiobrightness for a resolution cell would be to aggregate the predicted radiobrightnesses of typical landcover types for the cell according to their expected occurrence throughout an annual cycle. The bare field, or one that is covered by stubble, would be an expected occurrence in agricultural prairie -- especially during spring and fall when hydrologists would particularly like to know the quantity of water that is stored in soil or snow. Our overarching objective in this and a companion paper (Chapter 3) [71] is to develop an expected annual radiobrightness for these bare soils.

Several one-dimensional thermal models have been developed for bare rocks or soils to predict their thermal infrared (TIR) or thermal microwave (radiobrightness) signatures over diurnal periods. Watson [125] applied the Laplace transform method to develop a diurnal model for rock and dry soils. He proposed using diurnal temperature extremes – a measure of a rock's thermal inertia – to discriminate among rock types in TIR images. Kahle [59] developed a diurnal finite difference model for moist soils and proposed using thermal inertia to discriminate among various soils. Price [95, 96] developed a similar model and demonstrated that thermal inertia could be used to infer soil moisture. England [29] developed a diurnal finite element model for freezing and thawing soils to examine the empirical observation that a combination of 10 and 37 GHz radiobrightness from the Scanning Multichannel Microwave Radiometer (SMMR) could be used to map frozen and thawed prairie soils [30], and to extend the TIR-based, thermal inertia technique of estimating soil moisture to the SSM/I's spectral range of 19-85 GHz [31].

None of these diurnal models, nor any of the more recent remote sensing thermal models for vegetation covered terrains, place the diurnal thermal event in an annual context, nor do they incorporate physical models of freezing point depression or of coupled thermal and moisture transport. Using a variable time interval Laplace method to create an annual model for dry soils, Liou and England [69] found significant differences in predicted surface temperatures between the annual model and an equivalent diurnal model. Because soil temperature is a convolution of many past diurnal events, the seasonal history is embedded in the surface temperature. In our companion paper (Chapter 3) [71], we report on a finite difference, coupled temperature and moisture, diurnal radiobrightness model based upon the thermal modeling approach of de Vries [24] and advanced by Milly and others [79, 80, 77, 15, 78, 7].

However, this coupled model is too computationally intensive to become a practical annual model.

In this paper, we present the finite element annual thermal/radiobrightness model for moist soils that are subject to freezing and thawing, and compare the model's predictions with those of our equivalent diurnal model [29]. Our specific objectives are to extend our earlier findings for dry soils [69] to the more interesting case of the moist, freezing and thawing soils found in northern prairie; and to identify appropriate lower boundary temperatures by latitude and day-of-year for use as lower boundary temperatures in our coupled model for bare, moist soils (Chapter 3) [71]. The use of this lower boundary temperature places the coupled diurnal model in the approximate thermal context of an annual model. We also achieve a more rapid convergence of the coupled model by initializing its temperature profile with the temperature profile from this annual model for latitude and day-of-year.

2.2 THERMAL MODELS

2.2.1 Soil Constitutive Properties and Thermal Models

Soil temperatures are obtained by solving the one-dimensional heat flow equation within soil:

$$\frac{\partial}{\partial t}\left(C_{\mathrm{p}}(T_{\mathrm{g}})\cdot T_{\mathrm{g}}(z,t)\right)=\frac{\partial}{\partial z}\left(\lambda(T_{\mathrm{g}})\cdot\frac{\partial T_{\mathrm{g}}(z,t)}{\partial z}\right). \tag{2.1}$$

where C_{p} is the apparent volumetric heat capacity of the soil at constant pressure (J/m^3-K), $T_{\mathrm{g}}(z,t)$ is the ground temperature at depth z (m) and time t (s), and λ is the thermal conductivity (W/m-K). Following Andersland et al [6], the apparent volumetric heat capacity is described by

$$C_{\mathrm{p}}=C_{\mathrm{d}}+C_{\mathrm{i}}(\theta-\theta_{\mathrm{u}})+C_{\mathrm{u}}\theta_{\mathrm{u}}+L_{\mathrm{f}}\frac{\partial\theta_{\mathrm{u}}}{\partial T}. \tag{2.2}$$

where C_d is the volumetric heat capacity of dry soil matrix, C_i is the volumetric heat capacity of ice, C_u is the volumetric heat capacity of unfrozen water, θ is the total water content, (m^3/m^3), θ_u is the unfrozen water content, and L_f is the volumetric latent heat of fusion (J/m^3). Soil thermal conductivity is computed by using the de Vries' model [24]:

$$\lambda = \frac{\sum_{i=1}^{n} k_i \theta_i \lambda_i}{\sum_{i=1}^{n} k_i \theta_i}, \tag{2.3}$$

where $k_i, i = 1, \cdots, n$ is the weighting function of the i^{th} constituent; $\theta_i, i = 1, \cdots, n$ is the volumetric content of the i^{th} constituent; and $\lambda_i, i = 1, \cdots, n$ is the thermal conductivity of the i^{th} constituent.

Figure 2.1 shows the apparent volumetric heat capacity, unfrozen water content and thermal conductivity of 17 % and 38 % (by volume fraction) moist soils versus temperature.

Figure 2.1 (a) indicates that unfrozen water content decreases exponentially with decreasing temperature below the depressed freezing point (DFP) [6] and the rate of decrease depends upon soil texture. In general, the lower the moisture content, the lower the DFP. The DFP is 267.2 K for 17 % moist soil and 272.5 K for 38 % moist soils. In this paper, we chose a silt loam because it is typical of prairie soils. Typical silt loams have a porosity, field capacity and wilting point of 48 %, 28.6 %, and 13.3 %, respectively. Their dry substance consists of 19 % sand, 22.5 % clay, and 58.5 % silt [102]. Soil constituents, water, ice, and air have very different thermal properties as shown in Table 1. Figure 2.1 (b) shows that moist soils have an extremely high heat capacity as moisture begins to freeze at temperatures slightly lower than the DFP. Figure 2.1 (c) shows that soils with a higher moisture content have a higher thermal conductivity below the DFP, while those with a lower moisture content behaves weakly in the opposite sense.

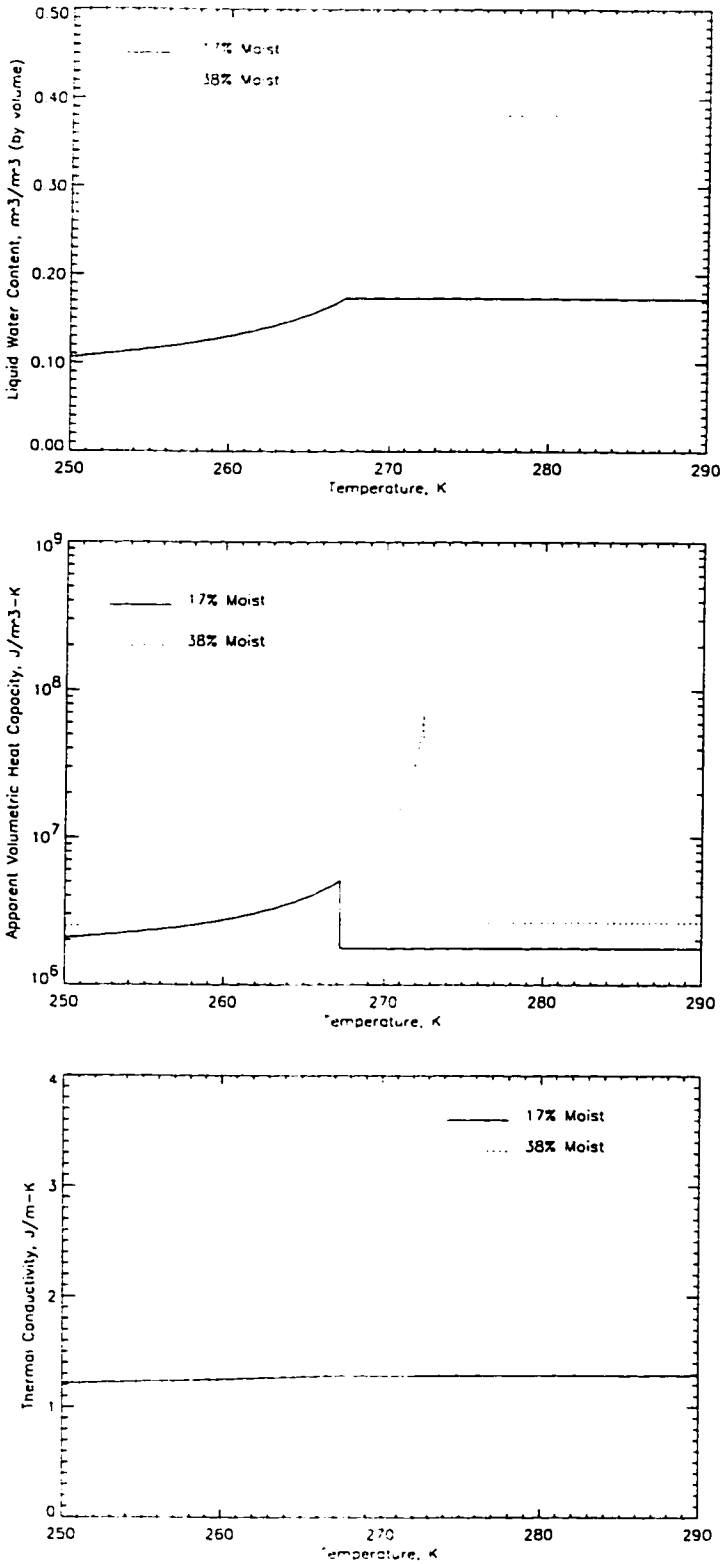

Figure 2.1: (a) Unfrozen water content. (b) Apparent volumetric heat capacity. (c) Thermal conductivity. These soil constitutive properties are applied to both diurnal and annual models.

Substance	λ, W/m-K	C, J/m^3-K	ρ, kg/m^3
Quartz	8.892	2.009×10^6	2660
Clay	2.930	1.894×10^6	2650
Water	0.586	4.194×10^6	1000
Ice	2.240	1.937×10^6	917
air	0.249	1.237×10^3	1.231

Table 2.1: Thermal conductivities, volumetric heat capacities, and densities of some soil materials, water, and air at 10°C and of ice at 0°C (after de Vries [24]).

C_p and λ are an aggregate of the physical properties of all of the soil constituents. Because some of these are temperature dependent, the heat flow equation is highly nonlinear with soil temperature. The problem becomes particularly difficult as the state of free water within soil changes and phase boundaries propagate. To solve (2.1), we used the finite element scheme of England's model [29] which tracks isotherms within the soil.

The term in parenthesis on the right of equation (2.1) is the negative of the energy flux at depth z and time t. Equation (2.1) is solved by imposing the following boundary conditions of weather forcing at the land-atmosphere interface and a zero energy flux at a depth beyond the annual thermal pulses.

2.2.2 Boundary Conditions

The energy budget at the land–atmosphere interface is a balance among radiant heat, sensible heat, and latent heat. The energy flux available to soil at the surface is

$$F(0,t) = F_{\text{sun}}(t) + F_{\text{sky}}(t) - F_{\text{sh}}(t) - F_{\text{lh}}(t) - F_{\text{g}}(t). \tag{2.4}$$

where F_{sun} is insolation reduced by cloud extinction, atmospheric absorption, albedo, and the cosine of the zenith angle; F_{sky} is sky brightness with a correction for cloud cover; F_{sh} is the sensible heat transfer from the land to the atmosphere; F_{lh} is the

latent heat transfer from the land to the atmosphere; and F_g is gray-body emission from the soil's surface. F_{sun}, F_{sky} and F_g have been further described in England [29]. The sensible heat transfer from the bulk transfer method may be expressed by [117]

$$F_{sh} = \rho_a \cdot c_{p,a} \cdot \left(\frac{T_g(0,t) - T_a(z_r,t)}{r_a} \right), \tag{2.5}$$

where r_a is the aerodynamic resistance (s/m), ρ_a is the air density (kg/m^3), $c_{p,a}$ is the air specific heat at constant pressure (J/kg-K), $T_a(z_r,t)$ is the air temperature at a reference height z_r and time t (K). The latent heat transfer is given by [91]

$$F_{lh} = f \cdot \frac{F_{sh}}{B}, \tag{2.6}$$

where f is evaporation efficiency, and B is the Bowen ratio. The evaporation efficiency, a ratio between real evaporation and potential evaporation, is chosen to be a linear function of soil moisture content with values between 0 and 1 corresponding to wilting point and saturation, respectively.

The Bowen ratio may be estimated by [91]

$$B = \gamma \cdot \frac{T_a(0,t) - T_a(z_r,t)}{e(0,t) - e(z_r,t)}, \tag{2.7}$$

where γ is the psychometric constant (Pa/K), $e(0,t)$ is surface water vapor pressure (Pa), and $e(z_r,t)$ is air vapor pressure at the reference height (Pa). Air temperature is assumed to be the climatic value for the time-of-day and day-of-year of the location for which the model was run. For our purposes, this location was chosen to be Sioux Falls, South Dakota. The partial pressure of the water vapor was arbitrarily chosen to be constant through a day and of a value that would yield a 40 % humidity at solar noon. The psychometric constant is expressed as [91]

$$\gamma = \frac{c_{p,a} \cdot p}{0.622 \cdot L_e}, \tag{2.8}$$

where p is the atmospheric pressure at the boundary layer (Pa), and L_e is the latent heat of evaporation of water (J/kg).

The saturation water vapor pressure is obtained by solving

$$log(0.01e) = 9.4041 - \frac{2354}{T}, \tag{2.9}$$

where *log* is decimal logarithm, and T is the temperature. Equation (2.9) is from the Clausius–Clapeyron equation with higher-order terms neglected [53].

2.2.3 Model Results

The ground warms quickly as the sun rises. Capturing these rapid changes with the numerical integrations requires time intervals of 10 minutes or less. Because there are over fifty thousand 10–minute intervals in an annual cycle, compared to only 144 intervals in a diurnal cycle, the numerical simulation of the annual model becomes computationally intensive. To gain quicker convergence, the annual equilibrium temperature (AET) is assigned as the initial temperature of soil at all depths and all time-steps. The AET is chosen so that the sum of incoming absorbed insolation and sky radiation and the outgoing emission from the surface are in balance. A similar treatment for the initial temperature is applied to the diurnal model.

The annual temperature at all depths and all time-steps generally differs from AET by less than 40 Kelvins so that its profile can be sufficiently described by 40 dynamic one-Kelvin isotherms. Similarly, 20 one-Kelvin isotherms are generally sufficient for a diurnal model. The actual number of isotherms is not only dependent upon time scale, but also dependent upon moisture content and state.

Figure 2.2 shows the surface temperatures for 17 % moist soil with latent heat transfer, and 38 % moist soil with and without latent heat transfer for March, June,

September, and December at a northern latitude of 43.5 degrees (that of Sioux Falls, South Dakota). Soils appear to resist changes in temperature as moisture freezes and thaws (Figure 2.2 for dates 03/22 and 12/22). A comparison of Figure 2.2 (a) and (b) shows 17 % moist soils respond to the weather forcing at the land-atmosphere interface faster and to a greater extent than to the 38 % moist soils, i.e., wetter soils have a higher apparent thermal inertia. The difference in the diurnal variation is 7.8 Kelvins for March, 6.8 Kelvins for June, 5.4 Kelvins for September, and 5.2 Kelvins for December. A comparison between Figure 2.2 (b) and (c) shows that latent heat exchanges with the atmosphere tend to suppress diurnal temperature variation. These decreases are 1 Kelvin for March, 4.4 Kelvins for June, 2.8 Kelvins for September, and 0.01 Kelvins for December. The decreases are in the direction to enhance the effect of moisture on apparent thermal inertia.

The thermal conductivity of 38 % moist soil is more than two times larger than that of 17 % moist soil at temperatures below the DFP so that the apparent thermal inertia is greater in March and December for more moist soils (Figure 2.1 (c)). More importantly, apparent volumetric heat capacity of 38 % moist soil is more than an order of magnitude greater than that of 17 % moist soil at temperatures between their DFPs (Figure 2.1 (b)).

Figure 2.3 shows the diurnal isotherms for 38 % moist soil with latent heat transfer for March and June. Notable characteristics include (1) isotherms are created after sunrise and start to merge some time after peak insolation; (2) temperature gradients in the first few centimeters are much larger during the day than during the night; (3) soil temperatures at depths below 0.8 meter remain approximately constant during a diurnal cycle; and (4) diurnal thermal pulses penetrate approximately 50 cm in June but less than 20 cm in March when a large fraction of the insolation is used to melt

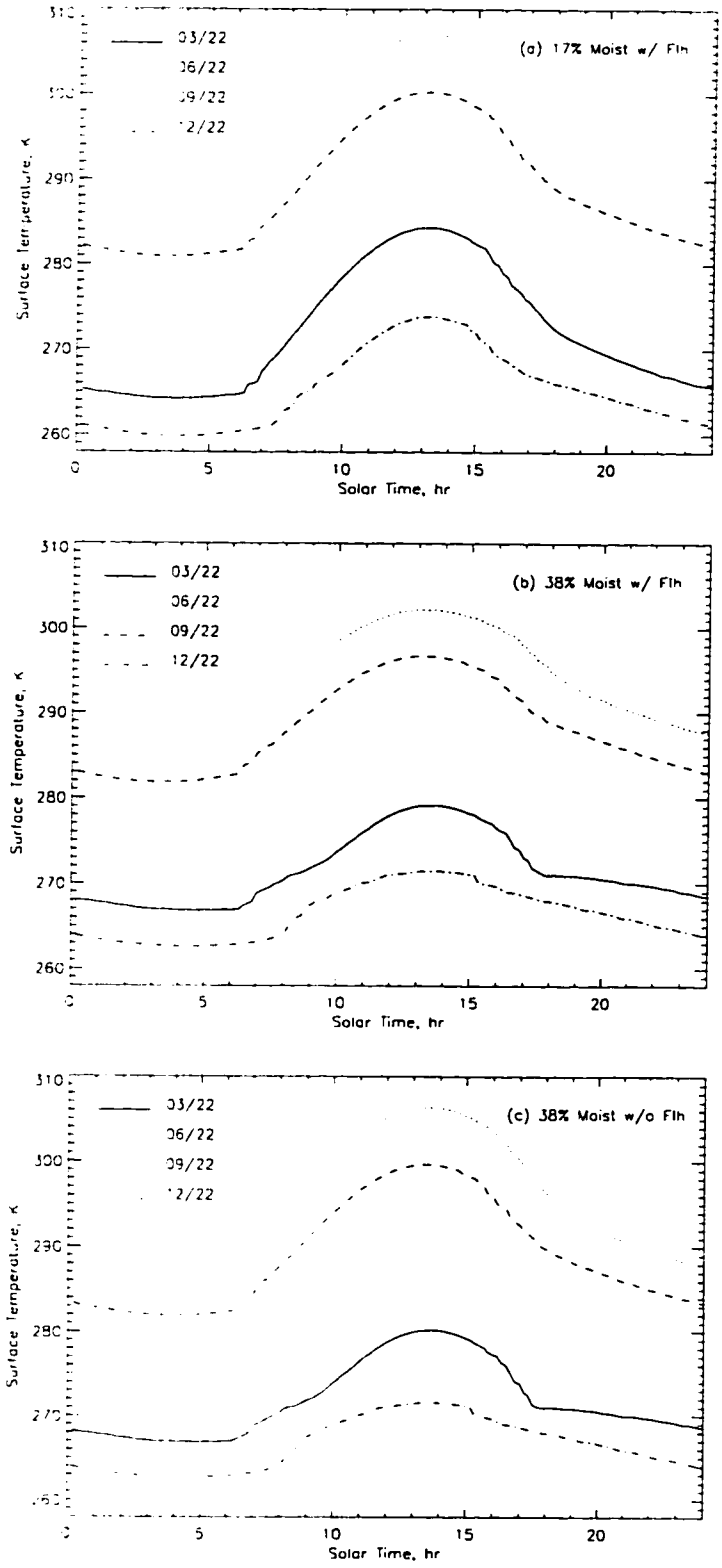

Figure 2.2: Diurnal surface temperatures for (a) 17 % with latent heat transfer, (b) 38 % moist soils with latent heat transfer, and (c) 38 % moist soils without latent heat transfer for 03/22, 06/22, 09/22 and 12/22.

water. We present only March and June isotherms because December isotherms are like those in March, and September isotherms are like those in June.

Figure 2.4 shows the diurnal isotherms for 17 % moist soil with latent heat transfer for March and June. Two major differences between Figure 2.3 and Figure 2.4 are (1) there are more one-Kelvin isotherms for 17 % moist soil than there are for 38 % moist soil; and (2) penetration depths of thermal pulses in winter are nearly 60 cm for 17 % moist soil, but only 20 cm for 38 % moist soil. Soil with 17 % moisture content is considered relatively dry and has a small amount of free water to freeze or thaw.

Figure 2.5 shows the diurnal isotherms for 38 % moist soil without latent heat transfer for March and June. A comparison between Figures 2.3 and 2.5 for March shows that the contours for the no latent heat case and for the latent heat case are nearly the same. Latent heat transfer is essentially turned off when the ground is frozen. For June, the latent heat case has fewer one-Kelvin isotherms than the no latent heat case because latent heat transfer reduces the change in soil temperature.

The differences in surface temperatures over a diurnal cycle between annual and diurnal models for 17 % and 38 % moist soils with latent heat transfer for March, June, September and December are shown in Figure 2.6. The range of the differences increases with increasing moisture content — from -3.5 to 2.8 Kelvins for 17 % moist soil and from -6.6 to 4.8 Kelvins for 38 % moist soil. This occurs because the drier soil with a lower thermal inertia is more easily modified by current weather forcing and is less dependent upon historical weather forcing.

Latent heat transfer is relatively more important when soils are unfrozen. For September, latent heat transfer and prior summer heating are opposing effects so that the differences between the two models are near zero during nighttime, and only

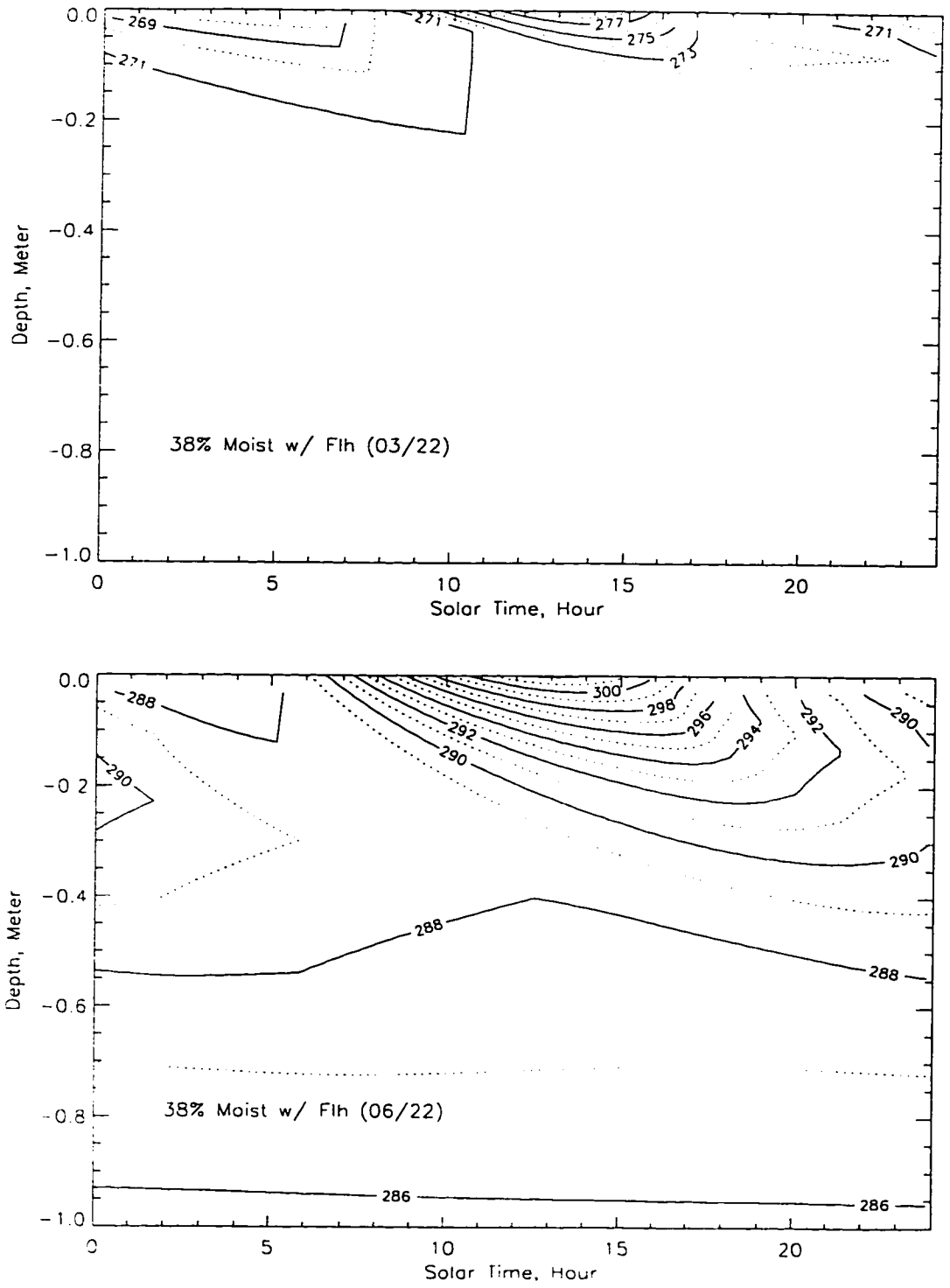

Figure 2.3: 38 % moist soil isotherms with latent heat transfer for 03/22 and 06/22.

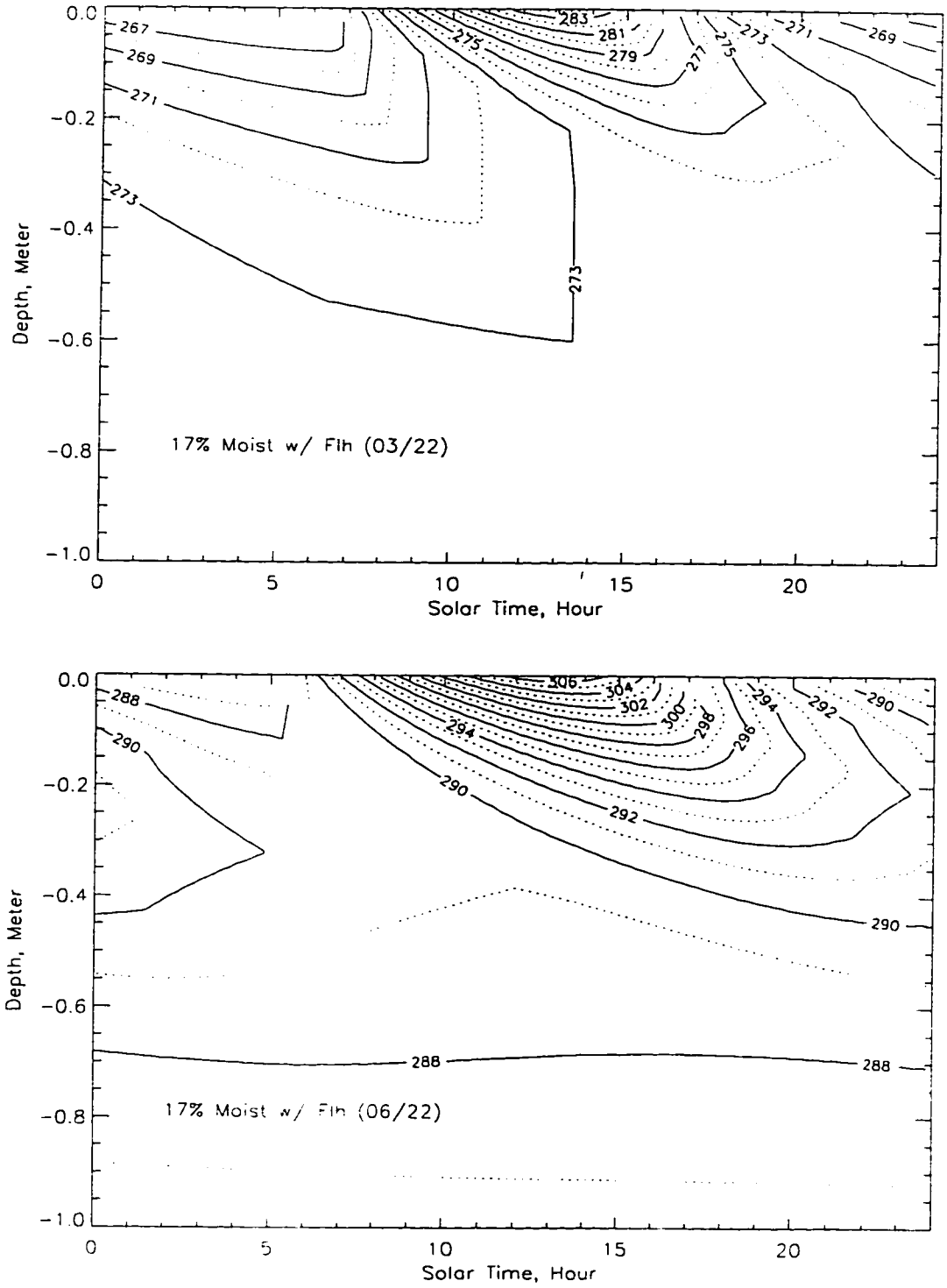

Figure 2.4: 17 % moist soil isotherms with latent heat transfer for 03/22 and 06/22.

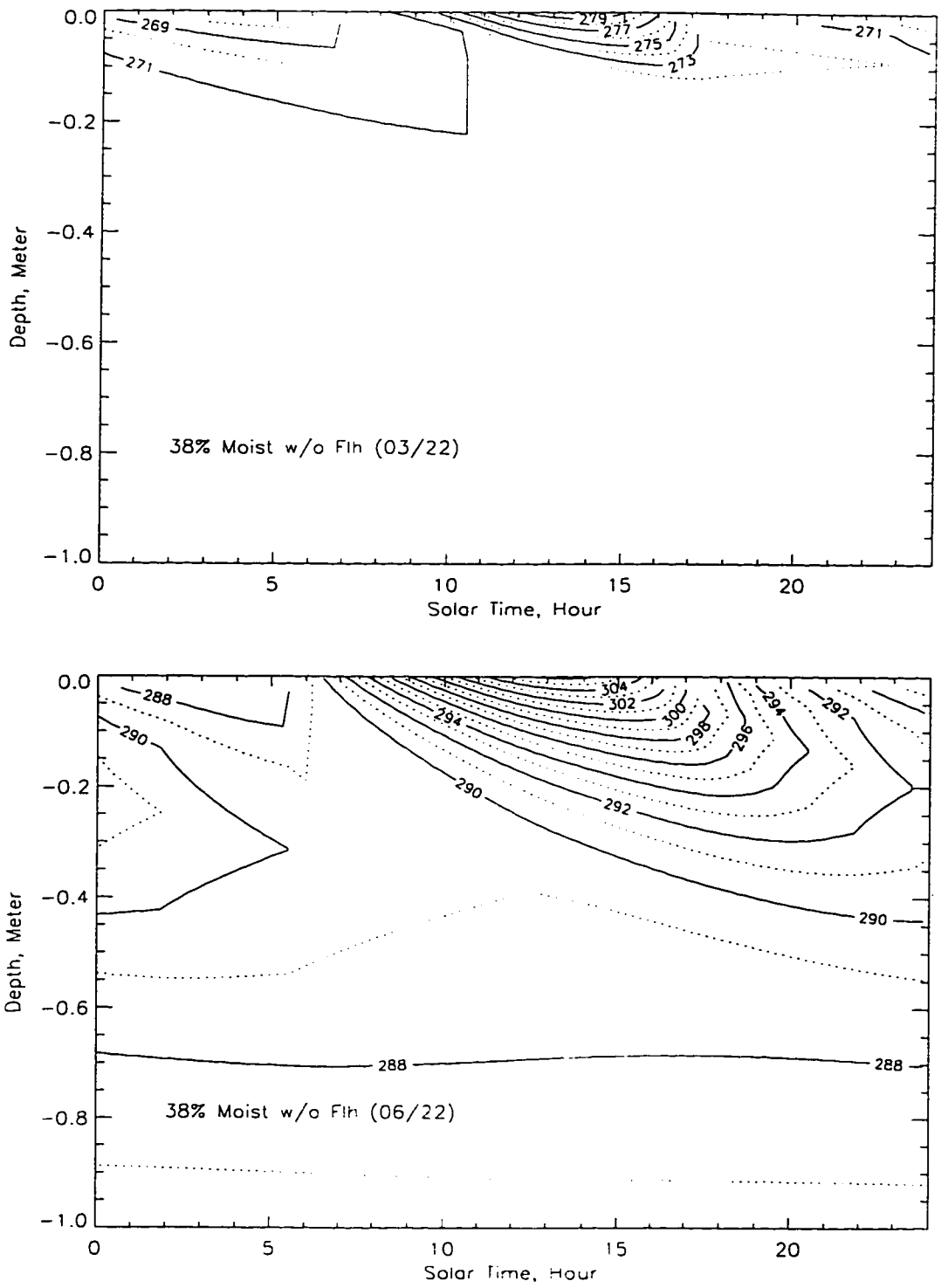

Figure 2.5: 38 % moist soil isotherms without latent heat transfer for 03/22 and 06/22.

	17 %	38 %
2 a.m.	30.7	29.1
6 a.m.	33.6	31.9
2 p.m.	37.5	34.1
6 p.m.	33.8	31.3

Table 2.2: The differences between the maximum and minimum surface temperatures over an annual cycle at four times for 17 % and 38 % moist soils.

slightly negative during daytime. For June, latent heat transfer and winter cooling contribute in the same sense so that the differences between the two models are about 3 Kelvins.

Figure 2.7 shows the annual surface temperature variations at four times: 2 a.m., 6 a.m., 2 p.m., and 6 p.m. for 17 % and 38 % moist soils. The differences between the maximum and minimum surface temperatures over an annual cycle for 17 % and 38 % moist soils are listed in Table 2. The differences are larger for 17 % moist soil than for 38 % moist soil at the four times by about 2 Kelvins. This indicates that annual extremes in soil temperature are weakly dependent upon moisture content. However, the annual model predicts significant perturbations in soil temperature with moisture content during the periods of spring thawing and winter freezing as noted in [69]. These perturbations are exaggerated in the temporal radiobrightness signature because of microwave emissivity's dependence upon moisture content and state.

2.3 RADIOBRIGHTNESS MODEL

2.3.1 Soil Dielectric Properties and Radiobrightness Model

Dielectric properties together with temperature and moisture content/state determine radiobrightness of soil. At temperatures above DFP, we estimate these dielectric

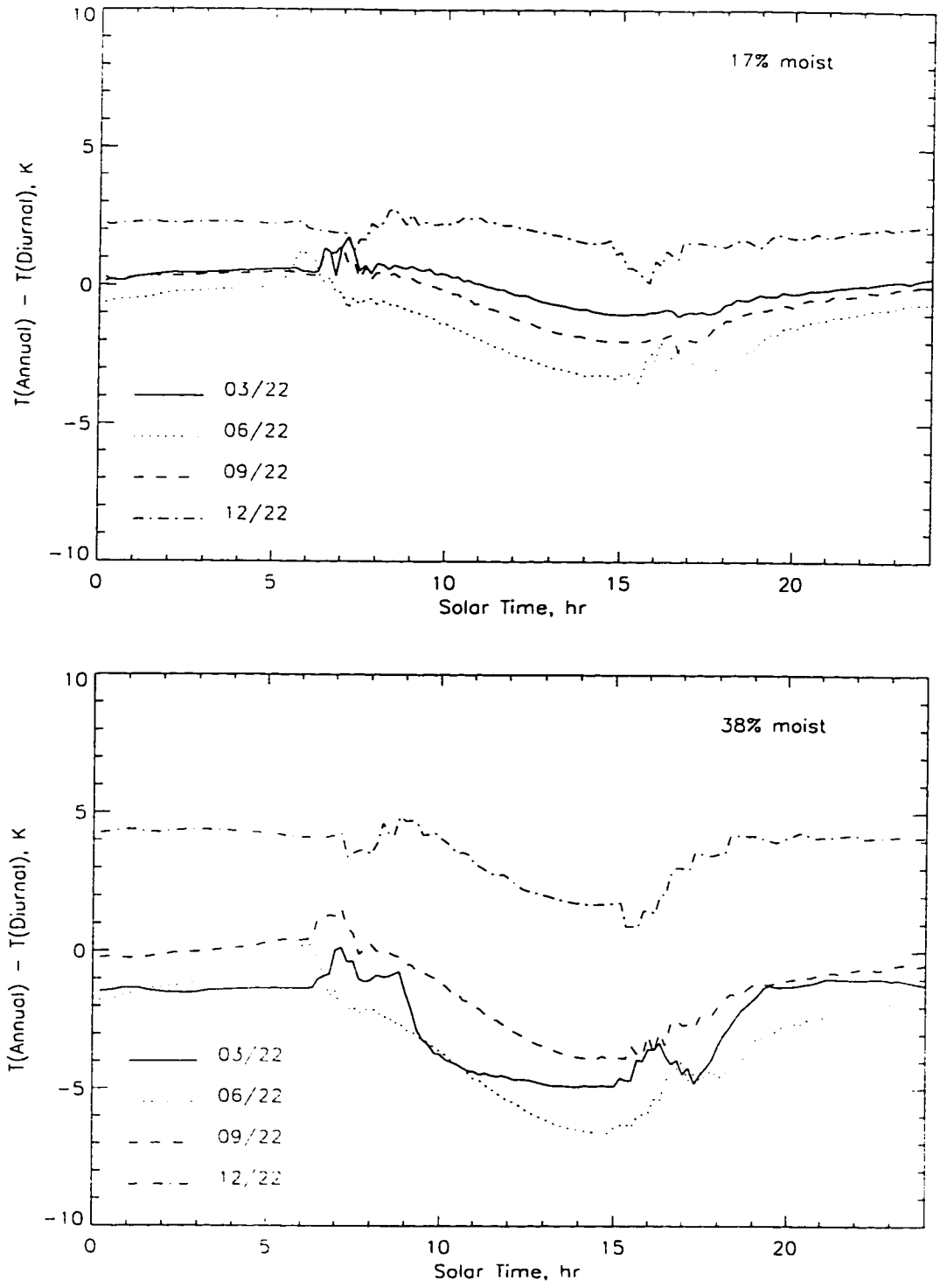

Figure 2.6: Differences in diurnal surface temperatures between annual and diurnal models for (a) 17 % moist soil and (b) 38 % moist soil for 03/22, 06/22, 09/22 and 12/22.

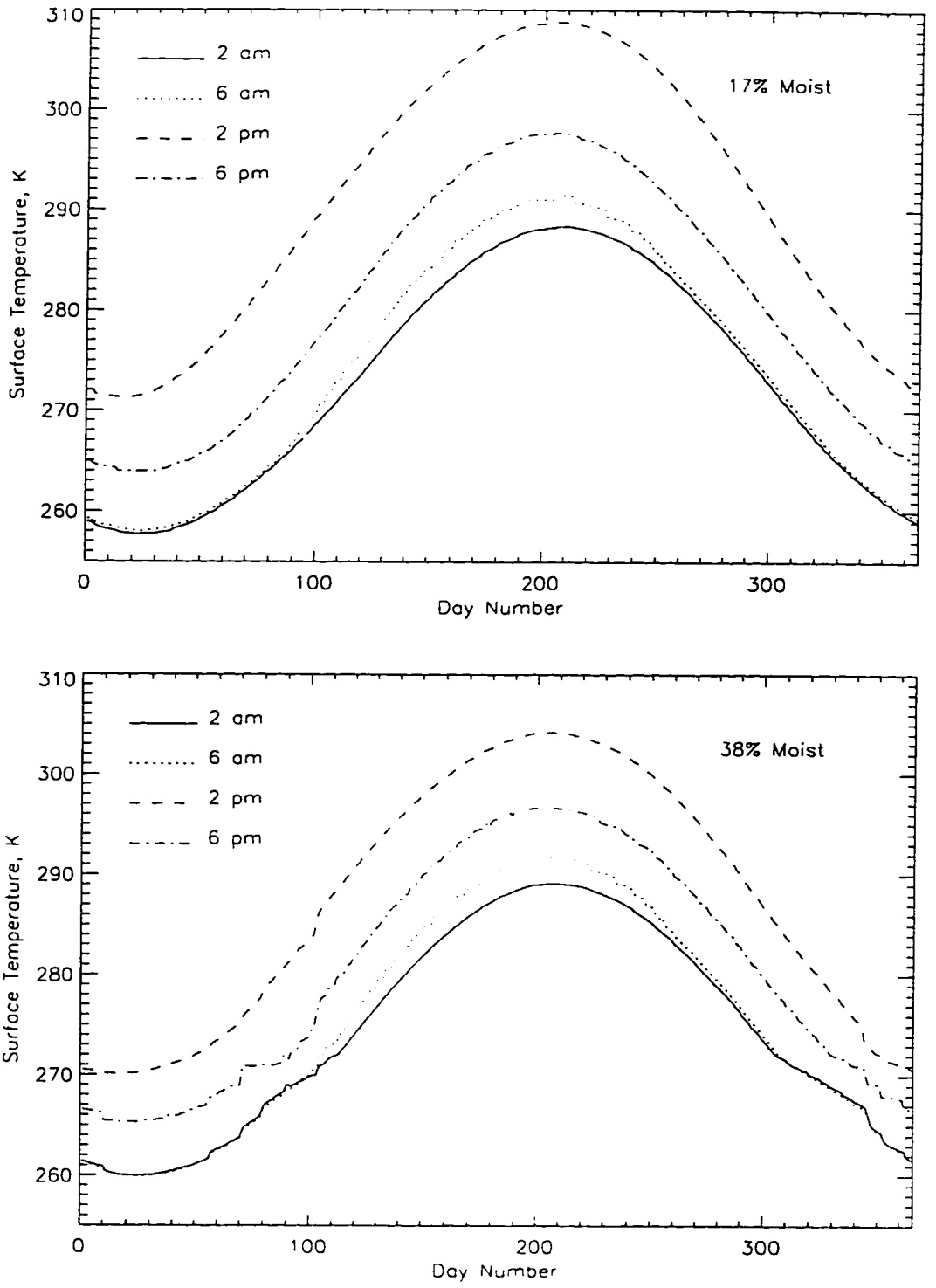

Figure 2.7: Annual surface temperature variations at four times: 2 a.m., 6 a.m., 2 p.m., and 6 p.m. for (a) 17 % moist soil and (b) 38 % moist soil.

α	0.65 [a]
ϵ_s	$(1.01 + 0.00044\rho_s)^2 - 0.062$ [a]
θ_{bw}	$10 \times dA\rho_b$ [a]
ϵ_{bw}	$31 + j15$ [a]
ρ_s	2658.9 kg/m^3 (soil density) [b]
ρ_b	1382.6 kg/m^3 (bulk density) [b]
d	3 $\AA$ (thickness of bound water layer) [a]
A	84000 m^2/kg (soil specific surface) [c]

a After Dobson et al [27].
b Estimates are based upon the values suggested by de Vries [24].
c After Andersland et al [6]. It is so chosen to be consistent with the model for computing liquid water content below DFP.

Table 2.3: Parameters required for computing radiometric properties of the soil-water system.

properties with a four-component mixture model of soil solids, air, free water, and bound water [27, 119]. Below DFP, we include the ice component, i.e.,

$$\epsilon^\alpha = \theta_s\epsilon_s^\alpha + \theta_a\epsilon_a^\alpha + \theta_{fw}\epsilon_{fw}^\alpha + \theta_{bw}\epsilon_{bw}^\alpha + \theta_i\epsilon_i^\alpha, \tag{2.10}$$

where ϵ is the complex dielectric constant of the soil-water system, α is a constant shape factor, θ denotes the volumetric fraction (m^3/m^3), and the subscripts s, a, fw, bw, and i stand for soil solids, air, free water in the liquid water state, bound water, and ice, respectively. α, ϵ_s, θ_{bw}, and ϵ_{bw} are described in Table 3. The dielectric constants of free water and ice are described by the Debye equation [119]

$$\epsilon_{fw/i}^* = \epsilon_{w\infty/i\infty}^* + \frac{\epsilon_{w0\ /\ i0}^* - \epsilon_{w\infty/i\infty}^*}{1 + j2\pi f\tau_{w/i}}, \tag{2.11}$$

where $\epsilon_{w0\ /\ i0}^*$ is the static dielectric constant of liquid water or ice, $\epsilon_{w\infty/i\infty}^*$ is the high frequency limit of $\epsilon_{fw/i}^*$, $\tau_{w/i}$ is the relaxation time of liquid water or ice (s), and f is the frequency, Hz.

Figure 2.8 shows the dielectric constants for 17 % and 38 % moist soils at 19.35, 37 and 85.5 GHz. The magnitudes of both real and imaginary parts of the dielectric

constants of liquid water and, thus, of moist soil decrease with increasing frequency. Below DFP, the magnitudes of both real and imaginary parts of the dielectric constants follow the liquid water content and decrease with decreasing temperature.

Wet soils are sufficiently absorptive in the microwave region so that effective emission depths are usually less than a few tenths of a centimeter. This permits a first-order approximation to the radiobrightnesses of bare, quasi-specular, wet soils [29, 69],

$$T_b(t) = e \cdot T_{eff}(t), \tag{2.12}$$

where $e = 1 - \Gamma$ is the emissivity of the soil. Γ, the reflectivity of the ground at the land-air interface, is

$$\Gamma = \begin{cases} \left| \frac{\eta_a \cos\theta_a - \eta_g \cos\theta_g}{\eta_a \cos\theta_a + \eta_g \cos\theta_g} \right|^2 & \text{horizontal polarization} \\ \left| \frac{\eta_g \cos\theta_a - \eta_a \cos\theta_g}{\eta_g \cos\theta_a + \eta_a \cos\theta_g} \right|^2 & \text{vertical polarization,} \end{cases}$$

where $\eta_g(\eta_a)$ is the intrinsic impedance of the ground (air), θ_a is the incidence angle, and θ_g is the transmission angle. The assumption of a quasi-specular soil surface may be adequate at 19.35 GHz - the lowest of the SSM/I frequencies, but it becomes questionable at the higher SSM/I frequencies. Surfaces look increasingly "black" as they become rough so that we expect the observed radiobrightness of moist soil to be somewhat higher at 37.0 GHz and 85.5 than Equation (2.12) would predict. This rough-surface correction is beyond the scope of this paper.

The effective ground temperature, T_{eff}, is

$$T_{eff}(t) = T_g(0,t) + \frac{1}{\kappa_e \sec\theta_g} \cdot \left(\frac{\partial T_g(z,t)}{\partial z} \right)_{z=0}, \tag{2.13}$$

where κ_e in the first-order correction to surface temperature is the extinction in soil.

The magnitude of extinction for temperatures between 250 K and 320 K at SSM/I frequencies lies between 200 to 1700 for 17 % moist soil, and between 200 to 3600 for

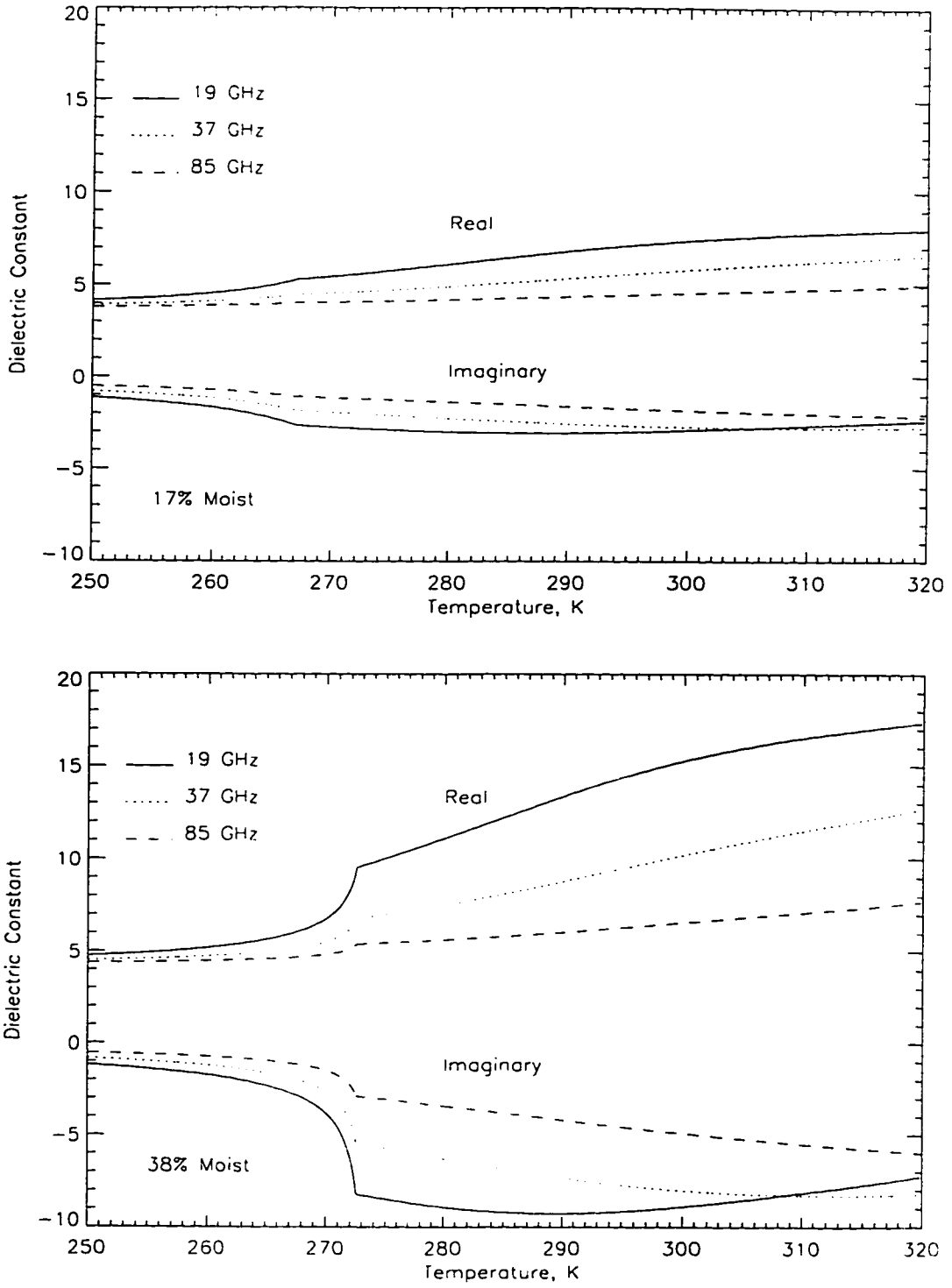

Figure 2.8: Dielectric constants of (a) 17 % moist soil and (b) 38 % moist soil at 19, 37 and 85 GHz.

38 % moist soil. Scattering is ignored because absorption dominates at temperatures above the DFP. At temperatures slightly below the DFP, scatter darkening might still be ignored because liquid water content continues to be significant. At temperatures sufficiently below the DFP, scatter darkening will become important [30].

2.3.2 Model Results

Emissivities at 19 GHz, 37 GHz, and 85 GHz for 17 % and 38 % moist soils are shown in Figure 2.9. Their magnitudes for both polarizations decrease slightly with increasing temperature. The 53° incidence angle is below the range of Brewster angles for 17 % moist soil — 63° to 71°, or for 38 % moist soil — 65° to 77°. The strong dependence of emissivity upon liquid water content is apparent in the differences between 2.9 (a) and 2.9 (b). These exceed 0.15 at temperatures above DFP, but are less than 0.05 at temperatures a few degrees below DFP.

The diurnal maxima and minima of the first-order terms $(\frac{1}{\kappa_e \sec\theta_t} \cdot \left(\frac{\partial T_g(z,t)}{\partial z}\right)_{z=0})$ for 19 GHz vertical and horizontal polarization for 17 % moist soil are shown in Figure 2.10. They range from -0.32 to 0.24 Kelvins for 19 GHz vertical polarization, and from -0.20 to 0.18 Kelvins for 19 GHz horizontal polarization. The temporal signatures for the diurnal maxima and minima of first-order terms for 37 GHz and 85 GHz are similar to those of 19 GHz, but with a smaller variation — from -0.16 to 0.17 Kelvins for 37 GHz vertical polarization, from -0.11 to 0.13 Kelvins for 37 GHz horizontal polarization, from -0.10 to 0.12 Kelvins for 85 GHz vertical polarization, and from -0.08 to 0.09 Kelvins for 85 GHz horizontal polarization. As soil moisture content increases, the first-order terms become even less important.

Figure 2.11 shows semiannual radiobrightness signatures for 19 GHz and 37 GHz

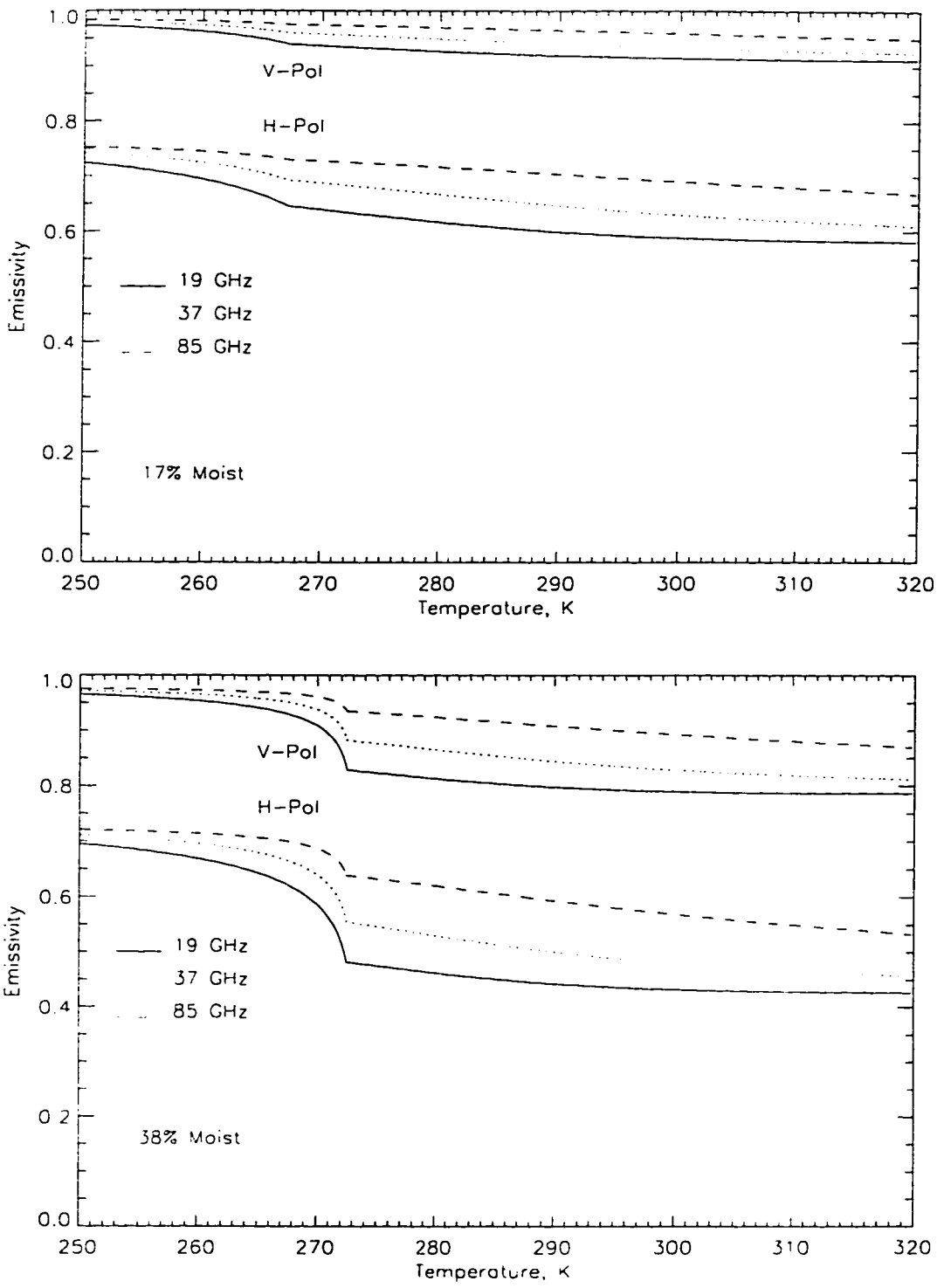

Figure 2.9: Emissivity versus temperature at the 53° angle of incidence of the SSM/I for (a) 17 % moist soil and (b) 38 % moist soil.

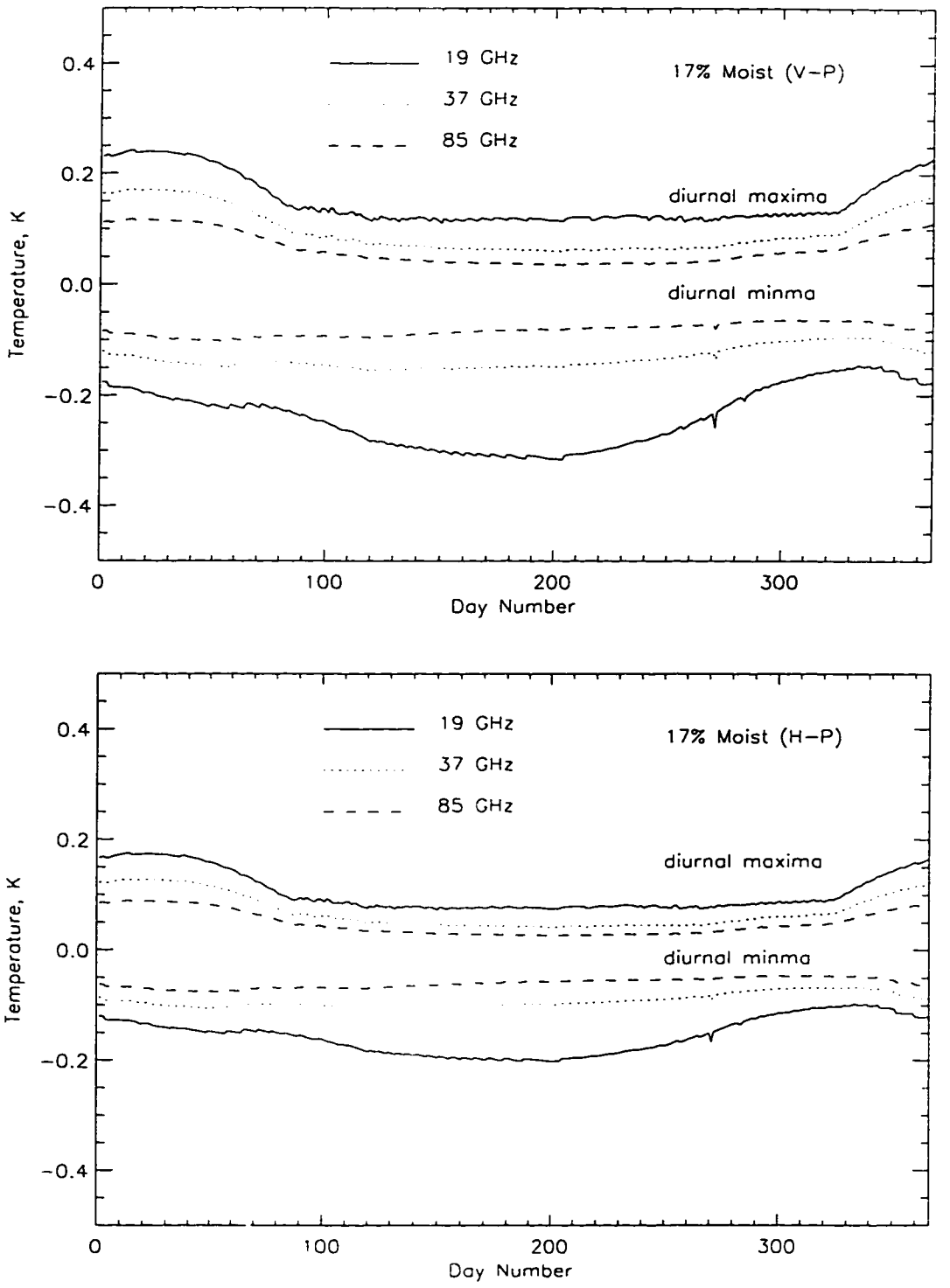

Figure 2.10: Diurnal maxima and minima of the first-order terms for (a) vertical polarization and (b) horizontal polarization for 17 % moist soil.

horizontal polarization for 17 % moist soil. In winter, nighttime radiobrightness corresponds to frozen (effectively dry) soil while daytime radiobrightness reflects melting (in the absence of vegetation and snow). Daytime decreases in radiobrightness are a response to increases in liquid water content.

In spring after soils are completely thawed, radiobrightnesses are nearly linear with temperature except for a small, second-order effect caused by emissivity's dependence upon temperature (Figure 2.9). An exponential decrease in radiobrightness occurs at the daytime in early winter. We only show semiannual results because the radiobrightness signatures for the second half year approximately mirror the first half year. The 85 GHz results are not shown because they are similar to but smaller in amplitude than the 19 and 37 GHz results. Results for vertical polarization are not shown for the same reason.

Figure 2.12 shows semiannual radiobrightness signatures for 19 and 37 GHz horizontal polarization for 38 % moist soil. A comparison between Figures 2.11 and 2.12 demonstrates that 17 % and 38 % moist soil have extremely different radiobrightness signatures during winter and spring when diurnal freezing and thawing have a more dramatic effect upon more moist soils. During winter or early spring, the day-to-night change in radiobrightness for 38 % moist soil could exceed 18 Kelvins at 19 GHz, and 9 Kelvins at 37 GHz. These variations are more than double those for 17 % moist soil. The maximum variations for 38 % moist soil occur in late February when soil is thawed during the daytime, but partially frozen at night. Figure 2.12 also shows that the day-to-night difference in 19 GHz horizontal radiobrightness is weakly positive in late spring by as much as 3 Kelvins, but that the equivalent 37 GHz difference is weakly negative by about -2 Kelvins. The contrast is caused by differing soil dielectric behavior with temperature at the two frequencies (Figure 2.8).

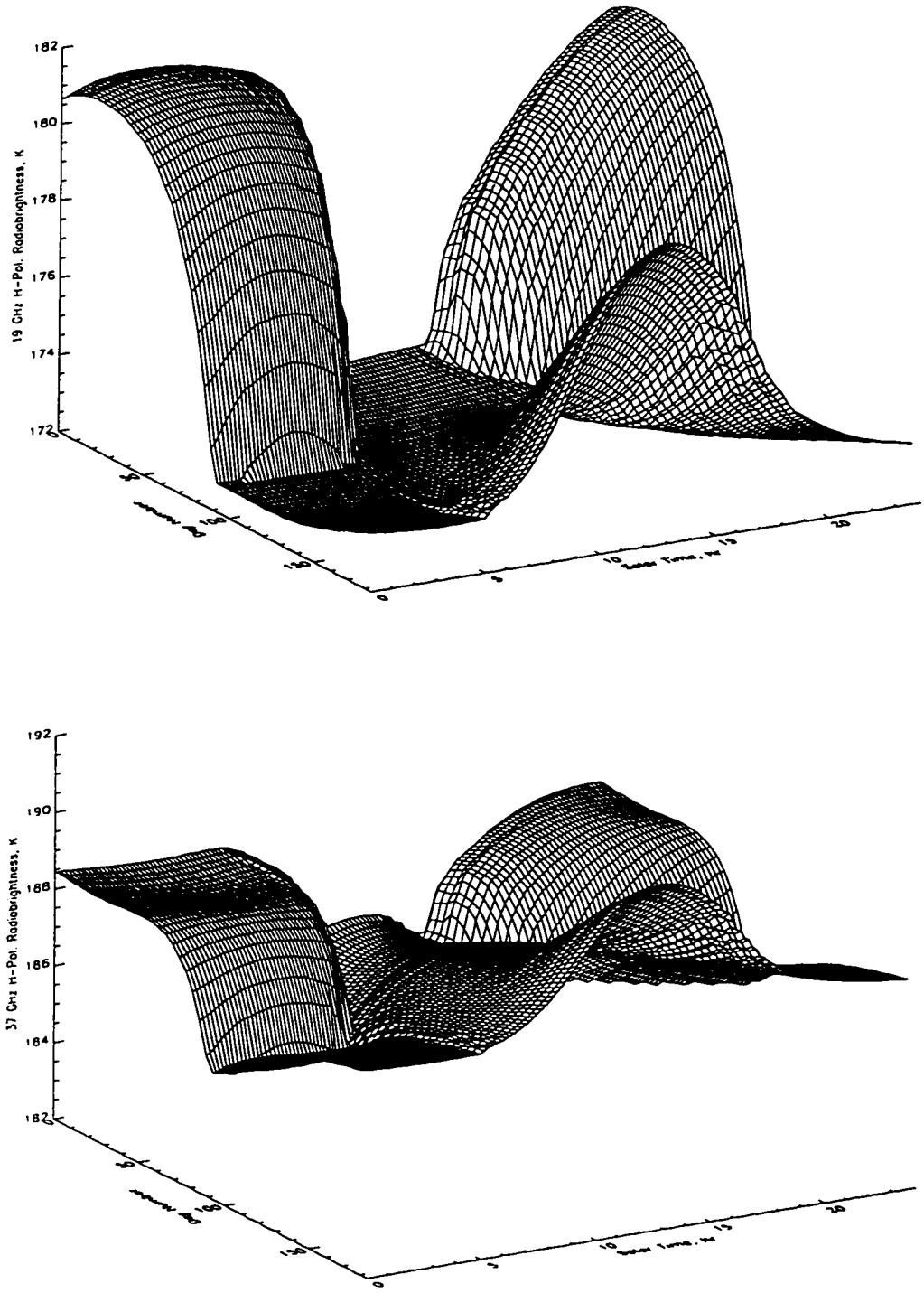

Figure 2.11: Semiannual radiobrightness signatures for (a) 19 GHz horizontal polarization, and (b) 37 GHz horizontal polarization for 17 % moist soil.

2.4 DISCUSSION

The predictions of this annual radiobrightness model should be compared with relevant data. The model in such a test would be forced by actual weather rather than by expected climate as we have done. As noted in the introduction, a comparison with satellite data (e.g., with data from the SSM/I), is difficult because of the low spatial resolution of these sensors. While there have been diurnal ground observations of bare soil that show the features of our diurnal model (e.g., Wegmüller et al [126]), there have been no seasonal or annual experiments. Our group has conducted a series of Radiobrightness Energy Balance Experiments in grassland prairie (REBEX-1 [39]) and in wet acidic tundra (REBEX-3 [60]), but have not yet examined the seasonal temperature and radiobrightness signatures of bare moist soil. We do plan such an experiment for the summer of 1996.

While we do not have the desired experimental verification, the annual model reported here indicates that diurnal predictions of land-atmosphere thermal and moisture exchanges should be set in an annual context, that the history of energy exchanges at the land-atmosphere interface has an increasing influence upon soil surface temperatures as moisture content increases, and that the strong moisture dependence of the diurnal extremes in surface temperature predicted by our diurnal model persists in an annual context. The last conclusion will be moderated in the companion paper. Coupling heat and moisture transport reduces the dependence of day-night temperature differences upon moisture content (Chapter 3) [71].

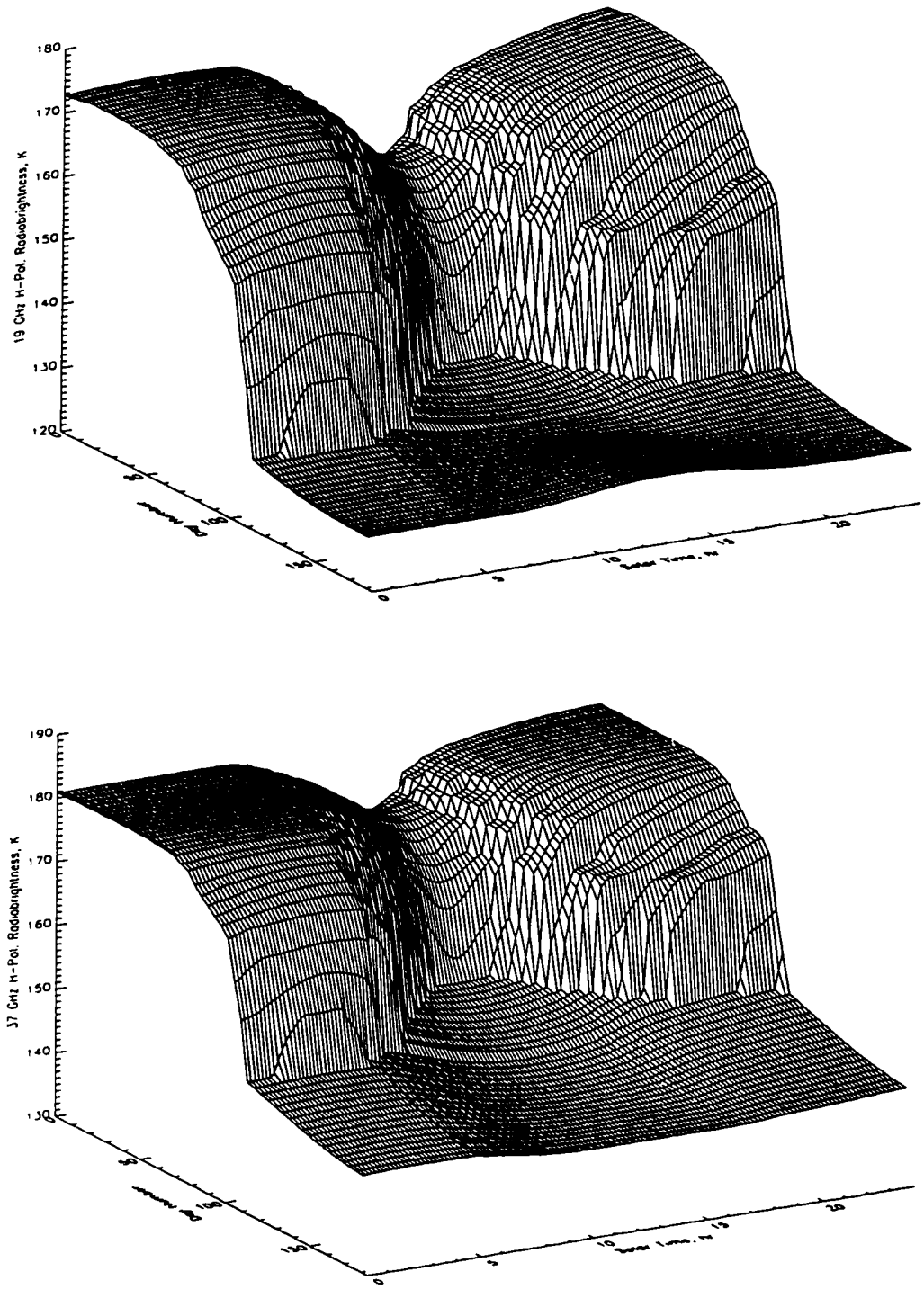

Figure 2.12: Semiannual radiobrightness signatures for (a) 19 GHz horizontal polarization, and (b) 37 GHz horizontal polarization for 38 % moist soil.

CHAPTER 3

The 1dH/R MODEL FOR BARE, UNFROZEN SOILS — A 1dHbu/R MODEL

Abstract — Heat and moisture transport in soil are coupled processes that jointly determine temperature and moisture profiles. We present a physically-based, one-dimensional, coupled heat and moisture transport hydrology (1dHu) model for bare, unfrozen, moist soils subject to insolation, radiant heating and cooling, and sensible and latent heat exchanges with the atmosphere. A 60-day simulation is conducted to study the effect of dry-down on soil temperature and moisture distributions in summer for bare soil in the U.S. Midwest. Given a typical initial moisture content of 38 % by volume, we find that temperature differences between the water transport and no water transport cases exhibit a diurnal oscillation with a slowly increasing amplitude, but never exceed 4.4 Kelvins for the 60-day period. However, moisture content of the surface decreases significantly with time for the water transport case and becomes only about 21 % at the end of the same period.

The 1dHu model is linked to a radiobrightness (1dHu/R) model as a potential means for soil moisture inversion. The model shows that radiobrightness thermal inertia (RTI) correlates with soil moisture if the two

radiobrightnesses are taken from times near the thermal extremes, e.g., 2 a.m. and 2 p.m., and that RTI appears temperature-dependent at the ending stages of the dry-down simulations where soils are dry and their moisture contents vary slowly. Near times of thermal crossover, the RTI technique is insensitive to soil moisture.

3.1 INTRODUCTION

The near-surface distributions of moisture and temperature influence the exchanges of moisture and energy between land and atmosphere, and, through these processes, affect weather and climate [100, 20, 73, 99, 81, 110, 68]. Atmospheric models that are used to study or predict weather or climate rely upon embedded Land Surface Process (LSP) models to estimate moisture and energy transfer within soils and vegetation that result in the land-atmosphere exchanges. LSP models, like the Biosphere-Atmosphere Transfer Scheme (BATS) [25] or the Simple Biosphere model (SiB) [106], characterize these transfer processes with relatively simple, almost cartoon-like parameterizations of the actual biophysical processes. The relative simplicity of these LSP models permits computational efficiencies in the demanding environment of numerical modeling of weather or climate.

Most LSP models are tuned to reproduce observed temperatures, humidities, and winds in the boundary layer rather than reproduce good estimates of moisture and temperature in the underlying soil or vegetation. It is possible to replace the LSP model with a 1-dimensional hydrology (1dH) model of the surface processes to achieve a greater fidelity in moisture and temperature profiles. While such use of a 1dH model is currently too computationally intensive for most atmospheric modeling applications, the approach can be used retrospectively to yield running estimates of

water stored in soil at specific points [74, 8, 9] or over selected regions. Because a 1dH model will accumulate errors over time in its estimate of stored water, the approach is potentially more powerful if point estimates can be checked periodically against an actual measurement, or if regional estimates can be refined through the assimilation of remotely sensed data. This process might also be used to examine the possible equivalence between an LSP model's estimate of soil wetness and the 1dHu/R model's estimate of stored water.

Of available remotely sensed data, radiobrightnesses are arguably the single class of measurements that are most sensitive to the critical parameters of surface temperature and moisture [124, 27, 44, 105, 55]. While L-band radiobrightness is recognized as the most desirable of the possibilities [105], radiobrightness at any frequency where emissivity is influenced by the Debye relaxation of water will be sensitive to moisture in vegetation or at the surface of bare soil. We have modeled and observed this sensitivity in field experiments at 19.35 and 37.0 GHz [37]. As satellite radiometers achieve adequate spatial resolutions at frequencies below the Special Sensor Microwave/Imager's (SSM/I's) 19 GHz, their sensitivities to soil moisture will become increasingly pronounced. For the purposes of this investigation, we focus on the temporal signature of radiobrightness at the SSM/I frequencies of 19.35, 37.0, and 85.5 GHz because these data have been available on a near-daily basis for the all of the Earth since 1987 [49].

Several investigators have developed one-dimensional thermal/emission models to predict thermal infrared (TIR) or thermal microwave (radiobrightness) signatures over a diurnal cycle for discrimination among rock types in TIR images [125] and among various soils [59], for inference about soil moisture [95, 96, 29, 31], and for mapping frozen and thawed prairie soils [30]. The diurnal thermal/radiobrightness

model of England [31] was expanded to simulate annual thermal and radiobrightness for dry soil [69]. Results from the annual model demonstrate that the seasonal history significantly influences the surface temperature. Liou and England [70] recently improved this annual thermal model to include freezing and thawing of soil moisture. However, none of these thermal models accounts for vertical transport of water in soil which is a dominant process governing temperature and moisture profiles and, consequently, TIR and radiobrightness signatures.

In this paper, we develop a 1-dimensional hydrology/radiobrightness (1dHu/R) model for unfrozen soils that incorporate coupled thermal and water transport. Radiobrightness is based upon a quasi-specular, microwave emission model ([29], [69], and [70]) which should be appropriate for 19.35 GHz over bare or sparsely vegetated soil, but increasingly less appropriate at 37.0 and 85.5 GHz where most soil surfaces appear increasingly rough.

Philip and de Vries [92] and de Vries [23] proposed a coupled heat and moisture transfer model for porous materials. In their work, liquid and vapor flux densities accounted for the total moisture flux density and liquid water was continuously in equilibrium with water vapor. Heat conduction, transfer of latent heat by vapor movement, and transfer of sensible heat in vapor and liquid comprised the total heat flux in a porous, unsaturated soil. Heat transfer by convection and radiation within the soil was assumed to be negligible. Moisture and temperature distributions in the soil were obtained by solving two coupled, nonlinear, partial differential equations in time and space.

Many attempts have been made to refine or support the Philip and de Vries theory. Working with laboratory soil columns, Gee [40] found that the theory predicted a moisture flux which was one-half to one-third that observed in a silt loam at inter-

mediate water content. In a fine sandy loam soil at low soil water content, Cassel et al [17] showed that the predicted net flux agreed with observation. Jackson et al [56] evaluated the theory for a clay loam soil under field conditions and found it adequate at intermediate soil water content, but an isothermal theory was better at high and very low water contents. Kimball et al [61] applied the coupled theory to calculate soil heat fluxes in a field of Avondale loam. They obtained a fair agreement with observation only after modifying the air shape factor curve and ignoring heat transfer due to water vapor movement. They concluded that situation-specific "calibrations" are required to reliably use the coupled theory.

Milly and Eagleson [79, 80] and Milly [77, 78] developed a matric-head formulation for simultaneous moisture and heat flow based upon the water-content formulation of Philip and de Vries. One of their goals was to generalize the Philip and de Vries' theory to accommodate the complications of hysteresis and inhomogeneity. Bach [7] used the Milly and Eagleson formulation to study thermally-driven water movement in Otero sandy loam soil and concluded that the Philip and de Vries theory provided an adequate description of nonisothermal transport processes. Other examples concerning coupled heat and moisture that are based upon the Philip and de Vries theory include Abdel-Hadi and Mitchell [1], Shah et al [107], Thomas [114], Ewen and Thomas [34], and Thomas and King [115].

The Philip and de Vries theory will be adopted in this study because its strengths and weaknesses are relatively well understood by the soil science community, and it appears to be the best theory available. Improved models for thermal conductivity [24], vapor diffusion coefficients [61], tortuosity factor for diffusion of gases in soil [66], and water retention [102] are incorporated in the original theory. For the purposes of this paper, we ignore hysteresis because our interest is in simulations of

soil dry-down, and not of infiltration.

The governing equations for the heat and moisture transport are too complicated to be solved analytically. Camillo et al [15] used a finite difference, numerical scheme with variable depth step. In their method, heat and moisture fluxes at all depths and at the surface were first computed. From these fluxes, they found the change in heat and moisture contents, and, hence, temperature and moisture content per unit volume for all layers. The process was repeated until the solutions met their criterion for convergence that the absolute value of the change in surface temperature between iterations was less than 0.1 Kelvins for all times in a diurnal cycle. Their solutions were compromised because no convergence criterion was required for moisture transport at the land-air boundary. We improve upon the Camillo et al model by using the Newton-Raphson method to match both heat and moisture fluxes at the land-air interface. To reduce the possibility of errors in the 1dHu model caused by omission of historical land-air exchanges of energy, initial temperatures and a continuing thermal flux at the lower boundary that is appropriate for time-of-year are obtained from the annual thermal model by Liou and England [70].

Based upon simulations using the 1dHu/R model, we discuss the effects of vertical transport of moisture in soil upon soil temperature, moisture profiles, and upon radiobrightness signatures for a 60-day simulation of drying in summer. Also, we re-examine the feasibility of the Radiobrightness Thermal Inertia (RTI) measure of soil moisture [31].

3.2 LAND SURFACE PROCESS MODEL

Our 1dHu model concerns vertical heat and moisture transfer in unsaturated soil, and at the land-air interface. For the soil, we chose a silt loam, a typical soil type in the U.S. Midwest, which consists of 19 % sand, 22.5 % clay, and 58.5 % silt, and has a porosity of 48 % [70]. The thermal and hydraulic properties of the soil-water system can be inferred from the soil texture and moisture content. These properties are thermal conductivity, heat capacity, liquid and vapor diffusivity, hydraulic conductivity, and water retention. Thermal conductivity and heat capacity have been presented in [70]; the other parameters are reviewed here.

3.2.1 Governing Equations of Heat and Moisture Transfer

The equations governing heat and moisture transport in soil may be derived from the equations for heat and moisture (liquid water, ice, and vapor) conservation, i.e.,

$$\frac{\partial X_m}{\partial t} = -\nabla \cdot \vec{q_m} \tag{3.1}$$

$$\frac{\partial X_h}{\partial t} = -\nabla \cdot \vec{q_h}, \tag{3.2}$$

where

- X_m is the total moisture content per unit volume, kg/m^3,
- X_h is the total heat content per unit volume, J/m^3,
- t is the time, s,
- $\vec{q_m} = \vec{q_v} + \vec{q_l}$ is the vector moisture flux density, kg/m^2-s, where $\vec{q_v}$ and $\vec{q_l}$ are the vector vapor and liquid flux densities, respectively, and
- $\vec{q_h}$ is the vector heat flux density, J/m^2-s.

For unfrozen ground, moisture and heat content per unit volume are

$$X_{\mathrm{m}} = \rho_{\mathrm{l}}\theta_{\mathrm{l}} + \rho_{\mathrm{v}}\theta_{\mathrm{a}} \tag{3.3}$$

$$X_{\mathrm{h}} = (C_{\mathrm{d}} + c_{\mathrm{l}}\rho_{\mathrm{l}}\theta_{\mathrm{l}} + c_{\mathrm{p}}\rho_{\mathrm{v}}\theta_{\mathrm{a}})(T - T_0) + L_{\mathrm{v}_0}\rho_{\mathrm{v}}\theta_{\mathrm{a}} - \rho_{\mathrm{l}}\int_0^{\theta_{\mathrm{l}}} W d\theta, \tag{3.4}$$

respectively, where

- ρ_{l} is the density of the liquid water, kg/m^3,
- θ_{l} is the volumetric liquid water content, m^3/m^3,
- ρ_{v} is the density of water vapor, kg/m^3,
- θ_{a} is the volumetric air content, m^3/m^3,
- C_{d} is the volumetric heat capacity of dry porous medium, J/m^3-K ,
- c_{l} is the specific heat of liquid water at constant pressure, J/kg-K,
- c_{p} is the specific heat of water vapor at constant pressure, J/kg-K,
- T is the temperature, K,
- T_0 is the reference temperature, K,
- L_{v_0} is the latent heat of vaporization at reference temperature, J/kg, and
- W is the differential heat of wetting [23], J/kg.

Following Philip and de Vries [92] and de Vries [23], the heat and moisture flux densities are described by

$$\frac{\vec{q_{\mathrm{m}}}}{\rho_{\mathrm{l}}} = -D_{\mathrm{T}}\nabla T - D_\theta \nabla\theta_{\mathrm{l}} - K\hat{k} \tag{3.5}$$

$$\vec{q_{\mathrm{h}}} = -\lambda\nabla T + L_{\mathrm{v}_0}\vec{q_{\mathrm{v}}} + c_{\mathrm{p}}(T - T_0)\vec{q_{\mathrm{v}}} + c_{\mathrm{l}}(T - T_0)\vec{q_{\mathrm{l}}}, \tag{3.6}$$

respectively, where

- $D_T = D_{T_l} + D_{T_v}$ is the thermal moisture diffusivity, $m^2/K\text{-}s$,
- $D_\theta = D_{\theta_l} + D_{\theta_v}$ is the isothermal moisture diffusivity, m^2/s,
- D_{T_l} is the thermal liquid diffusivity,
- D_{T_v} is the thermal vapor diffusivity,
- D_{θ_l} is the isothermal liquid diffusivity,
- D_{θ_v} is the isothermal vapor diffusivity,
- K is the hydraulic conductivity, m/s,
- $\hat{k}$ is a vertical unit vector, and
- λ is the thermal conductivity of a moist, porous medium, J/m-K-s.

Upon substituting equations (3.3) to (3.6) into equations (3.1) and (3.2), we get two coupled, nonlinear, partial differential equations for heat and moisture transfer, i.e.,

$$\begin{aligned} &\left[1 + \frac{(S-\theta_l)\rho_0}{\rho_l}\frac{\partial h_r}{\partial \theta_l} - \frac{\rho_v}{\rho_l}\right]\frac{\partial \theta_l}{\partial t} + \frac{(S-\theta_l)}{\rho_l}\left(h_r\frac{\partial \rho_0}{\partial T} + \rho_0\frac{\partial h_r}{\partial T}\right)\frac{\partial T}{\partial t} \\ = \quad &\nabla\cdot\left(D_T\nabla T + D_\theta\nabla\theta_l + K\hat{k}\right) \end{aligned} \tag{3.7}$$

$$\begin{aligned} &\left[L_v(S-\theta_l)\rho_0\frac{\partial h_r}{\partial \theta_l} - L_v\rho_v - \rho_l W\right]\frac{\partial \theta_l}{\partial t} + \left[C + L_v(S-\theta_l)\left(h_r\frac{\partial \rho_0}{\partial T} + \rho_0\frac{\partial h_r}{\partial T}\right)\right]\frac{\partial T}{\partial t} \\ = \quad &\nabla\cdot[(\lambda + L_v\rho_l D_{T_v})\nabla T] + L_v\rho_l\nabla\cdot(D_{\theta_l}\nabla\theta_l) + \rho_l\left[(c_p D_{\theta_v} + c_l D_{\theta_l})\nabla\theta_l\right. \\ &\left. + (c_p D_{T_v} + c_l D_{T_l})\nabla T + c_p K\hat{k}\right]\cdot\nabla T. \end{aligned} \tag{3.8}$$

We have used

$$\rho_v = \rho_0 h_r \tag{3.9}$$

$$\theta_a = S - \theta_l \tag{3.10}$$

$$L_v = L_{v_0} + (c_l + c_p)(T - T_0). \tag{3.11}$$

in Equations (3.7) and (3.8) where

- ρ_0 is the density of saturated water vapor, kg/m^3,
- h_r is the relative humidity, and
- S is the porosity.

Equations (3.7) and (3.8) are highly nonlinear in moisture and temperature because both thermal and hydraulic properties of the soil-water system are functions of moisture and temperature. They can be solved by the following numerical scheme.

3.2.2 Finite Difference Scheme

Figure 3.1 (a) shows the schematic diagram for the division of the soil profile into n layers, where $d_i, i = 1, \cdots, n$, is the thickness of the i^{th} layer, and $z_i, i = 1, \cdots, n$, is the depth from the surface to the center of the i^{th} layer. z_n must be beyond the thermal penetration of the period of interest (approximately less than 1 meter for a diurnal case and less than 3 meters for a seasonal case). The required number of soil layers is influenced by current and historical weather forcings, the time step of the numerical scheme, and soil texture. We typically use 60 layers in our simulations.

Soil layers near the surface are very likely to be modified by rapidly changing land-air interactions, while those at the bottom of the soil layer are insensitive to transient weather forcing. Consequently, thicknesses of the soil layers must be small near the surface, but may increase with depth. Layer thicknesses of a few tenths of a millimeter or less at the surface are generally required.

Figure 3.1 (b) is a flowchart of our algorithm for the 1dHu model. Major operations for each time step are listed as follows.

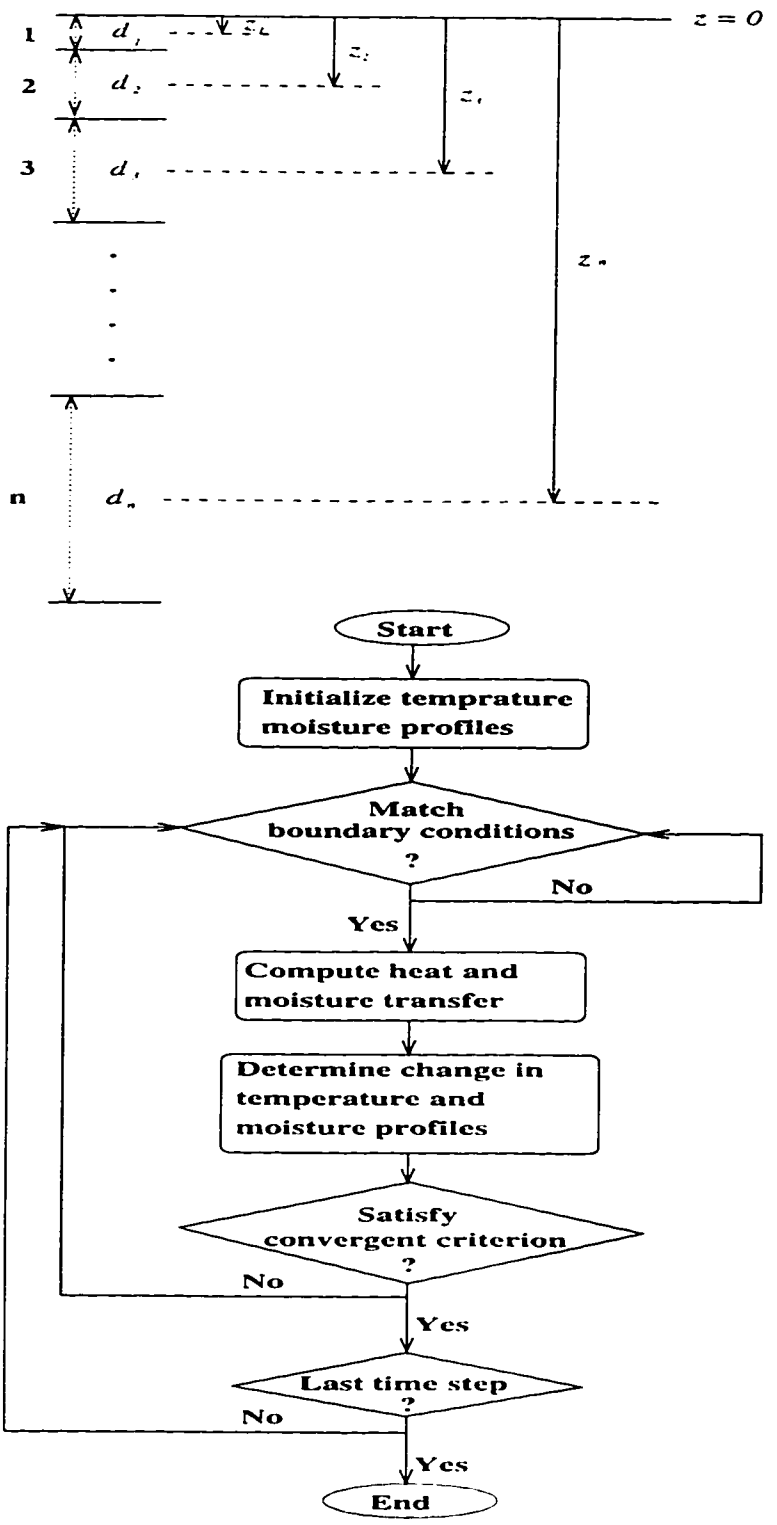

Figure 3.1: (a) Schematic diagram for the soil layers. (b) Flowchart of 1dHu model algorithm.

1. Initialize temperature and moisture profiles using results from the annual thermal model [70].

2. Match upper boundary conditions of heat and moisture fluxes using the Newton-Raphson method [94].

3. Compute heat and moisture fluxes between layers (excluding the bottom one) using Equations (3.7) and (3.8).

4. Match bottom boundary conditions of heat and moisture fluxes assuming the bottom layer has the same fluxes as the second to bottom layer so that its temperature and moisture content remain constant.

5. Determine the change in temperature and moisture content for all layers.

6. Check if the changes in temperature and moisture content between iterations are less than the criteria for convergence — 0.01 Kelvins for temperature, and 0.01 % for moisture content.

7. If criteria for convergence are not satisfied, then proceed to step 2 and repeat steps 3, 4, and 5. Otherwise, go to the next time step.

8. If the last time step has not been reached, then go to step 2 and repeat steps 3, 4, 5, and 6. Otherwise, end the process.

Approximations used in the numerical method were

$$\left(\frac{\partial x}{\partial t}\right)_i \rightarrow \frac{x_{i+1} - x_i}{t_{i+1} - t_i} \tag{3.12}$$

$$(\nabla x)_i \rightarrow \frac{x_{i+1} - x_i}{z_{i+1} - z_i} \tag{3.13}$$

$$(\bar{y})_i \rightarrow \frac{y_{i-1} y_i}{y_{i-1} + y_i}. \tag{3.14}$$

where

- x_i is the temperature or moisture content of the i^{th} layer, and
- y represents the constitutive quantities of those terms within each divergence, such as liquid/vapor diffusivity, latent heat of vaporization, heat capacity, thermal conductivity, liquid/vapor diffusivity, hydraulic conductivity, or their combinations.

3.2.3 Boundary Conditions

Boundary conditions include energy and moisture budgets both at the land-air interface and at the bottom of the soil layer. Following Liou and England [70], the energy budget at the land-air interface is a balance among solar radiation, sky brightness, sensible and latent heat transfer, and gray-body emission from the surface. At the bottom of the soil layer, we use a constant energy flux determined from our annual model [70] for the time-of-year. The moisture budget is assumed to be constant at the bottom of the soil layer. In the absence of precipitation, the moisture budget at the land-air interface is a product of latent heat exchanges between the land and atmosphere.

3.2.4 Hydraulic Conductivity and Water Retention

Mualem [82] proposes a closed-form equation for predicting the relative hydraulic conductivity. This model is based upon knowledge of the soil-water retention curve and the hydraulic conductivity at saturation, and can be described as

$$K_r = S_e \left[\int_0^{S_e} \frac{1}{\Psi} dS_e / \int_0^1 \frac{1}{\Psi} S_e dS_e \right] \tag{3.15}$$

$$S_e = \frac{\theta_l - \theta_r}{\theta_s - \theta_r} \tag{3.16}$$

$$= \left[\frac{1}{1+(l\Psi)^n}\right]^{1-1/n}. \tag{3.17}$$

where

- K_r is the relative hydraulic conductivity, m/s,
- S_e is the effective saturation,
- Ψ is the matric head, m,
- θ_r is the residual liquid water content, m^3/m^3,
- θ_s is the saturated liquid water content, m^3/m^3, and
- l and, n are constants.

Van Genuchten [121] generalizes the Mualem model by expressing the water retention as

$$S_e = \left[\frac{1}{1+(l\Psi)^n}\right]^m, \tag{3.18}$$

where $m = 1 - 1/n$ for the Mualem model. The van Genuchten model does relatively well for predictions of hydraulic conductivity at high and medium water content, but fails at lower water content [85, 101].

Rossi and Nimmo [102] recently developed two models for soil water retention -- the two-parameter sum model and the two-parameter junction model. Both are modified forms of the Brooks and Corey model [11] with residual liquid water content taken as zero and both fit observations over the entire range from saturation to oven dryness for seven sets of soil textural classes. The two-parameter junction model is analytically integrable so that its inclusion in the Mualem hydraulic conductivity model is straightforward. Water retention according to the two-parameter junction

model is

$$\frac{\theta_l}{\theta_s} = \theta_1 = 1 - a_1 \left(\frac{\Psi}{\Psi_0}\right)^2, \quad 0 \le \Psi \le \Psi_i \tag{3.19}$$

$$\frac{\theta_l}{\theta_s} = \theta_2 = \left(\frac{\Psi_0}{\Psi}\right)^{\eta}, \quad \Psi_i \le \Psi \le \Psi_j \tag{3.20}$$

$$\frac{\theta_l}{\theta_s} = \theta_3 = a_2 \ln\left(\frac{\Psi_d}{\Psi}\right), \quad \Psi_j \le \Psi \le \Psi_d, \tag{3.21}$$

where Ψ_0 and η are the two independent parameters characterizing the system, θ_s and Ψ_d, the value of Ψ at oven dryness, are assigned values based upon the measurements, and a_1, Ψ_i, Ψ_j, and a_2 are parameters that are determined as analytical functions of Ψ_d and η through the following relations

$$\begin{aligned} \theta_1(\Psi_i) &= \theta_2(\Psi_i) & \frac{\partial\theta_1}{\partial\Psi}(\Psi_i) &= \frac{\partial\theta_2}{\partial\Psi}(\Psi_i) \\ \theta_2(\Psi_j) &= \theta_3(\Psi_j) & \frac{\partial\theta_2}{\partial\Psi}(\Psi_j) &= \frac{\partial\theta_3}{\partial\Psi}(\Psi_j). \end{aligned} \tag{3.22}$$

Thus,

$$a_1 = \frac{\eta}{2}\left(1 + \frac{\eta}{2}\right)^{-(1+\frac{\eta}{2})} \tag{3.23}$$

$$\Psi_i = \Psi_0 \left(1 + \frac{\eta}{2}\right)^{1/\eta} \tag{3.24}$$

$$a_2 = \eta e \left(\frac{\Psi_0}{\Psi_d}\right)^{\eta} \tag{3.25}$$

$$\Psi_j = \Psi_d e^{-1/\eta}. \tag{3.26}$$

Figure 3.2 (a) shows the water retention curve for the Salkum silt loam, which is found to fit observations very well from saturation to oven dryness [102].

Finally, by applying the two-parameter junction model to the Mualem model, we obtain the relative hydraulic conductivity:

$$K_r(\theta_l) = \sqrt{\frac{\theta_l}{\theta_s}} \frac{I^2(\theta_l)}{I^2(\theta_s)}. \tag{3.27}$$

where

$$I(\theta_l) = \begin{cases} I_{III}(\theta_l) & 0 \le \theta_l \le \theta_j \\ I_{II}(\theta_l) & \theta_j \le \theta_l \le \theta_i \\ I_I(\theta_l) & \theta_i \le \theta_l \le \theta_s \end{cases}$$

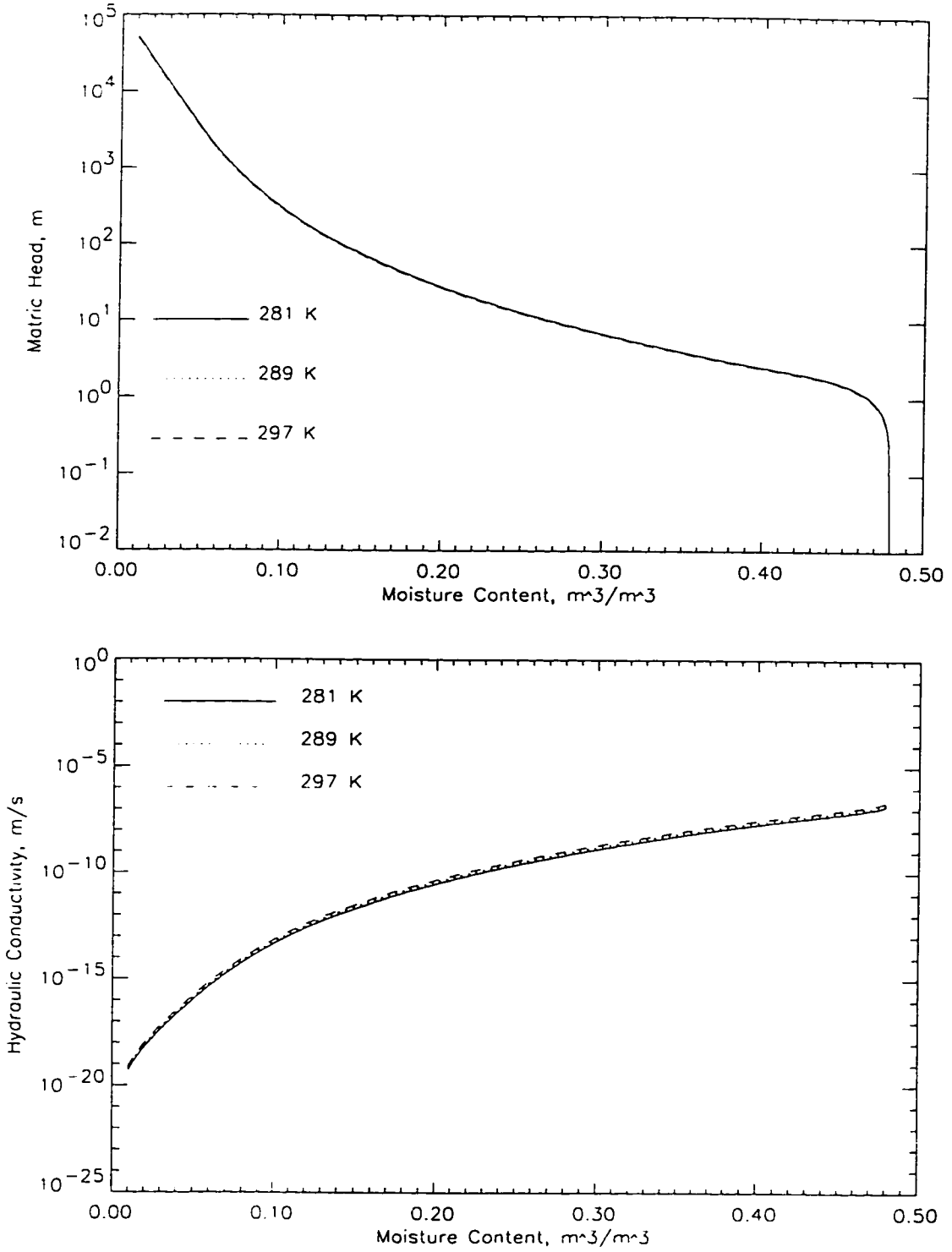

Figure 3.2: (a) Soil water retention for the Salkum silt loam. (b) Hydraulic conductivity as a function of moisture content.

and

$$I_{\mathrm{III}}(\theta_{\mathrm{l}}) = \frac{a_2}{\Psi_{\mathrm{d}}}\left[\exp\left(\frac{\theta_{\mathrm{l}}}{a_2\theta_{\mathrm{s}}}\right) - 1\right] \tag{3.28}$$

$$I_{\mathrm{II}}(\theta_{\mathrm{l}}) = I_3(\theta_j) + \frac{\eta}{\Psi_{\mathrm{o}}(\eta+1)}\left[\left(\frac{\theta_{\mathrm{l}}}{\theta_{\mathrm{s}}}\right)^{(\eta+1)/\eta} - \left(\frac{\theta_j}{\theta_{\mathrm{s}}}\right)^{(\eta+1)/\eta}\right] \tag{3.29}$$

$$I_{\mathrm{I}}(\theta_{\mathrm{l}}) = I_{\mathrm{II}}(\theta_i) + \frac{2a_1^{1/2}}{\Psi_{\mathrm{o}}}\left[\left(1 - \frac{\theta_i}{\theta_{\mathrm{s}}}\right)^{1/2} - \left(1 - \frac{\theta_{\mathrm{l}}}{\theta_{\mathrm{s}}}\right)^{1/2}\right] \tag{3.30}$$

in which $\theta_i = \theta_{\mathrm{l}}(\Psi_i)$ and $\theta_j = \theta_{\mathrm{l}}(\Psi_j)$ have been used. Subsequently, following Milly [77], one can get hydraulic conductivity:

$$K = K(\theta_{\mathrm{l}}, T) = K_0 K_{\mathrm{r}}(\theta_{\mathrm{l}})\frac{\vartheta(T_0)}{\vartheta(T)}, \tag{3.31}$$

where

- K_0 is the saturated hydraulic conductivity at a reference temperature T_0, and
- ϑ is the kinematic viscosity, kg/m-s.

Figure 3.2 (b) shows the hydraulic conductivity as a function of moisture for the silt loam. Equation (3.27) is used to estimate the hydraulic conductivity, but its performance has not been validated [102]. Therefore, estimates of the hydraulic conductivity are compared with those computed by Milly [77]. It appears that both models agree on the order of magnitude.

3.2.5 Liquid and Vapor Diffusivities

From Philip and de Vries [92] and de Vries [23], the moisture- and temperature-dependent liquid and vapor diffusivities can be expressed as

$$D_{\mathrm{T_l}} = K\partial\Psi/\partial T \tag{3.32}$$

$$D_{\mathrm{T_v}} = f D_{\mathrm{v}}\nu\beta h_{\mathrm{r}}\zeta/\rho_{\mathrm{l}} \tag{3.33}$$

$$D_{\theta_l} = K\partial\Psi/\partial\theta_l \tag{3.34}$$

$$D_{\theta_v} = \alpha\theta_a D_v \nu g \rho_v (\partial\Psi/\partial\theta_l)/\rho_l R_v T, \tag{3.35}$$

where

- $\partial\Psi/\partial T = (\Psi/\sigma)d\sigma/dT = \gamma\Psi$, where σ is the surface tension of water, J/m^2, and γ is the temperature coefficient of surface tension of water, K^{-1},
- f = porosity, S, for $\theta_l \leq \theta_{lk}$, $f = \theta_a + \theta_a\theta_l/(S - \theta_{lk})$ for $\theta_l > \theta_{lk}$ is a correction factor for the thermal vapor diffusivity, where θ_{lk} is the value of θ_l at which liquid continuity fails, m^3/m^3,
- $D_v = 4.42 \times 10^{-8} T^{2.3}/P$ is the molecular diffusion coefficient of water vapor in air, m^2/s, where P is the total gas pressure, Pa,
- $\nu = P/(P - p)$ is the mass flow factor, where p is the partial pressure of water vapor, Pa,
- $\alpha = 0.67$ is the tortuosity factor for diffusion of gases in soils,
- $\beta = \frac{d\rho_0}{dT}$, kg/m^3-K, where ρ_0 is the density of saturated water vapor, kg/m^3,
- $\zeta = (\nabla T)_a/\nabla T$, K/m, where ∇T is the average temperature gradient in the porous medium, K/m, and $(\nabla T)_a$ is the average temperature gradient in the air-filled pores, K/m,
- g is the acceleration due to gravity, m/s^2, and
- R_v is the gas constant of water vapor, J/kg-K.

Equations (3.32) to (3.35) are used to compute the four diffusivities: D_{T_l}, D_{T_v}, D_{θ_l}, and D_{θ_v} with the following modifications

$$D_v = 0.229(T/273.15)^{1.75} \text{ [61, 84]} \tag{3.36}$$

$$\alpha = (S - \theta_l)^{2/3} \text{ [66, 78, 84]} \tag{3.37}$$

$$\rho_0 = 10^{-3} e^{19.819 - 4975.9/T} \text{ [61, 84]} \tag{3.38}$$

Liquid and vapor diffusivities are shown in Figure 3.3. Since there are no experimental data that can be used to validate the predictions of liquid and vapor diffusivities, computed results are compared with those obtained by Milly [77]. It is found that estimates from the two models agree on the order of magnitude.

3.2.6 Simulation

The 1dHu model is run for a 60-day period starting from 06/22 for both water transport and no water transport in soil at a northern latitude of 43.5 degrees (that of Sioux Falls, South Dakota). The initial temperature and moisture profiles of the soil are results from the annual thermal model [70] in which soil moisture was fixed at 38 % for all layers.

Figure 3.4 (a) shows the surface moisture content over the 60-day period for both the water transport and the no water transport cases. For the no water transport case, the surface moisture content is simply constant. For the water transport case, surface moisture content exhibits a small diurnal oscillation with a quickly decreasing average. Diurnal peaks appear during nighttime due to condensation, and valleys appear during daytime due to evaporation. The difference in surface moisture content between the water transport and the no water transport cases approaches 19 % at 60 days.

Figure 3.4 (b) shows constant-moisture curves as a function of depth and day number for the 60-day period for the water transport case. We notice two major characteristics. First, near-surface soils are interacting with the air, while deep soils

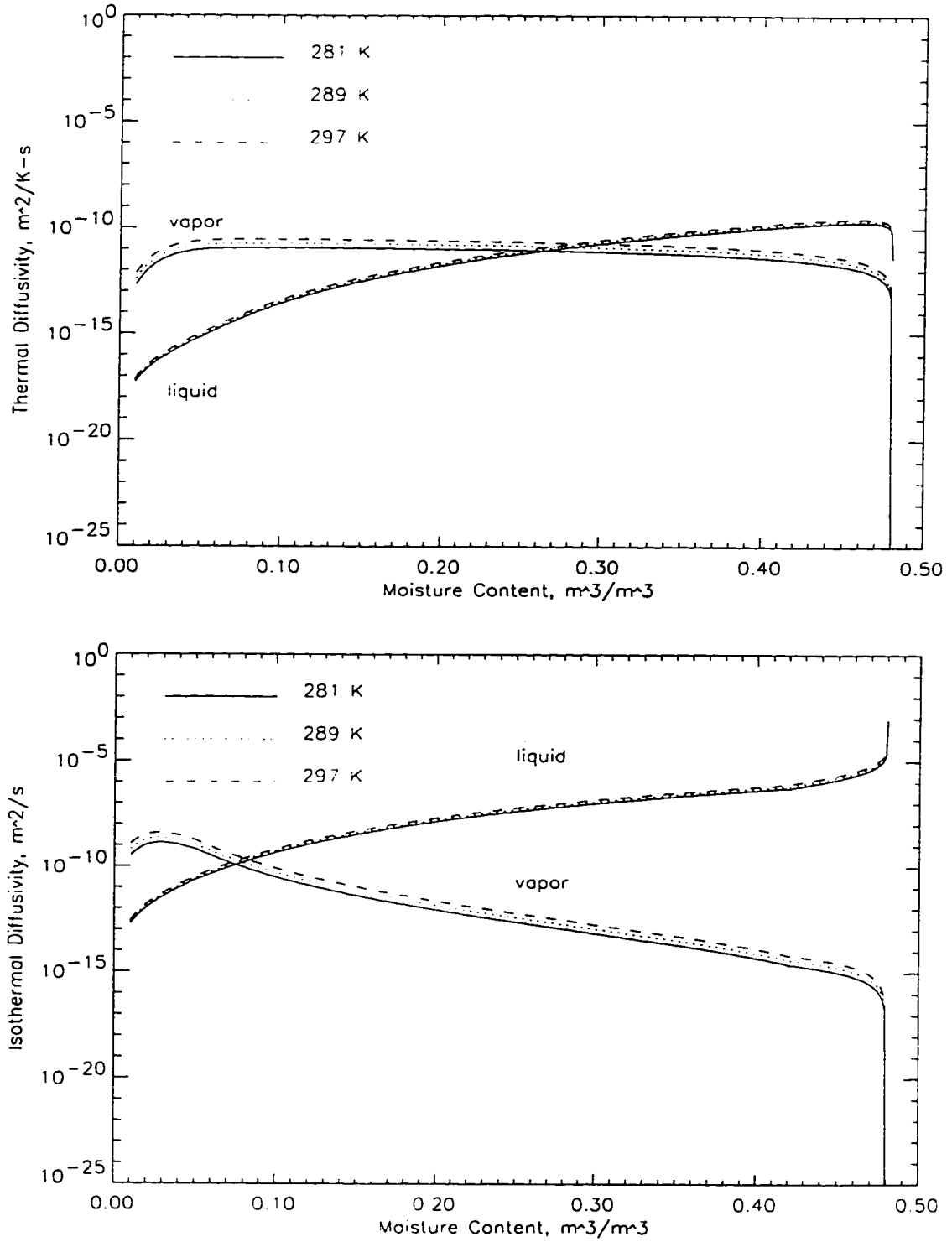

Figure 3.3: (a) Thermal liquid and vapor diffusivities. (b) Isothermal liquid and vapor diffusivities.

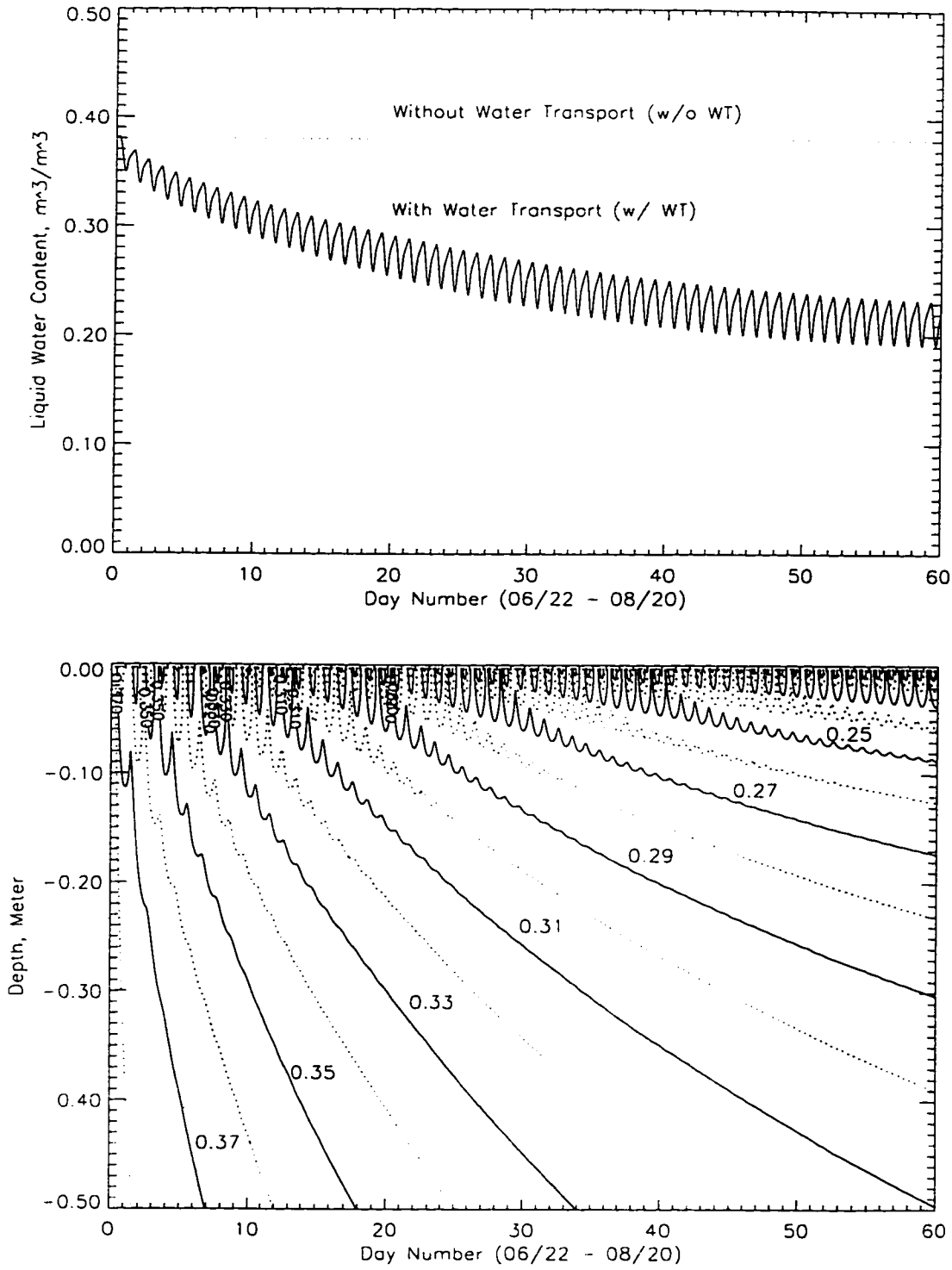

Figure 3.4: (a) Soil moisture content at the surface for the water transport and no water transport cases. (b) Soil moisture profile for the water transport case.

are not. This is clearly observable since downward-propagating constant-moisture curves exhibit a diurnal oscillation that damps out with depth. Second, there is an expected long term moisture loss at the surface and a commensurate net upward movement of water, i.e., evaporation dominates over condensation in the latent heat exchange at the land-air interface.

Surface temperatures for the water transport case are shown in Figure 3.5 (a). Notable characteristics include (1) a strong diurnal oscillation with a slowly increasing average for the first 40 days, and a slowly decreasing average after that; and (2) the day-to-night temperature difference increases with day number, from about 16 Kelvins at day 1 (06/22) to about 20 Kelvins at day 60 (08/20) because the thermal inertia of the soil decreases as the surface soils dry.

The differences in surface temperatures between the water transport and the no water transport cases are shown in Figure 3.5 (b). They exhibit a small diurnal oscillation with a slowly increasing average and amplitude. The maximum difference is only 4.4 Kelvins during daytime at day 60. The difference is small because thermal inertia is the integrated response of the soil over a diurnal cycle which penetrates beyond the dry surface soils.

Figure 3.6 shows the soil temperature profile on day 1 for the water transport case. It shows that (1) isotherms are created after sunrise and start to merge some time after peak insolation; (2) temperature gradients in the first few centimeters are much larger during the day than during the night; and (3) diurnal thermal pulses penetrate approximately 50 centimeters. We present only 06/22 isotherms because all diurnal isotherm patterns for the 60-day period were similar.

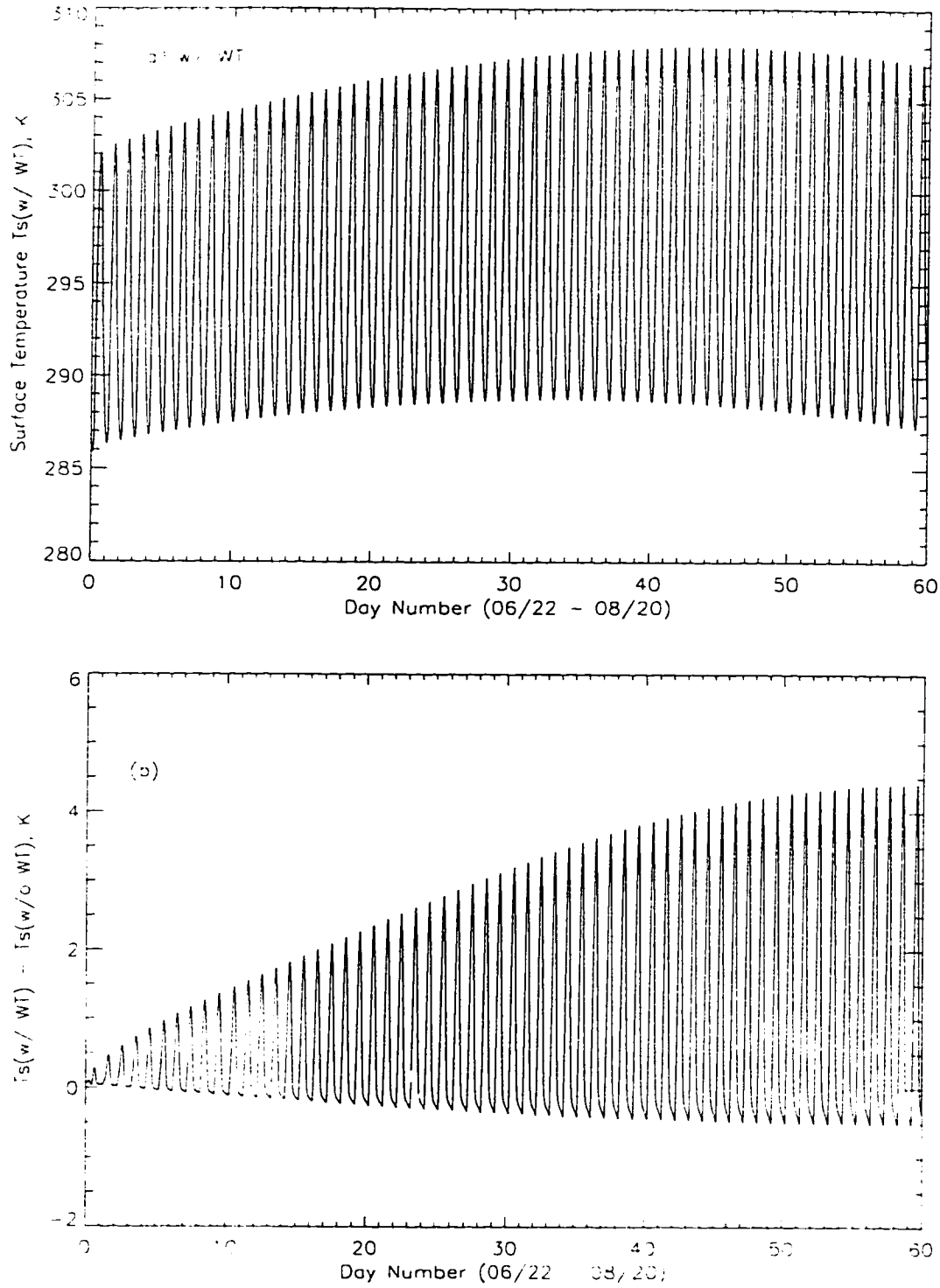

Figure 3.5: (a) Surface temperature for the water transport case. (b) Differences in surface temperatures between the water transport and no water transport cases.

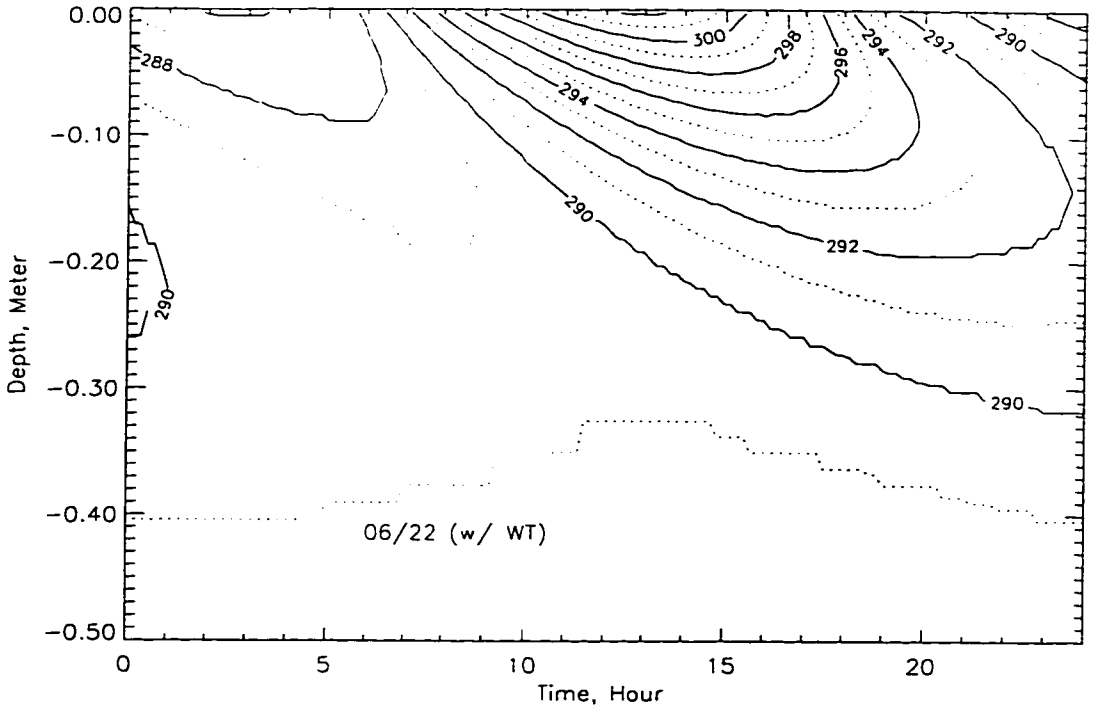

Figure 3.6: Soil temperature profile on 06/22 for the water transport case.

3.3 Remote Measure of Soil Moisture

3.3.1 Soil Dielectric Properties

Water content and temperature dominate the dielectric properties of soil. Water content is a key parameter because of a significant contrast in permittivity between water and soil constituents. Temperature is important because it governs the relaxation frequency, f_0, in the Debye relaxation equation for the relative permittivity of free water:

$$\epsilon_w = \epsilon_{w\infty} + \frac{\epsilon_{w0} - \epsilon_{w\infty}}{1 + jf/f_0}, \tag{3.39}$$

where

- ϵ_{w0} is the static dielectric constant of pure water,
- $\epsilon_{w\infty}$ is the high-frequency limit of ϵ_w, and

- f is the frequency, Hz.

For example, the relaxation frequency is about 14.5 GHz at 287 Kelvins and 23.5 GHz at 306 Kelvins [119].

The relative permittivity of the soil-water system can be estimated through use of a four-component mixture model of soil solids, air, free water, and bound water [70]. Figure 3.7 shows the complex relative permittivities and emissivities of the soil-water system for the water transport case. Estimates of both relative permittivity and emissivity are based upon the temperature and moisture content of the first soil layer. The magnitudes of both real and imaginary parts of the complex relative permittivity exhibit a diurnal oscillation with a decreasing average (Figure 3.7 (a)) that correlates with soil moisture in the uppermost soil layer. These averages also decrease with increasing microwave frequency.

The corresponding emissivities of soil based upon a quasi-specular interface exhibit a diurnal oscillation with a slowly increasing average (Figure 3.7 (b)). Their increase over the 60-day period for 19 and 37 GHz horizontal polarization is about 0.1, but is less for vertical polarization and for both polarizations at 85 GHz.

3.3.2 Soil Radiobrightnesses

The radiobrightnesses of bare, wet soil is

$$T_{\mathrm{b}}(t) = e \cdot T_{\mathrm{eff}}(t). \tag{3.40}$$

where e is the emissivity of the soil. The first order approximation to $T_{\mathrm{eff}}(t)$ is

$$T_{\mathrm{eff}}(t) = T_{\mathrm{g}}(0,t) + \frac{1}{\kappa_{\mathrm{e}} \sec\theta_t} \cdot \left(\frac{\partial T_{\mathrm{g}}(z,t)}{\partial z}\right)_{z=0}, \tag{3.41}$$

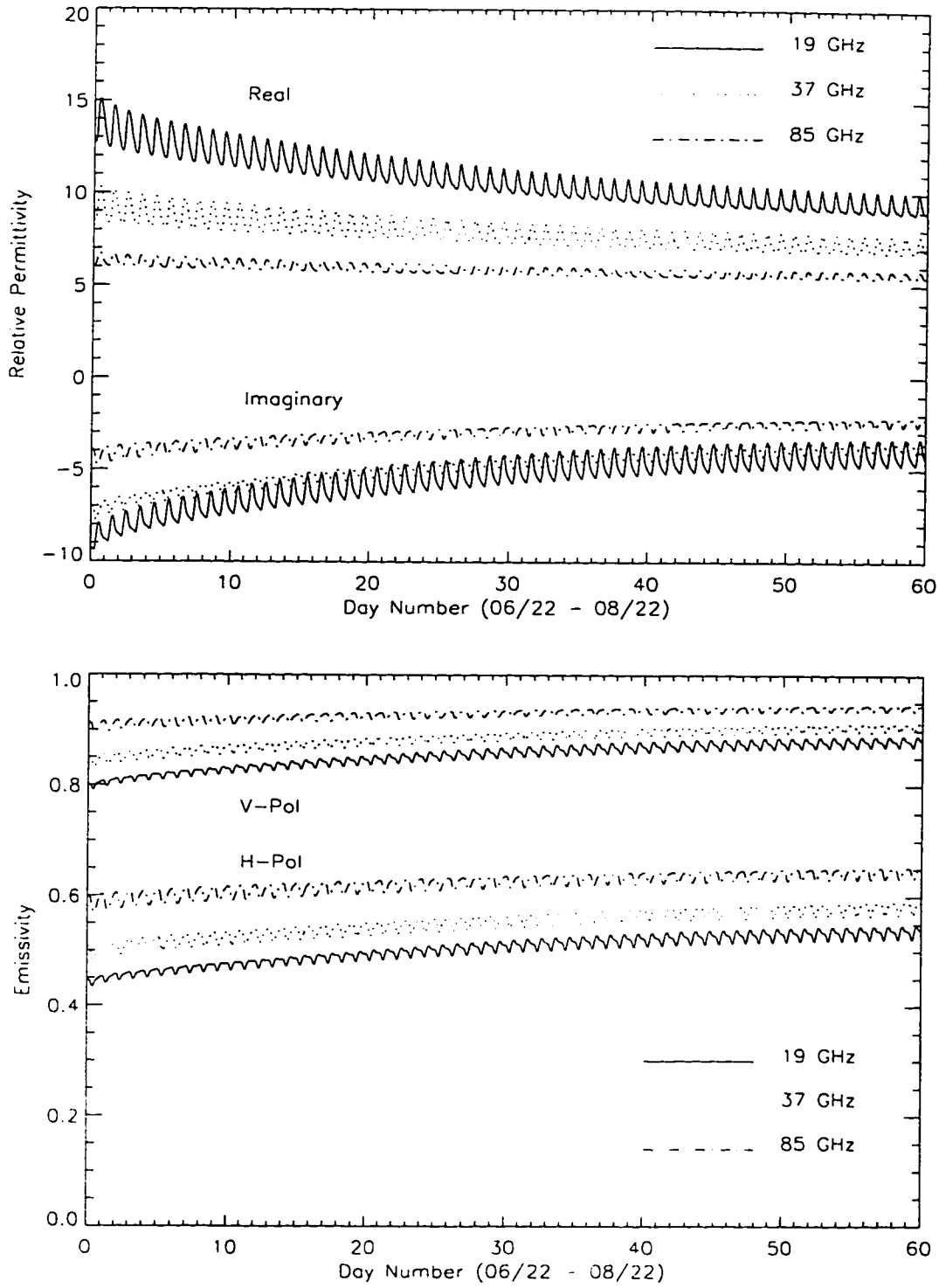

Figure 3.7: (a) Complex relative permittivities of soil at the surface conditions of the water transport case. (b) Emissivities associated with (a).

where κ_e is extinction of the soil and θ_t is a transmission angle. As shown in [70], the diurnal extremes of the first-order terms over an annual cycle are on the order of $\pm$0.3 Kelvins at 19 GHz for 17 % moist soil and decrease with increasing frequency and water content.

Figure 3.8 (a) shows 60-day radiobrightness signatures for the water transport case with 19 GHz horizontal polarization. The signatures are nearly linear with temperature except for a small, second-order effect caused by emissivity's dependence upon temperature. The change in diurnal average over the 60-day period is about 40 Kelvins for 19 GHz horizontal polarization, about 34 Kelvins for 37 GHz horizontal polarization, and about 26 Kelvins for 85 GHz horizontal polarization. Table 3.3.2 shows the maximum change in diurnal average radiobrightness over the 60-day simulation for both water transport and no water transport cases at 19, 37 and 85 GHz horizontal polarization. Radiobrightness at a fixed time in the diurnal cycle increases with day number because of a decrease in soil moisture. Similarly, daytime increases in maximum radiobrightness are also a response to decreases in liquid water content.

The largest variations in radiobrightness between 2 p.m. and the following 2 a.m. within the 60-day simulation are shown in Table 3.3.2 for both water transport and no water transport cases at 19, 37 and 85 GHz horizontal polarization. The 37 and 85 GHz results are not shown because they are similar to, but smaller in amplitude than, the 19 GHz results. Results for vertical polarization are not shown for the same reason.

The 60-day radiobrightness signatures for 19 GHz horizontal polarization for the no water transport case are shown in Figure 3.8 (b). The change in diurnal average radiobrightness over the 60-day period is within 3 Kelvins — much smaller than for the water transport case. The day-to-night variations in 19 GHz horizontal radiobright-

Changes (K)	19 GHz	37 GHz	85 GHz
60-day w/ WT	39.8	33.9	25.9
60-day w/o WT	2.3	2.5	2.1

Table 3.1: Change in the diurnal average radiobrightness over the 60-day simulation for both water transport and no water transport cases at 19, 37 and 85 GHz horizontal polarization.

Variations (K)	19 GHz	37 GHz	85 GHz
1-day w/ WT	12.7	8.8	8.8
1-day w/o WT	2.3	-1.6	-1.6

Table 3.2: Diurnal variations in radiobrightness between 2 p.m. and 2 a.m. for both water transport and no water transport cases at 19, 37 and 85 GHz horizontal polarization.

ness are weakly positive over the simulation period, while the equivalent variations for both 37 and 85 GHz are weakly negative. The contrast is caused by differing soil dielectric behavior with temperature at the three frequencies.

3.3.3 RTI Measure of Soil Moisture

Soil moisture is tied to radiometric signatures through its dominant influence upon diurnal soil temperatures and upon the dielectric properties of soil. Idso et al [52] addressed the importance of soil moisture in determining the visible reflectance of bare soil. Heilman and Moore [47, 48] conducted a thermal infrared experiment to discriminate among various rock and soil types based upon the differences in the near-surface storage of moisture.

England et al [31] proposed a Radiobrightness Thermal Inertia (RTI) scheme for estimates of soil moisture, and concluded that, of the SSM/I radiometer frequencies and polarizations, the 37.0 and 85.5 GHz, H-Polarized channels appear to be best suited to RTI. The RTI scheme was based on a knowledge of the relationship between

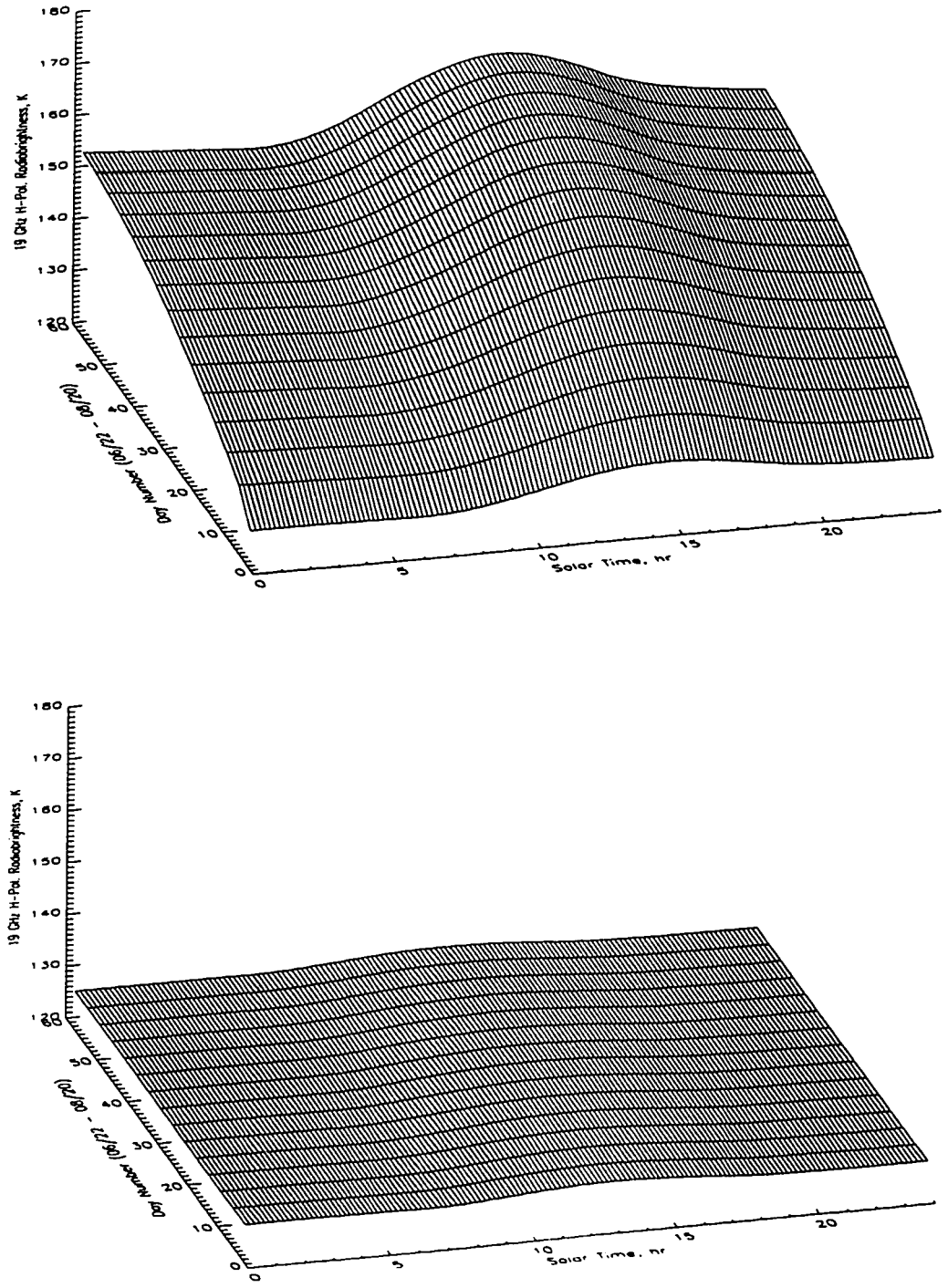

Figure 3.8: Radiobrightness signatures for 19 GHz horizontal polarization (a) for the water transport case, and (b) for the no water transport case.

the change in day-night radiobrightness and the soil moisture content derived from the predictions of the Michigan Cold Region Radiobrightness (MCRR/diurnal) model of England [29]. The major features of the scheme were (1) soils with higher water content have a smaller change in day-night radiobrightness because of increased thermal inertia and decreased emissivity; (2) potential masking contributions to radiobrightness from sparse vegetation vary minimally in a diurnal cycle and so their contribution does not greatly change the day-night difference; and (3) sun-synchronous satellites overfly a region at nearly 12 hour intervals. Unlike the 1dHu model, the MCRR/diurnal model ignored the dependences of thermal and moisture profiles upon latent heat transfer, historical weather forcing at the land-air interface, and soil water movements.

To re-examine the feasibility of the RTI measure of soil moisture over a wide range of moisture contents, we ran the 1dHu model for the cases with drier initial moisture contents of 24 % and 17 % for the same 60-day period as we did for the 38 % case. Figure 3.9 shows the surface soil moisture contents and temperatures at 2 a.m., 6 a.m., 2 p.m., and 6 p.m. for the 38 %, 24 %, and 17 % cases (all with vertical water movement in soil). We see that (1) soil moisture contents decrease monotonically with day number for the three dry-down simulations; (2) soil moisture decreases rapidly in the beginning few days of the 60-day period, but slowly in the rest of the same period; and (3) soil moisture contents never go below 13 % because evaporation ceases at the wilting point of 13 %. Figure 3.9 (b) shows that the surface temperatures increase with time for about the first 40 days and decrease with time for the rest of the simulation period. The temperature differences between 2 p.m. and 2 a.m. are largest for the driest soil — about 21 Kelvins over the 60-day period for the 17 % case, about 20 Kelvins for the 24 % case, and about 17 Kelvins for the

38 % case.

Figure 3.10 concerns the radiobrightness differences between 2 p.m. and 2 a.m., and between 6 p.m. and 6 a.m. for 19, 37, and 85 GHz horizontal and vertical polarization. The 60-day dry-down brightness differences are shown for the 38 %, 24 %, and 17 % initial moisture contents. The horizontal axis represents the averages of soil moisture contents between 2 p.m. and 2 a.m., and between 6 p.m. and 6 a.m. Note that the radiobrightness differences generally increase with decreased moisture content for the dry-down simulations in the 38 % and 24 % cases. Each of these differences decrease at the end of their simulation period where the decrease in soil moisture with time is small and diurnal temperature extremes are diminished as fall approaches. Only the final decrease is evident in the 17 % case where there is little free water available. If we connect the three ending points of the dry-down curve, and the three starting points of the same curve, respectively, there would be the six strips in Figure 3.10 (a). Each strip represents the area that radiobrightness differences may appear during a dry-down process. The slope of the strips is an estimate of the sensitivity of the RTI method to soil moisture, while the width of the strips in the vertical direction is an indicator of uncertainty caused by time since the last infiltration. Figure 3.10 (a) demonstrates that the three frequencies have about the same sensitivities to soil moisture in those ideal cases of quasi-specular interfaces. Figure 3.10 (a) and (b) show that the RTI scheme correlates with soil moisture for the 2 p.m.-2.a.m. case, but is insensitive to soil moisture for the 6 p.m.-6 a.m. case.

The magnitudes of RTI from the current model are smaller than those from the England et at [31] by approximately 6 Kelvins for horizontal polarization, and by about 20 Kelvins for vertical polarization. Such significant discrepancies between the two models demonstrate the importance of including latent heat transfer and historic

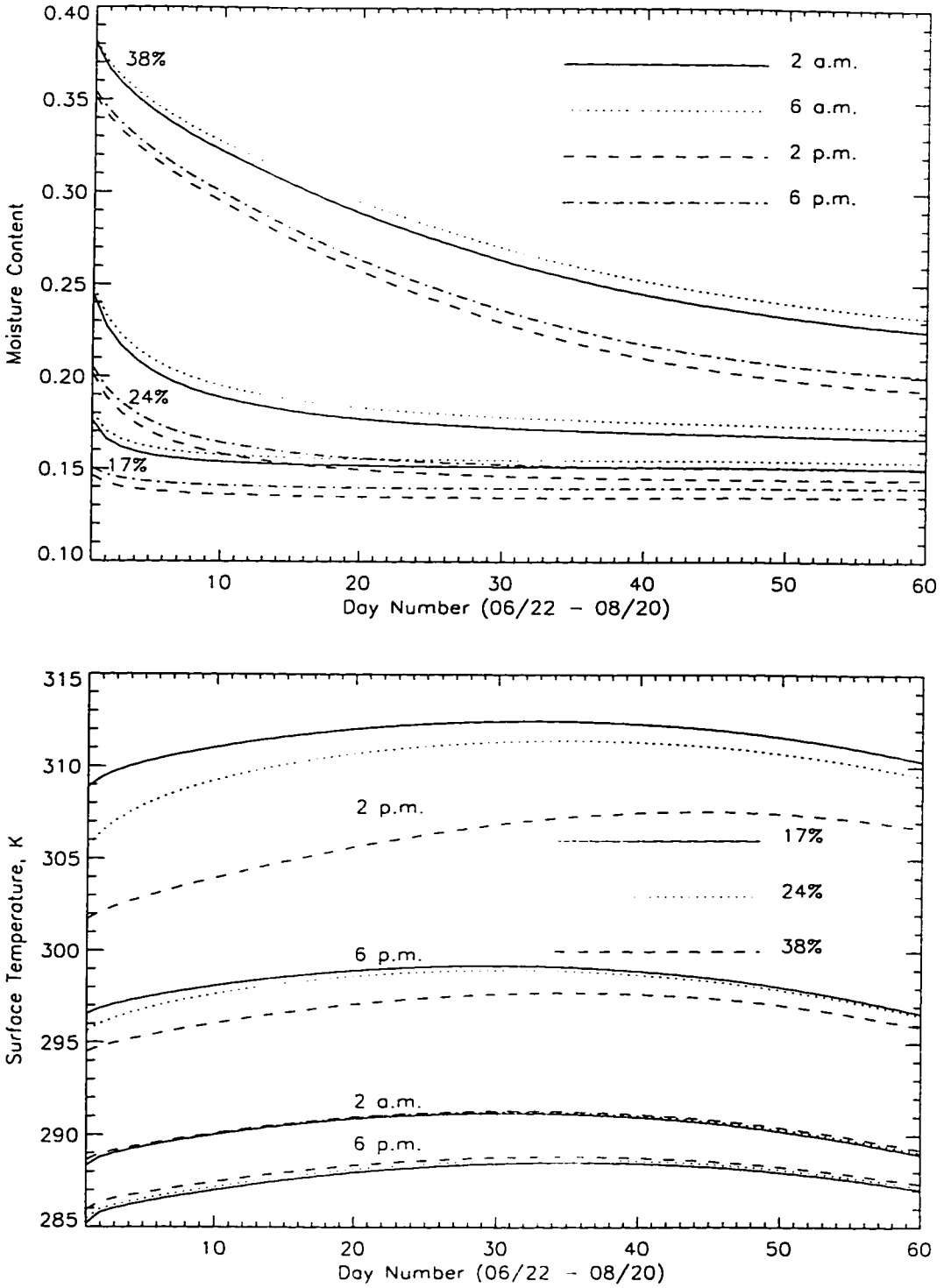

Figure 3.9: (a) Soil moisture content at the surface at four times: 2 a.m., 6 a.m., 2 p.m., and 6 p.m. for the 38 %, 24 %, and 17 % cases (all with water movement in the soil). (b) Surface temperature at four times: 2 a.m., 6 a.m., 2 p.m., and 6 p.m. for the 38 %, 24 %, and 17 % cases.

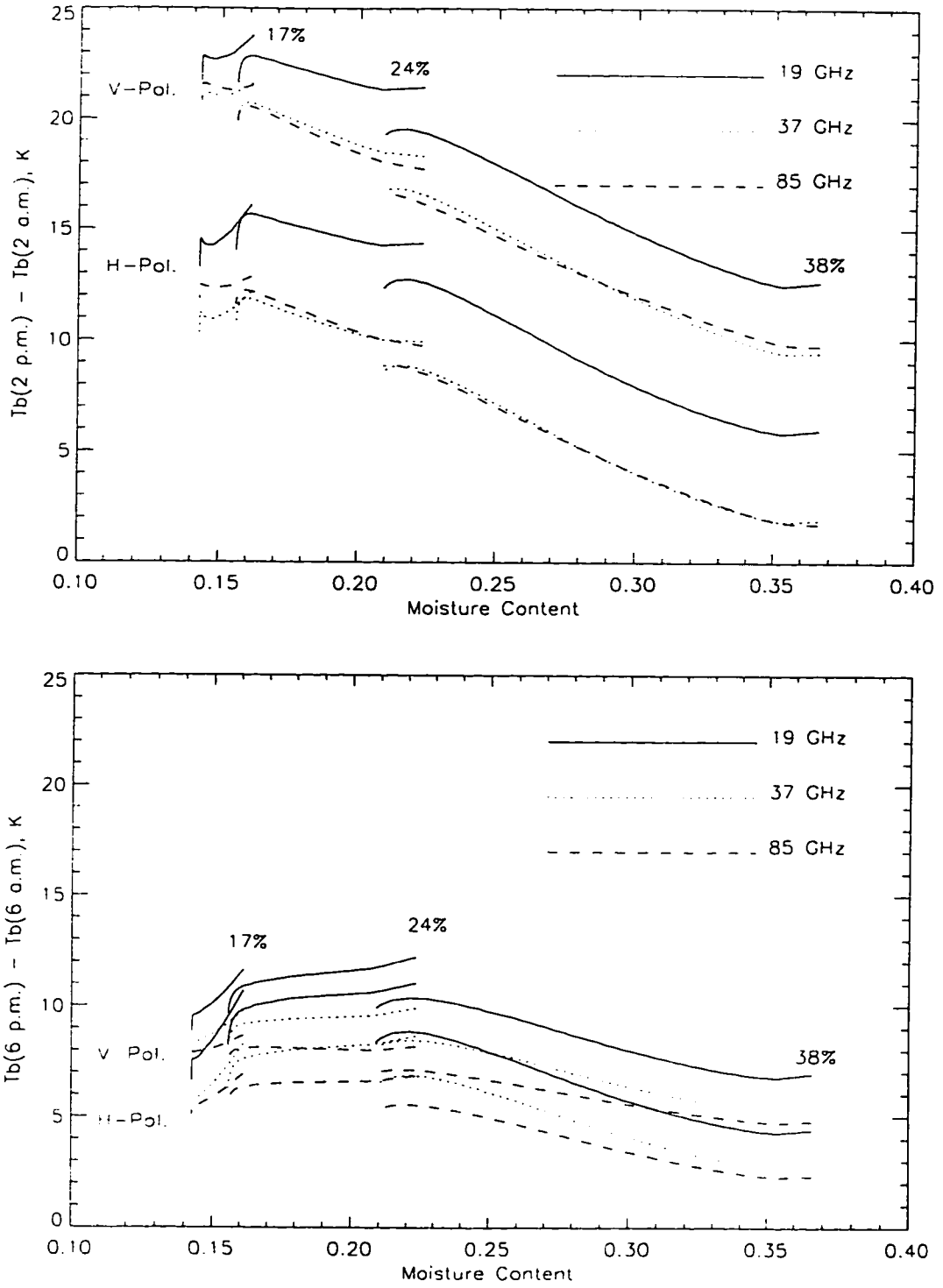

Figure 3.10: (a) Radiobrightness differences between 2 p.m. and 2 a.m. for the 38 %, 24 %, and 17 % cases. (b) Radiobrightness differences between 6 p.m. and 6 a.m. for the 38 %, 24 %, and 17 % cases.

weather forcing at the land-air interface, and of coupling water movement with temperature gradients in the thermal model. This diminished sensitivity casts the utility of the RTI method in some doubt and, because RTI is more sensitive than a thermal infrared-based measure of thermal inertia, it also explains the difficulty of deriving soil moisture from a TIR-based model.

3.4 DISCUSSION

We have presented a 1-dimensional hydrology/radiobrightness (1dHu/R) model for bare, unfrozen, moist soils. The 1dHu model includes coupled thermal and moisture transport within the soil and at the land-air interface, and soil thermal properties are realistically treated as functions of temperature and moisture. The radiobrightness model is based upon the temperature and moisture content of a quasi-specular upper soil layer. The physical fidelity of the 1dHu/R model affords some confidence in its predictions. Certainly, the 1dHu/R model is superior to our earlier model, the MCRR model, which successfully guided our earlier investigations of the radiobrightness of freezing and thawing soils.

The most significant prediction of the 60-day dry-down simulation is that SSM/I radiobrightnesses are sensitive to the dry-down process. The change for the 19 GHz horizontal polarization case was nearly 40 Kelvins over the 60-day period. This large dynamic range suggests that radiobrightness observations can be used to improve a model state estimate — at least for this simple case — if the precipitation history is known.

While RTI is sensitive to soil moisture, the sensitivity may not be significant enough for the practical use in field inversions of soil moisture for bare or sparsely-

vegetated lands. As vegetation cover increases, the interpretation of radiobrightness will become more complex. Vegetation that exceeds ~ 2 kg/m^2 column density appears nearly black at the SSM/I frequencies [32] so that enhancements in emissivity with water content are lost. Furthermore, vegetation actively maintains wetness levels by reducing transpiration as soils dry. Reduced transpiration will result in greater day-night differences in canopy temperature and radiobrightness, but the signature is sufficiently unique that its interpretation in terms of soil moisture may be difficult. Lower, more penetrating frequencies, like L-band, would greatly ease the interpretation where there is significant vegetation.

We recognize the need to validate the 1dHu/R model experimentally. Our group will conduct a field experiment on the prairie grassland near Sioux Falls, South Dakota, during the summer of 1996. Field data will be taken on both grassland and artificially bare soil at half-hour intervals throughout the growing season. Measurements will include horizontally and vertically polarized radiobrightnesses at SSM/I frequencies (only one polarization for 85 GHz), soil temperatures, soil and canopy moisture, soil heat flux, 10 m wind speed and direction, air temperature, relative humidity, downwelling and upwelling shortwave radiation, downwelling longwave radiation, precipitation, thermal infrared canopy temperature, and Bowen ratio.

CHAPTER 4

THE 1dH/R MODEL FOR BARE, FREEZING SOILS — A 1dHb/R MODEL

Abstract — Phase change of moisture is an important sink and source of energy and moisture within soils, and significant influence upon soil temperature and moisture profiles. These profiles play a crucial role in governing energy and moisture fluxes between bare soils and the atmosphere. They also codetermine radiobrightness so that the difference between modeled and observed radiobrightness becomes a measure of error in a model's estimate of temperature or moisture.

In this paper, we present a physically-based, coupled heat and moisture transport, one-dimensional Hydrology/Radiobrightness (1dH/R) model for bare, freezing and thawing moist soils that are subject to insolation, radiant heating and cooling, and sensible and latent heat exchanges with the atmosphere. We use this model to examine thermal, hydrologic, and SSM/I radiobrightness signatures for a three-month dry-down simulation in the fall and winter of the northern U.S. Great Plains as part of an investigation of the effects of coupling heat and moisture transport. Given a typical initial moisture content of 38%, we find that coupled transport results in a reduction of ice in the surface soil by 21 %. The range of

diurnal variations in temperature are not significantly affected by coupled transport. Diurnal variations in the 19 GHz, H-polarized radiobrightness can be greater in the coupled transport case by 37 Kelvins. Total diurnal variation can exceed 57 Kelvins during periods of diurnal freezing and thawing.

4.1 INTRODUCTION

Land surface processes are strongly coupled to the dynamics and thermodynamics of the atmosphere through the exchange of moisture, energy, and momentum [100, 20, 73, 99, 81, 110]. Surface temperature and moisture content/state are key parameters in partitioning land-atmosphere energy exchanges into radiant, sensible and latent heat processes, and they also govern the thermal and microwave brightness if soils are bare or sparsely vegetated. For example, satellite radiometry has been used to infer surface temperature [112] and moisture [19, 87, 88, 3], and to estimate surface heat fluxes [14, 111, 51, 65, 62, 41].

Land-Surface Process (LSP) models exchange moisture, energy, and momentum with atmospheric models to simulate the land-atmosphere interactions. The LSP models use the parameter soil wetness or soil water to denote the moisture in soil and vegetation that is available to the atmosphere through evaporation or transpiration. Errors in the magnitude of this parameter can cascade through consequent errors in the moisture and energy fluxes to produce significant errors in the atmospheric models [100, 20, 99].

We would like to use radiobrightness's sensitivity to surface moisture to obtain an estimate of the moisture content of surface soils, and to relate this soil moisture to an LSP model's soil wetness, that is, to assimilate radiobrightness to improve

the LSP estimate of soil wetness. This is not easily done. Current LSP models achieve computational efficiency by employing greatly simplified, or parameterized, caricatures of physical processes with the result that soil wetness may not be a true physical quantity that is measurable. Even if it is, current LSP models do not relate near-surface moisture to soil wetness.

A one-dimensional Hydrology (1dH) model can be substituted for an LSP model at the cost of computational efficiency. The stored water parameter in the hydrology model is the functional equivalent of soil wetness, but stored water is a measurable quantity. The hydrology model provides the linkage between near-surface soil moisture and stored water.

Mahfouf [74] used a 1dH model to estimate stored water from the history of screen-level temperature and humidity. Bouttier et al [8], using a sequential assimilation scheme, substituted their weather driven 1dH model for the LSP component of a mesoscale model [9]. Similarly, it should be possible to improve, retrospectively, an estimate of stored water by forcing a 1dH model with data from a model atmosphere, and refining the estimate through assimilation of radiobrightness.

We designate the combination of an hydrology model and a radiobrightness model as our 1dH/R model. Our first 1dH/R model with coupled heat and moisture transport was for bare, unfrozen soil (1dHbu/R) [71]. Through this model we demonstrated that water movement in unfrozen soils strongly influences radiobrightness.

Freezing soils present a very different problem (e.g., [38]). Modeling heat and moisture transfer in partially frozen soils differs from the unfrozen case in several ways: 1) liquid water and ice co-exist over a wide range of temperatures below the freezing depression point (FDP) [127, 4, 36, 116, 90, 12]; 2) liquid water content becomes the iterative solution of highly nonlinear, coupled temperature-suction and water-

retention equations; 3) temperature-moisture content curves for repeatedly freezing and thawing soils exhibit hysteresis [64, 50]; and 4) ice lensing and frost heaving occur as liquid water is drawn to the freezing front [5, 42, 16, 63]. One or more of these processes are frequently ignored to make the problem more tractable. For example, Harlan [45] ignored hysteresis, frost heaving, and the effects of the vapor phase on both heat and moisture transport in his study of coupled heat and moisture transport in partially frozen, unsaturated soils. The Harlan model was adopted by Guymon and Luthin [43], Taylor and Luthin [113], Jame and Norum [57], and Pikul et al [93]. Later, Flerchinger and Saxton included the effects of the vapor phase on heat and moisture transport [35], but used the simple water-retention model of Brooks and Corey [11].

Modern hydrologic models for porous, unsaturated soils are based upon the theory of heat and moisture transport by Philip and de Vries [92] and de Vries [23]. The Philip and de Vries theory includes heat and moisture transport due to temperature gradients, liquid water concentration gradients, pressure gradients, and gravity.

As ice content increases in freezing soils, intuition would suggest that the transport coefficients should decrease. Konrad and Duquennoi [63] recently proposed transport coefficients that are proportional to a power of the ratio between liquid water content and void space. Below FDP, liquid water is essentially a function of temperature alone [127]. Unless void space is interpreted as pore space less ice volume, allowing temperature to determine liquid water content means that the Konrad and Duquennoi transport coefficients are also determined even though ice content would vary with total water content. We avoid the ambiguity by reverting to the older theory of Taylor and Luthin [113] where transport coefficients unambiguously decrease with increasing ice content at a fixed temperature.

Our objective is to examine the influence of water transport upon soil temperature, moisture, and radiobrightness of bare soil during a 90-day dry-down simulation in the fall and winter at northern latitudes. For these simulations, we have intentionally ignored only the hysteresis in the freeze/thaw cycle.

4.2 HYDROLOGY MODEL

The principal differences between our 1dH model for non-freezing soils and that for freezing soils are the additional mass and energy terms associated with ice in the conservation equations, the ice-dependent reduction factors for the transport coefficients, a temperature-suction relation that is used iteratively to estimate liquid water content, and a modified numerical scheme.

4.2.1 Governing Equations and Associated Terms

Ice represents a lower energy state than liquid water so that the moisture and heat contents per unit volume (Equations (1) and (2) in [71]) become

$$X_{\mathrm{m}} = \rho_{\mathrm{l}}\theta_{\mathrm{l}} + \rho_{\mathrm{v}}\theta_{\mathrm{a}} + \rho_{\mathrm{i}}\theta_{\mathrm{i}} \tag{4.1}$$

$$\begin{aligned} X_{\mathrm{h}} = {} & (C_{\mathrm{d}} + c_{\mathrm{l}}\rho_{\mathrm{l}}\theta_{\mathrm{l}} + c_{\mathrm{p}}\rho_{\mathrm{v}}\theta_{\mathrm{a}} + c_{\mathrm{i}}\rho_{\mathrm{i}}\theta_{\mathrm{i}})(T - T_0) \\ & + L_{\mathrm{v}_0}\rho_{\mathrm{v}}\theta_{\mathrm{a}} - L_{\mathrm{f}_0}\rho_{\mathrm{i}}\theta_{\mathrm{i}} - \rho_{\mathrm{l}}\int_0^{\theta_{\mathrm{l}}} W d\theta, \end{aligned} \tag{4.2}$$

where

- X_{m} is the total mass of moisture per unit volume, kg/m^3,
- X_{h} is the total heat content per unit volume, J/m^3,
- ρ_{l} is the density of liquid water, kg/m^3,
- θ_{l} is the volumetric liquid water content, m^3/m^3,

- ρ_v is the density of water vapor, kg/m^3,
- θ_a is the volumetric air content, m^3/m^3,
- ρ_i is the density of ice, kg/m^3,
- θ_i is the volumetric ice content, m^3/m^3,
- C_d is the volumetric heat capacity of a dry porous medium, J/m^3-K ,
- c_l is the specific heat of liquid water at constant pressure, J/kg-K,
- c_p is the specific heat of water vapor at constant pressure, J/kg-K,
- c_i is the specific heat of ice at constant pressure, J/kg-K,
- T is the temperature, K,
- T_0 is the reference temperature, K,
- L_{v_0} is the latent heat of vaporization at the reference temperature, J/kg, and
- L_{f_0} is the latent heat of fusion at the reference temperature, J/kg, and
- W is the differential heat of wetting [23], J/kg.

The governing equations of heat and moisture transport become

$$\begin{aligned} &\left[1 + \frac{(S-\theta_l-\theta_i)\rho_0}{\rho_l}\frac{\partial h_r}{\partial \theta_l} - \frac{\rho_v}{\rho_l}\right]\frac{\partial \theta_l}{\partial t} \\ &+ \frac{(S-\theta_l-\theta_i)}{\rho_l}\left(h_r\frac{\partial \rho_0}{\partial T} + \rho_0\frac{\partial h_r}{\partial T}\right)\frac{\partial T}{\partial t} \\ &+ (\rho_i - \rho_v)\frac{\partial \theta_i}{\partial t} \\ = \quad &\nabla\cdot\left(D_T\nabla T + D_\theta\nabla\theta_l + K\hat{k}\right) \end{aligned} \tag{4.3}$$

$$
\begin{aligned}
&\left[L_v(S-\theta_l-\theta_i)\rho_0\frac{\partial h_r}{\partial \theta_l}-L_v\rho_v-\rho_l W\right]\frac{\partial \theta_l}{\partial t}\\
&+\left[C+L_v(S-\theta_l-\theta_i)\left(h_r\frac{\partial \rho_0}{\partial T}+\rho_0\frac{\partial h_r}{\partial T}\right)\right]\frac{\partial T}{\partial t}\\
&+(L_f\rho_i-L_v\rho_v)\frac{\partial \theta_i}{\partial t}\\
=\;&\nabla\cdot[(\lambda_*+L_v\rho_l D_{T_v})\nabla T]+L_v\rho_l\nabla\cdot(D_{\theta_l}\nabla\theta_l)\\
&+\rho_l[(c_p D_{\theta_v}+c_l D_{\theta_l})\nabla\theta_l\\
&+(c_p D_{T_v}+c_l D_{T_l})\nabla T+c_p K\hat{k}]\cdot\nabla T, \qquad (4.4)
\end{aligned}
$$

where

- S is the porosity,
- ρ_0 is the density of saturated water vapor, kg/m^3,
- h_r is the relative humidity,
- $D_T = D_{T_l} + D_{T_v}$ is the thermal moisture diffusivity, m^2/K-s,
- $D_\theta = D_{\theta_l} + D_{\theta_v}$ is the isothermal moisture diffusivity, m^2/s,
- D_{T_l} is the thermal liquid diffusivity,
- D_{T_v} is the thermal vapor diffusivity,
- D_{θ_l} is the isothermal liquid diffusivity,
- D_{θ_v} is the isothermal vapor diffusivity,
- K is the hydraulic conductivity, m/s,
- $\hat{k}$ is a vertical unit vector,
- $L_v = L_{v_0} + (c_l + c_p)(T - T_0)$,

- $L_f = L_{f_0} - (c_l - c_i)(T - T_0)$, and
- λ_* is the thermal conductivity of a moist porous medium, J/m-K-s.

The transport coefficients of heat and moisture for the partially frozen soil are obtained by dividing their corresponding values for an unfrozen soil with the same liquid water content by a reduction factor, i.e.,

$$D = D_u / I, \tag{4.5}$$

where D represents D_T, D_θ, D_{T_l}, D_{T_v}, D_{θ_l}, D_{θ_v}, or, K, and the subscript u denote an unfrozen value. The reduction factor, I, is given by [113] as

$$I = 10^{10\theta_i}. \tag{4.6}$$

4.2.2 Temperature-Suction Relation

The temperature-suction relation is [127]

$$\Psi = \frac{L_f(T) \cdot T_{fpd}}{Tg} \tag{4.7}$$

where

- Ψ is the suction (matric head) in meters,
- $L_f(T)$ is the latent heat of fusion of water at temperature T, J/kg,
- T_{fpd} is the freezing point depression in Kelvins, and
- g is the acceleration due to gravity, m/s^2.

The temperature-suction relation is combined with the Rossi and Nimmo [102] model of water retention to iteratively determine the liquid water content below the FDP.

4.2.3 Numerical Scheme

Differences between the non-freezing and freezing soil models that affect the numerical scheme are: 1) Moisture state may change from one time step to the next, 2) unfrozen water content is sensitive to temperature, and, 3) the two governing equations, (1) and (2), are independent above FED, but become dependent at temperatures below FDP. Convergence in the frozen case often requires multiple iterations for each layer at each time step—particularly for steps 3 and 5 in the following list of major operations (also shown by flowchart in Figure 4.1).

1. Initialize temperature, moisture content, and moisture state profiles using results from an annual thermal model [70].

2. Compute transfer coefficients including thermal conductivity, hydraulic conductivity and diffusion coefficients between layers (excluding the bottom one).

3. Match upper boundary conditions for heat and moisture fluxes using the Newton-Raphson method [94] — a two-dimensional (temperature and liquid water content) root finding problem for an unfrozen surface or a one-dimensional (temperature) problem for a frozen surface.

4. Compute heat and moisture fluxes between layers (excluding the bottom one).

5. Determine the changes in temperature and moisture content/state for all layers — a problem of algebraically solving two equations for unfrozen soil or a problem of one-dimensional root finding using the Newton-Raphson method for frozen soil.

6. If the bottom layer has not been reached, then return to step 5. Otherwise, match bottom boundary conditions for heat and moisture fluxes assuming the

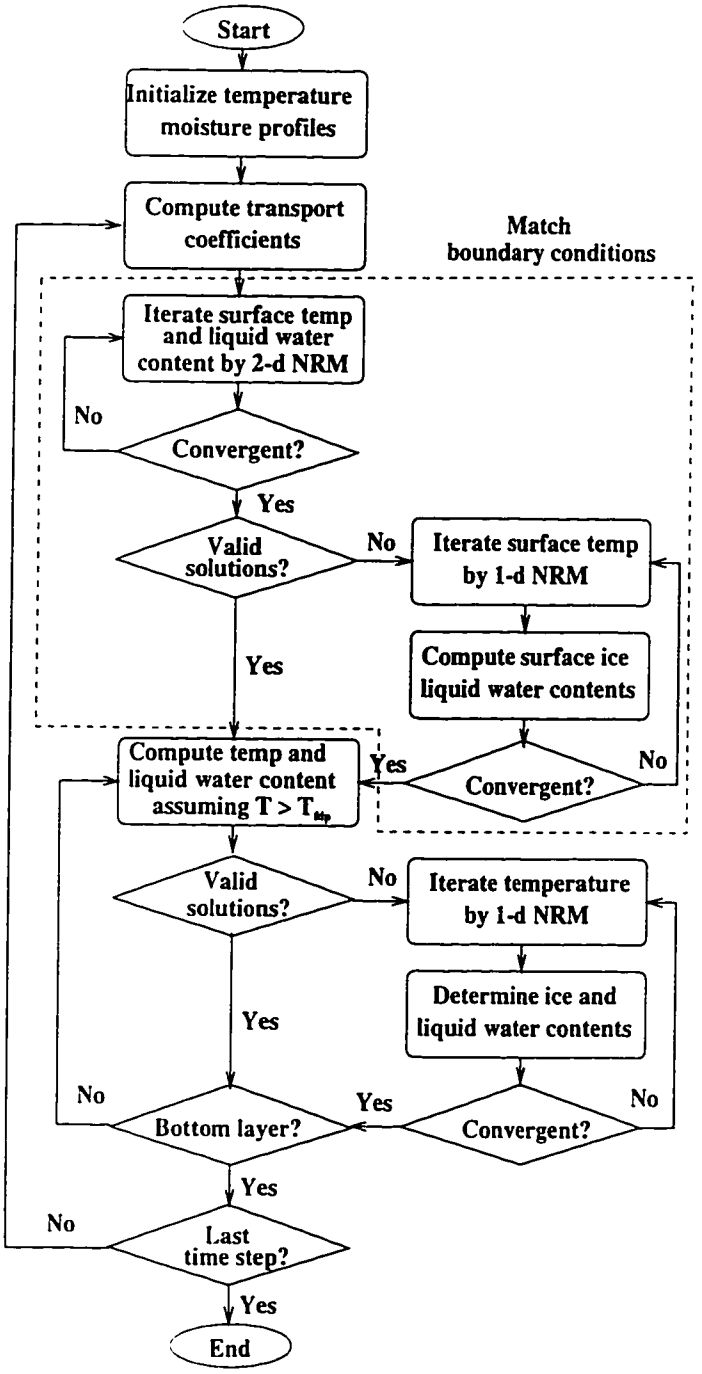

Figure 4.1: Flowchart of the 1dHb model algorithm for freezing soils. "NRM" denotes the Newton-Raphson Method.

bottom layer has the same fluxes as the second to bottom layer so that its energy and moisture fluxes remain constant, then go to the next time step.

7. If the last time step has not been reached, then return to step 2 and repeat steps 3, 4, 5, and 6. Otherwise, end the process.

For a 2-dimensional Newton-Raphson problem (unfrozen soil), the criteria for convergence include 1) the change in temperature between iterations is must be than 0.01 Kelvins, and 2) the change in liquid water content between iterations must be less than 0.01%. However, 1) is the only convergence criterion for a 1-dimensional Newton-Raphson problem (frozen soil).

4.2.4 Results

The model was run for a 90-day period for both water transport and no water transport cases in soil at a northern latitude of 43.5 degrees in fall and early winter (10/15-01/12). These times were chosen to span the transition between diurnal periods without freezing and diurnal periods without significant thawing. Initial temperature and moisture profiles are from an annual thermal model [70] in which soil moisture was a uniform 38% at all depths for the year. The heat flux at soil depths below the influence of the diurnal cycle was assigned to be that observed in the annual model.

Figure 4.2 shows the temperature, liquid water content, and ice content of the surface layer as a function of time for the water transport case. The 90-day simulation period can be divided into three sub-periods based upon surface wetness.

A. Day 1 to day 8: The first drying period

Both surface temperature and liquid water content exhibit regular diurnal os-

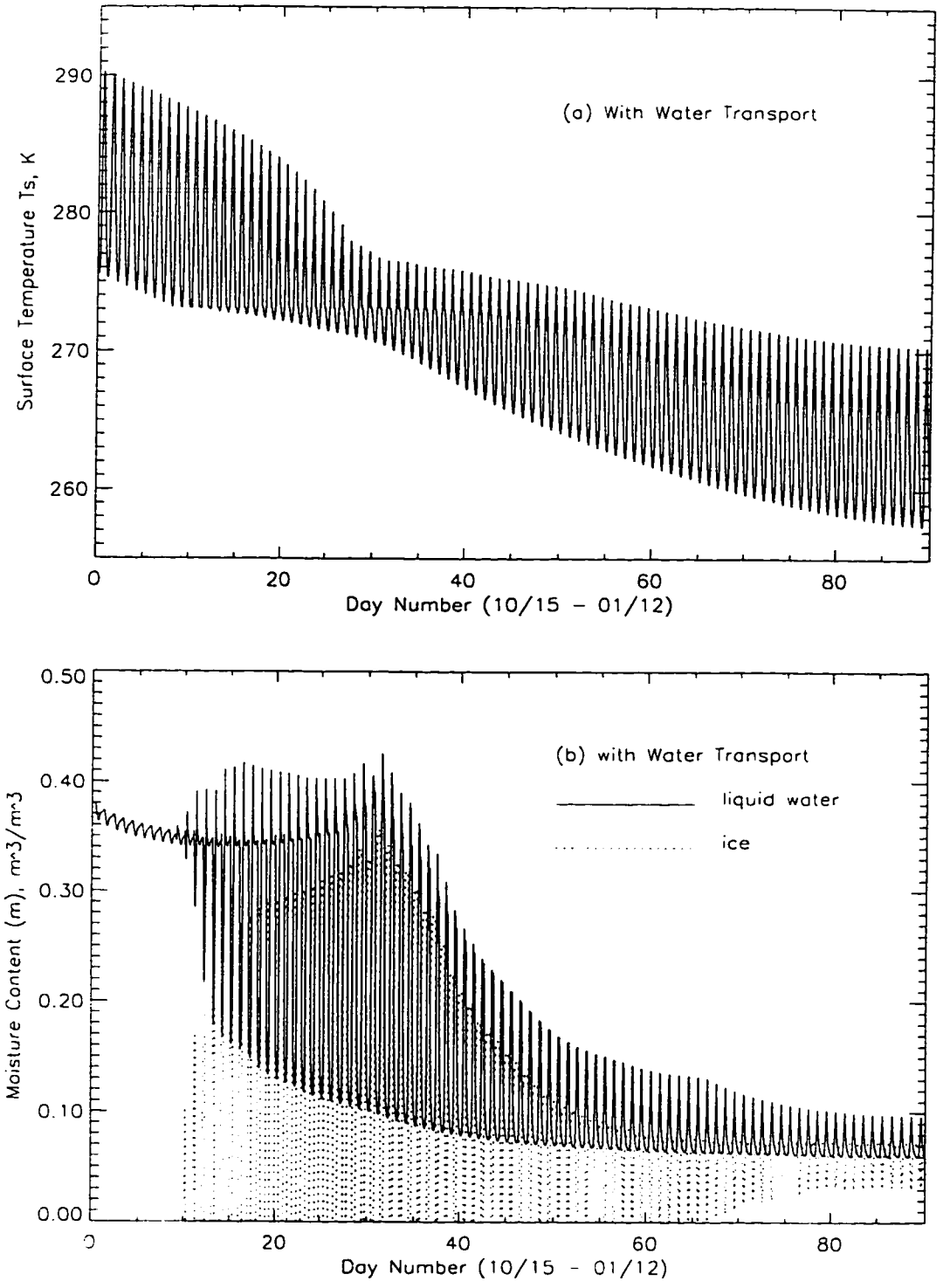

Figure 4.2: (a) Temperature and (b) liquid water and ice contents at the surface for the water transport case.

cillations with decreasing means.

B. Day 9 to day 30: The fluctuating period

Nighttime temperatures begin to drop below the FDP. Between day 9 and day 65, the diurnal variation in temperature is suppressed by the diurnal freezing and thawing of surface moisture. This fluctuating period is characterized by dramatic daytime increases and nighttime decreases in surface liquid water. Figure 4.3 shows the temperature, liquid water content, and ice content profiles over a typical diurnal cycle for the fluctuating period. We observe:

1. Freezing occurs toward the end of the previous night.
2. Updrawing of excess water from the soil layers below the freezing front significantly increases the total moisture content of the top soil layer.
3. As surface cooling moves the freezing front downward, more near-surface soil layers reach high moisture contents.
4. A large portion of the solar heating immediately after sunrise is spent melting the ice within the top soil layer, then the second layer, then the third layer, ... etc, so that the quantity of liquid water at the surface increases rapidly.
5. Ice within the top soil layer completely melts causing the liquid water content to surge to 41% at 9:20 a.m. After that maximum, moisture is removed by downward moisture transport and by upward evaporation (see Figures 4.7 (a) and (b)).
6. All of the forces that drive moisture — the water pressure gradient, liquid water content gradient, temperature gradient, gravity, and latent heat

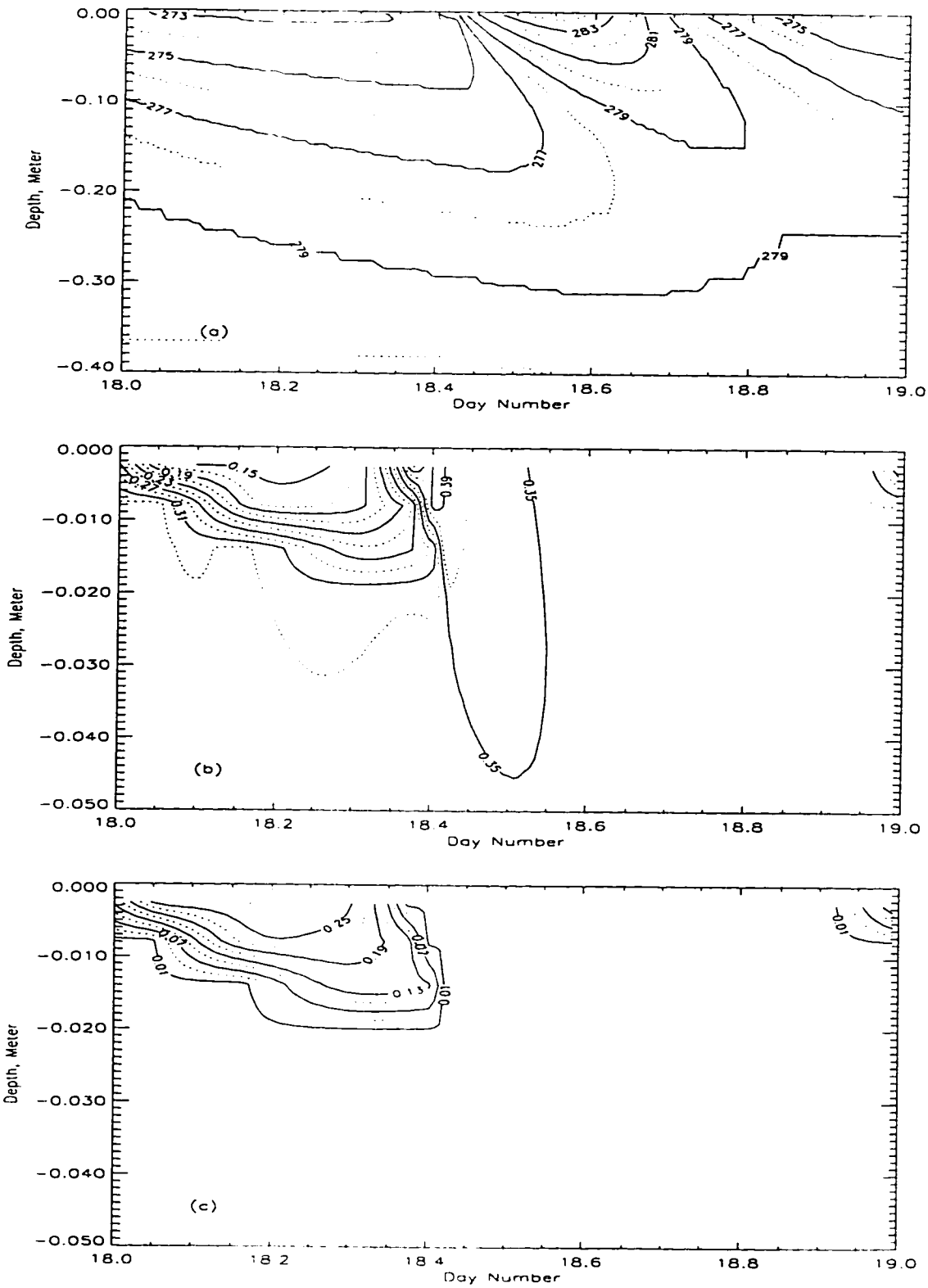

Figure 4.3: (a) Temperature, (b) liquid water content, and (c) ice content profiles over a diurnal cycle on day 19. Sunrise occurs at 7:10 a.m. with a peak insolation of 360 W/m^2 at 12:10 p.m.. The sun sets at 5:20 p.m. Note the change in vertical scales from 40 cm in (a) to 5 cm in (b) and (c).

transfer at the land-air interface — transport moisture away from the surface layer.

7. Ice within the second soil layer is completely melted by 10:00 a.m., the water pressure gradient between the first (unfrozen) and second (frozen) soil layers disappears, and the liquid water content gradient force drives moisture upward from the second to the first soil layer.

8. The first soil layer reaches another high moisture content of nearly 40 % at 10:10 a.m.

A similar process can occur at the interfaces between deeper soil layers to cause additional surges in surface liquid water content, but their significance is diminished for deeper layers. The discrete pattern of moisture surges is an artifact of layers of finite thickness. If layers were to become infinitely thin, the surges would smooth to a single diurnal surge. Diurnal surges appear in the surface liquid water content in Figure 4.2 (b).

C. Day 31 to day 90: The second drying period

The diurnal variation in temperature over this 60-day period increases with increasing day number from 6 Kelvins on day 31 to 13 Kelvins on the last day (Figure 4.2 (a)). The increase follows decreases in surficial liquid water and ice contents as the freezing front moves downward (also see Figure 4.5 (b)). The thickening of the frozen soil zone as the freezing front moves downward increasingly restricts the resupply of moisture to the surface layer from deeper soil layers.

From day 31 to day 50, the total water content of the top layer of soil decreases to about 25%, while, from day 50 to day 90, the decrease is only another 4 %.

Beginning with day 67, ice in the top soil layer never melts completely during daytime. After this date, there is little latent heat transfer between the air and the land.

The temperature, liquid water content, and ice content profiles for day 60 are shown in Figure 4.4. For temperatures below the FDP, liquid water content is a function of temperature so that Figure 4.4 (b) is highly correlated with Figure 4.4 (a). Figure 4.4 (c) shows that ice content generally decreases with increasing depth except near the surface where soil is subject to diurnal cooling and heating.

Temperature profiles for the 90-day water transport case are shown in Figure 4.5 (a). The near-surface, downward, lobe-shaped isotherms are a response of soil to diurnal heating and cooling at the land-air interface. Their penetration depths strongly correlate with the strength of diurnal weather forcing and inversely with the thermal inertia of the soil. The shallowest penetration, less than 6 cm, corresponds to the 273-Kelvin isotherm around day 30 when soil freezing and thawing are most extensive. This phase change of water dominates other factors in governing the thermal inertia of the soil. Similarly, the 273-K isotherm penetrates to deeper soils more slowly than do the the 281- and 285-Kelvin isotherms. The profiles of temperature (Figure 4.5 (a)) and of liquid water content (Figure 4.5 (b)) exhibit the correlation shown in Figures 4.4 (a) and (b) for one day.

Profiles of ice content for the water transport case are shown in Figure 4.5 (c). Frozen soil thickness increases until day 60. After day 60, there is insufficient cooling of the soil column for the freezing front to progress further downward. By day 31, a permanent frozen soil layer forms at about 3 cm depth. By day 43, the highest ice-content (43%) appears at about 4 cm depth. By the end of the 90-day simulation,

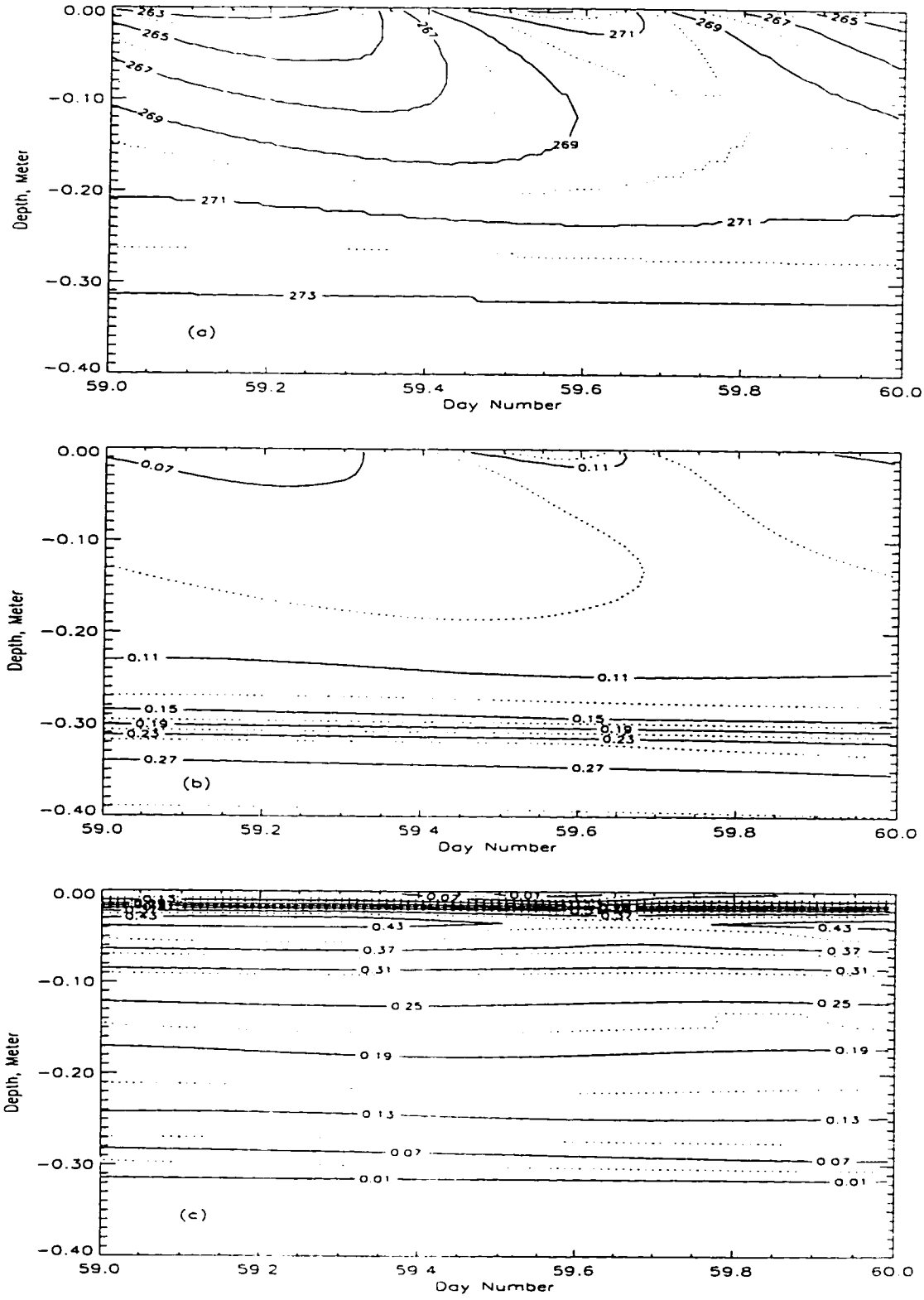

Figure 4.4: (a) Temperature, (b) liquid water content, and (c) ice content profiles over a diurnal cycle on day 60. Sunrise occurs at 7:20 a.m. with a peak insolation of 290 W/m^2 at 12:10 p.m. The sun sets at 5 p.m.

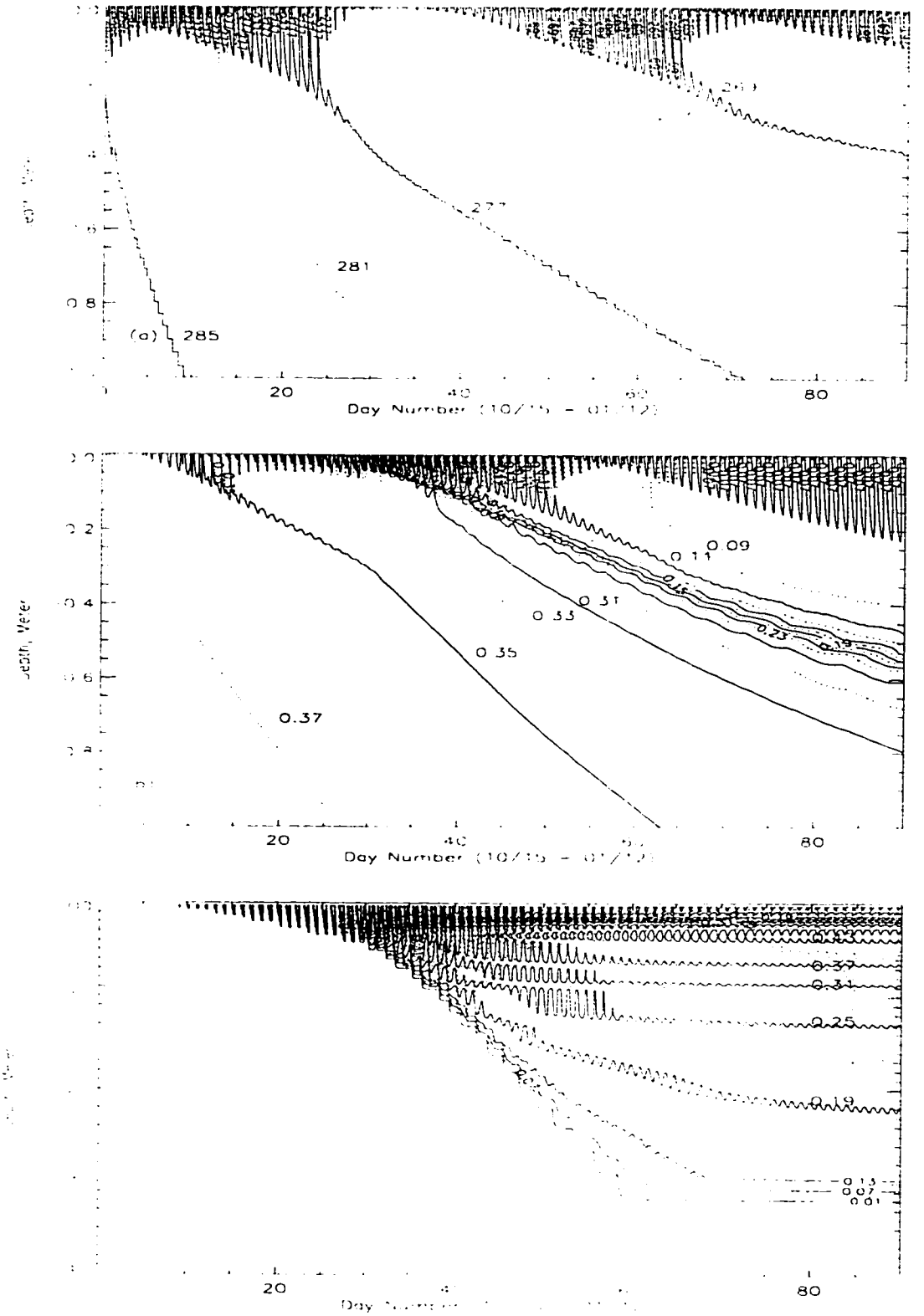

Figure 1.5: (a) Temperature, (b) liquid water content, and (c) ice content profiles for the water transport case. Note that the depth scale of (c) differs from that of (a) and (b).

this region of high ice-content is 1 cm thick and lies at a depth of 3.5 cm. Away from the ice maximum, ice content decreases monotonically with both increasing and decreasing depths.

Differences in surface liquid water and ice contents between the water transport and no water transport cases are shown in Figure 4.6 (a). The maximum difference in liquid water content over the 90-day simulation is 19 % on day 47. The maximum difference in ice content is 27 % during the last 30 days of the simulation. As expected in a dry-down simulation, surface moisture content (liquid water plus ice contents) for the water transport case is generally lower than that of the no water transport case. Exceptions occur when the freezing front is near the surface so that the surface layer can extract moisture from the soil layers below. This phenomenon can be seen during the nighttime between day 10 and day 33.

Total moisture content within the depth range of diurnal thermal pulses is lower for the water transport case than for the no water transport case. Consequently, the water transport case exhibits warmer surface temperatures during daytime and cooler surface temperatures during nighttime (Figure 4.6 (b)). Maximum differences near day 45 coincide with the period of maximum difference in liquid water content.

Figure 4.7 offers detailed views of diurnal variations in surface temperature and moisture content/state on days 19, 44, and 60 for both water transport and no water transport cases. Freezing and thawing are the dominant processes —- particularly on days 19 and 44.

4.3 RADIOBRIGHTNESS MODEL

Nearly-daily radiometric observations for higher latitudes from the Defense Meteorological Satellite's Special Sensor Microwave/Imager (SSM/I) [49] have been avail-

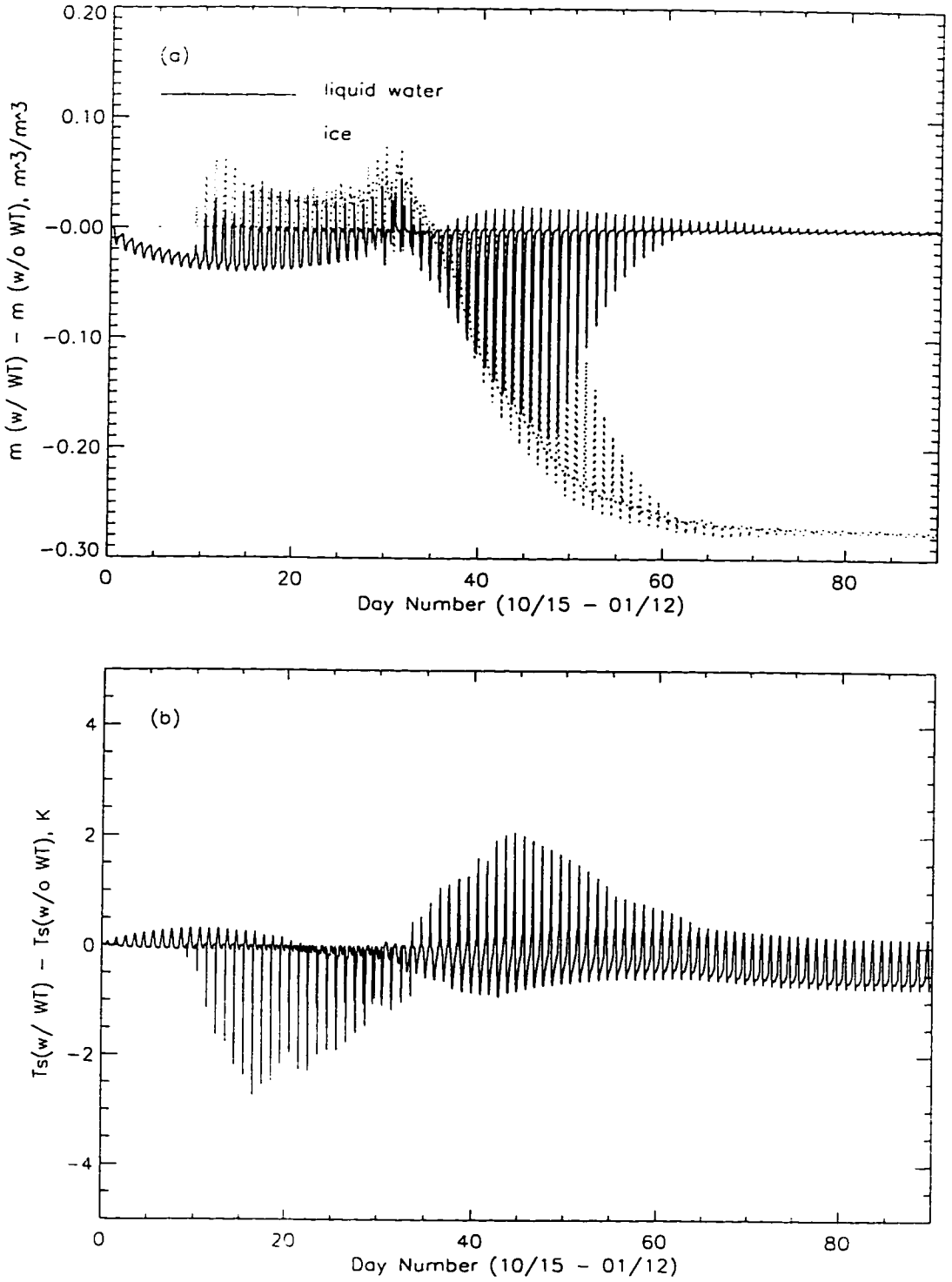

Figure 4.6: Differences in (a) liquid and ice contents and in (b) temperature at the surface between the water transport and no water transport cases.

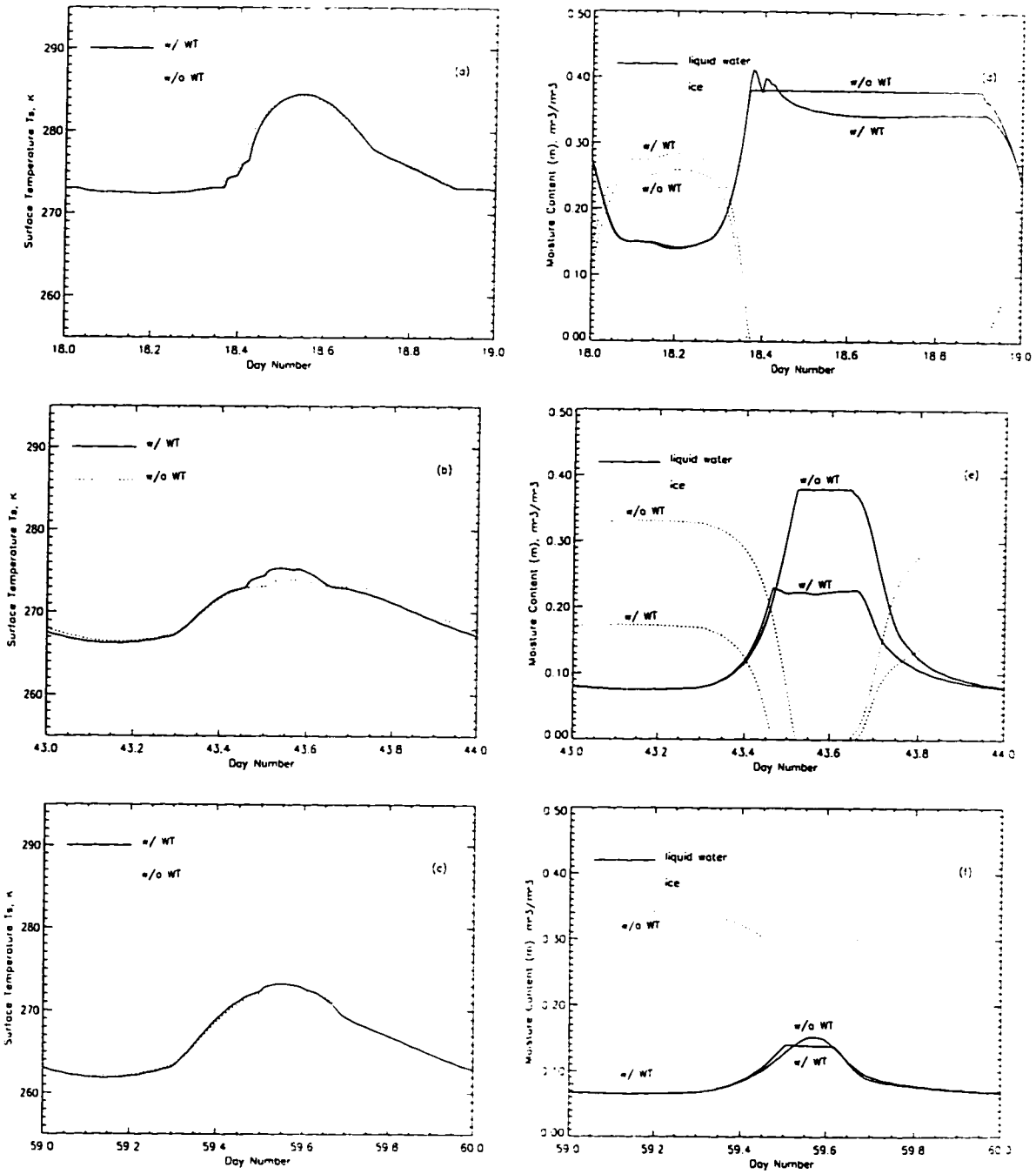

Figure 4.7: Surface temperatures on (a) day 19, (b) day 44, and (c) day 60. Liquid water and ice contents on (d) day 19, (e) day 44, and (f) day 60.

able since 1987. Radiobrightness is sensitive to moisture in bare or sparsely-vegetated soils through the Debye relaxation process of liquid water. Here, we examine the radiobrightness of freezing and thawing bare soils at the SSM/I frequencies.

The SSM/I radiobrightnesses of bare, wet soil are estimated with a microwave emission model for a quasi-specular, homogeneous soil,

$$T_b(t) = e \cdot T_{eff}(t), \tag{4.8}$$

where e is a Fresnel Reflectivity-based emissivity and $T_{eff}(t)$ is an effective surface temperature [71, 70]. This approximation is appropriate for bare or sparsely vegetated soil at 19 GHz, but increasingly less appropriate at 37 and 85 GHz where soil surfaces are increasingly rough at the scale of wavelength. The first order approximation to $T_{eff}(t)$ is

$$T_{eff}(t) = T_g(0,t) + \frac{1}{\kappa_e \sec\theta_t} \cdot \left(\frac{\partial T_g(z,t)}{\partial z}\right)_{z=0}, \tag{4.9}$$

where κ_e is extinction of the soil, θ_t is a transmission angle, and T_g is the ground temperature. As shown in [70], the diurnal extremes of the first-order terms are approximately ± 0.3 Kelvins at 19 GHz for 17% moist soil, and they decrease with increasing frequency and water content.

The 90-day, H-polarized, 19 GHz radiobrightness for the water transport case is shown in Figure 4.8 (a). A significant contrast in radiobrightness, more than 50 Kelvins between the first 10-day and the last 30-day periods, reflects the dominant influence of liquid water on radiobrightness. The difference in liquid water content between the two periods is 20 %. Similarly, differences in radiobrightness between daytime and nighttime are highly correlated with variations in the liquid water content over a diurnal cycle. The maximum diurnal variation in radiobrightness of 57 Kelvins is seen near day 30 when the surface liquid water content changes by 32% over a

Differences, K	maximum	minimum
2 a.m.	3.8	- 0.4
6 a.m.	3.5	- 3.4
2 p.m.	31.8	- 2.4
6 p.m.	12.7	- 2.6

Table 4.1: The maximum and minimum of T_b (water transport) - T_b (no water transport) for 19 GHz, horizontal polarization.

diurnal cycle (see Figure 4.2 (b)).

Differences in H-polarized, 19 GHz radiobrightness between the water transport and no water transport cases are shown in Figure 4.8 (b). The maximum difference of 37 Kelvins appears near day 48 when the difference in surface liquid water content between the two cases is the largest (Figure 4.6 (a)).

The maximum and minimum differences in 19 GHz, H-polarized radiobrightness between water transport and no water transport cases at 2 a.m., 6 a.m., 2 p.m. and 6 p.m. are shown in Table 4.1. Clearly, vertical water transport is an important influence upon the radiobrightness of bare soil. The 37 and 85 GHz differences are smaller.

Note that the effects of scatter darkening on the SSM/I radiobrightnesses are not accounted for in Equation (4.8). Scatter darkening within frozen soils results from the fact that freezing reduces the imaginary part of the soil dielectric constant [131] so that volume scattering becomes relatively significant at higher frequencies.

4.4 DISCUSSION

Water transport in bare or sparsely vegetated soils has a significant influence upon radiobrightness. The influence is particularly noticeable during periods of diurnal freezing and thawing.

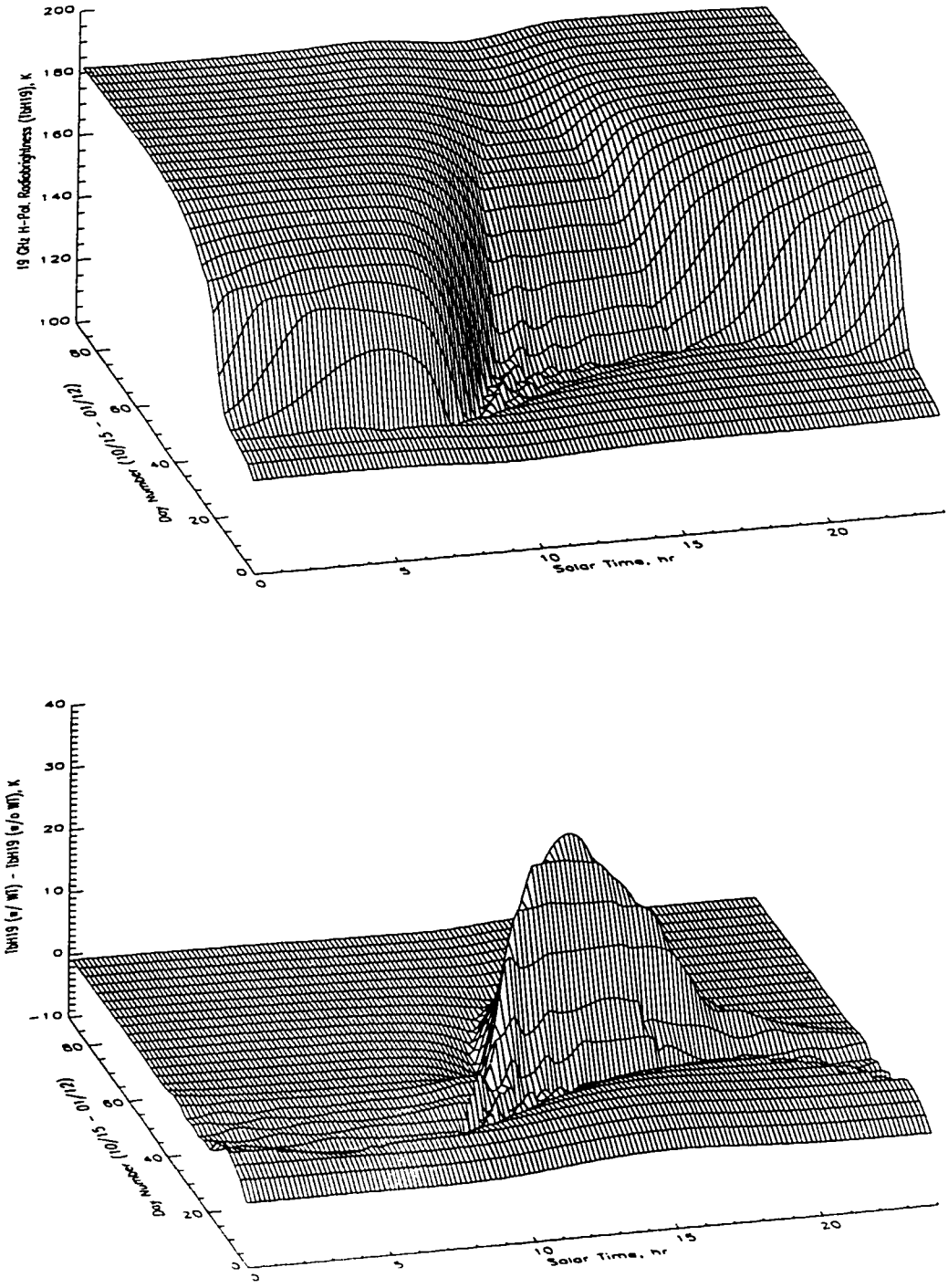

Figure 4.8: (a) H-polarized, 19 GHz radiobrightness for the water transport case. (b) Differences in H-polarized, 19 GHz radiobrightness between the water transport and no water transport cases.

The three significant hydrologic features of the 90-day dry down during fall for bare soils in northern latitudes are: 1) The decrease in the total moisture content at the surface is about 25 %, 2) There can be brief surges in daytime surface liquid water during periods of diurnal freezing and thawing, and 3) An ice-rich layer develops at a depth of about 3.5 cm. the significant radiobrightness feature of the 90-day dry-down is the dramatical diurnal variation in radiobrightness as soils freeze and thaw.

This LSP/R model for bare soil will be mixed with an LSP/R model for prairie grassland to model mixed terrains in the northern prairie. The LSP/R model for prairie grassland will be presented in a companion paper. Both models will be validated against our field data from REBEX-1 [38] and REBEX-4 (during the summer of 1996) on the prairie near Sioux Falls, South Dakota.

CHAPTER 5

THE 1dH/R MODEL FOR PRAIRIE GRASSLAND

Abstract — We present a biophysically-based, one-dimensional Hydrology/Radiobrightness (1dH/R) model for prairie grassland that is subject to solar heating, radiant heating and cooling, precipitation, and sensible and latent heat exchanges with the atmosphere. Vegetation coverage may vary from 0 % to 100 %. The 1dH/R model consists of two modules, a one-dimensional Hydrology (1dH) module that estimates the temperature and moisture profiles of the soil and the canopy, and a microwave emission module that predicts radiobrightness (R).

We validate the 1dH/R model by comparing its predictions with data from a field experiment. The model was driven by meteorological and sky radiance data from our Radiobrightness Energy Balance Experiment (REBEX-1) on prairie grassland near Sioux Falls, South Dakota, during the fall and winter of 1992-1993. Model predictions were compared with 995 consecutive REBEX-1 observations over a 14 day period in October. Average errors (predicted – measured) for canopy temperature are 1.1 K with a variance of 3.72, for soil temperatures at 2, 4, 8, 16, 32 and 64 cm depths are 2 K with a variance of 4, and for H-polarized radiobrightnesses

are − 0.06 K with a variance of 1.30 at 19 GHz and 6.01 K with a variance of 6.04 at 37 GHz. We attribute our overestimate of the 37 GHz radiobrightness to scatter darkening within the vegetation canopy.

We use the 1dH/R model to simulate a 60-day dry down of prairie grassland in summer. For grass with a column density of 3.7 kg/m^2 and soil with an initially uniform moisture content of 38 % by volume, the upper 5 mm of soil dries to 27 % by the end of the simulation. The corresponding L-band radiobrightness increases from an initial 143 K to a final 163 K. In contrast, none of the SSM/I radiobrightnesses nor the Radiobrightness Thermal Inertia (RTI) technique, either at L-band or at an SSM/I frequency, exhibits significant sensitivity to the soil dry-down.

5.1 INTRODUCTION

The water in soil and vegetation that is available to the atmosphere through evaporation or transpiration is often called soil wetness in the Land-Surface Process (LSP) models that are part of atmospheric models. Soil wetness affects the energy budget at the land-atmosphere interface through its influence upon the exchange of latent energy. Errors in the estimate of soil wetness contribute to errors in estimates of latent energy flux and, finally, to potentially significant errors in model-based predictions about weather or short-term climate [100, 20, 99].

The Biosphere-Atmosphere Transfer Scheme (BATS) [25], the Simple Biosphere model (SiB) [106], and the simplified biosphere model (SSiB) [130] are examples of commonly used LSP models. The computational requirement that LSP models interact at each time step with all of the near-surface grid points of an atmospheric model

has led to highly parameterized characterizations of the physical processes that occur at the land-atmosphere interface. Parameterizations within the LSP model are empirically tuned to yield an atmosphere whose behavior is consistent with observations. Self consistency is all that is required for validation of an LSP model, i.e., it is not required that the parameters in the LSP model be observable in the field.

LSP soil wetness estimates might be improved by the assimilation of observational data much as state estimates within atmospheric models are improved by the assimilation of observed atmospheric temperature and humidity profiles. Radiobrightness at lower microwave frequencies is known to be sensitive to soil moisture and temperature [124, 27, 44, 105, 55], and would be a candidate for assimilation if there were reliable relationships between the moisture content and temperature of surface soils and the soil wetness and temperature of LSP models. Finding those relationships is an objective of the Global Energy and Water Cycle Experiment (GEWEX) [128, 129]. In their absence, we can substitute a one-dimensional Hydrology (1dH) model for the LSP model, predict radiobrightness (R) based upon the more accurate soil moisture and temperature profiles of the 1dH model, and use the difference between observed and predicted radiobrightness as a measure of error in the 1dH model's estimate of stored water — the 1dH equivalent to the LSP model's soil wetness. A similar approach has been used by Mahfouf [74] and Bouttier et al [8] except that they assimilated local weather observations to improve point estimates of stored water.

Our group has conducted Radiobrightness Energy Balance Experiments in prairie grassland (REBEX-1) for fall and winter [39], and in arctic tundra (REBEX-3) for a full year [60]. We have also developed bare-soil models [70, 71, 72] that are being tested in REBEX-4, a joint experiment with the Canadian Atmospheric Environment Service, to measure the fluxes and radiobrightnesses of bare soil and prairie grassland

near Sioux Falls, South Dakota, during the spring and summer of 1996.

In this paper, we present a 1dH/R model of prairie grassland that is based upon a combination of our bare-soil model and a biophysical and radiative transfer model of the grass canopy. The new model is validated with observations from REBEX-1 in mid-October, and is then used to simulate a 60-day dry-down of grass-covered prairie in summer. Our objective is to examine the sensitivity of various radiobrightness frequencies and techniques for remotely measuring soil moisture.

5.2 THE GRASSLAND MODEL

5.2.1 Overview

The 1dH/R model consists of two modules, a 1dH module and a radiobrightness (R) module. The 1dH module simulates the land surface processes and estimates temperature and moisture profiles in soil and canopy for grass-covered fields. Assigned grass-coverage may vary from 0 % to 100 %. The R module is a radiative transfer model similar to that developed by the England and Galantowicz [32]. The soil is modeled as in Liou and England [71, 72] except that we account for the effects of transpiration on energy and moisture within the root zone.

The canopy is divided into two layers. The top layer links the soil and atmosphere through dynamic exchanges of energy and moisture, and the bottom layer, a thin insulating layer of thatch, is subject to radiant energy exchanges with the top layer, the atmosphere, and the underlying soil. Sensible and latent heat transfer are approximated as in Chehbouni et al [18] and Noilhan and Planton [86], respectively. Shortwave radiation absorbed by the two canopy layers is estimated using the non-scattering Beer's Law of radiative transfer [123].

Figure 5.1 is a schematic diagram of the 1dH/R model inputs and products. The

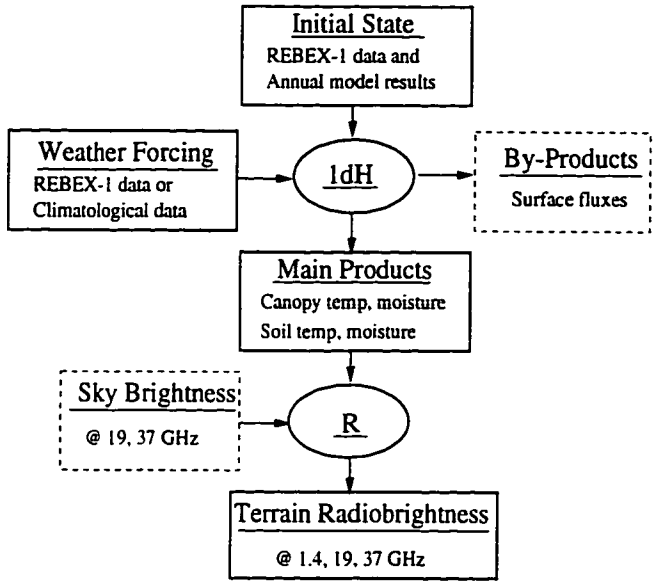

Figure 5.1: Schematic diagram of the 1dH/R model inputs and products.

1dH module initial state includes the temperature and moisture profiles of the soil and canopy. These profiles are derived from REBEX-1 observations and from the annual thermal model predictions [70]. In the current study, the 1dH module is driven by atmospheric data from REBEX-1 in order to validate the 1dH/R model. Once the model was verified, we drove the model using climatological data to examine the response of radiobrightness to a 60-day dry-down of a prairie grassland. The main products of the 1dH module are temperature and moisture profiles of the soil and canopy. They are the key parameters that are incorporated into the R module to compute radiobrightness. Sky brightnesses at 19 and 37 GHz from the REBEX-1 site are used only in the validation simulation. They modify terrain radiobrightness by less than a few degrees. By-products of the 1dH module are surface fluxes such as sensible heat transfer, and latent heat transfer through evaporation and transpiration.

5.2.2 The 1dH Module

A schematic diagram of the 1dH module land-air interactions for vegetated soils is shown in Figure 5.2. The vegetated field is subject to solar heating, $Q_{s,\,d}$, radiant heating from the sky, $Q_{l,\,d}$, radiant cooling of the canopy, Q_c, and of the bare soil, Q_s, sensible heat exchanges with the air from the canopy, H_c, and from the soil, H_s, evaporative heat loss from the wet foliage, $L_v E_c$, and from the bare soil, $L_v E_s$, heat loss due to transpiration, $L_v E_{tr}$, and heat exchange through precipitation, P_c. The other parameters in Figure 5.2 are gray-body emission from the thatch, Q_t, and from the soil, Q_s, energy flux, Q_h, and moisture flux, Q_m, within the soil, drainage from the canopy, D_c, runoff at the soil-canopy interface $Runoff$, total number of soil layers, N, and number of soil layers within the root zone, N_r.

The coupled transfer of energy and moisture governs the temperature and moisture profiles of the soil and canopy. The next sections describe details of the modeling of the upper canopy layer (canopy), the lower canopy layer (thatch), the soil layers, and the fluxes.

The Canopy Layer

For the canopy layer, equations for the conservation of energy and moisture are

$$\frac{\partial X_{hc}}{\partial t} = F_c \tag{5.1}$$

$$\frac{\partial X_{mc}}{\partial t} = \rho_l(P_c - D_c - E_c), \tag{5.2}$$

respectively, where

- $X_{hc} = (W_c c_c + W_l c_l)(T_c - T_0)$ is the total heat content per unit area of the canopy layer, J/m^2, where

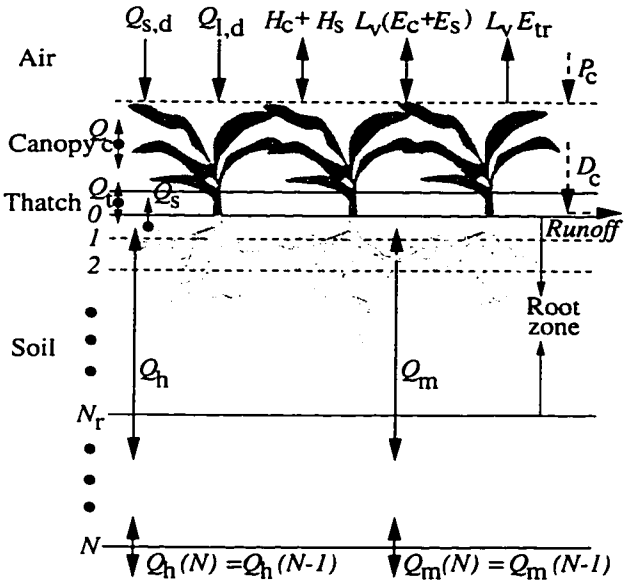

Figure 5.2: The 1dH module schematic diagram of land-air interactions for vegetated fields.

- W_c is the dry canopy mass, kg/m^2
- W_l is the canopy moisture mass, kg/m^2
- c_c is the canopy specific heat (typical = 2700 [123]), J/kg-K
- c_l is the specific heat of liquid water at constant pressure, J/kg-K
- T_c is the canopy temperature, K
- T_0 is the reference temperature, K

- $X_{mc} = W_l = W_{ls} + W_r$ is the total moisture per unit area of the canopy layer, kg/m^2, where
  - W_{ls} is the static moisture content in the canopy, kg/m^2,
  - W_r is the moisture stored on the foliage, kg/m^2
- t is the time, s

- $F_c = R_{nc} - H_c - \rho_l L_v E_{tr} - \rho_l L_v E_c$ is a function of the energy balance components of the canopy layer, W/m^2, where
  - R_{nc} is the net radiation absorbed by the canopy, W/m^2
  - H_c is the sensible heat flux between the atmosphere and canopy, W/m^2
  - L_v is the latent heat of vaporization of water, J/kg
  - E_{tr} is the rate of transpiration from the dry fraction of the canopy, m/s
  - E_c is the rate of vaporization from the wet fraction of the canopy, m/s
- ρ_l is the density of liquid water, kg/m^3
- P_c is the rate of precipitation, m/s
- D_c is the rate of water drainage, m/s
- E_c is the rate of vaporization, m/s.

The Thatch Layer

The thatch is a 2 cm layer of organic matter, like dead grass, that lies at the base of the grass canopy. It is subject to radiant heat exchange with the atmosphere, the canopy layer, and the underlying soil layers. Its energy budget is given by

$$\frac{\partial X_{ht}}{\partial t} = F_t, \tag{5.3}$$

where

- $X_{ht} = W_t c_t (T_t - T_0)$ the total heat content per unit area of the thatch, J/m^2, where
  - $W_t = r_{tc} W_{wc}$ is the mass of the thatch, kg/m^2

- r_{tc} is the ratio of the bottommost 2 cm wet biomass to the total wet biomass of the canopy (2 cm is chosen so that r_{tc} can be estimated using field observations given latter)
- $W_{wc} = W_c + W_{ls} + W_t$ is the mass of the wet canopy, kg/m^2
- c_t is the specific heat of the thatch, J/kg-K
- T_t is the thatch temperature, K

- $F_t = R_{nt}$ is a function of the thatch energy balance components, W/m^2, where
  - R_{nt} is the net radiation absorbed by the thatch, W/m^2.

The value of the parameter r_{tc} was obtained from a field study of the vertical distributions of biomass and moisture in a grass canopy at the University of Michigan's Matthaei Botanical Garden by Dahl et al [21]. The wet biomass was measured with 2 cm vertical resolution. The wet biomass of the grass at the REBEX-1 site was about 2.3 times the wet biomass of the grass at the Matthaei site.

The Soil Layers

Energy and moisture conservation equations within the soil have been given by Liou and England [71, 72]. They are

$$\frac{\partial X_h}{\partial t} = -\nabla \cdot \vec{Q}_h \tag{5.4}$$

$$\frac{\partial X_m}{\partial t} = -\nabla \cdot \vec{Q}_m, \tag{5.5}$$

respectively, where

- X_h is the total heat content per unit volume, J/m^3
- X_m is the total moisture content per unit volume, kg/m^3

- $\vec{Q}_{\mathrm{m}} = \vec{Q}_{\mathrm{v}} + \vec{Q}_{\mathrm{l}}$ is the vector moisture flux density, kg/m^2-s, where $\vec{Q}_{\mathrm{v}}$ and $\vec{Q}_{\mathrm{l}}$ are the vector vapor and liquid flux densities, respectively

- $\vec{Q}_{\mathrm{h}}$ is the vector heat flux density, J/m^2-s.

This current version of the soil module has been improved by incorporating the effect of transpiration on the moisture flux and on the energy flux within the root zone, i.e.,

$$\vec{Q}_{\mathrm{l}} = \vec{Q}_{\mathrm{l,\,b}} - \rho_{\mathrm{l}} E_{\mathrm{tr}} \hat{k}, \tag{5.6}$$

where

- $\vec{Q}_{\mathrm{l,\,b}}$ is the vector liquid water flux for bare soil given by Liou and England [72], kg/m^2-s

- $\hat{k}$ is a vertical unit vector.

The boundary conditions on energy and moisture fluxes at the soil-canopy interface (upper) and with soils below the modeled column (lower) are required to solve Equations (5.4) and (5.5). The lower boundary is chosen to be at a depth unaffected by diurnal thermal and moisture variations so that energy and moisture fluxes are constant (see Figure 5.2), i.e.,

$$Q_{\mathrm{h}}(N) = Q_{\mathrm{h}}(N-1) \tag{5.7}$$

$$Q_{\mathrm{m}}(N) = Q_{\mathrm{m}}(N-1), \tag{5.8}$$

where

- N is the the number of soil layers

- $Q_{\mathrm{h}}(N)$ is the heat flux density at the N^{th} layer boundary, J/m^2-s

- Q_{m} is the moisture flux density at the N^{th} layer boundary, kg/m^2-s.

At the upper boundary, the energy and moisture fluxes are

$$\vec{Q}_{\rm h}(0) = R_{\rm ns} - H_{\rm s} - \rho_{\rm l} L_{\rm v}(E_{\rm s} + E_{\rm tr}) \tag{5.9}$$

$$\vec{Q}_{\rm m}(0) = \rho_{\rm l}(D_{\rm c} - E_{\rm s} - E_{\rm tr} - Runoff), \tag{5.10}$$

respectively, where

- $R_{\rm ns}$ is the net radiation absorbed by the soil, W/m^2
- $H_{\rm s}$ is the sensible heat flux from bare soil, W/m^2
- $E_{\rm s}$ is the rate of evaporation from bare soil, m/s
- $Runoff$ is the rate of runoff, m/s.

Radiation Fluxes

Longwave and shortwave radiation transfer occur among the vegetation, thatch, and soil. Shortwave radiation is described by the non-scattering Beer's law of radiative transfer so that the transmissivity of shortwave radiation for the canopy becomes [123]

$$\tau_{\rm c} = \exp(-\kappa_{\rm c} {\rm LAI}), \tag{5.11}$$

where

- $\kappa_{\rm c}$ is the extinction coefficient of the canopy ($= 0.4/\cos Z$ for crops and grass)
- LAI is the leaf area index, m^2/m^2.
- Z is the solar zenith angle, degrees.

Similarly, the transmissivity of shortwave radiation for the thatch is

$$\tau_{\rm t} = \exp(-\kappa_{\rm c} {\rm LAI}_{\rm t}), \tag{5.12}$$

where

- $\mathrm{LAI_t} = r_{\mathrm{tc}}\mathrm{LAI}$ is the leaf area index of thatch, $\mathrm{m^2/m^2}$.

The net radiation absorbed by the canopy and by the thatch layers is

$$\begin{aligned} R_{\mathrm{nc}} &= \mathrm{veg}[(1-\tau_{\mathrm{c}})(1-A_{\mathrm{c}})Q_{\mathrm{s,\,d}} \\ &\quad + e_{\mathrm{c}}Q_{\mathrm{l,\,d}} + e_{\mathrm{c}}e_{\mathrm{t}}\sigma T_{\mathrm{t}}^4 - 2e_{\mathrm{c}}\sigma T_{\mathrm{c}}^4] \qquad (5.13) \\ R_{\mathrm{nt}} &= \mathrm{veg}[\tau_{\mathrm{c}}(1-A_{\mathrm{c}})(1-A_{\mathrm{t}})(1-\tau_{\mathrm{t}})Q_{\mathrm{s,\,d}} \\ &\quad + e_{\mathrm{t}}e_{\mathrm{c}}\sigma T_{\mathrm{c}}^4 + e_{\mathrm{t}}e_{\mathrm{s}}\sigma T_{\mathrm{s}}^4 - 2e_{\mathrm{t}}\sigma T_{\mathrm{t}}^4], \qquad (5.14) \end{aligned}$$

respectively, where

- veg is the fraction of the canopy cover
- A_{c} is the albedo of the canopy
- A_{t} is the albedo of the thatch
- $Q_{\mathrm{s,\,d}}$ is the down-welling shortwave radiation, $\mathrm{W/m^2}$
- $Q_{\mathrm{l,\,d}}$ is the down-welling longwave radiation, $\mathrm{W/m^2}$
- e_{c} is the emissivity of the canopy
- e_{t} is the emissivity of the thatch
- e_{s} is the emissivity of the soil
- σ is the Stefan-Boltzmann constant, $\mathrm{W/m^2 - K^4}$
- T_{c} is the canopy temperature, K
- T_{t} is the thatch temperature, K
- T_{s} is the soil temperature (top layer), K.

The four terms between the brackets of Equation (5.13) represent: 1) the absorbed shortwave radiation corrected by the transmissivity and albedo of the canopy, 2) the absorbed downwelling sky thermal radiation, 3) the absorbed thermal emission from the underlying thatch, and 4) the gray-body emission from the canopy in both upward and in downward directions. The four terms between the brackets in Equation (5.14) are the absorbed shortwave radiation, the absorbed canopy thermal emission, the absorbed soil thermal emission, and the thermal emission of the thatch, respectively.

The net radiation absorbed by the soil is

$$\begin{aligned} R_{ng} &= \text{veg}[e_s e_t \sigma T_t^4 + \tau_c \tau_t (1 - A_c)(1 - A_t) \\ &\quad (1 - A_s) Q_{s,\,d}] + (1 - \text{veg}) \\ &\quad [(1 - A_s) Q_{s,\,d} + e_s Q_{l,\,d}] - e_s \sigma T_s^4 \end{aligned} \tag{5.15}$$

- A_s is the albedo of the soil

Between the first set of brackets, the first term is the downwelling thermal emission absorbed from the thatch, and the second term is the downwelling shortwave radiation modified by the transmissivity and albedo of both the thatch and the canopy, and by the albedo of the soil. The two terms between the second set of brackets are the shortwave and longwave radiation absorbed by the bare soil, respectively. The last term of the equation is gray-body emission from the soil.

Sensible and Latent Heat Fluxes

Sensible Heat Transfer

Sensible heat exchanges between the atmosphere and the vegetation and between

the atmosphere and the soil are modeled with the bulk aerodynamic approach [117]:

$$H_c = \text{veg}\rho_a c_{p,a}\frac{T_c - T_{a,r}}{r_{ac}} \tag{5.16}$$

$$H_s = (1 - \text{veg})\rho_a c_{p,a}\frac{T_s - T_{a,r}}{r_{as}}, \tag{5.17}$$

respectively, where

- ρ_a is the air density, kg/m^3
- $c_{p,a}$ is the specific heat of air, J/kg-K
- r_{ac} is the aerodynamic resistance between the atmosphere and canopy, s/m
- r_{as} is the aerodynamic resistance between the atmosphere and bare soil, s/m
- $T_{a,r}$ is the temperature of the air at the first reference height (1.8 m), K

The aerodynamic resistance is described by [18]

$$r_{ax} = \frac{\{\ln[(z_{r2} - d + z_0)/z_0]\}^2}{k^2 u_{r2}}, \tag{5.18}$$

where

- ax = ac (air-canopy) or as (air-soil),
- z_{r2} is the second reference height (= 10), m
- z_0 is the surface roughness (= 0.028 h_c for the prairie [122]; = 0.015 for bare soil), m
- d is the zero plane displacement (= 0.71 h_c for the prairie [122]; negligible for bare soil), m
- h_c is the canopy height (= 0.6), m

- u_{r2} is the wind speed at the second reference height, m
- k is Von Karman's constant (= 0.4).

Latent Heat Transfer — Evaporation and Condensation

Evaporation occurs over the fraction of foliage that is covered by a film of water, while transpiration occurs over the fraction of foliage that is dry. The fraction of the foliage covered by a film of water is given by [106]

$$\begin{aligned} \delta_w &= \frac{W_r}{W_{r,\,max}}, \text{ if } e_{sat}(T_c) > e_a \\ &= 1, \qquad \text{otherwise} \end{aligned} \tag{5.19}$$

where

- $W_{r,\,max} = (0.2 \sim 0.5)$ LAI [106] is the maximum stored moisture on the foliage, kg/m^2
- $e_{sat}(T_c)$ is the saturation water vapor pressure at T_c, Pa
- e_a is the atmospheric water vapor pressure, Pa.

Evaporation from the canopy and bare soil are described by

$$\rho_l L_v E_c = veg L_v \rho_a \frac{q_{sat}(T_c) - q(T_a)}{r_{ac}} \delta_w \tag{5.20}$$

$$\rho_l L_v E_s = (1 - veg) L_v \rho_a \times \frac{RH_s q_{sat}(T_s) - q(T_a)}{r_{as}}, \tag{5.21}$$

respectively, where

- $q_{sat}(T_c)$ is the saturation specific humidity at T_c

- $q(T_a)$ is the atmospheric specific humidity at T_a
- RH_s is the relative humidity of the first soil layer.

The relative humidity is given by [92]

$$RH_s = \exp(-\Psi g / RT_s), \tag{5.22}$$

where

- Ψ is the suction of the first soil layer, m
- g is the acceleration due to gravity, m/s^3
- R is the gas constant of water vapor, J/kg-K.

Equations (5.20) and (5.21) also describe condensation which occurs when evaporation ceases.

Latent Heat Transfer — Transpiration

Transpiration is modeled as

$$\rho_l L_v E_{tr} = veg L_v \rho_a \frac{q_{sat}(T_c) - q(T_a)}{r_{ac} + r_c}(1 - \delta_w) \tag{5.23}$$

where

- r_c is the canopy resistance, s/m.

Transpiration stops if the air temperature is lower than the freezing point or if condensation occurs. The canopy resistance is primarily affected by incoming solar radiation, the air vapor pressure deficit, soil moisture (matric head), and air temperature [86], i.e.,

$$r_c = \frac{r_{c,\,min}}{LAI\ F_1(Q_{s,\,d})F_2(\theta_l)F_3(q_{sat})F_4(T_a)} \tag{5.24}$$

where $r_{c,\,min}$ is the minimum canopy resistance, s/m, and θ_l is the water content volume fraction.

The fractional parameters $F_x, x = 1, \ldots, 4$, are defined as follows [86].

$$F_1 = \frac{r_{c,\,min}/r_{c,\,max} + f}{1 + f} \tag{5.25}$$

$$F_2 = \min(1, 40/\Psi_{s,\,r}) \text{ [123]} \tag{5.26}$$

$$F_3 = 1 - 0.06(q_{sat}(T_a) - q_a), \quad \text{and } F_3 \geq 0.33 \tag{5.27}$$

$$F_4 = 1 - 1.6 \times 10^3 \times (298 - T_a) \tag{5.28}$$

where

- $r_{c,\,max}$ is the maximum canopy resistance (= 5000), s/m
- $f = 0.55\frac{2Q_{s,\,d}}{LAIQ_{sd1}}$ is a dimensionless term representing incoming photosythetically active shortwave radiation
- Q_{sd1} is 30 W/m^2 for trees to 100 W/m^2 for crops [54]
- $\Psi_{s,\,r}$ is the the minimum moisture suction of the soil layers within the rooting zone, m.

The amount of water extracted from the root zone due to transpiration is governed by the distribution of roots and the surrounding moisture profile. Similar to the approach of Verseghy et al [123], we compute the fraction of extracted water from the i^{th} soil layer using

$$F_{r,i} = \frac{Root_i(\Psi_{max,i} - \Psi_i)}{\sum_{i=1}^{N_r} Root_i(\Psi_{max,i} - \Psi_i)}, \tag{5.29}$$

where

- $Root_i$ is the fractional root volume within the i^{th} soil layer

- $\Psi_{max,i}$ is the soil moisture suction corresponding to the wilting point at the i^{th} soil layer

- Ψ_i is the soil moisture suction at the i^{th} soil layer.

$\Psi_{max,i}$ and Ψ_i are described by Liou and England [71, 72]. The fractional root volume below a given depth z is given by [123]

$$Root(z) = \frac{\exp(-3z) - \exp(-3z_r)}{1 - \exp(-3z_r)} \tag{5.30}$$

where

- z_r is the averaged canopy root depth (= 0.3), m.

The fractional root volume within the i^{th} soil layer is

$$Root_i(z) = Root(z_{i-1}) - Root(z_i), \tag{5.31}$$

where z lies between z_{i-1} and z_i — the depths of the top and bottom of the soil layer, respectively.

Numerical Scheme

We use the numerical scheme developed by Liou and England [70, 71] to solve Equations (5.1), (5.2), (5.3), (5.4), and (5.5) for the temperatures and moisture contents of the soil layers and two canopy layers. As shown in Figure 5.2, the soil profile is divided into N layers including N_r layers in the root zone. We typically use 40 soil layers in our simulations. The thickness of the first layer is 5 mm, and the thicknesses of the other layers increase exponentially with depth. To increase computational efficiency, the time step is adjustable based upon two factors, the speed of convergence

and the strength of the weather forcings (solar heating and precipitation). For example, the time step is about 2 to 3 minutes when there is no precipitation and solar radiation is less than 10 W/m^2. Otherwise, it is assigned a value of several tens of seconds.

5.2.3 The Radiobrightness Module

Dielectric Properties of Moist Soils

We estimate the dielectric properties of moist soils with a five-component mixture model of soil solids, air, free water, bound water, and ice. The dielectric properties are functions of temperature and moisture content/state. They were discussed in our previous work [70, 71], and will not be re-addressed here.

Dielectric Properties and Optical Thickness of the Canopy

The relative permittivity of a wet canopy is found using the dual-dispersion model of Ulaby and El-Rayes [120], i.e.,

$$\begin{aligned} \epsilon_{wg} &= \epsilon_r + v_{fw}[4.9 + \frac{75}{1+jf/18} - j\frac{18\sigma}{f}] \\ &\quad + v_{bw}[2.9 + \frac{55}{1+(jf/0.18)^{0.5}}], \end{aligned} \tag{5.32}$$

where

- $\epsilon_r = 1.7 - 0.74m_g + 6.16m_g^2$ is the residual dielectric constant, and m_g is the gravimetric moisture constant of the wet grass, kg/kg
- $v_{fw} = m_g(0.55m_g - 0.076)$ is the volume fraction of free water in the grass
- $v_{bw} = 4.64m_g^2/(1 + 7.36m_g^2)$ is the volume fraction of bound water in the grass

- $\sigma = 1.27$ is the ionic conductivity of the free water solution, S/m
- f is the frequency, GHz.

While the Ulaby and El-Rayes model was based upon dielectric measurements of corn leaves, we are unaware of a model that would be more suitable for grass.

Subsequently, we can find the refractive index of the wet canopy by

$$n_{wg} = \sqrt{\epsilon_{wg}} \tag{5.33}$$

and the total refractive index of the air-grass mixture layer using an additive approach [32]:

$$n_t = 1 + v_{wg} n_{wg}, \tag{5.34}$$

where

- $v_{wg} = 9.26 \times 10^{-3} e^{-z/0.1149}$ is the volume fraction of the wet grass.

Finally, the optical thickness of the air-grass mixture layer can be determined, i.e.,

$$\tau_0 = -\int_0^{\infty} 2k_0 \kappa dz \tag{5.35}$$

where

- k_0 is the vacuum wavenumber, 1/m
- κ is the imaginary part of the total refractive index.

For a canopy layer of height h_c, Equation (5.35) becomes

$$\begin{aligned} \tau_0 &= -\int_0^{h_c} 2k_0 \kappa dz \\ &= 0.0022128 k_0 \sqrt{\epsilon_{wg}} [e^{-h_c/0.1149} - 1] \end{aligned} \tag{5.36}$$

where we have applied Equation (5.34) to perform the integration.

The Radiative Transfer Model

The radiative transfer model used for this study is similar to the England and Galantowicz [32] approach. As shown in Figure 5.3, the total model brightness is comprised of four components: Tb_{s}, the soil brightness attenuated by one trip through the canopy; $Tb_{\mathrm{c,\,d}}$, the downwelling canopy brightness reflected by the soil and attenuated by one trip through the canopy; $Tb_{\mathrm{c,\,u}}$, the upwelling canopy brightness; and Tb_{sky}, the sky brightness reflected by the soil and attenuated by two trips through the canopy. That is,

$$Tb_{\mathrm{s}} = T_{\mathrm{s,\,e}}(1 - R_{\mathrm{p}}(\mu))e^{-\tau_0/\mu} \tag{5.37}$$

$$Tb_{\mathrm{c,\,d}} = T_{\mathrm{c,\,e}}(1 - e^{-\tau_0/\mu})R_{\mathrm{p}}(\mu)e^{-\tau_0/\mu} \tag{5.38}$$

$$Tb_{\mathrm{c,\,u}} = T_{\mathrm{c,\,e}}(1 - e^{-\tau_0/\mu}) \tag{5.39}$$

$$Tb_{\mathrm{sky}} = T_{\mathrm{sky}}R_{\mathrm{p}}(\mu)e^{-2\tau_0/\mu} \tag{5.40}$$

where

- $T_{\mathrm{s,\,e}}$ is the effective emitting temperature of the soil [70, 71], K
- R_{p} is the Fresnel reflectivity of the moist soil for polarization p
- μ is the cosine of the SSM/I incidence angle of 53^0
- $T_{\mathrm{c,\,e}}$ is the effective emitting temperature of the canopy, K.

The total model brightness is

$$Tb = Tb_{\mathrm{s}} + Tb_{\mathrm{c,\,d}} + Tb_{\mathrm{c,\,u}} + Tb_{\mathrm{sky}}. \tag{5.41}$$

Microwave emission comes from all parts of the canopy. Since the canopy is divided into two layers in the current study, we take their average temperature as the effective

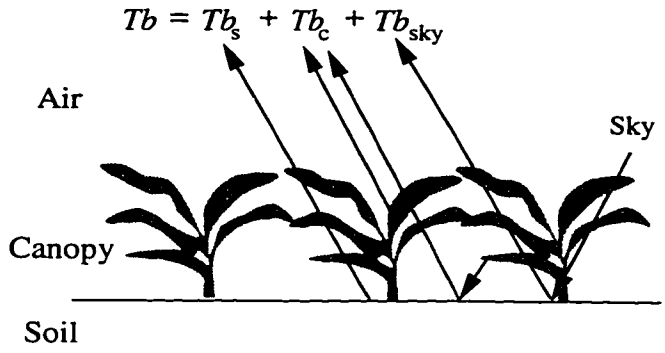

Figure 5.3: Radiobrightness components of the 1dH/R model.

emitting temperature, i.e.,

$$T_{c,e} = \frac{1}{2}(T_c + T_t). \tag{5.42}$$

5.3 VALIDATION OF GRASSLAND MODEL

We validated the 1dH/R model by driving the model with observed weather and downwelling radiation during REBEX-1 and comparing model predictions of temperatures, heat flux, and radiobrightness with equivalent observations. For the 14 day period from day 287 to day 300 of REBEX-1, the grass was green and there was no snow cover.

5.3.1 REBEX-1

REBEX-1 was conducted on the grounds of the US. Geological Survey's EROS Data Center near Sioux Falls, South Dakota, at 43°43'N latitude and 96°30'W longitude from October, 1992 through April, 1993. Measurements included horizontally polarized radiobrightnesses and sky brightnesses at the SSM/I frequencies, soil temperatures at depths of 2, 4, 8, 16, 32, and 64 cm, soil heat flux at 2 cm depth, 10 m wind speed, air temperature at 1.8 m height, air relative humidity, downwelling shortwave radiation, net radiation, precipitation, and thermal infrared (TIR) canopy

temperature. Soil moisture was measured only occasionally.

5.3.2 Initial Conditions

Key initial conditions are the temperature and moisture profiles in soil and canopy. The 1dH/R model was run beginning at 3 p.m. on day 287. At that time, soil and grass temperatures were measured and core samples were taken from the REBEX-1 site to determine moisture profiles. Reliable initial conditions not only allow rapid convergence of algorithms, but also reduce propagation errors in the algorithm.

Soil Moisture

Six soil columns were collected with a 7.2 cm (inner) diameter cylindrical coring tool between day 287 and day 290. Soil moisture contents at 0-2, 2-4, 4-6, 6-8, and 8-10 cm depths were measured. The average of the 30 moisture contents (6 $\times$ 5) is 34.1 % and the bound water is 3.5 %. The method of estimating the bound water has been discussed by Liou and England [70]. Soil moistures at two arbitrary depths between 9 cm (average of 8 and 10 cm) and 1 m were linearly interpolated to constrain moisture content within reasonable values. Finally, the complete initial moisture profile was determined using cubic spline interpolation [94].

Soil Temperature

Soil temperatures were measured at 6 points between the surface and 64 cm. All of these depths experience diurnal effects so that none exhibits the constant energy

and moisture fluxes for that are characteristics of the lower boundary of the model. We used the annual thermal model [70] to provide temperatures and heat fluxes for deeper soil layers that were appropriate for the time-of-year. The temperature predicted by the annual thermal was first matched with the measured soil temperature at 64 cm. The difference between the predicted and measured temperatures was used to adjust the temperature profile below 64 cm. This difference was about 1 K. A cubic spline was used to estimate soil temperatures between 0 and 64 cm.

Canopy Temperature and Moisture

Grass samples were taken over many of the core samples. These were dried at 70° C for 9 days. The average column density of the six dry canopy samples was 2.281 kg/m^2 and the corresponding average moisture was 1.4 kg/m^2. The total wet biomass of the canopy was 3.681 kg/m^2, and was regarded as constant throughout the 14 day simulation period. This should be an acceptable assumption for the 14 day period because vegetation maintains its moisture content even as soil moisture varies within relatively broad limits.

The surface of the foliage holds extra moisture depending upon antecedent weather, latent heat exchange with the atmosphere, and the Leaf Area Index (LAI). We arbitrarily chose a value of 0.14 kg/m^2 as the initial moisture on foliage. A higher value of this initial foliage moisture was found to give an initially smaller day-night variation in the canopy temperature, but had a negligible effect on the canopy temperature after the second day of the simulation. We assumed that the initial temperature of the thatch was the average of the soil surface temperature and the TIR canopy temperature.

Leaf Area Index

We used non-scattering radiative transfer theory (Beer's law) to estimate the shortwave radiation absorbed by the canopy as a function of LAI. Since this absorbed radiation controls the canopy temperature, a correct value of LAI is important for reliable predictions of canopy temperature. LAI was not available from REBEX-1. We estimated LAI from a survey of the literature, and the subsequent performance of the 1dH module.

LAI values for a variety of plant species have been reported (i.e., Table 5.1). The prairie grassland at the REBEX-1 site was fully developed, denser and taller than the Konza prairie so that the LAI should be greater than 2.18.

Plant Type	LAI Range	Investigators
Rice	$2.19 \sim 4.97$	Shibayama and Akiyama [108]
Rice	$1.16 \sim 5.31$	Shibayama et al [109]
Wheat	$0.39 \sim 2.42$	Richardson and Wiegand [98]
Corn	$1.33 \sim 3.32$	[98]
Cotton	$0.42 \sim 3.60$	[98]
Sorghum Canopy	3.35	[98]
Konza Prairie	$0.12 \sim 2.18$	Middleton [76]
Prairie	$0.3 \sim 3.0$	Verma et al [122]
Alfalfa	3.8	Paloscia and Pampaloni [89]

Table 5.1: Observations of LAI for a variety of vegetation.

The 1dH module was run using 4 values of LAI between 2 to 5. We found that the module gives the best fit between predictions and observations when the LAI is 3. In general, the canopy temperature increases for a given time-of-day with increasing LAI.

Minimum Canopy Resistance

Verseghy et al [123] found that low values of the minimum canopy resistance ($25 < r_{c,\,min} < 100$s/m) are appropriate for dense, green, unstressed canopies. A higher value of canopy resistance ($r_{c,\,min} = 450$s/m) is appropriate for mature canopies [86]. Our grass was certainly mature and probably senescent. We set $r_{c,\,min}$ to 400 in our simulations.

5.3.3 Downwelling Longwave Radiation and Canopy Albedo

Downwelling longwave radiation, an important forcing for the 1dH module, was not measured during REBEX-1. We estimated values based upon the observed downwelling shortwave radiation, net radiation and TIR canopy temperature, and the model-estimated canopy albedo. The measured net radiation is

$$\begin{aligned} R_{net} &= Q_{s,\,d} + Q_{l,\,d} - Q_{s,\,u} - Q_{l,\,u} \\ &\quad - \text{veg}\,e_c\sigma T_c^4 - (1 - \text{veg})e_s\sigma T_s^4 \end{aligned} \tag{5.43}$$

where

- $Q_{s,\,u}$ is the up-welling shortwave radiation, W/m^2
- $Q_{l,\,u}$ is the up-welling longwave radiation, W/m^2 due to reflected $Q_{s,\,u}$.

Equation (5.43) gives

$$Q_{l,\,d} = R_{net}/e_c + \sigma T_c^4 - (1 - A_c)Q_{s,\,d}/e_c \tag{5.44}$$

where we have applied

- $Q_{s,\,d} - Q_{s,\,u} = (1 - A_c)Q_{s,\,d}$

- $Q_{l,\,d} - Q_{l,\,u} = e_c Q_{l,\,d}$
- veg = 1, which is appropriate for the prairie grass of this study with a high wet biomass of 3.681 kg/m^2.

The albedo, A_c, is the only unknown on the right-hand side of Equation (5.44); so we can estimate $Q_{l,\,d}$ given a knowledge of A_c. We determine the albedo as follows:

1. Estimate the spectral reflectance of the canopy at 0.662 and 0.826 microns using the Ahmad and Deering [2] model of reflectance, i.e.,

$$R_x = A_1 + A_2 \cos Z + A_3 \cos^2 Z \tag{5.45}$$

   where A_1, A_2, and A_3 are model coefficients, and the subscript x = r (red = 0.662 microns), or NIR (near infrared = 0.826 microns).

2. Find the spectral reflectance of the canopy in the green band by

$$R_g = R_r + 3\%. \tag{5.46}$$

   Reflectance is higher for the green band than for the red band over the prairie by a few % [67].

3. Compute the albedo using the inversion model of Brest and Goward [10] for vegetated land, i.e.,

$$A_c = 0.526 R_g + 0.418 R_{NIR}. \tag{5.47}$$

The maximum and minimum of the model-estimated albedos in the 2-week simulation period are 0.398 and 0.202, respectively. This range of albedos should be reasonable. Ranson et al [97] have found the albedo of grass to lie between about 20 % to 30 %. Hasson [46] reported albedos between 21 % and 35 % for crops (pepper and tomato).

To evaluate the above method for estimating down-welling longwave radiation $Q_{l,d}$, we have compared its predictions with those of models developed by Brutsaert [13], Satterlund [104], and Kahle [59]. These models are based upon known air temperature and humidity, i.e.,

$$Q_{l,d} = 1.24\sigma T_a^4 (100 e_v / T_a)^{1/7} \text{ [13]} \tag{5.48}$$

$$Q_{l,d} = 1.08\sigma T_a^4 (1 - e^{-e_v T_a / 20.16}) \text{ [104]} \tag{5.49}$$

$$Q_{l,d} = \sigma T_a^4 (0.61 + 0.00433\sqrt{e_v \mathrm{RH}_a}) \text{ [59]} \tag{5.50}$$

where

- e_v is the water vapor pressure, Pa
- T_a is the air temperature at screen height, K
- RH_a is the air relative humidity.

Figure 5.4 shows the down-welling longwave radiation obtained using Equations (5.44), and (5.48)–(5.50). The lower limit of $Q_{l,d}$ is obtained using Equation (5.44), and an albedo of 0.1 (reference case 1), while the upper limit is found assuming an albedo of 0.4 (reference case 2). Given the upper and lower limits of $Q_{l,d}$, we may determine whether or not the model predictions fall within a reasonable range.

1. During Nighttime:

   $Q_{l,d}$ is independent of albedo since the shortwave radiation is zero. Results from the two reference cases overlap and Equation (5.44) gives the best estimate of downwelling longwave radiation. The Satterlund [104], Brutsaert [13], and Kahle [59] methods generally underestimate $Q_{l,d}$ compared to the two reference cases, except that the Satterlund [104] method overestimates $Q_{l,d}$ near days 296 and 297.

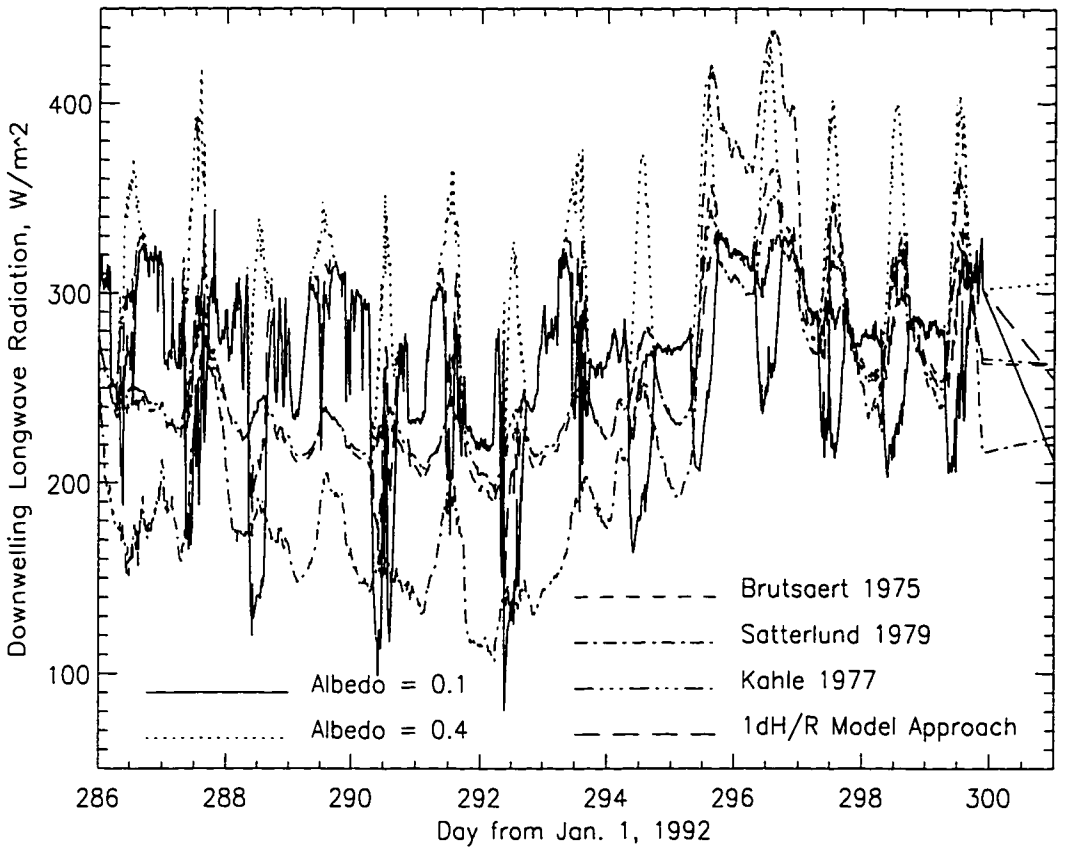

Figure 5.4: Predicted $Q_{l,d}$ using the current proposed approach and the models proposed by Brutsaert [1975], Satterlund [1979], and Kahle [1977].

2. During Daytime:

   Results from the the Satterlund [104], Brutsaert [13], and Kahle [59] methods, and the proposed approach all fall within the envelope enclosed by the two reference curves. The exception is that the Satterlund [104] method again overestimates $Q_{l,\,d}$ near days 296 and 297. The Brutsaert [13], the Kahle [59] methods, and the 1dH module approach always give the reasonable values of $Q_{l,\,d}$.

We chose the 1dH module approach to estimate $Q_{l,\,d}$ because the approach gives the best estimate of $Q_{l,\,d}$ during nighttime and always predicts reasonable $Q_{l,\,d}$ values during daytime. Table 5.2 lists the average of the differences (AD) between the model-predicted downwelling longwave radiation and the $Q_{l,\,d}$ obtained from the first reference case. The table also lists the corresponding standard deviations (SD). We computed the AD using

$$\mathrm{AD} = \frac{\sum_{i=1}^{N_o}[(Q_{l,\,d})_p - (Q_{l,\,d})_x]}{N_o} \tag{5.51}$$

and the SD using

$$\mathrm{SD} = \frac{\sqrt{\sum_{i=1}^{N_o}[(Q_{l,\,d})_p - (Q_{l,\,d})_x]^2}}{N_o}, \tag{5.52}$$

where

- N_o is the number of observations (= 995)
- $(Q_{l,\,d})_p$ is the predicted $Q_{l,\,d}$ from Equations (5.44), and (5.48)–(5.50)
- $(Q_{l,\,d})_x$ is the predicted $Q_{l,\,d}$ from the reference case of albedo x (x = 0.1 or 0.4).

As in Table 5.2, Table 5.3 shows the AD and SD, but the comparisons are made between the model-predicted $Q_{l,\,d}$ and the second reference case of albedo 0.4.

Method	AD, W/m^2	SD, W/m^2
Brutsaert [13]	-14.5	98.8
Satterlund [104]	-36.5	144.9
Kahle [59]	-16.4	99.8
1dH/R	16.5	32.9

Table 5.2: The AD and SD from comparisons between the model-predicted $Q_{l,\,d}$ and reference case 1 (Equation (5.44) with albedo = 0.1).

Method	AD, W/m^2	SD, W/m^2
Brutsaert [13]	-51.0	103.4
Satterlund [104]	-72.9	162.8
Kahle [59]	-53.0	106.5
1dH/R	-20.0	40.1

Table 5.3: The AD and SD from comparisons between the model-predicted $Q_{l,\,d}$ and reference case 2 (Equation (5.44) with albedo = 0.4).

The two tables show that the AD values are all negative using the Satterlund [104], Brutsaert [13], and Kahle [59] methods, while the SD values are all large. The negative values of AD are caused by the consistent nighttime biases of Equations (5.48)–(5.50) (Figure 5.4). Although the Satterlund [104] method overestimates $Q_{l,\,d}$ on days 296 and 297, its strong nighttime underestimates result in the most negative AD and the largest SD.

5.3.4 Comparing the Model to Observations

We compare the 1dH/R model-predicted and measured soil heat flux at 2 cm depth, soil temperatures at 2, 4, 8, 16, 32, and 64 cm depths, canopy temperature, and 19, and 37 GHz horizontally polarized radiobrightnesses. In general, the model predictions agree with the corresponding measured values very well.

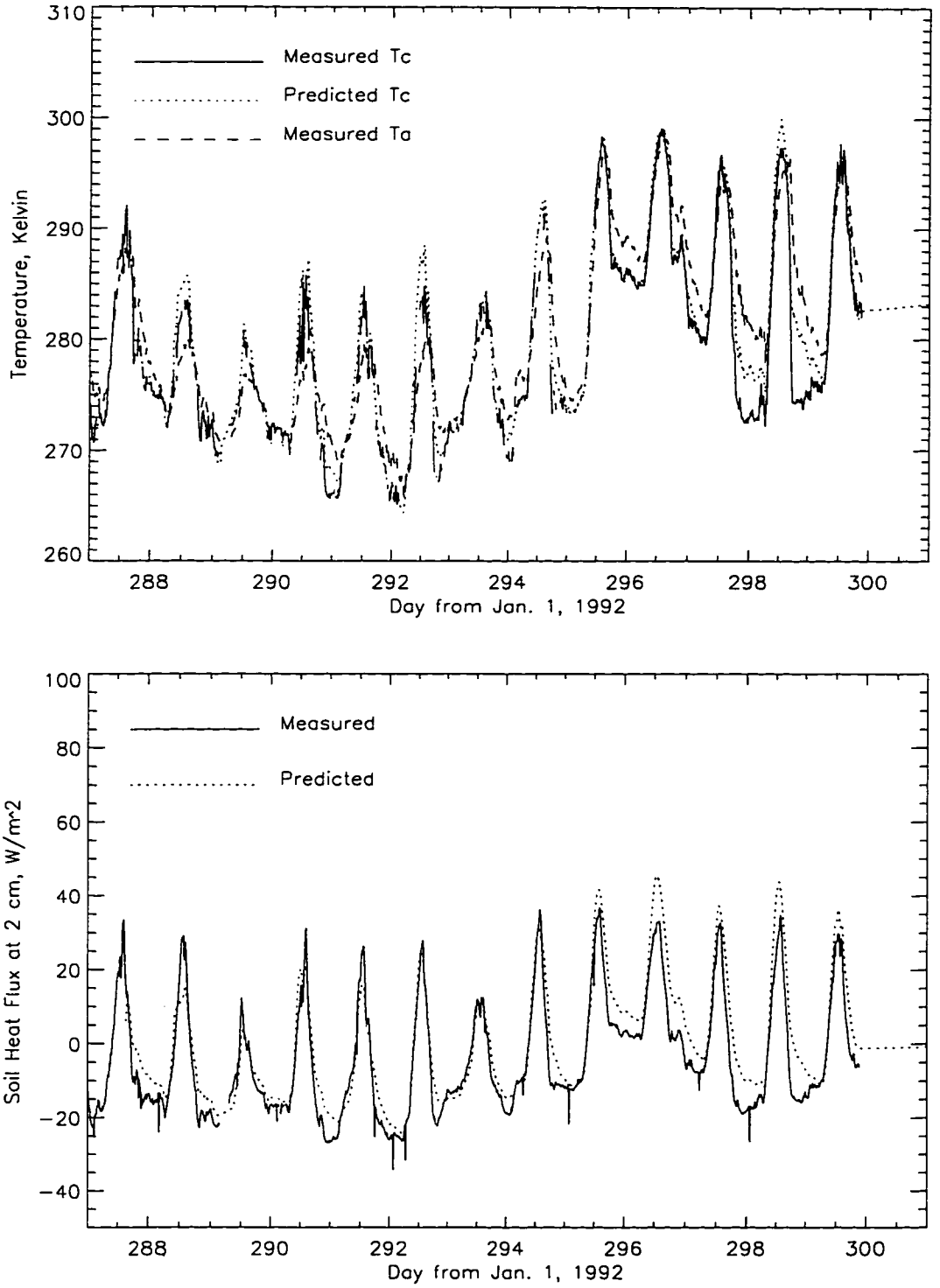

Figure 5.5: (a) Measured canopy and air temperatures, and predicted canopy temperature. (b) Measured and predicted soil heat fluxes at 2 cm depth.

Thermal and Hydrologic Signatures

Figure 5.5 shows the measured and predicted canopy temperatures as well as the measured air temperatures. The predicted canopy temperature agrees with the measured temperature except that there are differences of 2 - 3 K near the diurnal peaks of solar heating on days 288, 292, and 298. The AD and SD of the model-predicted versus measured canopy temperatures are 1.1 and 1.9 K, respectively. Estimates of AD and SD are computed similarly to Equations (5.51) and (5.52), respectively.

Figure 5.5 (a) also shows that the diurnal variation is generally larger for the canopy temperature than for the air temperature. This is because the canopy is heated by solar radiation during the day and cools through longwave radiation at night, and it is primarily the canopy that heats and cools the air.

Figure 5.5 (b) shows the 14-day soil heat flux at 2 cm depth versus daynumber. The modeled heat flux closely mimics the measured heat flux signature. For the first four days of the simulation, the model sightly underestimates the diurnal peaks of the soil heat flux. This could be due to the use of too high a value of LAI or too low a shortwave transmissivity (too large an extinction coefficient) so that too little shortwave radiation reaches the soil. The former should be the dominant factor because we set the extinction coefficient to be $0.4/\cos Z$ (Equation (5.11)) and that leads to low-end values of the coefficient for solar radiation. Verseghy et at [123] suggested extinction coefficients of $0.4/\cos Z$ and $0.5/\cos Z$ for near-infrared and visible radiation, respectively.

The model begins to overestimate the soil heat flux on day 295. These increasing differences between the predictions and observations may be caused by accumulated algorithm errors. That is, constant updating of soil temperature and moisture may be needed to obtain reliable predictions in a long term simulation. This is beyond

the scope of the current presentation.

Although the predictions diverge from the observations over time, the degree of divergence is small. The errors are only a few watts per square meter. The AD between the predicted and measured soil heat fluxes is 4.6 W/m^2 and the corresponding SD is 6.9 W/m^2.

Figure 5.6 shows the 14-day soil temperatures at 2, 4, 8, 16, 32, and 64 cm depths versus daynumber. The 1dH module slightly overestimates soil temperatures. This is associated with the overestimates of net downward soil heat flux. The figure also shows that near-surface soils are more easily affected by weather forcing than are the deeper soils. The AD and SD based upon comparisons between measured and predicted soil temperatures at 2, 4, 8, 16, 32, and 64 cm depths are listed in Table 5.4. Both AD and SD decrease with depth because of the constant energy and moisture flux constraints at the lower boundary.

Depth	AD, K	SD, K
2 cm	1.9	2.1
4 cm	1.8	2.0
8 cm	1.6	1.7
16 cm	1.3	1.5
32 cm	1.1	1.2
64 cm	0.6	0.8

Table 5.4: The AD and SD based upon comparisons between measured- and predicted-soil temperatures at 2, 4, 8, 16, 32, and 64 cm depths.

Radiobrightness

Figure 5.7 shows the predicted 1.4 GHz, and the measured and predicted 19 and 37 GHz horizontally polarized radiobrightnesses. The predicted and measured 19 GHz radiobrightnesses match very well. The major differences occur only when the corresponding canopy temperature differences are large. The AD between the

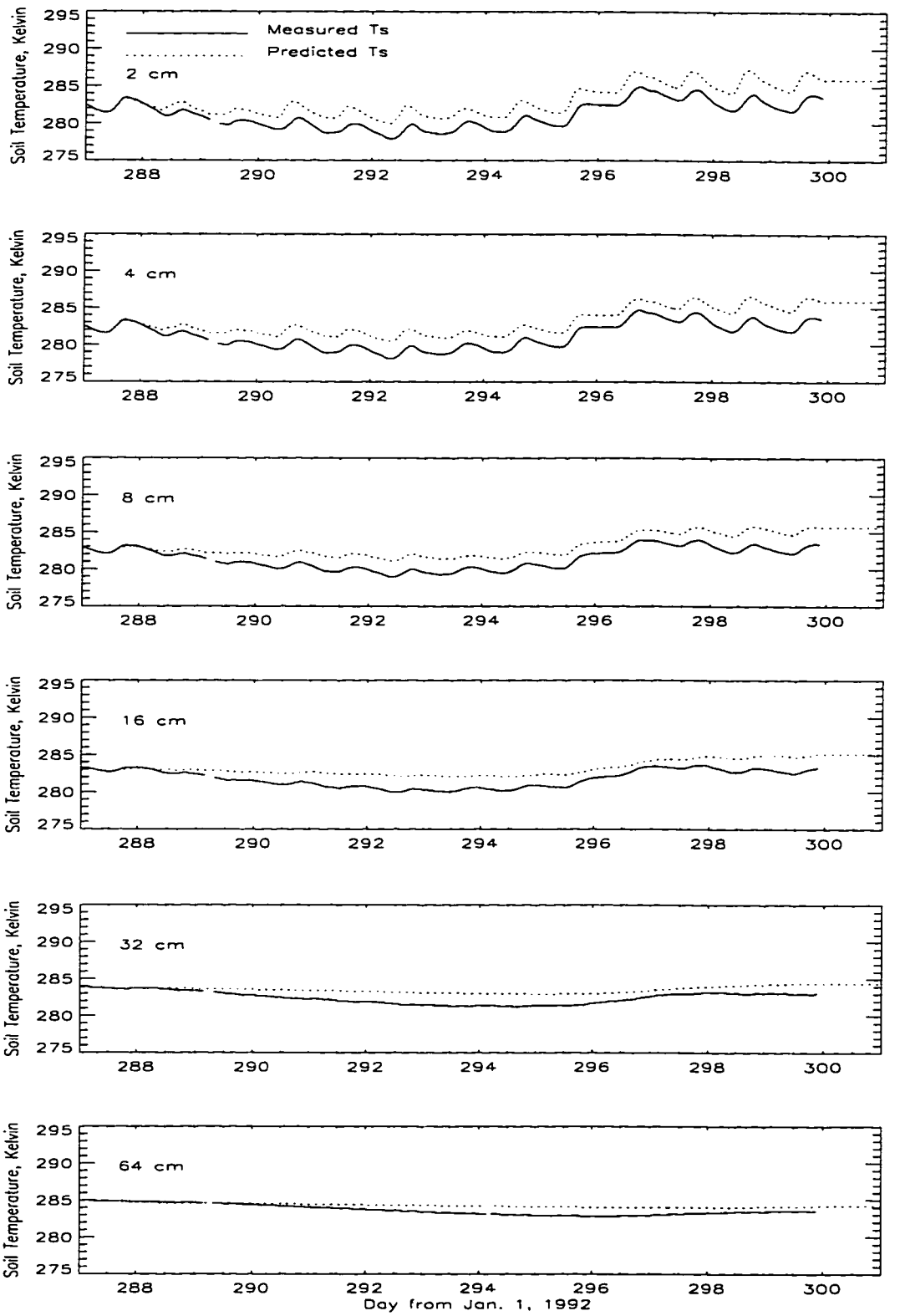

Figure 5.6: Soil temperatures at 2, 4, 8, 16, 32, and 64 cm depths.

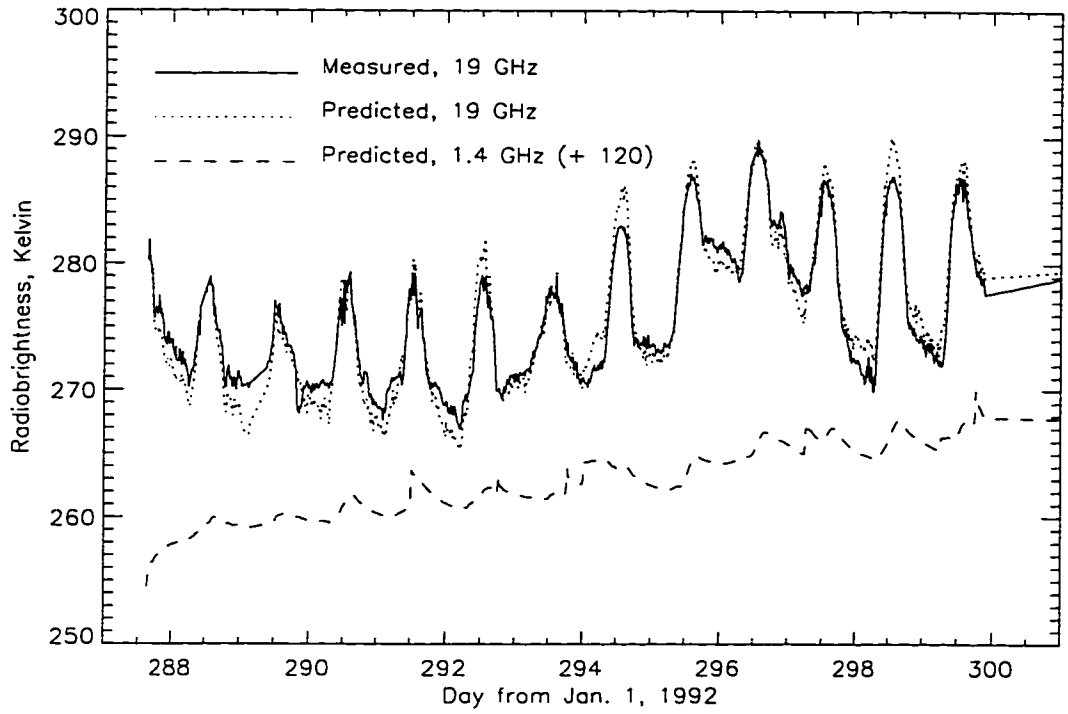

Figure 5.7: 1.4, 19, and 37 GHz horizontally polarized radiobrightnesses.

predicted and measured 19 GHz radiobrightnesses is −0.06 K. The corresponding SD is 1.1 K.

We also computed the 1.4 GHz radiobrightness and found that radiobrightness at L-band is sensitive to soil moisture, but radiobrightness at 19 and 37 GHz is not sensitive to soil moisture. The increase in L-band radiobrightness is about 12 K for the 14-day simulation period and the decrease in soil moisture is about 7 % for the same period.

We do not show the comparisons for the 37 GHz radiobrightness because scatter darkening becomes significant causing the the 1dH/R model to overestimate the 37 GHz radiobrightness by about 6.0 K. The corresponding SD is 2.5 K.

5.4 SIMULATION OF A 90-DAY DRY-DOWN

The 1dH/R model was run for a 60-day dry-down simulation in summer to study the sensitivity of radiobrightness to soil moisture over a 100 % grass-cover area. The simulation differs from the validation study in the following two respects. First, the model is driven by climatological data as discussed in Liou and England [70, 71]. Second, the simulation started on day 173 (June 23, 1992) so that some of the initial conditions needed to be changed.

The differences in initial conditions between the dry-down simulation and the model validation cases were:

1. The soil moisture is initialized to be a uniform profile of 38 %.

2. The soil temperature profile for the time-of-year is derived entirely from the annual thermal model by Liou and England [70].

3. The initial canopy temperature is assumed to be the air temperature from the climatological data.

4. The minimum canopy resistance is arbitrarily chosen to be 200 s/m, which is half the 400 s/m used in the model validation case.

5. Sky brightness is not accounted for when we compute radiobrightnesses. This may modify total radiobrightnesses by a few degrees.

We compare the predictions from the 1dH/R 60-day dry-down simulation for prairie grass with those from the 1dHbu/R model for bare soils [71]. We also examine the feasibility of using the RTI measure of soil moisture in prairie grassland.

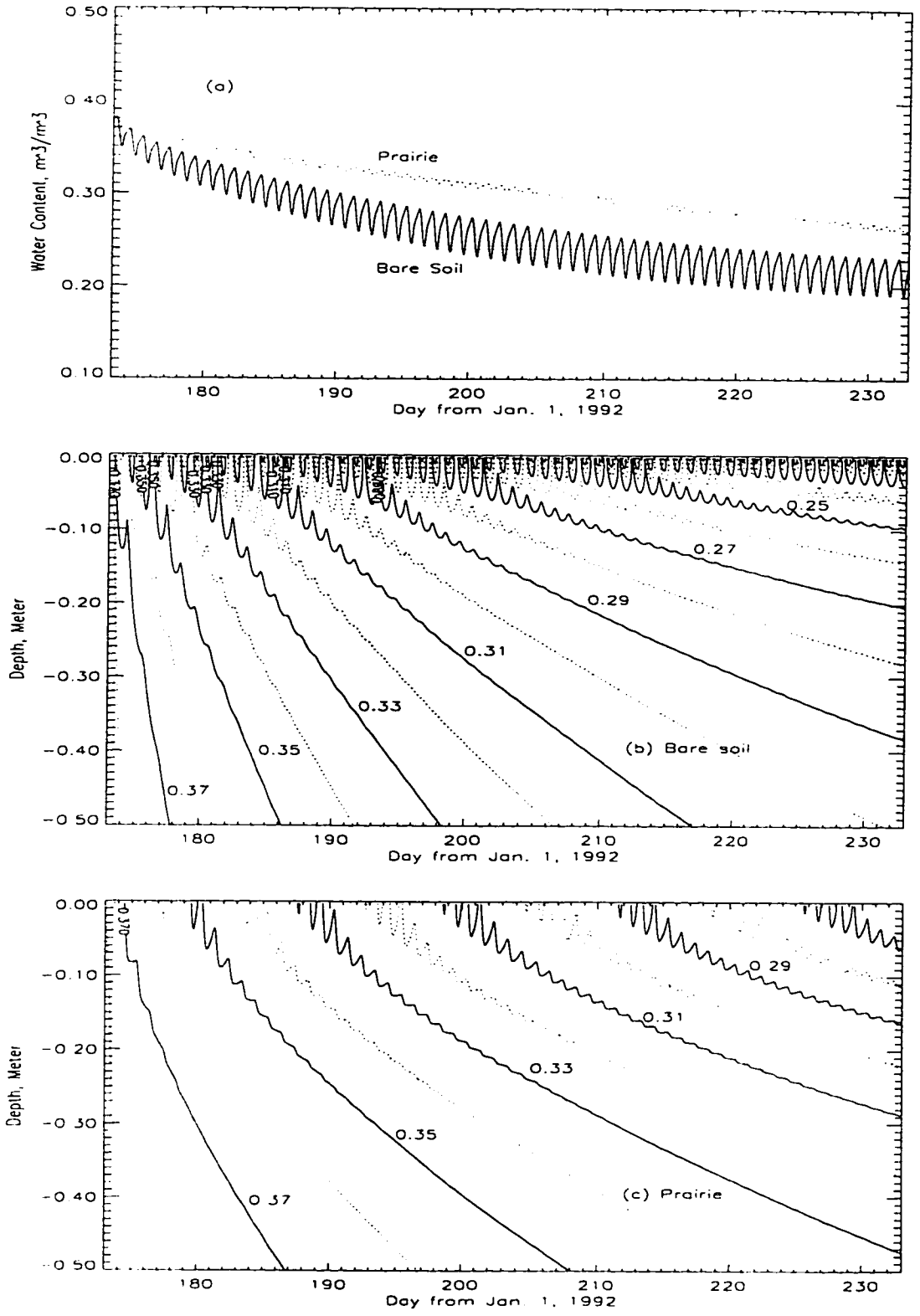

Figure 5.8: (a) Soil moisture content at the surface for the prairie and bare soil cases. (b) Soil moisture profile for the bare soil case. (c) Soil moisture profile for the prairie case.

5.4.1 Thermal and Hydrologic Signatures

Figure 5.8 (a) shows the surface moisture content over the 60-day period for both the prairie and the bare soil cases. For the bare soil case, the surface moisture content exhibits small diurnal oscillations with a rapidly decreasing average. Diurnal peaks appear during nighttime due to condensation, and valleys appear during daytime due to evaporation. For the prairie case, surface moisture content remains almost constant over a diurnal cycle, but decreases more moderately with daynumber. The decrease in moisture content is due to transpiration. Because the transfer resistance for moisture is greater for the prairie case than for the bare soil case, surface moisture content decreases more slowly for the former than for the latter. At the end of the 60-day simulation, the decrease in surface soil moisture is about 17 % for the bare soil case, while it is only 11 % for the prairie case since re-charge of the surface moisture is only from the upward movement of a small amount of moisture. Unlike the bare soil case, condensation does not deposit moisture on the soil surface so that the diurnal variation in surface moisture is much larger for the bare soil case ($\sim$ 4 %) than for the prairie case ($\sim$ 0.5 %).

Figures 5.8 (b) and (c) show constant-moisture curves as a function of depth and day number for the 60-day period for bare soil and prairie grass, respectively. From a comparison between the two figures, we see that the vegetation increases the resistance for latent heat transfer from soil to the air so that drying in soils is less pronounced for prairie grass than for bare soil. Constant-moisture curves appear to propagate downward more rapidly for bare soil. Both cases exhibit an expected long term moisture loss at the surface and a net upward movement of water in the soil and across the land-air boundary, i.e., evaporation and transpiration dominate over condensation in the latent heat exchange at the land-air interface for the bare soil

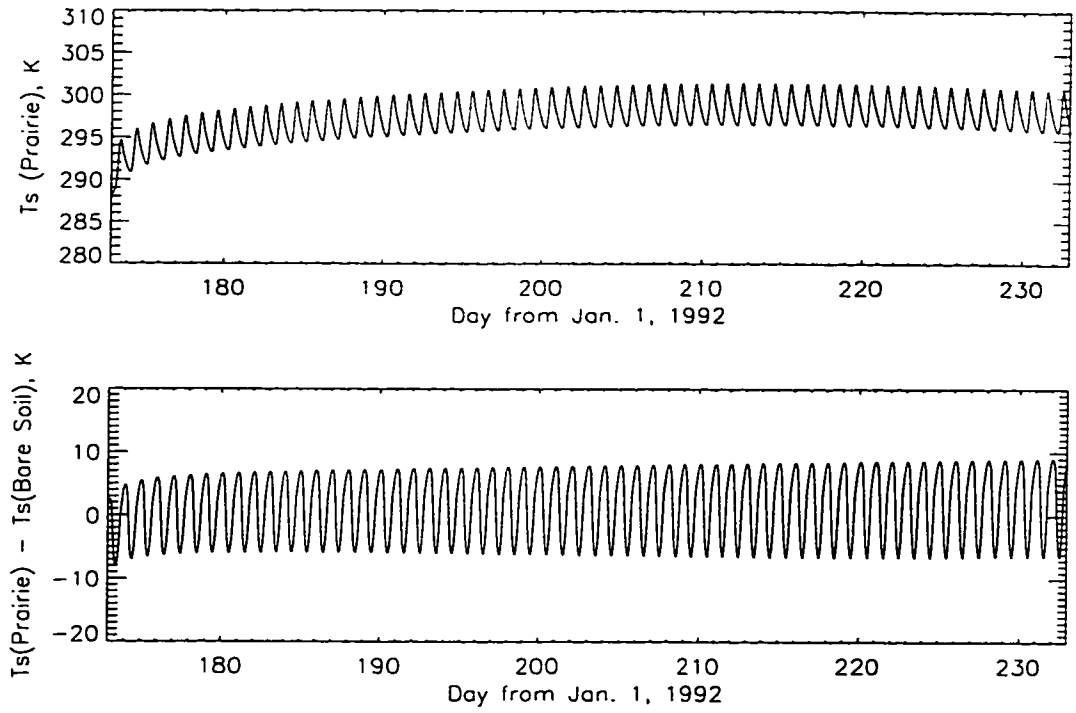

Figure 5.9: (a) Surface temperature for the prairie case. (b) Difference in surface temperatures between the prairie and bare soil cases.

and prairie cases.

Surface temperatures for prairie grass are shown in Figure 5.9 (a). There is a weak diurnal oscillation with a slowly increasing average. The amplitude of the diurnal oscillation remains almost constant at about 5 Kelvins for the entire simulation period.

The difference in surface temperatures between prairie grass and bare soil is shown in Figure 5.9 (b). There is a moderate diurnal oscillation with a slowly increasing amplitude of 12 Kelvins on day 174 to 16 Kelvins on day 232. This is an indication that prairie vegetation is an effective thermal insulating medium.

Figure 5.10 shows the soil temperature profiles on day 173 (a) for bare soil and (b) for prairie grass. For both cases, notable characteristics are 1) isotherms are created after sunrise and start to merge some time after peak insolation and 2) temperature

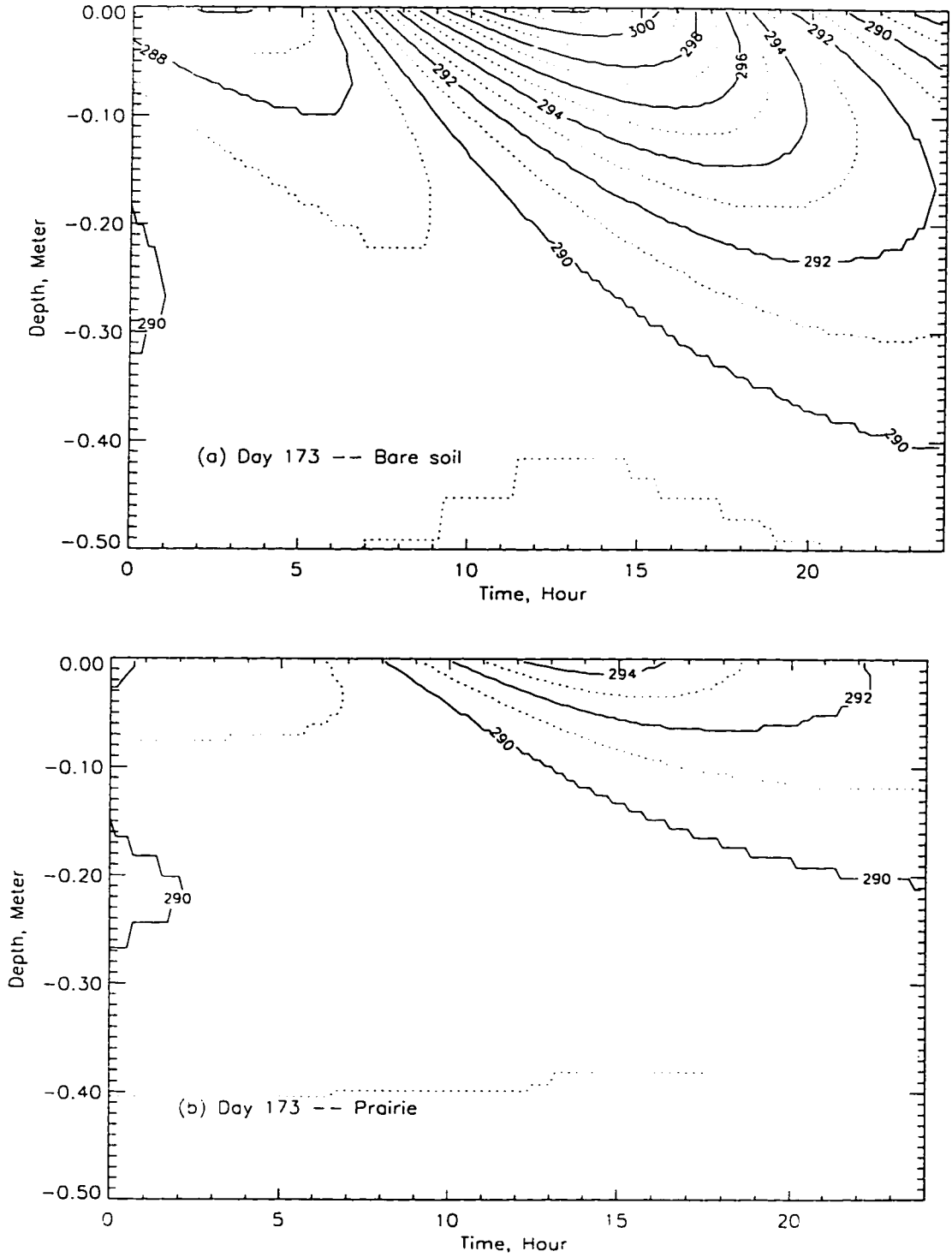

Figure 5.10: Soil temperature profiles on 06/22 (a) for the bare soil case and (b) for the prairie case.

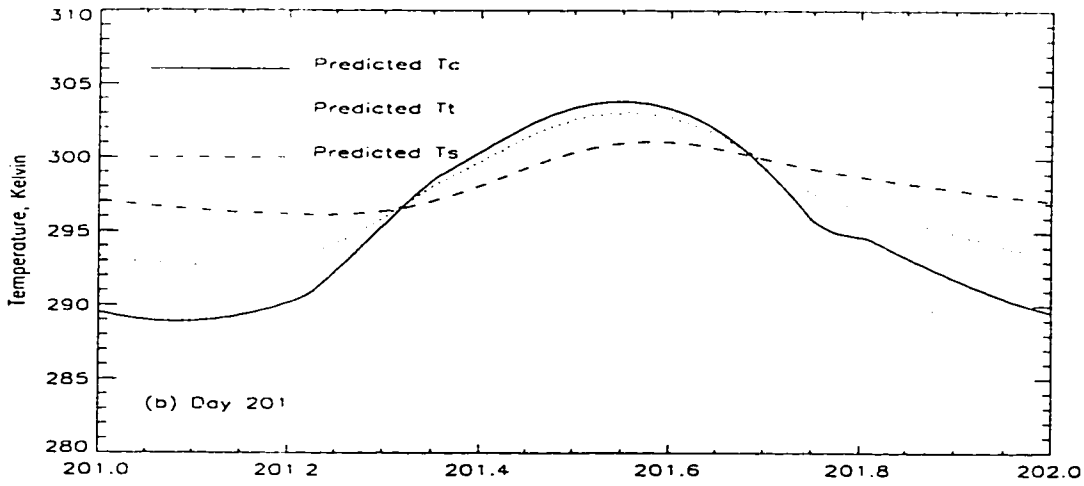

Figure 5.11: Temperature for the canopy, thatch, and surface on day 201.

gradients in the first few centimeters are much larger during the day than during the night. A comparison between the two figures demonstrates two major differences. First, diurnal thermal pulses penetrate approximately 50 centimeters for bare soil, but only about 25 centimeters for prairie grass. Second, the number of 1-K isotherms for bare soil is more than double that of prairie grass. That is, the vertical temperature gradient for the former is more than double that of the latter. This significant contrast in temperature gradients is due to the insulating effect of the vegetation. All diurnal isotherm patterns for the 60-day period were similar so that we have presented only the 06/22 isotherms.

Figure 5.11 shows the temperatures for the canopy, thatch, and surface on day 201. The diurnal variations in temperature are largest for the canopy, and smallest for the surface. They are approximately 15, 10, and 5 Kelvins for the canopy, thatch, and surface, respectively. We present only the day 201 temperatures because they are typical for the entire 60-day simulation period.

5.4.2 Radiobrightness

Terrain radiobrightnesses are computed using Equation (5.41), but sky brightnesses are omitted. Sky brightnesses at 1.4, 19, and 37 GHz have a negligible effect on sensitivity studies of radiobrightness to soil moisture since they are usually small (less than several Kelvins). Brightnesses from the soil (Equation (5.37)) and vegetation (Equations (5.38) + (5.39)) make up the total model brightness here.

Figure 5.12 shows the predicted horizontally-polarized radiobrightnesses at 1.4 , 19 and 37 GHz versus daynumber for prairie grass. We observe three characteristics. First, radiobrightnesses at 19 and 37 GHz exhibit diurnal oscillations with an extremely slowly increasing average before about day 210, and with a decreasing average after that. Second, L-band radiobrightnesses exhibit diurnal oscillations with a rapidly increasing average from about 143 Kelvins on day 173 to 163 Kelvins at the end of the 60-day period. Note that L-band radiobrightnesses are shown shifted by + 120 Kelvins for easier comparison with the other radiobrightness signatures. Third, the amplitudes of the diurnal oscillations in radiobrightness are almost constant throughout the 60-day period, about 3 Kelvins for L-band, 8 Kelvins at 19 GHz, and 11 Kelvins at 37 GHz. These characteristics imply that the 19 and 37 GHz radiobrightnesses are not sensitive to soil moisture, but that the L-band radiobrightnesses are. Figure 5.12 (b) shows the 1.4, 19, and 37 GHz radiobrightnesses versus soil moisture for the prairie case.

To better demonstrate the different sensitivities of 1.4, 19 and 37 GHz radiobrightnesses to soil moisture, we also present the percentage of radiobrightness contributed by the soil in Figure 5.12 (c). Figure 5.12 (c) shows that soil radiobrightness weightings (SRW) are considerably smaller for the 19 and 37 GHz cases, about 10 % for the former and 3 % for the latter. These almost constant SRW are an indication of the

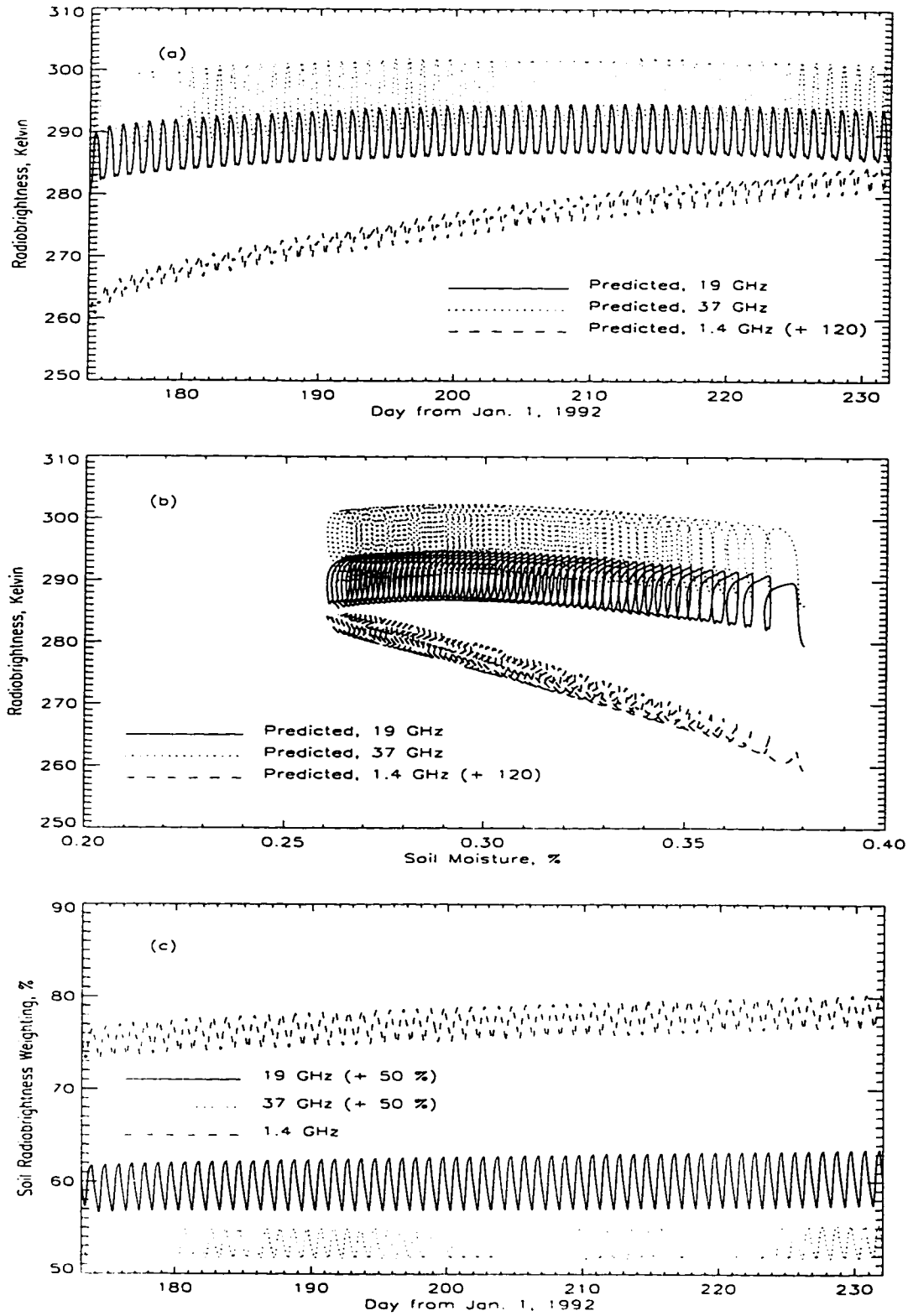

Figure 5.12: Horizontally polarized radiobrightnesses at 1.4 , 19 and 37 GHz (a) versus daynumber and (b) versus soil moisture for the prairie case. (c) The percentage of radiobrightness contributed by the soil.

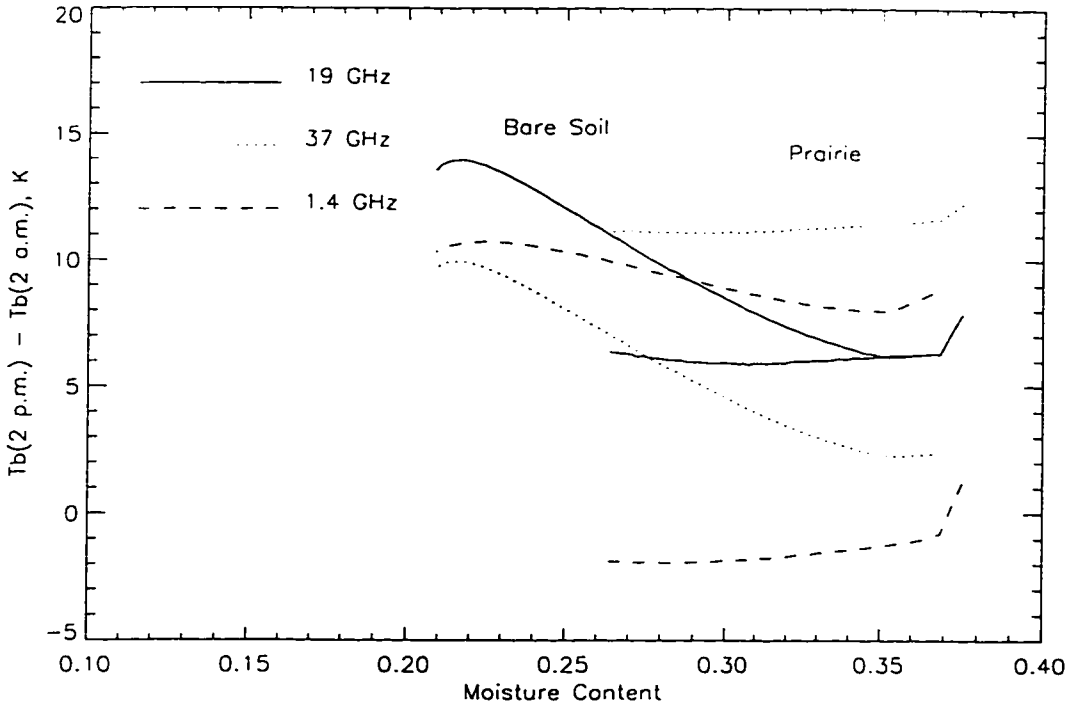

Figure 5.13: Differences in radiobrightness between 2 p.m. and 2 a.m. versus soil moisture for both the bare soil and prairie cases.

insensitivity of 19 and 37 GHz radiobrightness to soil moisture in the prairie case.

In contrast, the L-band SRW varies from about 75 % on day 173 to 79 % on day 232. This indicates that vegetation has a small influence on the predicted L-band radiobrightnesses so that L-band should be a potential candidate for sensing soil parameters such as moisture and temperature in vegetated fields. The 4 % change in the SRW corresponds to a change of about 20 Kelvins in L-band radiobrightness. To discuss the feasibility of the RTI measure of soil moisture, the 2 p.m. - 2 a.m. radiobrightness differences versus soil moisture for both bare soil and prairie grass are shown in Figure 5.13.

For bare soil, the day-night difference changes by about 7 Kelvins for both the 19 and 37 GHz cases for a 16 % change in soil moisture. The change is only about 3

Kelvins at L-band. The L-band emission comes from a greater depth in the moist soil than is true of emission at the SSM/I frequencies. The first-order terms darken L-band radiobrightnesses by as much as 12 Kelvins at 2 p.m., while the first-order terms at the SSM/I frequencies would be an order of magnitude smaller. The darkening occurs because deeper soils are cooler and wetter than surface soils. The first-order terms increase L-band brightness by as much as 7 Kelvins at 2 a.m. because deep soils are warmer and drier than surface soils. The combined effect is that the day-to-night difference in radiobrightness is reduced. That is, RTI at L-band is less sensitive to soil moisture than at 19 and 37 GHz over bare soils. These large first-order terms for L-band radiobrightness suggest that higher-order terms should be considered.

RTI is not sensitive to soil moisture in a prairie grass canopy at any of the three frequencies. The 19 and 37 GHz emission from soil does not penetrate the grass canopy. While the canopy does not absorb all of the L-band emission, the amplitude of diurnal variations in soil temperature is only about 5 Kelvins (Figure 5.11).

5.5 DISCUSSION

The 1dH/R model simulates land surface processes for northern prairie to obtain temperature and moisture profiles of the canopy and soil, and predicts terrain radiobrightness signatures. We validated the model with field measurements from REBEX-1 and found that model predictions generally agree very well with the observations. These predictions include canopy temperature, soil heat flux at 2 cm depth, soil temperatures at 2, 4, 8, 16, 32, and 64 cm depths, and horizontally-polarized radiobrightness at 19 GHz. The good agreement gives us confidence in using the model to examine the linkage between radiobrightness and moisture stored in prairie grassland.

Although the 1dH/R model may be too computationally intensive to be incorporated into an operational weather prediction model, it can be used as a non-interactive model to check estimates of stored water at selected grid points. Comparisons between predicted and observed radiobrightnesses for these points are a measure of the quality of the stored water estimates.

Based upon a 60-day dry-down simulation for a 100 % grass-covered prairie in summer, the 1dH/R model predicts that L-band radiometry is highly sensitive to soil moisture. L-band radiobrightness increased 20 Kelvins in response to an 11 % decrease in soil moisture. The model also predicts that, while the SSM/I frequencies of 19, 37, and 85 GHz are sensitive to moisture in bare soil, they are not sensitive to soil moisture in grassland having wet vegetation column densities over 3 kg/m^2. If this is true, the observed SSM/I sensitivity to soil moisture in prairie must come from bare or sparsely vegetated areas within each SSM/I pixel. Thus, land cover must be included in any algorithm using SSM/I data for a quantitative estimate of soil moisture.

While the current 1dH/R model is capable of aggregating bare soil and grassland according to their appearance within a grid cell, it is a prototype. Further validation of the model may be necessary. In a future study [58], we will re-examine the model predictions against REBEX-4 observations including temperature and moisture profiles of the soil and canopy.

CHAPTER 6

CONCLUSIONS

This chapter concludes the dissertation with a summary of its major contributions and recommendations for future research.

6.1 Contributions

The major contributions of the dissertation are the development of the four models, the AT/R, 1dHbu/R, 1dHb/R, and 1dH/R models. Table 6.1 is a list of inputs, forcings, and products of the these models.

Models	Thermal/Hydrology Modules			R
	Inputs	Forcings	Products	Modules
AT/R	Uniform $T_g(z)$ and $\theta(z)$	Climatological data	$T_g(z), Q_{lh}$, Q_{sh}, and Q_g	T_b
1dHbu/R	Uniform $\theta(z)$ $T_g(z)$ from AT module	Climatological data	$T_g(z), \theta(z), Q_{lh}$, Q_{sh}, and Q_g	T_b
1dHb/R	Uniform $\theta(z)$ $T_g(z)$ from AT module	Climatological data	$T_g(z), \theta(z), Q_{lh}$, Q_{sh}, and Q_g	T_b
1dH/R	Uniform $\theta(z)$ $T_g(z)$ from REBEX-1 & AT module	Climatological & REBEX-1 data	$T_g(z), \theta(z), Q_{lh}$, Q_{sh}, Q_g, T_c, and θ_c	T_b

Table 6.1: Summary of the inputs, forcings, and products of the four models presented in the dissertation. The notations are: $T_g(z)$, soil temperature profile; $\theta(z)$, soil moisture profile; Q_{lh}, latent heat transfer; Q_{sh}, sensible heat transfer; T_c, canopy temperature; θ_c, canopy moisture; Q_g, thermal emission from the terrain; and T_b, terrain radiobrightness.

The AT/R model in Chapter 2 was the first to examine annual thermal and

radiobrightness signatures for bare, freezing/thawing moist soils. The model does not account for water movement within the soil, but does permit soil freezing and thawing — key processes in determining the temperature profile. I compared predictions from the model with those of an equivalent diurnal model. The comparison demonstrated that diurnal predictions of land-atmosphere thermal and moisture exchanges should be set in an annual context. Consequently, I used the temperature profile from the annual model for the time-of-year to initialize the three 1dH models to achieve more rapid convergence. I also used the energy flux below the depth of the diurnal wave for the time-of-year as the lower boundary condition in the three 1dH models.

The 1dHbu/R model in Chapter 3 links a hydrology model to a radiobrightness model. The 1dHb/R model in Chapter 4 is the revised 1dHbu/R model without the restriction against soil freezing/thawing. The two models were used to examine the thermal, hydrology and radiobrightness signatures for the dry-down of bare soils as an investigation of the influence of water transport on these signatures. A comparison of results from the water transport and no water transport cases demonstrates that water transport is significant and that water transport greatly influences radiobrightness.

The 1dH/R model in Chapter 5 represents a combination of the bare-soil model and a biophysical and radiative transfer model of a grass canopy. Through comparisons with observations from REBEX-1, I showed that the model accurately reproduced canopy temperature, soil temperature profile, soil heat flux at 2 cm, and H-polarized 19 GHz radiobrightness. I used the model to investigate the moisture sensitivity of various radiobrightness frequencies and techniques, and found that L-band is sensitive to soil moisture in prairie grassland, while the SSM/I frequencies are sensitive to moisture in the canopy. I also found that the RTI scheme is not sensitive to soil moisture at any of the microwave frequencies. Since radiobrightness

is sensitive to moisture in the soil and the canopy, the model is potentially useful for retrospectively estimating stored water in soil through the assimilation of radio-brightness observations.

6.2 Recommendations for Future Research

There are issues that follow my dissertation. They involve further validations, sensitivity studies, and refinements of the presented models.

1. Validations:

   The usefulness of a model depends upon its reliability, which cannot be judged without model validation. The 1dH/R model accurately reproduces the observed data from REBEX-1. However, the soil moisture dynamics predicted by the model were not verified because moisture profiles were not recorded during the experiment. Validating the 1dH moisture dynamics should be the first priority of future research.

2. Sensitivity Studies:

   The 1dH/R model is concerned with energy and moisture transport in the soil and their exchanges between the land and the atmosphere. Any field parameters that influence these transport processes must be carefully examined. These field parameters fall into two categories — grass parameters such as moisture, temperature, albedo, height, root distribution and LAI, and soil parameters such as moisture, temperature, and albedo. I have found the model to be very sensitive to LAI and canopy and soil albedos because they determine the shortwave radiation that is available to canopy and soil.

3. Refinements:

The 1dH/R model is the most complicated model among the four models presented in this dissertation. The model considers the land surface processes for a bare or grass-covered field. It inevitably consists of many sub-models for the parameters that are associated with energy and moisture transport. These include thermal and hydraulic conductivities, energy and moisture diffusion coefficients, apparent heat capacity, water-retention characteristics, unfrozen liquid water content, and canopy surface resistance. The 1dH/R model also includes sub-models associated with estimates of terrain radiobrightness such as the dielectric properties of soil and canopy. Certainly, each of these sub-models can be improved, but further sensitivity studies are required to determine where improvements would be most beneficial.

The treatment of the downwelling longwave radiation should be improved. The downwelling longwave radiation is currently estimated using the measured net radiation, the measured canopy temperature, and a model-estimated canopy albedo. The albedo model could likely be improved.

Other relevant issues include chemical material dynamics in the canopy, surface heterogeneity or scaling, and scatter darkening. The model might also be incorporated into a snow model such as the one developed by Galantowicz [37].

APPENDICES

APPENDIX A

THE AT/R MODEL

A.1 The AT Module

```
C=====================================================================
      PROGRAM ANNUAL
C=====================================================================
C
C     This program is written to investigate the response of annual
C temperature and radiobrightness to weather for freezing/thawing, moist,
C bare soils [Chapter 2 of the dissertation].  The soils are subject to
C annual insolation, radiant heating and cooling, and sensible and latent
C heat exchanges with the atmosphere.
C
C   Weather forcing primarily follows [England 1990].
C   Heat capacity is after [Andersland et al 1978].
C   Thermal conductivity uses de Vries model [de Vries, 1963].
C
C   Written by Yuei-An Liou, 1993-1994
C
C=====================================================================
C
C     DECL(366)     : daily declination
C     DELTMAX       : convergent criterion for ground temperature between
C                     iterations
C     FGND(I)       : gray-body emission from the ground, W/m^2
C     FSKY(I)       : sky brightness, W/m^2
C     FSOLAR(I)     : solar heating, W/m^2
C     FWIND(I)      : sensible heat transfer, W/m^2
C     FNET(I)       : net heat flow into the ground, W/m^2
C     HOUR          : time step
C     INERTIA       : thermal inertia
C     NDAY          : the day number of the year, ranging from 1 on 1
C                     January to NDAYY on 31 December
C     NDAYM(I)      : the number of days in one month
C     NDAYMS(0:12)  : the number of days to the end of the month
C     NDAYY         : the number of days in a year
C     NSAM2         : the number of time steps starting from the midnight
C     NSAMD         : the number of time steps in a day
C     NSAMMS(0:12)  : the number of time steps to the end of the month
C     NSAMDS(0:366): the number of time steps to the end of the day
C     NSAMY         : the number of time steps in a year
C     SOLAR(I)      : solar heating components
C     TAIR(I)       : average air temperature within the time step
C     TGRAD(I)      : surface temperature gradient
C     TOLD(I)       : ground temperatures between iterations
C     TNEW(I)       : ground temperatures between iterations
C     TOAIR(366)    : daily average air temperature
C     TSKY(I)       : sky temperature
C     Z(0:nodep,0:I): soil layers as a function of space and time
```

```
C     ZOLD(0:nodep): depths between iterations
C     ZNEW(0:nodep): depths between iterations
C
C     Some parameters are described in the subroutine SPARA.
C
C     !--------------------bounds for statements----------------------!
C
      implicit none
C=== main program
      integer NODEP,IMAX,NSAMD,N,NOITER,I,ITEST,JS,JE,IA,II,
     1        II0,II1,nhr_step,NSMAX,NWRITE
      REAL PI,SIGMA,Flh
      PARAMETER (NODEP=40,IMAX=52704,PI=3.1415927,SIGMA=5.6696E-8,
     1           NWRITE=NODEP/10)
      DOUBLE PRECISION STARTIME,ENDTIME,COMPUTIME,EXECTIME(35),
     1 deltaTAG
      REAL TGOLD(0:IMAX),COSRLAT,SINRLAT,WATERV25,SOLARCL,EMSI,
     1     TGRAD(0:IMAX),RHR,CONVERTHR,TIMEH,fwind0,Bowen,
     2     PI2,RLAT1,COS,SIN,ABS,ES,DELTG
      COMMON /CMAIN_FCL_INIT/COSRLAT,SINRLAT
     1       /CMAIN_INIT/WATERV25,SOLARCL
     2       /CMAIN_INIT_ITER/EMSI
     3       /CMAIN_ITER/NSMAX
      external es
C--- subroutine spara
      REAL RLAT,CL,WIND,EM,WATERV,SO,RHOAIR,CPAIR,DRAG,
     1     DELTMAX,ALB,ALBCL,psychro1
      INTEGER ITERMAX,NOZ
      COMMON /CPARA_MAIN/RLAT,CL,WIND,EM,WATERV,SO,RHOAIR,CPAIR,DRAG,
     1                   ITERMAX,DELTMAX,ALB,ALBCL,psychro1
     2       /CPARA_MAIN_INIT_ITER/NOZ
     3       /CPARA_MAIN_YEAR/NSAMD
C--- subroutine syear
      INTEGER NDAYY,NSAMY,NSAMDS(0:366),NSAMMS(0:12)
      COMMON /CYEAR/NDAYY
     1       /CYEAR_MAIN_INIT_ITER/NSAMY,NSAMDS,NSAMMS
C=== subroutine sf2
      REAL AIRF,F20
      COMMON /CMAIN_F2/F20
     1       /CMAIN_F2_INIT_ITER/AIRF
C--- function
      REAL PERIODD,PI2PER
      COMMON /CMAIN_FCL/PERIODD,PI2PER
C--- subroutine sinit
      INTEGER Tmi,Tma
      PARAMETER (Tmi=150,Tma=450)
      DOUBLE PRECISION Z(0:NODEP,0:IMAX),e_sfc(Tmi:Tma),e_air(0:IMAX)
      REAL TG(0:IMAX),TAIR(0:IMAX),TSKY(0:IMAX),FSOLAR(0:IMAX)
      INTEGER HR,T(0:NODEP,0:IMAX)
      COMMON /CINIT_MAIN_ITER/e_sfc,e_air,Z,TG,TAIR,TSKY,FSOLAR,T
C--- function
      real Vf_l,Le_water
      external Vf_l,Le_water
c===== data
      double precision L_f(6),Tk_Lf(6),de_Lf_T(6),L_v(16),Tk_Lv(16),
     1 de_Lv_T(16),YP1,YP2
      common /CMAIN_Lf2/Tk_Lf,L_f,de_Lf_T
      common /CMAIN_Lv2/Tk_Lv,L_v,de_Lv_T
       data L_f/2.035e5,2.357e5,2.638e5,2.889e5,3.119e5,3.337e5/
     1   Tk_Lf/223.15, 233.15, 243.15, 253.15, 263.15, 273.15/
c      data L_s/2.832e6, 2.834e6, 2.837e6, 2.8383e6,2.8387e6,
c     1         2.8387e6,2.8383e6,2.8366e6,2.8345e6/
c     2   Tk_Ls/193.15,  203.15,  213.15,  223.15,  233.15,
c     3         243.15,  253.15,  263.15,  273.15/
      data L_v/2.6348e6,2.6030e6,2.5749e6,2.5494e6,2.5247e6,2.5008e6,
     1         2.4891e6,2.4774e6,2.4656e6,2.4535e6,2.4418e6,2.4300e6,
     2         2.4183e6,2.4062e6,2.3945e6,2.3823e6/
     3   Tk_Lv/223.15,  233.15,  243.15,  253.15,  263.15,  273.15,
```

```
     4         278.15,  283.15,  288.15,  293.15,  298.15,  303.15,
     5         308.15,  313.15,  318.15,  323.15/
C     !-------------------bounds for statements----------------------!
      YP1 = dble(1e30)
      YP2 = dble(1e30)
C
C--- Call subroutines to compute latent heat of fusion and evaporation
C
      CALL TIME(STARTIME)
      CALL SPLINE(Tk_Lf,L_f,6,YP1,YP2,de_Lf_T)
      CALL SPLINE(Tk_Lv,L_v,16,YP1,YP2,de_Lv_T)
      CALL SPARA
      CALL SYEAR
C
C       Some common constants.
C
      AIRF = RHOAIR * CPAIR * DRAG * (WIND + 2)
      IF (WIND.EQ.0) AIRF = 0.
      PERIODD = 24
      PI2 = 180. / PI
      PI2PER = PI * 2. / PERIODD
      RLAT1 = RLAT / PI2
      COSRLAT = COS(RLAT1)
      SINRLAT = SIN(RLAT1)
      F20 = (CL/2.)*SO*(1.-ALB)/PERIODD
      WATERV25 = (0.61 + 0.05 * WATERV ** .5) ** .25
      SOLARCL = SO*((1.0-CL)+CL*(1.0-ALBCL))*(1.0-ALB)
      EMSI = EM * SIGMA
       write(6,*)' call SDECL'
      CALL SDECL
        write(6,*)' call SF2'
      CALL SF2
        write(6,*)' call STOAIR'
      CALL STOAIR
        write(6,*)' call SINIT'
      CALL SINIT
        write(6,*)' SINIT ends'
C
C   Subroutine siter iterates Z(N,HR), T(N,HR), and surface temperature,
C TG(HR).  Convergent criterion is |TG(HR)-TGOLD(HR)| < DELTMAX  for all HR,
C or iterations = IMAX.
C
      I = 1
   21 ITEST = 0
      NSMAX = 100
      DO 25 HR = 1, NSAMY
         TGOLD(HR)=TG(HR)
   25 CONTINUE
      IF(I.GT.7) NSMAX = 120
      IF (I.GT.11) NSMAX = 150
       write(6,*)' call SITER'
      CALL SITER
      CALL TIME(EXECTIME(I))
      WRITE (6,27) I
   27 FORMAT(' The iteration ',I2,' is completed.')
      write(6,*)'The CPU time is ',EXECTIME(I),' seconds!'
      DO 35 HR = 1, NSAMY
        DELTG = ABS(TG(HR)-TGOLD(HR))
        IF (DELTG.GT.DELTMAX) THEN
          ITEST = 1
          IF (I.LT.ITERMAX) THEN
            DO 31 N=0,NOZ
              Z(N,0)=Z(N,NSAMY)
              T(N,0)=T(N,NSAMY)
   31       CONTINUE
            TG(0)=TG(NSAMY)
            I = I + 1
            GOTO 21
```

```
          ENDIF
        ENDIF
   35 CONTINUE

      DO 37 HR = 0, NSAMY
         TGRAD(HR)=(FLOAT(T(1,HR))-TG(HR))/REAL(Z(1,HR))
   37 CONTINUE

      NOITER = I
C      IAEND = NODEP / 10
      CONVERTHR = 24.0/REAL(NSAMD)
C
C   Write results to data files.
C  22T.dat stores daynumber (I), time in a day (TIMEH), groung temp (TG),
C temp gradient at the surface (TGRAD), sky temp (TSKY), air temp (TAIR),
C Bowen ratio (Bowen), sensible heat transfer (fwind0), Solar radiation
C (FSOLAR), liquid water content (Vf_1) on days 03/22, 06/22, 09/22, and
C 12/22.
C  22TZ.dat stores temp profile (T) and the associated depths (Z) on days
C 03/22, 06/22, 09/22, and 12/22.
C  T.dat stores the same data as 22T.dat does, but the data are for the
C whole year and for the midnight only.
C  TZ.dat stores the same data as 22TZ does, but the data are for the
C whole year and for the midnight only.  TZ.dat is further used in the
C dry-down simulation in Chapter 5.
C
      OPEN(UNIT=82,STATUS= 'UNKNOWN',FILE='T.dat')
      OPEN(UNIT=81,STATUS= 'UNKNOWN',FILE='TZ.dat')
      OPEN(UNIT=80,STATUS= 'UNKNOWN',FILE='22T.dat')
      OPEN(UNIT=79,STATUS= 'UNKNOWN',FILE='22TZ.dat')

      DO 51 I = 82, 266, 92
        JS = NSAMDS(I-1) + 1
        JE = NSAMDS(I)
        RHR = 0.
        DO 49 HR = JS, JE
          RHR = RHR + 1.0
          TIMEH = RHR * CONVERTHR
C
C         Calculate sensible heat transfer and Bowen ratio. (10/20/93)
C
          deltaTAG = DBLE(TAIR(HR) - TG(HR))
          fwind0 = AIRF * deltaTAG
          if (dabs(deltaTAG).ne.0.d0) then
            Bowen =(psychro1/Le_water(TG(HR)))*deltaTAG/
     1             (e_air(HR)-es(TG(HR)))
          else
            Bowen = 0.
          endif
          if(Bowen.eq.0) pause'Bowen = 0'
          Flh = fwind0/Bowen
          WRITE(80,50)I,TIMEH,TG(HR),TGRAD(HR),TSKY(HR),TAIR(HR),
     1                Bowen,fwind0,FSOLAR(HR),Vf_1(TG(HR))
          DO 45 IA = 1, NWRITE
            II0 = (IA - 1) * 10 + 1
            II1 = IA * 10
            WRITE(79,52)(T(II,HR), II=II0,II1)
   45     CONTINUE
          DO 47 IA = 1, NWRITE
            II0 = (IA - 1) * 10 + 1
            II1 = IA * 10
            WRITE(79,54)(Z(II,HR), II=II0,II1)
   47     CONTINUE

   49   CONTINUE
   51 CONTINUE

   50 FORMAT(I3,' ',F5.2,' ',F6.2,' ',f7.2,2(' ',F6.2),' ',f9.3,
```

```
     1          ' ',F7.2,' ',F7.2,' ',1pe9.3)
  52 FORMAT(10('    ',I4,'  '))
  54 FORMAT(10(' ',1pe9.2))
     DO 63 I = 357, 357
       JS = NSAMDS(I-1) + 1
       JE = NSAMDS(I)
       RHR = 0.
       DO 61 HR = JS, JE
         RHR = RHR + 1.0
         TIMEH = RHR * CONVERTHR
         deltaTAG = DBLE(TAIR(HR) - TG(HR))
         fwind0 = AIRF * deltaTAG
         if (dabs(deltaTAG).ne.0.D0) then
           Bowen =(psychro1/Le_water(TG(HR)))*deltaTAG/
     1             (e_air(HR)-es(TG(HR)))
         else
           Bowen = 0.
         endif
         WRITE(80,50)I,TIMEH,TG(HR),TGRAD(HR),TSKY(HR),TAIR(HR),
     1               Bowen,fwind0,FSOLAR(HR),Vf_1(TG(HR))
         DO 57 IA = 1, NWRITE
           II0 = (IA - 1) * 10 + 1
           II1 = IA * 10
           WRITE(79,52)(T(II,HR), II=II0,II1)
  57     CONTINUE
         DO 59 IA = 1, NWRITE
           II0 = (IA - 1) * 10 + 1
           II1 = IA * 10
           WRITE(79,54)(Z(II,HR), II=II0,II1)
  59     CONTINUE
  61   CONTINUE
  63 CONTINUE

     DO 73 I = 1, NDAYY
       JS = NSAMDS(I-1) + 1
       RHR = 0.
       HR = JS
       RHR = RHR + 1.0
       TIMEH = RHR * CONVERTHR
       deltaTAG = DBLE(TAIR(HR) - TG(HR))
       fwind0 = AIRF * deltaTAG
       if (dabs(deltaTAG).ne.0.D0) then
         Bowen =(psychro1/Le_water(TG(HR)))*deltaTAG/
     1           (e_air(HR)-es(TG(HR)))
       else
         Bowen = 0.
       endif
       WRITE(82,50)I,TIMEH,TG(HR),TGRAD(HR),TSKY(HR),TAIR(HR),
     1             Bowen,fwind0,FSOLAR(HR),Vf_1(TG(HR))
       DO 67 IA = 1, NWRITE
         II0 = (IA - 1) * 10 + 1
         II1 = IA * 10
         WRITE(81,52)(T(II,HR), II=II0,II1)
  67     CONTINUE
         DO 69 IA = 1, NWRITE
           II0 = (IA - 1) * 10 + 1
           II1 = IA * 10
           WRITE(81,54)(Z(II,HR), II=II0,II1)
  69     CONTINUE
  73   CONTINUE
     WRITE(80,*)'Day# Time Tgnd   Tgrad(K/m) Tsky Tair  Bowen    Fsh',
     1' Fsun  Vf_1(by vol.)'
     WRITE(82,*)'Day# Time Tgnd   Tgrad(K/m) Tsky Tair  Bowen    Fsh',
     1' Fsun  Vf_1(by vol.)'
     CLOSE(79)
     CLOSE(80)
     CLOSE(81)
     CLOSE(82)
```

```
C
C   Write results to data file annualb.dat.
C
      OPEN (UNIT=90,STATUS= 'UNKNOWN',FILE='annualb.dat')
C
C   nhr_step is the rate of storing data.  Typically, data is stored
C every 6 minutes.  nhr_step = 2 implies that data will be stored
C every 12 mintues.
C
      nhr_step = 1
      DO 89 I = 1, NDAYY
        JS = NSAMDS(I-1) + 1
        JE = NSAMDS(I)
        RHR = 0.
        DO 87 HR = JS, JE, nhr_step
          RHR = RHR + nhr_step
          TIMEH = RHR * CONVERTHR
C
C   Calculate sensible heat transfer and Bowen ratio. (10/20/93)
C
          deltaTAG = DBLE(TAIR(HR) - TG(HR))
          fwind0 = AIRF * deltaTAG
          if (dabs(deltaTAG).ne.0D0) then
            Bowen =(psychro1/Le_water(TG(HR)))*deltaTAG/
     1             (e_air(HR)-es(TG(HR)))
          else
            Bowen = 0.
            pause ' Bowen = 0'
          endif
         WRITE(90,50)I,TIMEH,TG(HR),TGRAD(HR),TSKY(HR),TAIR(HR),Bowen,
     1              fwind0,FSOLAR(HR),Vf_1(TG(HR))
   87   CONTINUE
   89 CONTINUE
      WRITE(90,*)'Day# Time Tgnd   Tgrad(K/m) Tsky Tair  Bowen    Fsh',
     1' Fsun  Vf_1(by vol)'
      CLOSE(90)
C
C   Write computer time to data file annual.time.
C
      CALL TIME(ENDTIME)
      OPEN(UNIT=99,STATUS= 'UNKNOWN',FILE='annual.time')
        COMPUTIME = (ENDTIME - STARTIME)/60.0D0
        WRITE(99,*) 'The number of iterations is ',NOITER,'.'
        WRITE(99,*)' The code starts at ',STARTIME,'!'
        DO 95 I = 1, NOITER
          WRITE(99,94)I,EXECTIME(I)
   94     FORMAT(' After ',I2,' iterations, the CPU time is ',
     1          f30.15,' seconds!')
   95   CONTINUE
        WRITE(99,*)' The code ends at ',ENDTIME,' seconds!'
        WRITE(99,*)' The computer time is ',COMPUTIME,' minutes!'
        IF(ITEST.EQ.0) then
          WRITE(99,97)DELTMAX
   97     format('Solution converges < ',F6.4,' K!')
        ELSEIF(ITEST.EQ.1) THEN
          WRITE(99,98)DELTMAX
   98     format('Solution does not converge < ',F6.4,' K!')
        ENDIF
      CLOSE(99)

      STOP
      END
C=====================================================================
      SUBROUTINE  SPARA
C=====================================================================
C   annual.prm lists some parameters used in the code.  All units are
C in SI.
C
```

```
      implicit none
      REAL RLAT,MOIS,CL,WIND,EM,RHODRY,CP,KDRY,DIELECT,LOSSTAN,TAIRO,
     1     TAIR1,THETALAG,TDEL,WATERV,SO,RHOAIR,CPAIR,DRAG,DELTMAX,
     2     ALB,ALBCL,psychro1,fe,inv_psy,inv_psy_ln,humidity
      DOUBLE PRECISION ZINCR
      INTEGER ITERMAX,TAU,YEAR,NSAMD,NOZ
      COMMON /CPARA_MAIN/RLAT,CL,WIND,EM,WATERV,SO,RHOAIR,CPAIR,DRAG,
     1                   ITERMAX,DELTMAX,ALB,ALBCL,psychro1
     2       /CPARA_MAIN_INIT_ITER/NOZ
     3       /CPARA_MAIN_YEAR/NSAMD
     4       /CPARA_YEAR/YEAR
     5       /CPARA_TOAIR/TAIRO,TAIR1,THETALAG
     6       /CPARA_INIT/fe,MOIS,RHODRY,CP,KDRY,TDEL,humidity
     7       /CPARA_INIT_ITER/TAU
     8       /CPARA_ITER/ZINCR,inv_psy,inv_psy_ln
     9       /CPARA_TB/DIELECT,LOSSTAN
C
C     !--------------------bounds for statements----------------------!
C
C   Read parameters from annual.prm.  Many parameters are from [England
C 1990].
C
      OPEN(110,FILE='annual.prm',STATUS='OLD')
C       LAT: latitude(typical = 47. N).
      READ(110,*) RLAT
        IF ((RLAT.lt.-90.0).or.(RLAT.gt.90.0)) RLAT=47.0
C       MOIS: soil moisture(typical MOIS = 7% for dry soil).
      READ(110,*) MOIS
C       CL: cloud cover(typical = 0.2)
      READ(110,*) CL
C       WIND: average winds(typical = 5 m/s).
      READ(110,*) WIND
C       EM: thermal IR emissivity(typical = .95).
      READ(110,*) EM
C       RHODRY: 7% moist soil density(typicaL = 1000.0 kg/m^3).
      READ(110,*) RHODRY
C       CP: 7% moist soil specific heat(typical = 1000.0 J/kg-K).
      READ(110,*) CP
C       KDRY: 7% moist soil thermal conductivity(typical = .36 W/m-K).
      READ(110,*) KDRY
C       DIELECT: 7% moist soil dielectric constant(typical = 3.3).
      READ(110,*) DIELECT
C       LOSSTAN: 7% moist soil loss tangent(typical = .23).
      READ(110,*) LOSSTAN
C       TAIRO: average air temperature(typical = 278.3 K).
      READ(110,*) TAIRO
C       TAIR1: annual air temperature variation(typical = 16.9 K).
      READ(110,*) TAIR1
C       THETALAG: temperature phase lag(typical = 1.12 months).
      READ(110,*) THETALAG
C       TDEL: diurnal temperature variation(typical = 5 K).
      READ(110,*) TDEL
C       WATERV: water vapor pressure(typical = .76 mmHg).
      READ(110,*) WATERV
C       SO: solar constant(typical = 1385 W/m^2).
      READ(110,*) SO
C       RHOAIR: air density at surface(typical = 1.25 kg/m^3).
      READ(110,*) RHOAIR
C       CPAIR: specific heat of the air, (typical = 1000.0 J/kg-K).
      READ(110,*) CPAIR
C       DRAG: drag coefficient(typical = 0.002).
      READ(110,*) DRAG
C       IMAX: maximum number of iterations before an abort.
      READ(110,*) ITERMAX
C       DELTMAX: convergent criterion for ground temperature, K
      READ(110,*) DELTMAX
C       TAU: the range of temperatures as ice and liquid water co-exist.
      READ(110,*) TAU
```

```
C       ALB: albedo of soil
        READ(110,*) ALB
C       ALBCL: albedo of clouds
        READ(110,*) ALBCL
C       YEAR: the year in number.
        READ (110,*) YEAR
C       NSAMD: the number of time steps in a day.
        READ (110,*) NSAMD
C       NOZ: the number of soil layers, less than 100, typical = 60
        READ(110,*) NOZ
C       ZINCR: increment in depth per layer or iteration, in m.
        READ(110,*) ZINCR
C       fe: ratio of real to potential evaporation
        READ(110,*) fe
C       humidity: typical relative humidity in South Dakota
        READ(110,*) humidity
        CLOSE(110)
C
C     Psychometric constant is from Peixoto and Oort 1992.
c       psychro1 = CPAIR*1.01325e5/(0.622*2.501E6), in K-Newton/m^2
c                * .01 ==> mbar-K
c       psychro1 = CPAIR*1.01325e5/(0.622*2.501E6)
        psychro1 = CPAIR*1.01325e5/0.622
        inv_psy = 1. / psychro1
        inv_psy_ln = 2354.*ALOG(10.)*inv_psy

        RETURN
        END
C=======================================================================
        SUBROUTINE SYEAR
C=======================================================================
C   Determine whether or not it is a leap year and the numbers for some
C parameters, like number of days in a month and in a year.
C
        implicit none
C--- syear
        INTEGER NDAYY,NDAYM(12),NSAMY,N1,N2,N3,LEAP,RY(12),LY(12),
     1          NDAYMS(0:12),NSAMMS(0:12),NSAMDS(0:366),NS,I
        COMMON /CYEAR/NDAYY
     1        /CYEAR_MAIN_INIT_ITER/NSAMY,NSAMDS,NSAMMS
C--- spara
        INTEGER YEAR,NSAMD
        COMMON /CPARA_MAIN_YEAR/NSAMD
     1        /CPARA_YEAR/YEAR

        DATA RY/31,28,31,30,31,30,31,31,30,31,30,31/,
     1      LY/31,29,31,30,31,30,31,31,30,31,30,31/
C
C       !---------------range of statements-------------------------------!
C
        N1 = MOD(YEAR,4)
        N2 = MOD(YEAR,100)
        N3 = MOD(YEAR,400)
        IF (N1.EQ.0) THEN
          IF (N2.NE.0) THEN
            LEAP = 1
          ELSEIF (N3.EQ.0) THEN
            LEAP = 1
          ELSE
            LEAP = 0
          ENDIF
        ELSE
          LEAP = 0
        ENDIF
        NS = 0
        NDAYMS(0) = 0
        NSAMMS(0) = 0
        NSAMDS(0) = 0
```

```
C
C      Typically, a time step is 10 minutes.  Hence, a leap year has
C    52704 time steps, and a regular year has 52560 time steps.
C
      IF (LEAP.EQ.1) THEN
        NDAYY = 366
c        NSAMY = 52704
        DO 151 I = 1, 12
          NDAYM(I) = LY(I)
          NS = NDAYM(I) + NS
          NDAYMS(I) = NS
          NSAMMS(I) = NDAYMS(I) * NSAMD
  151   CONTINUE
      ELSE
        NDAYY = 365
c        NSAMY = 52560
        DO 155 I = 1, 12
          NDAYM(I) = RY(I)
          NS = NDAYM(I) + NS
          NDAYMS(I) = NS
          NSAMMS(I) = NDAYMS(I) * NSAMD
  155   CONTINUE
      ENDIF
      NSAMY = NDAYY * NSAMD
      DO 159 I = 1, NDAYY
        NSAMDS(I) = NSAMDS(I-1) + NSAMD
  159 CONTINUE
      RETURN
      END
C=======================================================================
      SUBROUTINE SDECL
C=======================================================================
C Calculate average daily declination.
C
      implicit none
C--- sdecl
      integer I
      REAL DECL,GAMMA,DUM,COSDECL(366),SINDECL(366)
      COMMON /CDECL_FCL_INIT/COSDECL,SINDECL
C--- syear
      INTEGER NDAYY
      COMMON /CYEAR/NDAYY

      DUM = 2. * 3.141592654 / NDAYY
      DO 203 I = 1, NDAYY
        GAMMA = (I-1) * DUM
        DECL = .006918-.399912*COS(GAMMA)+.070257*SIN(GAMMA)
     1           -.006758*COS(2.*GAMMA)+.000907*SIN(2.*GAMMA)
     2           -.002697*COS(3.*GAMMA)+.00148*SIN(3.*GAMMA)
        COSDECL(I) = COS(DECL)
        SINDECL(I) = SIN(DECL)
  203 CONTINUE

      RETURN
      END
C=======================================================================
      SUBROUTINE SF2
C========================================= ========================
C       Compute irradiance from clouds.
C
      implicit none
C--- sf2
      integer I,NDAY
      real F2(366)
      COMMON /CF2_INIT/F2
     1       /CF2_FCL/NDAY
C=== subroutine syear
      INTEGER NDAYY
```

```
      COMMON /CYEAR/NDAYY
      REAL AIRF,F20,FC
      COMMON /CMAIN_F2_INIT_ITER/AIRF
     1       /CMAIN_F2/F20
C--- function
      real FCLOUD
      EXTERNAL FCLOUD

      DO 253 I = 1, NDAYY
        NDAY = I
        FC = 0.
        CALL QTRAP(FCLOUD,0.,24.,FC)
        F2(I) = F20 * FC
  253 CONTINUE
      RETURN
      END
C=======================================================================
      FUNCTION FCLOUD(HOUR)
C=======================================================================
C       FCLOUD is a function for estimates of irradiance from clouds.
C
      implicit none
      real DUM1,FCLOUD

      INTEGER NDAY
      REAL COSRLAT,SINRLAT,COSDECL(366),SINDECL(366),PERIODD,HOUR,
     1     PI2PER
      COMMON /CMAIN_FCL_INIT/COSRLAT,SINRLAT
      COMMON /CMAIN_FCL/PERIODD,PI2PER
     1       /CF2_FCL/NDAY
     2       /CDECL_FCL_INIT/COSDECL,SINDECL
      DUM1 = COSRLAT*COSDECL(NDAY)*(-COS(PI2PER*HOUR)+
     1       SINRLAT*SINDECL(NDAY))
      IF (DUM1.GT.0.) THEN
        FCLOUD = DUM1 - 0.2 * DUM1 ** 0.5
        IF (FCLOUD.LE.0.) FCLOUD = 0.
      ELSE
        FCLOUD = 0.
      ENDIF
      RETURN
      END
C=======================================================================
      SUBROUTINE QTRAP(FCLOUD,A,B,S)
C=======================================================================
C       Subroutines QTRAP and TRAPZD are from Numerical Recipes [Press et
C   al 1989].
C
C       Returns as S the integral of the function FUNC from A to B.  The
C   parameters EPS can be set to the desired fractional accuracy and
C   JMAX so that 2 to the (JMAX-1)th power is the maximum allowed number
C   of steps.  Integration is performed by the trapezoidal rule.
C
      implicit none
      real EPS,A,B,OLDS,ABS,S,FCLOUD
      integer JMAX,J
      EXTERNAL FCLOUD
      PARAMETER (EPS=1.E-5, JMAX=18)
C
C       OLDS is any number that is unlikely to be the average of the
C     function at its endpoints will do here.
C
      OLDS=-1.E30
      DO 303 J=1,JMAX
        CALL TRAPZD(FCLOUD,A,B,S,J)
        IF (ABS(S-OLDS).LT.EPS*ABS(OLDS)) RETURN
        OLDS=S
  303 CONTINUE
      RETURN
```

```
      END
C=======================================================================
      SUBROUTINE TRAPZD(FCLOUD,A,B,S,N)
C=======================================================================
C     This routine computes the N'th stage of refinement of an extended
C  trapezoidal rule.  FUNC is input as the name of the function to be
C  integrated between limits A and B, also input.  When called with
C  N = 1, the routine returns as S the crudest estimate of the integral.
C  Subsequent calls with N = 2, 3, ... (in that sequential order) will
C  improve the accuracy of S by adding 2 to the (N-1)th power additional
C  interior points. S should not be modified between sequential calls.
C
      implicit none
      real FCLOUD,S,B,A,DEL,X,SUM,TNM
      integer IT,J,N
      EXTERNAL FCLOUD
      SAVE IT

      IF (N.EQ.1) THEN
        S=0.5*(B-A)*(FCLOUD(A)+FCLOUD(B))
C
C       IT is the number of points to be added on the next call.
C
        IT=1
      ELSE
        TNM=real(IT)
C
C       DEL is the spacing of the points to be added.
C
        DEL=(B-A)/TNM
        X=A+0.5*DEL
        SUM=0.
        DO 353 J=1,IT
          SUM=SUM+FCLOUD(X)
          X=X+DEL
  353   CONTINUE
C
C       This replaces S by its refined value.
C
        S=0.5*(S+(B-A)*SUM/TNM)
        IT=2*IT
      ENDIF
      RETURN
      END
C=======================================================================
      SUBROUTINE STOAIR
C=======================================================================
C  Calculate average daily air temperature.
C
      implicit none
      real TAIRO,TAIR1,PLAG2,P2,COS,THETALAG,NDAY2
      integer I
      COMMON /CPARA_TOAIR/TAIRO,TAIR1,THETALAG
      INTEGER NDAYY,NDUM
      COMMON /CYEAR/NDAYY
      REAL TOAIR(0:366)
      COMMON /CTOAIR_INIT_ITER/TOAIR

      PLAG2 = 2. * 3.141592654 * THETALAG / 12.
      P2 = 2. * 3.141592654 / NDAYY
      IF(NDAYY.EQ.366) THEN
        NDUM = 10
      ELSE
        NDUM = 9
      ENDIF
      DO 403 I = 1, NDAYY
        NDAY2 = I + NDUM
C       TOAIR(I) = TAIRO-TAIR1*COS(2.*PI*(MON-THETALAG)/12.)
```

```
        TOAIR(I)=TAIR0-TAIR1*COS(P2 * real(NDAY2) - PLAG2)
  403 CONTINUE
      CLOSE(630)
        TOAIR(0) = TOAIR(NDAYY)
      RETURN
      END
C=======================================================================
      SUBROUTINE SINIT
C=======================================================================
C  Initialize soil temperature profile.  The equilibrium temperature at
C the land-air interface is used as the initial temperature.  It is
C obtained when energy balance is reached at the interface.
C
      implicit none
C==== sinit
      INTEGER HR,TMIN,TDRY,IMAX,NODEP,TI,N,I,JS,JE,Tmi,Tma
      REAL PI,SIGMA
      PARAMETER (Tmi=150,Tma=450)
      PARAMETER (NODEP=40,IMAX=52704,PI=3.1415927,SIGMA=5.6696E-8)
      INTEGER T(0:NODEP,0:IMAX),noon
      DOUBLE PRECISION FSKY(0:IMAX),RCP2(Tmi:Tma),KWET(Tmi:Tma),
     1  Z(0:NODEP,0:IMAX),SUM,e_sfc(Tmi:Tma),e_air(0:IMAX),f(Tmi:Tma),
     2  f_d(Tmi:Tma),e_max
      REAL TG(0:IMAX),TAIR(0:IMAX),TSKY(0:IMAX),COS,
     1     FSOLAR(0:IMAX),PIHR,SOLAR,COSZ,RHOWET
      COMMON /CINIT_MAIN_ITER/e_sfc,e_air,Z,TG,TAIR,TSKY,FSOLAR,T
     1       /CINIT_ITER/FSKY,RCP2,KWET,f,f_d,RHOWET,TI,TMIN
C---- sapra
      REAL MOIS,RHODRY,CP,KDRY,TDEL,fe,humidity
      INTEGER NOZ,TAU
      COMMON /CPARA_MAIN_INIT_ITER/NOZ
     1       /CPARA_INIT/fe,MOIS,RHODRY,CP,KDRY,TDEL,humidity
     2       /CPARA_INIT_ITER/TAU
C***   main
      REAL COSRLAT,SINRLAT,WATERV25,SOLARCL,EMSI
      COMMON /CMAIN_FCL_INIT/COSRLAT,SINRLAT
     1       /CMAIN_INIT/WATERV25,SOLARCL
     2       /CMAIN_INIT_ITER/EMSI
C===   syear
      INTEGER NDAYY,NSAMY,NSAMDS(0:366),NSAMMS(0:12)
      COMMON /CYEAR/NDAYY
     1       /CYEAR_MAIN_INIT_ITER/NSAMY,NSAMDS,NSAMMS
C***  sdecl
      REAL COSDECL(366),SINDECL(366)
      COMMON /CDECL_FCL_INIT/COSDECL,SINDECL
C--- subroutine sf2
      REAL AIRF,F2(366)
      EXTERNAL FCLOUD
      COMMON /CMAIN_F2_INIT_ITER/AIRF
     1       /CF2_INIT/F2
C=== subroutine stoair
      REAL TOAIR(0:366)
      COMMON /CTOAIR_INIT_ITER/TOAIR
      real es
      external es
C
C     !--------------------bounds for statements----------------------!
C
      PIHR = PI / 72.0
C       Find SOLAR, TAIR(I), TSKY(I), FSKY(I), FSOLAR and FWIND(I).
      DO 457 I = 1, NDAYY
        JS = NSAMDS(I-1) + 1
        JE = NSAMDS(I)
        DO 453 HR = JS, JE
          COSZ=COSRLAT*COSDECL(I)*(-COS(REAL(HR)*PIHR)
     1         + SINRLAT*SINDECL(I))
          IF (COSZ.GT.0.0) THEN
            SOLAR = COSZ - .2 * COSZ ** .5
```

```
            IF (SOLAR.LT.0.0) SOLAR = 0.0
          ELSEIF (COSZ.LE.0.) THEN
            SOLAR = 0.0
          ENDIF
          TAIR(HR)= TOAIR(I)-TDEL*COS((HR-12.)*PIHR)
          TSKY(HR)= TAIR(HR)*WATERV25
          FSKY(HR)= SIGMA*TSKY(HR) ** 4.+F2(I)
          FSOLAR(HR) = SOLAR * SOLARCL
  453   CONTINUE
  457 CONTINUE
          TAIR(0) = TAIR(NSAMY)
          TSKY(0) = TSKY(NSAMY)
          FSKY(0) = FSKY(NSAMY)
          FSOLAR(0) = FSOLAR(NSAMY)
C
C   Compute delta-enthalpy term, RCP2(TK) = Rho*Cp(TK), and thermal
C conductivity, KWET.
C
      call scond(RCP2,KWET,f,f_d,fe,MOIS)
C
C   Balance the radiation budget at the land-air interface to
C obtain initial temperature profile of the soil.
C
      SUM = 0.0D0
      DO 463 HR = 1, NSAMY
        SUM=SUM+FSKY(HR)+DBLE(FSOLAR(HR))
  463 CONTINUE
        TI=NINT((REAL(SUM)/(REAL(NSAMY)*EMSI))**0.25)
        DO 465 N=0,NOZ
          Z(N,0)=0.01D0*DBLE(N)
          T(N,0)=TI
  465   CONTINUE
      e_air(0) = DBLE(es(TAIR(0)))
      noon  = NSAMDS(1)/2
      DO 469 I = 1, NDAYY
        JS = NSAMDS(I-1) + 1
        JE = NSAMDS(I)
        e_max = dble(es(TAIR(JS+noon)))
        DO 467 HR = JS, JE
          DO 466 N=0,NOZ
            Z(N,HR)=0.01D0*DBLE(N)
            T(N,HR)=TI
  466     CONTINUE
          TG(HR)=REAL(TI)
          e_air(HR) = DBLE(es(TAIR(HR)))
          if (e_air(HR).gt.e_max) e_air(HR) = e_max
  467   CONTINUE
  469 CONTINUE
      DO 473 TDRY = Tmi,Tma
         e_sfc(TDRY) = DBLE(es(real(TDRY)))
  473 CONTINUE
      RETURN
      END
C=======================================================================
      SUBROUTINE SITER
C=======================================================================
C    SITER tracks isotherms T(n,0) at Z(n,0) using a finite element
C  scheme [England 1992].  Each time step is sub-divided into NSMAX
C  intervals for a higher resolution in tracking isotherms.  NSMAX is
C  adjustable depending on speed of convergence.  Linear interpolations
C  are used to find values of variables at each sub-interval.
C
      implicit none
C=== subroutine siter
      INTEGER IMAX,NODEP,NOZO
      PARAMETER (IMAX=52704,NODEP=40,NOZO=NODEP-1)
      DOUBLE PRECISION ZOLD(0:NODEP),ZNEW(0:NODEP),FDIF,FS,ZMIN,FSKY1,
     1       FSKY2,FSKY3,ZLIN,ZDUM,ZPLUS,ZMINUS,UPLUS,UMINUS,DELH,DELZ,
```

```
     2       DNSMAX,DELT60,i_e_delt
      REAL DELTG,NUM,DEN,TGNEW,TAGDEL,rTO,fTO
      INTEGER TPLUS,TZERO,TMINUS,TOLD(0:NODEP),
     1        TNEW(0:NODEP),NUHR,I,JS,JE,NS,M,N,NSMAX0,
     2        MN,KDIF,KABS,IABS,NSMAX
C--- subroutine spara
      real inv_psy,inv_psy_ln
      DOUBLE PRECISION ZINCR
      INTEGER TAU,NOZ
      COMMON /CPARA_MAIN_INIT_ITER/NOZ
     1       /CPARA_INIT_ITER/TAU
     2       /CPARA_ITER/ZINCR,inv_psy,inv_psy_ln
C***  main
      REAL EMSI
      COMMON /CMAIN_INIT_ITER/EMSI
     1       /CMAIN_ITER/NSMAX
C=== subroutine syear
      INTEGER NDAYY,NSAMY,NSAMDS(0:366),NSAMMS(0:12)
      COMMON /CYEAR/NDAYY
     1       /CYEAR_MAIN_INIT_ITER/NSAMY,NSAMDS,NSAMMS
C=== subroutine sf2
      REAL AIRF
      COMMON /CMAIN_F2_INIT_ITER/AIRF
C=== subroutine stoair
C      REAL TOAIR(0:366)
C      COMMON /CTOAIR_INIT_ITER/TOAIR
C--- subroutine sinit
C      PARAMETER (SIGMA=5.6696E-8)
      INTEGER HR,T(0:NODEP,0:IMAX),TI,DELT,Tmi,Tma,TMIN
      PARAMETER (Tmi=150,Tma=450)
      DOUBLE PRECISION FSKY(0:IMAX),RCP2(Tmi:Tma),KWET(Tmi:Tma),
     1  Z(0:NODEP,0:IMAX),e_sfc(Tmi:Tma),e_air(0:IMAX),f(Tmi:Tma),
     2  f_d(Tmi:Tma)
      REAL TG(0:IMAX),RHOWET,TAIR(0:IMAX),TSKY(0:IMAX),
     1       FSOLAR(0:IMAX)
      COMMON /CINIT_MAIN_ITER/e_sfc,e_air,Z,TG,TAIR,TSKY,FSOLAR,T
     1       /CINIT_ITER/FSKY,RCP2,KWET,f,f_d,RHOWET,TI,TMIN
C==== functions
      real es,Le_water
      external es,Le_water
C
C     !---------------range of statements-----------------------------!
C
C       Extrapolate for each hr (= 0 to 1439 1 minute intervals in 1 day)
C     to obtain Z and T at nuhr=hr+1
C
      ZMIN=0.00001D0
      DNSMAX = DBLE(NSMAX)
      DELT60 = 600.0D0 / DNSMAX
      NSMAX0 = NSMAX - 1
C      NOZ0 = NOZ - 1

      DO 593 I = 1, NDAYY
        JS = NSAMDS(I-1)
        JE = NSAMDS(I) - 1
        DO 591 HR = JS, JE
          NUHR=HR+1
          FSKY1 = FSKY(HR)+FSOLAR(HR)
          FSKY2 = FSKY(NUHR)+FSOLAR(NUHR)
          FSKY3 = FSKY2 - FSKY1
C
C       Extrapolate from hour to hour using:  Z(n,hr+1)=Z(n,hr)+DELZ
C     where: DELZ = -DelFlux/DELH.
C       Perform extrapolation in nsmax increments per minute
C
          DO 503 N=0,NOZ
            ZOLD(N)=Z(N,HR)
            TOLD(N)=T(N,HR)
```

```
  503     CONTINUE
          FDIF = FSKY3/(FSKY1*DMSMAX)
          DO 581 MS=0,MSMAXO
            FS = FSKY1 * (1.0DO+FDIF*DBLE(MS))
            M=1
            DO 521  M=1,MOZO
              TMINUS=TOLD(M-1)
              TZERO=TOLD(M)
              TPLUS=TOLD(M+1)
              IF(TMINUS.eq.TPLUS) THEN
                ZDUM=ZOLD(M)
                ZLIM=0.0DO
                IF (M.GT.1) ZLIM = ZNEW(M-1)
                IF (ZDUM.GT.(ZLIM+ZMIN)) THEN
                  ZNEW(M)=ZDUM
                  TNEW(M)=TPLUS
                  M=M+1
                ENDIF
              ELSE
                ZPLUS=ZOLD(M+1)-ZOLD(M)
                ZMINUS=ZOLD(M)-ZOLD(M-1)
                UPLUS=KWET(TZERO)*DBLE(TPLUS-TZERO)
                UMINUS=KWET(TZERO)*DBLE(TZERO-TMINUS)
                IF(TMINUS.EQ.TZERO)THEN
                  IF(TZERO.GT.TPLUS)THEN
                    DELH=RCP2(TZERO)
                  ELSE
                    DELH=-RCP2(TPLUS)
                  ENDIF
                ELSEIF(TMINUS.GT.TZERO)THEN
                  IF(TZERO.EQ.TPLUS)THEN
                    DELH=RCP2(TMINUS)
                  ELSE
                    DELH=(RCP2(TZERO)+RCP2(TMINUS))
                  ENDIF
                ELSE
                  IF(TZERO.LT.TPLUS)THEN
                    DELH=-(RCP2(TZERO)+RCP2(TPLUS))
                  ELSE
                    DELH=-RCP2(TZERO)
                  ENDIF
                ENDIF

                DELZ=(UPLUS/ZPLUS-UMINUS/ZMINUS)*DELT6O/DELH
                ZDUM=ZOLD(M)+DELZ
                ZLIM=0.0DO
                IF (M.GT.1) ZLIM=ZNEW(M-1)
                IF (ZDUM.GT.(ZLIM+ZMIN)) THEN
                  ZNEW(M)=ZDUM
                  TNEW(M)=TZERO
                  M=M+1
                ENDIF
              ENDIF
  521       CONTINUE
C
C       Extrapolate M=50, i.e., M = MOZ
C
            TMINUS=TOLD(MOZO)
            TZERO=TOLD(MOZ)
            TPLUS=TZERO
            IF (TMINUS.EQ.TZERO) THEN
              ZDUM=ZOLD(MOZ)
              ZLIM=0.0DO
              IF (M.GT.1) ZLIM = ZNEW(M-1)
              IF (ZDUM.GT.(ZLIM+ZMIN)) THEN
                ZNEW(M)=ZDUM
                TNEW(M)=TPLUS
                M=M+1
```

```
              ENDIF
            ELSE

              ZMINUS=ZOLD(NOZ)-ZOLD(NOZO)
              UMINUS=KWET(TZERO)*DBLE(TZERO-TMINUS)
              IF(TMINUS.LT.TZERO)THEN
                DELH=-RCP2(TZERO)
              ELSE
                DELH=RCP2(TZERO)
              ENDIF
              DELZ=-(UMINUS/ZMINUS)*DELT60/DELH
              ZDUM=ZOLD(NOZ)+DELZ
              ZLIM=0.0D0
              IF (M.GT.1) ZLIM=ZNEW(M-1)
              IF (ZDUM.GT.(ZLIM+ZMIN)) THEN
                ZNEW(M)=ZDUM
                TNEW(M)=TZERO
                M=M+1
              ENDIF
            ENDIF
C
C       Fill out depth and temp arrays
C
            IF (M.LE.NOZ) THEN
              DO 531 MM=M,NOZ
                ZNEW(MM)=ZNEW(MM-1)+ZINCR
                TNEW(MM)=TNEW(MM-1)
  531         CONTINUE
            ENDIF
C
C       Set TG(nuhr)
C
            TZERO=TNEW(1)
            TAGDEL=TAIR(HR)-REAL(TZERO)
C
C          Calculate DELTG= Tgnd - Tzero.
C
            rTO = real(TZERO)
            fTO = f(TZERO)
            NUM=REAL(ZNEW(1) * (FS + DBLE(AIRF*(TAGDEL+fTO*
     1 inv_psy*Le_water(rTO)*(e_air(HR)-e_sfc(TZERO)))-EMSI*rTO**4)))
            DEN=REAL( KWET(TZERO)+ZNEW(1)*DBLE(AIRF*(1.+fTO*
     1 inv_psy_ln*Le_water(rTO)*e_sfc(TZERO)/rTO**2)+4.0*EMSI*rTO**3))
            DELTG=NUM/DEN
            TGNEW=rTO+DELTG
C
C       Set T(0,nuhr) and Z(0,nuhr)
C
            ZNEW(0)=0.0D0
            TNEW(0)=TNEW(1)
            IF (ABS(DELTG).GT.0.001) then
              DELT=-1
              IF (DELTG.LT.0.0) DELT=1
              DELZ=DABS(ZNEW(1)/DBLE(DELTG))
              ZNEW(0)=ZNEW(1)-DELZ
              TNEW(0)=TNEW(1)-DELT
  541         IF (ZNEW(0).GT.0.0D0) THEN
                DO 545 MM=NOZ,1,-1
                  ZNEW(MM)=ZNEW(MM-1)
                  TNEW(MM)=TNEW(MM-1)
  545           CONTINUE
                ZNEW(0)=ZNEW(1)-DELZ
                TNEW(0)=TNEW(1)-DELT
                GOTO 541
              ENDIF
            ENDIF
C
C   Fill in missing T(n): Insert temp's if the temp difference
```

```
C between T(n) and T(n+1) is greater than 2 K.
C
            DO 575 N=1,NOZO
              KDIF=TNEW(N+1)-TNEW(N)
              KABS=IABS(KDIF)
              IF (KABS.GT.1) THEN
                DELZ=(ZNEW(N+1)-ZNEW(N))/REAL(KABS)
                DELT=-1
                IF (KDIF.GT.0) DELT=1
                DO 573 NN=NOZ,N+1,-1
                  ZNEW(NN)=ZNEW(NN-1)
                  TNEW(NN)=TNEW(NN-1)
  573           CONTINUE
                ZNEW(N+1)=ZNEW(N)+DELZ
                TNEW(N+1)=TNEW(N)+DELT
              ENDIF
  575       CONTINUE
C
C   Migrate T(50,nuhr) toward TI
C
            IF (TNEW(NOZ).NE.TI) THEN
              TZERO=TNEW(NOZ)
              DELT=1
              IF (TZERO.GT.TI) DELT=-1
              IF (TNEW(NOZO).EQ.TZERO) TNEW(NOZ)=TZERO+DELT
            ENDIF
            IF (NS.LT.NSMAX-1) THEN
              DO 579 N=0,NOZ
                  ZOLD(N)=ZNEW(N)
                  TOLD(N)=TNEW(N)
  579         CONTINUE
            ENDIF
  581     CONTINUE
          DO 585 N=0,NOZ
            Z(N,NUHR)=ZNEW(N)
            T(N,NUHR)=TNEW(N)
  585     CONTINUE
          TG(NUHR)=TGNEW
  591   CONTINUE
  593 CONTINUE
      RETURN
      END
C=======================================================================
      real function es(Tz)
C=======================================================================
C    es is after [Iribarne and Godson, 1981].
C
      implicit none
      real Tz
      es = 1.e2 * 10.**(9.4041-2354./Tz)
      return
      end
C=======================================================================
      SUBROUTINE TIME(T)
C=======================================================================
      implicit none
      DOUBLE PRECISION T
CSGLE REAL T
      REAL ETIME,TARRAY(2)
C
C ETIME  returns the elapsed run time in seconds for the calling process.
C The argument array TARRAY returns user time in the first element and
C system time in the second element.  The function value is the sum of
C user and system time.
C This routine will run on apollos, decs, suns, alliant, etc.
C Type 'man etime' for more information.
C On the apollos, due to a bug in sr10.1, this routine works fine
C only on nodes running sr10.2 or greater.
```

```
      T =  DBLE(ETIME(TARRAY))
CSGLE T =       ETIME(TARRAY)
      RETURN
      END
C=======================================================================
       subroutine scond(RCP2,KWET,f,f_d,fe,MOIS)
C=======================================================================
C   The program computes thermal conductivity of moist soils.  Moist
C soil consists of air, water(and ice), and dry soil.
C
C     K = thermal conductivity, cal/cm-K --> J/m-K
C     Cp = specific heat, cal/g-K
C     Rho = density, g/cm^3 --> kg/m^3
C     RCp = heat capacity, cal/cm^3-K --> J/m^3-K
C     Tmi,Tma = minimum temperature and maximum temperature, K
C     TmiH,TmaL = low end and high end of the temperatures in a field.
C     scale = a weighting factor used to compute thermal conductivity
C     Vf = volume fraction
C     alpha,beta= parameters used to determine unfrozen liquid water
C     Wu = unfrozen water content, kg H2O/ kg bulk soil
C     T_step = temperature step to compute heat capacity, 0.01 K
C     Tf = freezing point of pure water, 273.16 K
C     Tfpd = freezing pt depression of water within soil, < 273.16K
C     ratio = ratio of void space to solid soil
C     b_dry,c_dry,denom_dry,kwater_dry,K_airdry,r_dry
C     b_sat,c_sat,denom_sat,kwater_sat,K_airsat,r_sat
C               = parameters used to compute ga, shape factor
C     unsatH    = field capacity
C     unsatL    = wilting point
C     f  = evaporation efficiency
C
C     !--------------------bounds for statements-----------------------!
C
      implicit none
      INTEGER Tmi,Tma,TmiH,TmaL,T1
      PARAMETER (Tmi=150,Tma=450,TmiH=250,TmaL=300)
      DOUBLE PRECISION  RCP2(Tmi:Tma),KWET(Tmi:Tma),f(Tmi:Tma),
     1       f_d(Tmi:Tma)
      real MOIS,T_step,K_soil_ave,RCp_soil_ave,Rho_soil,f_ave,fe,
     1       f_d_stepH, f_d_stepL

      real  T,Tf,Tfpd,Tfpd_K,RH,alpha,beta,porosity,Wu_water,Wu_H2O,
     1  Vf_space,Vf_solid,Vf_sat,Vf_unsatH,Vf_unsatL,es0,
     2  Vf_H2O,Vf_dry,scale_total,ratio_H2O,Vf_H2O_free15

      real Vf_clay,  ratio_clay,  K_clayf,  scale_clay,  scale_clayK,
     1     Vf_org,   ratio_org,   K_orgf,   scale_org,   scale_orgK,
     2     Vf_water,              K_waterf, scale_water, scale_waterK,
     3     Vf_ice,                K_icef,   scale_ice,   scale_iceK,
     4     Vf_air,   ratio_air,   K_airf,   scale_air,   scale_airK,
     5     Vf_quartz,ratio_quartz,K_quartzf,scale_quartz,scale_quartzK

      real Cp_clayT,  K_clayT,  Rho_clayT,  RCp_clay,  kclay,
     1     Cp_orgT,   K_orgT,   Rho_orgT,   RCp_org,   korg,
     2     Cp_waterT, K_waterT, Rho_waterT, RCp_water,
     3     Cp_iceT,   K_iceT,   Rho_iceT,   RCp_ice,   kice,
     4     Cp_airT,   K_airT,   Rho_airT,   RCp_air,   kair,
     5     Cp_quartzT,K_quartzT,Rho_quartzT,RCp_quartz,kquartz

      real Wt_H2O,Wt_water,D_waterT,Le_waterT,K_vaporT,esT,Rho_bulk,
     1     T2,Wt_water2,T15,Rho_water15,Rho_bulk15

      real ga,ga_sat,ga_unsatH,ga_soil,ga_ice,ga_water,
     1     gc,gc_sat,gc_soil,gc_ice,gc_water,ga_dry,ga_dry_sat,
     2     RCp_soil, K0,K_soildry,K_soil,K_unsatL,
     3     b_dry,c_dry,denom_dry,kwater_dry,K_airdry,r_dry,
     4     b_sat,c_sat,denom_sat,kwater_sat,K_airsat,r_sat
```

```
      common /COND_VFL/Vf_H2O,Tfpd_K,Vf_space,alpha,beta,Tf,Wt_H2O,
     1 Vf_clay,Vf_org,Vf_quartz
c
c      This section is needed to calculate Tb.
c      Revised on Thu Apr 21 12:01:25 EDT 1994.
c
      real Vf_H2O_free,  Vf_H2O_free_ave,  Vf_H2O_fr(Tmi:Tma),
     1  Vf_water_free,Vf_water_free_ave,f_water_fr(Tmi:Tma),dummy,
     2  K_airTO,Vf_waterL,Vf_iceL,Vf_airL,Wu_waterL,Wt_waterL,gaL,gcL
c
      real     Cp_clay,  K_clay,  Rho_clay,  L_f2,
     1         Cp_org,   K_org,   Rho_org,
     2         Cp_water, K_water, Rho_water,  D_water, Le_water,
     3         Cp_ice,   K_ice,   Rho_ice,    K_vapor, es,
     4         Cp_air,   K_air,   Rho_air,
     5         Cp_quartz,K_quartz,Rho_quartz
      external Cp_clay,  K_clay,  Rho_clay,  L_f2,
     1         Cp_org,   K_org,   Rho_org,
     2         Cp_water, K_water, Rho_water,  D_water, Le_water,
     3         Cp_ice,   K_ice,   Rho_ice,    K_vapor, es,
     4         Cp_air,   K_air,   Rho_air,
     5         Cp_quartz,K_quartz,Rho_quartz
C
C     !--------------------bounds for statements----------------------!
C
C  Prescribed parameters
C
      porosity     = 48
      ratio_clay   = .225
      ratio_quartz = .775
      ratio_org    = 1. - (ratio_clay+ratio_quartz)
      Tf           = 273.16
      T_step       = .01
C
C  Formula used to compute unfrozen water content follows
C [Andersland et al, 1978]. alpha and beta are two model parameters.
C
      alpha = .2380
      beta  = -.360
C
C   ga_XXXX are shape factors used to compute thermal conductivity
C after [de Vries, 1963].
C
      ga_soil  = .144
      ga_ice   = .144
      ga_water = .144
C
C  Parameters that do not depend upon moisture content
C
      Vf_space   = porosity / 100.
      Vf_solid   = 1. - Vf_space
      Vf_clay    = ratio_clay * Vf_solid
      Vf_org     = ratio_org  * Vf_solid
      Vf_quartz  = ratio_quartz  * Vf_solid
C
C     Typically, I assume porosity = 47%, field capacity = 28%, and
C   wilting point = 13%. ==> .27659574 = 13/47;  0.59574468 = 28/47.
C   These parameters may be changed if a different porosity is given.
C
      Vf_sat    = Vf_space
      Vf_unsatH = 5.9574468e-1 * Vf_sat
      Vf_unsatL = 2.7659574e-1 * Vf_sat
      Vf_dry    = .0
      ga_sat    = 1./3.
      gc_sat    = 1. - 2. * ga_sat
      gc_soil   = 1. - 2. * ga_soil
      gc_ice    = 1. - 2. * ga_ice
      gc_water  = 1. - 2. * ga_water
```

```
      es0   = es(Tf)

      T15   = Tf+15.
      Rho_bulk15=(Rho_air(T15)*Vf_space+Rho_clay(T15)*Vf_clay+
     1          Rho_org(T15)*Vf_org  +Rho_quartz(T15)*Vf_quartz)
      Rho_water15 = Rho_water(T15)

      write(6,*)'Rho_bulk(288.16 K) = ',Rho_bulk15
      write(6,*)Vf_sat,Vf_unsatH,Vf_unsatL
      write(6,*)'Saturated  Field Capacity  Wilting Pt (Vol Fraction)'
      write(6,*)Vf_sat*Rho_water15/Rho_bulk15,Vf_unsatH*
     1     Rho_water15/Rho_bulk15,Vf_unsatL*Rho_water15/Rho_bulk15
      write(6,*)'Saturated  Field Capacity  Wilting Pt (mixing ratio)'

      open(95,file='free.dat',STATUS= 'UNKNOWN')
      open(97,file='conduct.dat',STATUS= 'UNKNOWN')
      open(99,file='scale.dat',STATUS= 'UNKNOWN')

      Vf_H2O = (MOIS/Rho_water15)/(1./Rho_bulk15)
      if (Vf_H2O.ge.Vf_sat) Vf_H2O = Vf_sat
      ratio_H2O = Vf_H2O/Vf_space
      write(6,*)'The vol fraction of water at 288.16 K is ',Vf_H2O
      if(Vf_H2O.ge.Vf_unsatL)then
        Vf_H2O_free15 = Vf_H2O - Vf_unsatL
      else
        Vf_H2O_free15 = 0.
      endif
c      Do 90 ratio_H2O = 0.,1.,.2
       if(ratio_H2O.eq.0.)ratio_H2O=1.e-5
C
C  Parameters that depend upon moisture content
C
      ratio_air = 1. - ratio_H2O
      Vf_air    = ratio_air * Vf_space
      Wt_H2O    = Vf_H2O * Rho_water(T15)

      Rho_bulk=(Rho_air(Tf)*Vf_space+Rho_clay(Tf)*Vf_clay+
     1          Rho_org(Tf)*Vf_org  +Rho_quartz(Tf)*Vf_quartz)
      Wu_H2O = Vf_H2O * Rho_water(Tf) / Rho_bulk
      Tfpd = (Wu_H2O / alpha)**(1./beta)
      Tfpd_K = Tf - Tfpd

      open(98,file='Dielect.dat',STATUS= 'UNKNOWN')
      Do 80 T1 = TmiH,TmaL,1
        K_soil_ave   = 0.
        RCp_soil_ave = 0.
        f_ave        = 0.
        Vf_H2O_free_ave   = 0.
        Vf_water_free_ave = 0.
        do 60 T = real(T1-0.5), real(T1+0.5), T_step
          Cp_clayT    = Cp_clay(T)
          K_clayT     = K_clay(T)
          Rho_clayT   = Rho_clay(T)
          RCp_clay    = Rho_clayT * Cp_clayT

          Cp_orgT     = Cp_org(T)
          K_orgT      = K_org(T)
          Rho_orgT    = Rho_org(T)
          RCp_org     = Rho_orgT * Cp_orgT

          Cp_quartzT  = Cp_quartz(T)
          K_quartzT   = K_quartz(T)
          Rho_quartzT = Rho_quartz(T)
          RCp_quartz  = Rho_quartzT * Cp_quartzT

          Cp_waterT   = Cp_water(T)
          K_waterT    = K_water(T)
          Rho_waterT  = Rho_water(T)
```

```
          D_waterT    = D_water(T)
          Le_waterT   = Le_water(T)
          RCp_water   = Rho_waterT * Cp_waterT
          Cp_airT     = Cp_air(T)
          K_airTO      = K_air(T)
          Rho_airT    = Rho_air(T)
          RCp_air     = Rho_airT * Cp_airT
          K_vaporT    = K_vapor(T)
          esT      = es(T)
          KO = K_waterT
          if (T.ge.Tfpd_K) then
            Vf_water = Vf_H2O
            Vf_ice   = 0.
            Vf_air   = Vf_space - Vf_water
            RCp_soil = RCp_clay*Vf_clay+RCp_org*Vf_org
     1      +RCp_quartz*Vf_quartz+ RCp_water*Vf_water+RCp_air*Vf_air
          else
            Cp_iceT  = Cp_ice(T)
            K_iceT   = K_ice(T)
            Rho_iceT = Rho_ice(T)
            RCp_ice  = Rho_iceT * Cp_iceT
            Wu_water = alpha * (Tf-T)**beta
C
C   Rho_bulk is defined as the bulk density of soil with
C space filled by air only.  Vf_air = Vf_space.
C
            T2 = Tf-T+T_step
            Rho_bulk=(Rho_airT*Vf_space+Rho_clayT*Vf_clay+
     1              Rho_orgT*Vf_org  +Rho_quartzT*Vf_quartz)

            Wt_water = Wu_water * Rho_bulk
            Wt_water2=  alpha * (T2**beta)* Rho_bulk
c            Vf_water = Wt_water, cgs system  / rho = mks
            Vf_water = Wt_water / Rho_waterT
C
C  Note water mass must be conserved.
C
            Vf_ice   = (Wt_H2O - Wt_water)/Rho_iceT
            Vf_air   = Vf_space - (Vf_water+Vf_ice)
            if (Vf_air.le.0.) then
              Vf_air = 0.0
              Vf_ice = Vf_space - Vf_water
            endif
            RCp_soil = RCp_clay*Vf_clay+RCp_org*Vf_org+RCp_quartz*
     1       Vf_quartz+RCp_water*Vf_water+RCp_air*Vf_air+RCp_ice*Vf_ice
     2        + L_f2(T)*(Wt_water-Wt_water2)/T_step
          endif
          if (T.eq.288.)then
            Rho_soil=Rho_clayT*Vf_clay+Rho_orgT*Vf_org+Rho_quartzT*
     1       Vf_quartz+Rho_waterT*Vf_water+Rho_iceT*Vf_ice+
     2       Rho_airT*Vf_air
          endif
C
C     !--------------------bounds for statements----------------------!
C  It is assumed that the continuous medium is water if Vf_water >=
C Vf_unsatL.  The apparent thermal conductivity of a gas-filled pore is
C due to both the normal heat conduction K_air and vapor movement K_vapor.
C Hence, K_air = K_air + K_vapor.
C   K_vapor = K_vapor for saturated vapor if Vf_water >= Vf_waterH
C   K_vapor = RH * K_vapor for unsaturated vapor if Vf_water < Vf_waterH
C  RH is determined using a linear interpolation scheme between
C Vf_water=Vf_dry and Vf_water=Vf_unsatH.
C
          K_airsat = K_airTO + K_vaporT
          r_sat    = K_airsat/K_waterT -1.
          kwater_sat=(2./(1.+ (K_waterT/K_airsat -1.)*ga_water)+
     1               1./(1.+ (K_waterT/K_airsat -1.)*gc_water))/3.
          denom_sat = -6.*r_sat**2 / kwater_sat
```

```
            b_sat =(3.*(r_sat-1)/kwater_sat+3.)*r_sat/denom_sat
            c_sat =(3.*(1+r_sat)/kwater_sat-(3.+2.*r_sat))/denom_sat
            ga_dry_sat = (-b_sat-sqrt(b_sat**2 - 4.*c_sat))/2.
            if(Vf_H2O.ge.Vf_unsatH)then
              ga = ga_sat -(Vf_air/Vf_sat) * (ga_sat-ga_dry_sat)
              gc = 1. - 2. * ga
              K_airT = K_airTO + K_vaporT
            else
              K_airdry = K_airTO
              r_dry    = K_airdry/K_waterT -1.
              dummy = K_waterT/K_airdry -1.
              kwater_dry=(2./(1.+dummy*ga_water) +
     1                    1./(1.+dummy*gc_water))/3.
              denom_dry = -6.*r_dry**2 / kwater_dry
              b_dry =(3.*(r_dry-1)/kwater_dry+3.)*r_dry/denom_dry
              c_dry =(3.*(1+r_dry)/kwater_dry-(3.+2.*r_dry))/denom_dry
              ga_dry = (-b_dry-sqrt(b_dry**2 - 4.*c_dry))/2.
              ga_unsatH=ga_sat-(1.-Vf_unsatH/Vf_sat)*
     1                 (ga_sat-ga_dry_sat)
              ga =ga_dry+Vf_water/Vf_unsatH *(ga_unsatH-ga_dry)
              gc = 1. - 2. * ga
              RH = Vf_water/Vf_unsatH
              K_airT = K_airTO + RH * K_vaporT
              if(Vf_H2O.lt.Vf_unsatL) then
C
C  The continuous medium is air at Vf_water = 0.
C K_soildry is soil conductivity at Vf_water = 0.
C  K_soil is linearly interpolated between the two values,
C Vf_water = 0 and Vf_water = Vf_unsatL.
C
                dummy = K_clayT/K_airdry -1.
                kclay=ga_sat*(2./(1.+dummy*ga_soil)+
     1                        1./(1.+ dummy*gc_soil))
                dummy = K_orgT/K_airdry -1.
                korg =ga_sat*(2./(1.+dummy*ga_soil)+
     1                        1./(1.+dummy*gc_soil))
C     !--------------------bounds for statements-----------------------!
                dummy = K_quartzT/K_airdry -1.
                kquartz =ga_sat*(2./(1.+dummy*ga_soil)+
     1                           1./(1.+dummy*gc_soil))
                K_soildry=1.25*(kclay*Vf_clay*K_clayT+korg*Vf_org*
     1           K_orgT+kquartz*Vf_quartz*K_quartzT+Vf_sat*K_airdry)/
     2          (kclay*Vf_clay+korg*Vf_org+kquartz*Vf_quartz+Vf_sat)
C
C  Note Vf_air = Vf_space = Vf_sat above.
C
                gaL =ga_dry+Vf_unsatL/Vf_unsatH *(ga_unsatH-ga_dry)
                gcL = 1.D0 - 2.D0 * gaL
                if(T.ge.Tfpd_K)then
                  Vf_waterL = Vf_H2O
                  Vf_iceL   = 0.
                  Vf_airL   = Vf_space - Vf_waterL
                else
                  Wu_waterL = alpha * (Tf-T)**beta
                  Wt_waterL = Wu_waterL * Rho_bulk
                  Vf_waterL = Wt_waterL / Rho_waterT
                  Vf_iceL   = (Wt_H2O - Wt_waterL)/Rho_iceT
                  Vf_airL   = Vf_space - (Vf_waterL+Vf_iceL)
                  if (Vf_airL.le.0.) then
                    Vf_airL = 0.0
                    Vf_iceL = Vf_space - Vf_waterL
                  endif
                endif
                dummy = K_clayT/KO -1.
                kclay=ga_sat*(2./(1.+ dummy*ga_soil)+
     1                        1./(1.+ dummy*gc_soil))
                dummy = K_orgT/KO -1.
                korg =ga_sat*(2./(1.+ dummy*ga_soil)+
```

```
     1                        1./(1.+ dummy*gc_soil))
               dummy = K_quartzT/K0 -1.
               kquartz =ga_sat*(2./(1.+ dummy*ga_soil)+
     1                        1./(1.+ dummy*gc_soil))
               dummy = K_airT/K0 -1.
               kair =ga_sat*(2./(1.+ dummy*gaL)+
     1                        1./(1.+ dummy*gcL))
               dummy = K_iceT/K0 -1.
               kice =ga_sat*(2./(1.+ dummy*ga_ice)+
     1                        1./(1.+ dummy*gc_ice))
               K_unsatL=(kclay*Vf_clay*K_clayT+korg*Vf_org* K_orgT+
     1           kquartz*Vf_quartz*K_quartzT  +kair*Vf_air*K_airT +
     2           kice*Vf_ice*K_iceT           +Vf_unsatL*K_waterT)/
     3          (kclay*Vf_clay  +korg*Vf_org  +kquartz*Vf_quartz  +
     4           kair*Vf_air    +kice*Vf_ice  +Vf_unsatL)
C
C  Note Vf_water = Vf_unsatL above when calculate K_unsatL.
C
                K_soil=K_soildry+Vf_H2O*((K_unsatL-K_soildry)
     1           /(Vf_unsatL-Vf_dry))
                goto 50
              endif
            endif
            dummy = K_clayT/K0 -1.
            kclay=ga_sat*(2./(1.+dummy*ga_soil)+1./(1.+dummy*gc_soil))
            dummy = K_orgT/K0 -1.
            korg =ga_sat*(2./(1.+dummy*ga_soil)+1./(1.+dummy*gc_soil))
            dummy = K_quartzT/K0 -1.
            kquartz =ga_sat*(2./(1.+ dummy*ga_soil)+
     1                      1./(1.+ dummy*gc_soil))
            dummy = K_airT/K0 -1.
            kair =ga_sat*( 2./(1.+ dummy*ga)+1./(1.+ dummy*gc))
            dummy = K_iceT/K0 -1.
            kice =ga_sat*( 2./(1.+dummy*ga_ice)+1./(1.+dummy*gc_ice))
            K_soil=(kclay*Vf_clay*K_clayT  +korg*Vf_org* K_orgT +
     1        kquartz*Vf_quartz* K_quartzT +kair*Vf_air*K_airT  +
     2        kice*Vf_ice*K_iceT           +Vf_water*K_waterT)  /
     3       (kclay*Vf_clay  +korg*Vf_org  +kquartz*Vf_quartz   +
     4        kair*Vf_air    +kice*Vf_ice  +Vf_water)
C
C     !--------------------bounds for statements-----------------------!
C  Note Vf_water = Vf_sat since soil is saturated.
C
   50       scale_clay   = kclay*Vf_clay
            scale_org    = korg*Vf_org
            scale_quartz = kquartz*Vf_quartz
            scale_water  = Vf_water
            scale_ice    = kice*Vf_ice
            scale_air    = kair*Vf_air

            scale_clayK  = scale_clay*K_clayT
            scale_orgK   = scale_org*K_orgT
            scale_quartzK= scale_quartz*K_orgT
            scale_waterK = scale_water*K_waterT
            scale_iceK   = scale_ice *K_iceT
            scale_airK   = scale_air*K_airT
            scale_total  = (scale_clay +scale_org   +scale_quartz+
     1                      scale_air  +scale_water +scale_ice)
            K_clayf   = scale_clayK / scale_total
            K_orgf    = scale_orgK / scale_total
            K_quartzf = scale_quartzK / scale_total
            K_waterf  = scale_waterK / scale_total
            K_icef    = scale_iceK / scale_total
            K_airf    = scale_airK / scale_total
            K_soil_ave = K_soil_ave + K_soil
            RCp_soil_ave = RCp_soil_ave + RCp_soil
c           if(Vf_water.ge.Vf_unsatL) then
c             f_ave = f_ave +(Vf_water-Vf_unsatL)/(Vf_sat-Vf_unsatL)
```

```
c            else
c              f_ave = f_ave
c            endif
            if (Vf_H2O.gt.Vf_unsatL) then
              if (Vf_ice.le.0.) then
                Vf_H2O_free = Vf_H2O - Vf_unsatL
                Vf_water_free = Vf_H2O_free
              else
                Vf_H2O_free = Vf_water + Vf_ice - Vf_unsatL
                if(Vf_water.gt.Vf_unsatL) then
                  Vf_water_free = Vf_water - Vf_unsatL
                else
                Vf_water_free = 0.
              endif
            endif
          else
            Vf_H2O_free = 0.
            Vf_water_free = 0.
          endif
c
c           if (T.eq.0.) then
c             f_d_stepL = fe * Vf_water_free
c           endif
c           if (T.eq.T_step) then
c             f_d_stepH = fe * Vf_water_free
c           endif
          Vf_H2O_free_ave   = Vf_H2O_free_ave  + Vf_H2O_free
          Vf_water_free_ave = Vf_water_free_ave + Vf_water_free
          write(98,58)T,K_soil,Vf_water,Vf_ice,RCp_soil
   58     format(f7.3,3(' ',f6.4),' ',1pe9.3)
   60   continue
C
C   f = evaporation efficiency, a ratio between real evaporation and
C potential evaporation, it is assumed to be a linear function of
C moisture content with maximum 1. and minimum 0 corresponding to
C field capacity and wilting point, respectivity.
C
        K_soil_ave   = K_soil_ave * T_step
        RCp_soil_ave = RCp_soil_ave * T_step
        KWET(T1)     = dble(K_soil_ave)
        RCP2(T1)     = dble(RCp_soil_ave/2.)
        Vf_H2O_fr(T1)  = Vf_H2O_free_ave   * T_step
        f_water_fr(T1) = Vf_water_free_ave * T_step / Vf_H2O_fr(T1)
        f(T1)          = fe * Vf_water_free_ave *T_step / Vf_sat
        f_d(T1)        = f(T1) - f(T1-1)
        write(95,68)T1,Vf_H2O_fr(T1),f_water_fr(T1),f_d(T1)
   68   format(I4,3(' ',1pe9.3))
        write(97,72)T,K_soil,Vf_ice,Vf_air,K_iceT,K_vaporT,RCp_soil,
     1      Vf_water,Vf_quartz,K_waterT,K_quartzT
        write(99,76)T,K_soil,K_clayf,K_orgf,K_waterf,K_icef,K_airf,
     1  scale_clay,scale_org,Vf_water,scale_ice,scale_air,K_quartzf,
     2  scale_quartz
   72   format(f6.2,' ',10(' ',1pe9.3))
   76   format(f6.2,13(' ',1pe9.3))
   80 continue
      write(98,*)'  T     K_s    Vf_w   Vf_i  RCp_soil'
      write(98,*)'To get this dat file, change TmiH and TmiL to '
      write(98,*)'the values you like'
      close(98)
      do 82 T1 = Tmi, TmiH-1, 1
        KWET(T1)     = KWET(TmiH)
        RCP2(T1)     = RCP2(TmiH)
        f(T1)        = f(TmiH)
        f_d(T1)      = f_d(TmiH)
        Vf_H2O_fr(T1)  = Vf_H2O_fr(TmiH)
        f_water_fr(T1) = f_water_fr(TmiH)
   82 continue
      do 84 T1 = TmaL+1, Tma, 1
```

```
        KWET(T1)     = KWET(TmaL)
        RCP2(T1)     = RCP2(TmaL)
        f(T1)        = f(TmaL)
        f_d(T1)      = f_d(TmaL)
        Vf_H2O_fr(T1)  = Vf_H2O_fr(TmaL)
        f_water_fr(T1) = f_water_fr(TmaL)
   84 continue
      write(97,92)
   92 format(' Temp  K_soil  Vf_ice    Vf_air   K_ice  K_vapor RCp_soil'
     1'(MKS)  Vf_water  Vf_quartz  K_water  K_quartz ')
      write(99,93)
   93 format(' Temp    K_soil    K_clayf   K_orgf     K_waterf  K_icef '
     1' K_airf scale_clay  sca_org  Vf_water  sca_ice  scale_air  K_qu'
     2'artz  sca_quartz')
      write(95,*) Tfpd,Tfpd_K,Vf_H2O_free15
      write(95,94)
   94 format('Temp  Vf_H2O_free  f_water_fr  evap_eff  evap_eff_deri')
      close(95)
      close(97)
      close(99)
      return
      end
C=======================================================================
      real function Cp_clay(T)
C=======================================================================
C  specific heat of clay, J/kg-K
C
      implicit none
      real T
      Cp_clay = 669.76 + 1.610 * (T - 255.16)
      return
      end
C=======================================================================
      real function K_clay(T)
C=======================================================================
C     conductivity of clay, J/m-s-K
C
      implicit none
      real T
      K_clay = 2.9302
      return
      end
C=======================================================================
      real function Rho_clay(T)
C=======================================================================
C       clay density, kg/m^3
C
      implicit none
      real T
      Rho_clay = 2.65e3
      return
      end
C=======================================================================
      real function Cp_org(T)
C=======================================================================
C  specific heat of org, J/kg-K
C
      implicit none
      real T
      Cp_org = 1.932e3
      return
      end
C=======================================================================
      real function K_org(T)
C=======================================================================
C  conductivity of org, J/m-s-K
C
      real T
```

```
      K_org= 2.5116e-1
      return
      end
C=======================================================================
      real function Rho_org(T)
C=======================================================================
C  org density, kg/m^3
C
      real T
      Rho_org = 1.3 e3
      return
      end
C=======================================================================
      real function Cp_quartz(T)
C=======================================================================
C  specific heat of quartz, J/kg-K
C
      implicit none
      real T
      Cp_quartz = 7.5536843e2
      return
      end
C=======================================================================
      real function K_quartz(T)
C=======================================================================
C  conductivity of quartz, J/m-s-K
C
      real T
      K_quartz= -1.9027254e-6 * T**3 + 1.8922227e-3* T**2
     1         -6.517895e-1 * T      + 8.493394 e1
      return
      end
C=======================================================================
      real function Rho_quartz(T)
C=======================================================================
C  quartz density, kg/m^3
C
      real T
      Rho_quartz = 2.66 e3
      return
      end
C=======================================================================
      real function Cp_water(T)
C=======================================================================
C  specific heat of water, J/kg-K
C
      implicit none
      real T
      Cp_water=(T**4) * (1.6744e-5) -( T**3.) * (2.0646315e-2)
     1   + (T**2)*(9.55735) - T * (1.96851e3) + 1.5639356e5
      return
      end
C=======================================================================
      real function K_water(T)
C=======================================================================
C   conductivity of water, J/m-s-K
C
      implicit none
      real T
      K_water= 0.58604 + 1.15115e-3 *(T - 283.16)
      return
      end
C=======================================================================
      real function Rho_water(T)
C=======================================================================
C  water density, kg/m^3
C
      implicit none
```

```
      real T
      Rho_water = 1.e3
      return
      end
C=======================================================================
      real function D_water(T)
C=======================================================================
C  The diffusion coefficient of water vapor in air, m^2/sec
C
      implicit none
      real T
      D_water = .217e-4 * (T/273.16)**1.8
      return
      end
C=======================================================================
      real function Le_water(T)
C=======================================================================
C  heat of evaporation, J/kg
C
      implicit none
      double precision Tk_Lv(16),L_v(16),de_Lv_T(16),L_v2
      real T
      common /CMAIN_Lv2/Tk_Lv,L_v,de_Lv_T
      call SPLINT(Tk_Lv,L_v,de_Lv_T,16,dble(T),L_v2)
      Le_water = real(L_v2)
      return
      end

C=======================================================================
      real function L_f2(T)
C=======================================================================
C   heat of fusion, J/kg
C===== main
      double precision Tk_Lf(6),L_f(6),de_Lf_T(6),L_fd
      real T
      common /CMAIN_Lf2/Tk_Lf,L_f,de_Lf_T
      call SPLINT(Tk_Lf,L_f,de_Lf_T,6,dble(T),L_fd)
      L_f2 = real(L_fd)
      return
      end

C=======================================================================
      real function Cp_ice(T)
C=======================================================================
C  specific heat of ice, J/kg-K
C
      implicit none
      real T
      Cp_ice = 1.959048e3 + 7.3255 * (T - 253.16)
      return
      end
C=======================================================================
      real function K_ice(T)
C=======================================================================
C  conductivity of ice, J/m-s-K
C
      implicit none
      real T
      K_ice = (T**2) * (1.6744e-4) + T*(-9.7754821e-2) + 16.448468
      return
      end
C=======================================================================
      real function Rho_ice(T)
C=======================================================================
C  ice density, kg/m^3
C
      implicit none
      real T
```

```
      Rho_ice = .92e3
      return
      end
C=======================================================================
      real function Ls_ice(T)
C=======================================================================
C       heat of sublimation, J/kg
C
      implicit none
      real T
      Ls_ice = 2.8376894e6 - 188.37 * (T- 253.16)
      return
      end
C=======================================================================
      real function Cp_air(T)
C=======================================================================
C      specific heat of air, J/kg-K.
C
      implicit none
      real T
      Cp_air = 1004.64
      return
      end
C=======================================================================
      real function K_air(T)
C=======================================================================
C      conductivity of air, J/m-s-K
C
      real T
      K_air = 2.28137e-2 + 7.046433e-5 * (T - 253.16)
      return
      end
C=======================================================================
      real function Rho_air(T)
C=======================================================================
C  air density, kg/m^3
C
      implicit none
      real T
      Rho_air = 3.4855216e2/T
      return
      end

C=======================================================================
      real function K_vapor(T)
C=======================================================================
C      conductivity for saturated vapor, J/m-s-K
C
      implicit none
      real T,Le_water,D_water,es2,es,p,R_vapor
      external Le_water,D_water,es

      p = 1.101325e5
      es2 = es(T)
      R_vapor = 4.6151e3
      K_vapor=Le_water(T)**2 *D_water(T)*p*es2
     1    /((R_vapor**2)*(T**3)*(p-es2))
      return
      end
C=======================================================================
      real function Vf_l(T)
C=======================================================================
C  Calculate liquid water content.
C
      implicit none
      real T,Rho_bulk,Vf_water,Vf_ice,Vf_air,Wu_water,Wt_water,
     1 Rho_airT,Rho_clayT,Rho_orgT,Rho_quartzT,Rho_waterT,
     2 Rho_iceT
```

```
c=====scond
      real Vf_H2O,Tfpd_K,Vf_space,alpha,beta,Tf,Wt_H2O,Vf_clay,
     1 Vf_org,Vf_quartz
      common /COMD_VFL/Vf_H2O,Tfpd_K,Vf_space,alpha,beta,Tf,Wt_H2O,
     1 Vf_clay,Vf_org,Vf_quartz
      external Rho_air,Rho_clay,Rho_org,Rho_quartz,Rho_water,Rho_ice
      real Rho_air,Rho_clay,Rho_org,Rho_quartz,Rho_water,Rho_ice

      if (T.ge.Tfpd_K) then
        Vf_l = Vf_H2O
      else
        Rho_airT    = Rho_air(T)
        Rho_clayT   = Rho_clay(T)
        Rho_orgT    = Rho_org(T)
        Rho_quartzT = Rho_quartz(T)
        Rho_waterT  = Rho_water(T)
        Rho_iceT = Rho_ice(T)
        Wu_water = alpha * (Tf-T)**beta
        Rho_bulk=(Rho_airT*Vf_space+Rho_clayT*Vf_clay+
     1           Rho_orgT*Vf_org  +Rho_quartzT*Vf_quartz)
        Wt_water = Wu_water * Rho_bulk
        Vf_l = Wt_water / Rho_waterT
      endif
      return
      end
C=======================================================================
      SUBROUTINE SPLINE(X,Y,N,YP1,YPN,Y2)
C=======================================================================
C       Subroutines SPLINE and SPLINT are from Numerical Recipes
C   [Press et al 1989].
      implicit none
      integer NMAX,I,N,K
      PARAMETER (NMAX=500)
      double precision X(N),Y(N),Y2(N),U(NMAX),YP1,YPN,SIG,P,QN,UN
      IF (YP1.GT..99E30) THEN
        Y2(1)=0.DO
        U(1)=0.DO
      ELSE
        Y2(1)=-dble(0.5)
        U(1)=(dble(3.)/(X(2)-X(1)))*((Y(2)-Y(1))/(X(2)-X(1))-YP1)
      ENDIF
      DO 11 I=2,N-1
        SIG=(X(I)-X(I-1))/(X(I+1)-X(I-1))
        P=SIG*Y2(I-1)+2.DO
        Y2(I)=(SIG-1.)/P
        U(I)=(dble(6.)*((Y(I+1)-Y(I))/(X(I+1)-X(I))-(Y(I)-Y(I-1))
     1      /(X(I)-X(I-1)))/(X(I+1)-X(I-1))-SIG*U(I-1))/P
11    CONTINUE
      IF (YPN.GT..99E30) THEN
        QN=0.DO
        UN=0.DO
      ELSE
        QN=5DO
        UN=(3.DO/(X(N)-X(N-1)))*(YPN-(Y(N)-Y(N-1))/(X(N)-X(N-1)))
      ENDIF
      Y2(N)=(UN-QN*U(N-1))/(QN*Y2(N-1)+1.DO)
      DO 12 K=N-1,1,-1
        Y2(K)=Y2(K)*Y2(K+1)+U(K)
12    CONTINUE
      RETURN
      END
C=======================================================================
      SUBROUTINE SPLINT(XA,YA,Y2A,N,X,Y)
C=======================================================================
      implicit none
      integer N
      double precision XA(N),YA(N),Y2A(N),X,Y,H,A,B
      integer KLO,KHI,K
```

```
      KLO=1
      KHI=N
1     IF (KHI-KLO.GT.1) THEN
        K=(KHI+KLO)/2
        IF(XA(K).GT.X)THEN
          KHI=K
        ELSE
          KLO=K
        ENDIF
      GOTO 1
      ENDIF
      H=XA(KHI)-XA(KLO)
      IF (H.EQ.0.) PAUSE 'Bad XA input.'
      A=(XA(KHI)-X)/H
      B=(X-XA(KLO))/H
      Y=A*YA(KLO)+B*YA(KHI)+
     1      ((A**3-A)*Y2A(KLO)+(B**3-B)*Y2A(KHI))*(H**2)/6.D0
      RETURN
      END

C=====================================================================
C=====================================================================
C  The following is the parameter file, annual.prm
C=====================================================================
 43.5     { LAT: latitude(typical = 47. N).
 .125     { MOIS: soil moisture(typical MOIS = 7% for dry soil).
 .2       { CL: cloud cover(trpical = 0.2)
 5.       { WIND: average wind(typical = 5 m/s).
 .95      { EM: thermal IR emissivity(typical = .95).
 1000.0   { RHODRY: 7% moist soil density(typicaL = 1000.0 kg/m^3).
 1000.0   { CP: 7% moist soil specific heat(typical = 1000.0 J/kg-K).
 .36      { KDRY: 7% moist soil thermal conductivity(typical = .36 W/m-K).
 3.3      { DIELECT: 7% moist soil dielectric constant(typical = 3.3).
 .23      { LOSSTAN: 7% moist soil loss tangent(typical = .23).
 278.3    { TAIRO: average air temperature(typical = 278.3 K).
 16.9     { TAIR1: annual air temperature variation(typical = 16.9 K).
 1.12     { THETALAG: temperature phase lag(typical = 1.12 months).
 5.       { TDEL: diurnal temperature variation(typical = 5 K).
 .76      { WATERV: water vapor pressure(typical = .76 mmHg).
 1385.    { SO: solar constant(typical = 1385 W/m^2).
 1.25     { RHOAIR: air density at surface(typical = 1.25 kg/m^3).
 1000.0   { CPAIR: dry air specific heat(typical = 1000.0 J/kg-K).
 .002     { DRAG: drag coefficient(typical = 0.002).
 25       { ITERMAX: maximum number of iterations.
 .01      { DELTMAX: convergent criterion for ground temperature
 3        { TAU: the range of temp's when ice and liquid water co-exist
 .3       { ALB: soil albedo
 .7       { ALBCL: albedo of clouds
 1996     { YEAR: the year number
 144      { NSAMD: the number of time steps in a day
 40       ( NOZ: number of soil layers, typical = 40
 .01D0    { ZINCR: increment in depth per layer or iteration, in m.
 1.       { fe: ratio of real to potential evaporation
.40       { humidity: typical relative humidity in South Dakota
```

A.2 The Radiobrightness Module

```
C ================================================================
      PROGRAM TBMU
C ================================================================
C  The code is written to compute bare soil radiobrightness for the AT/R
C model.
C
C  Yuei-An Liou, 1995
C
C     FF : fraction of free water in liquid,
C     TK   : ground temperature, K
C     TC : ground temperature, C (Centigrade)
C     TG        : temperature gradient w.r.t. depth at the surface
C  Vf_H2O_fr    : volume fraction of free water
C
      implicit none
      real CO,PIR,PID
      PARAMETER(CO=3.E8,PIR=3.14159,PID=180.)
      real zefftemp,zefftemp1,THETAR,Tsky,Tair,Flh,Fsh,Fsun,
     1 Vf_w,Vf_i,Vf_a
      INTEGER DAY,ifreq,I
      COMPLEX COSRO,Es,EGND(3),NGND(3)
     1     ,COSTO(3),NCOS1(3), NCOS2(3),AMPV(3),AMPH(3)
      CHARACTER MO*2,LATENT*1
      REAL PIRD,COSR,SINR,ANGF(3),ZEFFO(3),TIME,TG,FF,THETAT(3),
     1 COST(3),TEFF(3),ZEFFCM(3),ZEFFMIN(3),ZEFFMAX(3),TGMIN,TGMAX,
     2 ZEFF(3),RV(3),RH(3),EH(3),EV(3),TBV(3),TBH(3),FREQ,TK,TC,
     3 TbV6a(366,3),TbV6p(366,3),TbH6a(366,3),TbH6p(366,3),Vf_H2O_fr,
     4 Tg6am(366),Tg6pm(366),Vf_H2O_fr_6am(366),FF_6am(366),TBVO(3),
     5 TBHO(3)
      COMMON /CMAIN_WATER_ICE/FREQ
     1       /CMAIN_WATER/TC
     2       /CMAIN_ICE/TK
C
C     !-------------------bounds for statements----------------------!
C==== spara
C
      REAL MOIS,EsR,LTAN,THETA,FREQ2(3),fe,Vf_s,Vf_bw,alpha
      INTEGER NSAMD,NSAMY,NDAY_ST,NDAY_ED,NSAMT
      CHARACTER DATAI*45
      COMMON /CPARA_MAIN/MOIS,EsR,LTAN,THETA,Vf_s,Vf_bw,alpha,
     1       NSAMD,NSAMY,NDAY_ST,NDAY_ED,FREQ2,fe,DATAI
C
C==== ewater,eice
C
      COMPLEX Ew,Ei,Ebw,Ea
      COMMON/CEWATER_MAIN/Ew
      COMMON/CEICE_MAIN/Ei
      CALL SPARA
      TGMIN = 1.
      TGMAX = 0.
      PIRD = PIR / PID
      THETAR = THETA * PIRD
      COSR = COS(THETAR)
      COSRO = CMPLX(COSR,0.)
      SINR = SIN(THETAR)
      do 11 ifreq = 1,3
        FREQ = FREQ2(ifreq)
        ZEFFMIN(ifreq)= 1.
        ZEFFMAX(ifreq) = 0.
        ANGF(ifreq) = 2. * PIR * FREQ
        ZEFFO(ifreq) = CO / (2. * ANGF(ifreq))
   11 continue
      Es = CMPLX(EsR,-EsR*LTAN)
      Es = CMPLX(4.7, 0.)
      Ebw   = cmplx(35., -15.)
```

```
      Ea  = cmplx(1., 0.)
C
C   Determine the ouput file name.
C  Note that MOIS is moisture content by volume, but MO is
C moisture content by weight.  MOIS = .3802, MO = .275;
C  MOIS = .1728, MO = .125
C
        IF (MOIS.EQ.0.1728) THEN
          MO = '12'
        ELSEIF (MOIS.EQ.0.3802) THEN
          MO = '27'
        ELSE
          WRITE(6,*)'Please enter moisture .07, .1, .15, ',
     1             '.20, or .25!'
          PAUSE
        ENDIF
       if(fe.gt.0.01)then
         LATENT = 'M'
       else
         LATENT = 'N'
       endif
       OPEN(UNIT=50,FILE=DATAI,STATUS='OLD')
       OPEN(UNIT=70,FILE='Tb'//LATENT//MO//'.dat',STATUS= 'UNKNOWN')
       OPEN(UNIT=74,FILE='Tb'//LATENT//MO//'_d.dat',STATUS= 'UNKNOWN')
   22 FORMAT(I3,' ',F5.2,' ',F6.2,6(' ',f8.3))
   23 FORMAT(I3,' ',F5.2,' ',F6.2,6(' ',1pe10.3))
       NSAMT = NSAMD*(NDAY_ED-NDAY_ST+1)
       DO 30 I = 1, NSAMY
         read(50,*)DAY,TIME,TK,TG,Tsky,Tair,Flh,Fsh,Fsun,Vf_H2O_fr
         if(Vf_H2O_fr.ge.Vf_bw)then
           Vf_w = Vf_H2O_fr - Vf_bw
         else
           Vf_w = 0.
         endif
         Vf_i = MOIS - Vf_w - Vf_bw
         Vf_a = 1. - MOIS - Vf_s
         IF (TG.GT.TGMAX) THEN
           TGMAX = TG
         ELSEIF (TG.LT.TGMIN) THEN
           TGMIN = TG
         ENDIF
         TC = TK - 273.15
         do 15 ifreq = 1,3
           FREQ = FREQ2(ifreq)
           CALL SEWATER
           CALL SEICE
           EGND(ifreq)=(Vf_s*Es**alpha+Vf_a*Ea**alpha+Vf_w*Ew**alpha+
     1                  Vf_i*Ei**alpha+Vf_bw*Ebw**alpha)**(1./alpha)
           NGND(ifreq) = CSQRT(EGND(ifreq))
           THETAT(ifreq) = ASIN(SINR/REAL(NGND(ifreq)))
C Compute reflectivity.
           COST(ifreq) =  COS(THETAT(ifreq))
           COSTO(ifreq) = CMPLX(COST(ifreq),0.)
           NCOS1(ifreq) = NGND(ifreq)*COSR
           NCOS2(ifreq) = NGND(ifreq)*COST(ifreq)
           AMPV(ifreq) = (NCOS1(ifreq)-COSTO(ifreq)) /
     1                   (NCOS1(ifreq)+COSTO(ifreq))
           AMPH(ifreq) = (COSRO-NCOS2(ifreq)) /
     1                   (COSRO+NCOS2(ifreq))
C Compute reflectivity
           RV(ifreq) = CABS(AMPV(ifreq)) ** 2
           RH(ifreq) = CABS(AMPH(ifreq)) ** 2
           EV(ifreq) = 1. - RV(ifreq)
           EH(ifreq) = 1. - RH(ifreq)
           zefftemp = ABS(AIMAG(NGND(ifreq)))
           zefftemp1 = ZEFFO(ifreq)/zefftemp
           ZEFF(ifreq)=COST(ifreq)*zefftemp1
           ZEFFCM(ifreq) = ZEFF(ifreq) * 100.0
```

```
          IF (ZEFFCM(ifreq).GT.ZEFFMAX(ifreq)) THEN
            ZEFFMAX(ifreq) = ZEFFCM(ifreq)
          ELSEIF (ZEFFCM(ifreq).LT.ZEFFMIN(ifreq)) THEN
            ZEFFMIN(ifreq) = ZEFFCM(ifreq)
          ENDIF
          TEFF(ifreq) = TK + ZEFF(ifreq) * TG
          TBV(ifreq) = EV(ifreq) * TEFF(ifreq)
          TBH(ifreq) = EH(ifreq) * TEFF(ifreq)
          TBVO(ifreq) = EV(ifreq) * TK
          TBHO(ifreq) = EH(ifreq) * TK
          if(TIME.EQ.6.)THEN
            TbV6a(DAY,ifreq) = TBV(ifreq)
            TbH6a(DAY,ifreq) = TBH(ifreq)
            Tg6am(DAY) = TK
            FF_6am(DAY) = FF
            Vf_H2O_fr_6am(DAY) = Vf_H2O_fr
          elseif(TIME.EQ.18.)THEN
            TbV6p(DAY,ifreq) = TBV(ifreq)
            TbH6p(DAY,ifreq) = TBH(ifreq)
            Tg6pm(DAY) = TK
          endif
   15   continue
        WRITE(70,22)DAY,TIME,TK,TBV(1),TBH(1),TBV(2),TBH(2),
     1            TBV(3),TBH(3)
        WRITE(74,23)DAY,TIME,TK,TBV(1)-TBVO(1),TBH(1)-TBHO(1),
     1  TBV(2)-TBVO(2),TBH(2)-TBHO(2),TBV(3)-TBVO(3),TBH(3)-TBHO(3)

C     !--------------------bounds for statements----------------------!
   30 CONTINUE
      WRITE(70,*)'DAY Time  Tgnd TBV(1),TBH(1),TBV(2),TBH(2) 3 3 '
      WRITE(70,*)'The effective emitting depth limits are ',
     1  ZEFFMIN(1),' to ',ZEFFMAX(1),' cm.'
      WRITE(70,*)'The effective emitting depth limits are ',
     1  ZEFFMIN(2),' to ',ZEFFMAX(2),' cm.'

      WRITE(70,*)'The temperature gradient limits are ',
     1  TGMIN,' to ',TGMAX,' K/meter.'
      CLOSE(50)
      CLOSE(70)
      CLOSE(74)
      OPEN(UNIT=90,FILE='Tb6'//LATENT//MO//'.dat',STATUS= 'UNKNOWN')
      OPEN(UNIT=94,FILE='Tg6'//LATENT//MO//'.dat',STATUS= 'UNKNOWN')
       do 84 DAY = NDAY_ST,NDAY_ED
         write(90,82)DAY,(TbV6a(DAY,ifreq),TbV6p(DAY,ifreq),
     1   ifreq =1,3),(TbH6a(DAY,ifreq),TbH6p(DAY,ifreq),ifreq =1,3)
   82    format(I4,12(' ',f8.3))
         write(94,83)DAY,Tg6am(DAY),Tg6pm(DAY),TbH6a(DAY,1),
     1     FF_6am(DAY),Vf_H2O_fr_6am(DAY)
   83    format(I4,3(' ',f8.3),2(' ',1pe10.3))
   84  continue
       write(90,*)'day  6aV  6pV  2_freq 3_freq 6aH 6pH 2_freq 3_freq'
       write(94,*)' day Tg6am Tg6pm  TbH6a FF_6am Vf_H2O_fr_6am'
      CLOSE(90)
      CLOSE(94)
      STOP
      END
C ====================================================================
      SUBROUTINE  SPARA
C ====================================================================
C  Read some parameters.  All units are in SI.
C
      implicit none
      REAL MOIS,EsR,LTAN,THETA,FREQ2(3),fe,Vf_s,Vf_bw,alpha
      INTEGER NSAMD,NSAMY,NDAY_ST,NDAY_ED
      CHARACTER DATAI*45
      COMMON /CPARA_MAIN/MOIS,EsR,LTAN,THETA,Vf_s,Vf_bw,alpha,
     1                   NSAMD,NSAMY,NDAY_ST,NDAY_ED,FREQ2,fe,DATAI
C
```

```
      OPEN(110,FILE='TbA.prm',STATUS='OLD')
C       MOIS: soil moisture(typical MOIS = 7% for dry soil).
      READ(110,*) MOIS
C       EsR: 7% moist soil dielectric constant(typical = 3.3).
      READ(110,*) EsR
C       LTAN: 7% moist soil loss tangent(typical = .23).
      READ(110,*) LTAN
C       NSAMD: the sample number in one day(typical=144)
      READ (110,*) NSAMD
C       NSAMY: the number of time steps in a year(leap=52704,reg=52560)
      READ (110,*) NSAMY
C       NDAY_ST: the starting day number of simulation
      READ(110,*) NDAY_ST
C       NDAY_ST: the ending day number of simulation
      READ(110,*) NDAY_ED
C       FREQ: frequency, Hz(typical=SSM/I frequencies)
        READ(110,*) FREQ2(1)
        READ(110,*) FREQ2(2)
        READ(110,*) FREQ2(3)
C       fe = 0, without latent heat ; = 1,  otherwise.
      READ (110,*) fe
C       THETA(1): incident angle, degrees(typical=53.1)
      READ(110,*) THETA
C         Vf_s = volumetric content of soil solids
      READ(110,*) Vf_s
C         Vf_bw = vloumetric content of bound water
      READ(110,*) Vf_bw
C         alpha = a constant shape factor to determine dielect costant
C                 of moist soils
      READ(110,*) alpha
C       DATAI: input file name,
      READ(110,*) DATAI
      CLOSE(110)
      RETURN
      END
C ===============================================================
      SUBROUTINE SEWATER
C ===============================================================
C  This subroutine computes the complex dielectric constant of water.
C [Ulaby et al 1986] Volume III.
C
C  TC : ground temperature, C
C  FREQ : frequency, Hz
C
      implicit none
      REAL EWATO,EWAT9,DELTAEW,RELAXT,RELAXTF,PORTEW,
     1     EREAL,EIMAG
      COMPLEX Ew
      COMMON/CEWATER_MAIN/Ew
c main ======
      real FREQ,TC
      COMMON /CMAIN_WATER_ICE/FREQ
     1       /CMAIN_WATER/TC

      EWAT9=4.9
C Eq. E.19 in [Ulaby et al 1986] Volume III.
      EWATO=88.045-(0.4147*TC)+(6.295E-4)*(TC**2)+(1.075E-5)*
     1      (TC**3)
C Eq. E.16
      DELTAEW = EWATO - EWAT9
C The relaxation time of pure water is given by Eq. E.17
      RELAXT=1.1109E-10 -3.824E-12 * TC+6.938E-14 * TC**2
     1        - 5.096E-16 * TC**3
      RELAXTF=RELAXT * FREQ
      PORTEW=DELTAEW/(1.+RELAXTF**2)
C Eq. E.15a
      EREAL=EWAT9 + PORTEW
C Eq. E.15b
```

```
      EIMAG = - RELAXTF * PORTEW
      Ew= CMPLX(EREAL,EIMAG)
      RETURN
      END
C ===============================================================
      SUBROUTINE SEICE
C ===============================================================
C  This subroutine computes the complex dielectric constant of ice
C [England 1990].
C
C TK      : ground temperature, K **
C FREQ    : operating frequency, Hz
C BOLTZMAN: Boltzmann's constant, J/K
C
      implicit none
C eice ======
      REAL PIR,RELAXO,BOLTZMAN,BOLC,Ei9,Ei0,RELAXT,PORTEI,
     1     EREAL,EIMAG
      COMPLEX Ei
      COMMON /CEICE_MAIN/Ei
c main ======
      real FREQ,TK
      COMMON /CMAIN_WATER_ICE/FREQ
     1       /CMAIN_ICE/TK

      PIR = 3.141592654
      RELAXO = 2. * PIR * FREQ * 4.76E-16
      BOLTZMAN = 1.3806 E -23
      BOLC = 9.24E-20/BOLTZMAN
      Ei9 = 3.2
      Ei0 = 20715. / (TK-38.)
      RELAXT = RELAXO * EXP(BOLC/TK)
      PORTEI = Ei0/(1.+RELAXT**2)
      EREAL = Ei9 + PORTEI
      EIMAG = - RELAXT * PORTEI
      Ei = CMPLX(EREAL,EIMAG)
      RETURN
      END

C=====================================================================
C=====================================================================
C  Input file of parameters, Tb.prm.
C=====================================================================
.1728  {MOIS: soil moisture (by volume)
3.3    {ESOILR: 7% moist soil dielectric constant(typical = 3.3).
.23    {LTAN: 7% moist soil loss tangent(typical = .23).
144    {NSAMD: number of time steps in one day(typical=144->72)
52704  {NSAMY: number of time steps in a year(leap=52704,reg=52560
              => 26352, 26280)
 173   {NDAY_ST: the starting day number of simulation
 232   {NDAY_ED: the ending day number of simulation
19.35e9{FREQ2: frequency, Hz
37.00e9{FREQ: frequency, Hz
85.50e9{FREQ2: frequency, Hz
1.     {fe: =0, without latent heat; 1, otherwise
53.1   {THETA: SSM/I incident angle, degrees(typical=53.1)
.52    {Vf_s : volumetric content of soil solids
.035   {Vf_bw: volumetric content of bound water
.65    {alpha = a constant shape factor to determine dielect costant
        of moist soils
'/usr/users/yueian/BARE/ANN/TH/M12/annualb.dat'
```

APPENDIX B

THE 1dH/R MODEL

B.1 The 1dH Module

```
C=====================================================================
      PROGRAM dH
C=====================================================================
c  The program is written to simulate the exchange of energy and moisture
c between the land and atmosphere, and coupled energy and moisture
c transport in soil for prairie grassland [Chapter 5 of the dissertation].
c Grass coverage may vary from 0 % to 100 %.  The soil module of this code
c is primarily based on the codes for the bare soil cases [Chapters 3 and
c 4 of the dissertation] except that I also account for the influence of
c transpiration on energy and water transport within the root zone.
c
c  Initial state includes the temperature and moisture profiles of the
c canopy and soil.  These profiles are from the REBEX-1 and the annual
c thermal model [Chapter 2].
c
c  Forcings and inputs are downwelling short- and long-wave radiation,
c and air temperature and relaitve humidity at 1.8 m, infrared temp of
c the canopy, soil temp's and moisture contents at 2, 4, 8, 16, 32, and
c 64 cm, and wind speed at 10 m. These are data from the REBEX-1.
c
c  Products are sensible heat transfer, latent heat transfer of
c evaporation and transpiration, and temperature and moisture profiles
c of the canopy and soil.
c
c     Written by Yuei-An Liou, 1995-1996
c=====================================================================
c
c     T          : temperatures of the canopy, and soil layers
c                  T(0) : canopy
c                  T(i) : soil, i : 1, 2, ... Ns
c     NZ         : number of soil layers
c     Nr         : number of soil layers within the root zone
c     IMAX       : number of available measurements in the period of
c                  interest typically 1 measurement per 10 to 15 minutes
c                  from the REBEX-1
c     NDAY_ST    : daynumber of the starting day, 1 : 1st january
c     NDAY_ED    : daynumber of the ending day
c     YEAR       : the year number
c     RHa        : air relative humidity
c     e_ar(I)    : atmospheric vapor pressure, Pa
c     e_asat(I)  : saturated vapor pressure, Pa
c     q_ar(I)    : atmospheric speific humidity
c     q_asat(I)  : saturated specific humidity
C     DECL(366)  : daily declination
C     DELTMAX    : convergent criterion for ground temp between iterations
C     FGND(I)    : gray-body emission from the ground, W/m^2
```

```
C     Qldc(I)    : absorbed downwelling longwave radiation by canopy, W/m^2
C     Qld(I)     : absorbed downwelling longwave radiation by soil, W/m^2
C     Qsdc(I)    : absorbed downwelling shortwave radiation by canopy, W/m^2
C     Qsd(I)     : absorbed dwonwelling shortwave radiation by soil, W/m^2
C     FWIND(I)   : sensible heat transfer, W/m^2
C     FNET(I)    : net heat flow into the ground, W/m^2
C     HOUR       : local solar time of the (NSAM2)th time step
C     INERTIA    : thermal inertia
C     NDAY       : the day number of the year, ranging from 1 on 1 January
C                  to NDAYY on 31 December
C     NDAYM(I)   : the number of days in the month
C     NDAYMS(0:12) : the number of days to the end of the month
C     NDAYY      : the number of days in a year
C     NSAM2      : the number of time steps starting from the midnight
C     NSAMD      : the number of time steps in a day
C     NSAMMS(0:12) : the number of time steps to the end of the month
C     NSAMDS(0:366): the number of time steps to the end of the day
C     NSAMY      : the number of time steps in a year
C     TGrad(I)   : surface temperature gradient
C     T_OLD(I)   : ground temperatures between iterations
C     T_NEW(I)   : ground temperatures between iterations
C     TOAIR(366): daily average air temperature
C     TSKY(I)    : sky temperature
C     Z(0:nodep,0:I): soil layers as a function of space and time
C     ZOLD(0:nodep): depths
C     ZNEW(0:nodep): depths
C     L_v2       : a function used to compute latent heat of vaporization
C     Lv0        : latent heat of vaporization at reference temp, T0
C     L_vT       : latent heat of vaporization at temp, T
C     Lv         : Lv + (Cp_a - Cp_w) * (T -T0)
C
C     Some parameters are given in the subroutine SPARA.
C
C     !--------------------bounds for statements----------------------!
C
      implicit none
C=== main program
      integer NODEP,IMAX,NSAMD,NOITER,I
      DOUBLE PRECISION PI,SIGMA
      PARAMETER (NODEP=60,IMAX=16000,PI=3.1415927,SIGMA=5.6696E-8)
      DOUBLE PRECISION
     1 COSRLAT,SINRLAT,EMSI,PI2,RLAT1,COS,SIN,YP1,YP2,PERIODD,PI2PER,
     2 EMSIc,EMSIt
      COMMON /CMAIN_FCL_INIT/COSRLAT,SINRLAT
     1 /CMAIN_FCL/PERIODD,PI2PER
     3 /CMAIN_INIT_ITER/EMSI,EMSIc,EMSIt
      double precision Tk_visc(11),visc(11),de_viscT(11),L_f(6),Lv0,
     1 Tk_Lf(6),de_Lf_T(6),L_v(16),Tk_Lv(16),de_Lv_T(16),X1,X2,TACC,
     2 Lf0,Lf0i,NF,Tk_Ls(9),de_Ls_T(9),L_s(9),phi_d(27),Tk_phi(27),
     3 de_phi(27)
      common /CMAIN_RTBI/X1,X2,TACC
     1 /CMAIN_ITER/Tk_visc,visc,de_viscT
     2 /CMAIN_Lf2/Tk_Lf,L_f,de_Lf_T
     3 /CMAIN_Lv2/Tk_Lv,L_v,de_Lv_T
     3 /CMAIN_Ls2/Tk_Ls,L_s,de_Ls_T
     4 /CMAIN_ITER_COND/Lv0,Lf0i,NF
     5 /CMAIN_phi2/Tk_phi,phi_d,de_phi
c===== sdepth
      double precision Z(NODEP),depth(0:NODEP),
     1  Z2(0:NODEP),depth1(NODEP),depth2(0:NODEP)
      common /cdept_MAIN_INIT_ITER/Z,Z2
     1 /cdept_MAIN_ITER/depth,depth1,depth2
C--- spara
      DOUBLE PRECISION RLAT,EM,DELTMAX,psychro,Cp_a,DVfMax,veg,veg1,EMc,
     1 LAI,EMt
      INTEGER NOZ,NDAY_ST,NDAY_ED,drydown
      COMMON /CPARA_MAIN/RLAT,drydown
     2 /CPARA_MAIN_INIT_ITER/EM,EMc,EMt,LAI,veg,veg1,NOZ,NDAY_ST,NDAY_ED
```

```
      4 /CPARA_MAIN_ITER/psychro,DELTMAX,DVfMax
      5 /CPARA_MAIN_ITER_COND/Cp_a
C--- syear
      INTEGER NDAYY
      COMMON /CYEAR/NDAYY
C--- function
      DOUBLE PRECISION es,L_v2,L_f2,L_s2,phi_2,T2
      external es,L_v2,L_f2,L_s2,phi_2
C--- sinit
      INTEGER Nr,NSAM
      DOUBLE PRECISION e_ar(IMAX),pp(0:IMAX),TAIR(IMAX),Qld(IMAX),
     1 TSKY(IMAX),Qldc(IMAX),Qsdc(IMAX),Qsd(IMAX),T(0:NODEP),Wr_max,
     3 Vf(0:NODEP),AIRF(IMAX),FFF(IMAX),RHR_i(IMAX),RDAY(0:IMAX),
     4 Qsdt(IMAX)
      COMMON /CINIT_MAIN_ITER/e_ar,pp,TAIR,AIRF,Qldc,TSKY,Qsdc,T,
     4 Qld,Qsd,Qsdt,Vf,FFF,RDAY,RHR_i,Wr_max,Nr,NSAM
c===== data
      data visc/1.7921e-3, 1.5188e-3, 1.3077e-3, 1.1404e-3, 1.0050e-3,
     1  .8937e-3,.8007e-3,  .7225e-3,  .6560e-3,  .5988e-3,  .5494e-3/
     2 Tk_visc/273.15D0,278.15D0,283.15D0,288.15D0,293.15D0,298.15D0,
     3         303.15D0,308.15D0,313.15D0,318.15D0,323.15D0/
      data L_f/2.035e5,2.357e5,2.638e5,2.889e5,3.119e5,3.337e5/
     1   Tk_Lf/223.15, 233.15, 243.15, 253.15, 263.15, 273.15/
      data L_s/2.832e6, 2.834e6, 2.837e6, 2.8383e6,2.8387e6,
     1         2.8387e6,2.8383e6,2.8366e6,2.8345e6/
     2   Tk_Ls/193.15,  203.15,  213.15,  223.15,  233.15,
     3         243.15,  253.15,  263.15,  273.15/
      data L_v/2.6348e6,2.6030e6,2.5749e6,2.5494e6,2.5247e6,2.5008e6,
     1         2.4891e6,2.4774e6,2.4656e6,2.4535e6,2.4418e6,2.4300e6,
     2         2.4183e6,2.4062e6,2.3945e6,2.3823e6/
     3   Tk_Lv/223.15,  233.15,  243.15,  253.15,  263.15,  273.15,
     4         278.15,  283.15,  288.15,  293.15,  298.15,  303.15,
     5         308.15,  313.15,  318.15,  323.15/
      data phi_d/2655., 2343., 2019., 1685., 1342., 990.6, 631.8, 266.1,
     1   114.8, 114.1, 113.4, 112.7, 112.0, 111.3, 110.6, 109.9, 109.2,
     2   108.5, 107.8, 107.2, 106.5, 105.8, 105.2, 104.5, 103.9, 103.2,
     3   102.6/
     4    Tk_phi/250.,  253.,  256.,  259.,  262.,  265.,  268.,  271.,
     5   274.,   277.,  280.,  283.,  286.,  289.,  292.,  295.,  298.,
     6   301.,   304.,  307.,  310.,  313.,  316.,  319.,  322.,  325.,
     7   328./
C
C     !--------------------bounds for statements----------------------!
C
      YP1 = dble(1e30)
      YP2 = dble(1e30)
      X1 = 120.D0
      X2 = 273.17D0
      TACC = 1.e-8
C
C  Call subroutines to compute viscosity, latent heat of fusion,
c evaporation, and sublimation, and matric head.
C
      CALL SPARA
      call sdepth
      CALL SPLINE(Tk_visc,visc,11,YP1,YP2,de_viscT)
      CALL SPLINE(Tk_Lf,L_f,6,YP1,YP2,de_Lf_T)
      CALL SPLINE(Tk_Lv,L_v,16,YP1,YP2,de_Lv_T)
      CALL SPLINE(Tk_Ls,L_s,9,YP1,YP2,de_Ls_T)
      CALL SPLINE(Tk_phi,phi_d,27,YP1,YP2,de_phi)
      Lv0 = L_v2(273.15D0)
      Lf0 = L_f2(273.15D0)
      Lf0i= Lf0 * .92e3
      i = 0
      CALL SYEAR
C
C  Some common constants.
C
```

```
      PERIODD = 24.DO
      PI2 = 180. / PI
      PI2PER = PI * 2. / PERIODD
      RLAT1 = RLAT / PI2
      COSRLAT = COS(RLAT1)
      SINRLAT = SIN(RLAT1)
      EMSI = EM * SIGMA
      EMSIc = EMc * SIGMA
      EMSIt = EMt * SIGMA
      CALL SDECL
c
c   Model validation or dry-down simulation?
c
      if(drydown.eq.0)then
        CALL SINIT
      else
        CALL SF2
        CALL STOAIR
        CALL SINIT2
      endif
c
c  SITER computes temp and moisture profiles of the canopy and soil.
c Also find sensible and latent heat exchanges between the land and air.
c
      CALL SITER
      STOP
      END
C=======================================================================
      SUBROUTINE  SPARA
C=======================================================================
C       dH.prm lists some parameters used in the code.  All units are
C   in SI.
C
      implicit none
      DOUBLE PRECISION RLAT,WIND,EM,DELTMAX,psychro,TIME_ST,veg,veg1,
     2 Cp_w_i,ZINCR,Cp_a,mh_s,DVfMax,hc,zm,zr,LAI,EMc,Wr,rsmin_max,
     2 rsmin,rsmax,ALB,ALBt,ALBc,EMt
      INTEGER YEAR,NOZ,NDAY_ST,NDAY_ED,NSMAX,write_coe,wea_coe,drydown
      COMMON /CPARA_MAIN/RLAT,drydown
     1 /CPARA_MAIN_INIT_ITER/EM,EMc,EMt,LAI,veg,veg1,NOZ,NDAY_ST,NDAY_ED
     2 /CPARA_MAIN_ITER/psychro,DELTMAX,DVfMax
     3 /CPARA_YEAR/YEAR
     4 /CPARA_MAIN_ITER_COND/Cp_a
     5 /CPARA_ITER/Wr,rsmin_max,rsmin,Cp_w_i,ZINCR,NSMAX,
     5             write_coe,wea_coe
     6 /CPARA_ITER_mhRo/mh_s
     7 /CPARA_F2_INIT_ITER/ALB,ALBt,ALBc
      double precision porosity,ratio_c,ratio_q,Tf,delta_T,ga_soil,ga_i,
     1 ga_w,ratio_o,Tstep,Vf_space,Vf_solid,Vf_c,Vf_o,Vf_q,Vf_sat,
     2 Vf_unsatH,Vf_unsatL,Vf_dry,ga_sat,gc_sat,gc_soil,gc_i,gc_w,Dc2,
     3 no_Tstep,Vf_H2Ok,HK_s,b,Cp_c,K_c,coe_mhi,coe_mhj,coe_alpha,
     4 Rho_c,Cp_o,K_o,Rho_o,Cp_q,Rho_q,Cp_w,Rho_w,Cp_i,Rho_i,viscO,
     5 mh_OT,mh_dT,lambda,Vf_H2O_s,c,tension_aw,mh_O2c,lambda1,RCp_c,
     6 RCp_o,RCp_i,RCp_w,RCp_q,Cp_aw,RCp_solid,zinc,Z_1,mh_0,mh_d,mh_i,
     6 Vf_H2O_i,Vf_H2O_j,coef_I1,coef_I2,coef_I3,I3_exp,Vf_H2O_i_s,
     7 Vf_H2O_j_s,I3_j,I2_i,Is,alpha,mh_j,trans_ct
      COMMON /CPARA_INIT/hc,zm,zr,TIME_ST,trans_ct
     1 /CPARA_ITER_COND/Tstep,RCp_w,Rho_w,Cp_w,Cp_aw,Rho_i,Cp_i
     2 /CPARA_ITER_COND_Vfwa_mhRo/Vf_H2O_s,Vf_sat  /CPARA_ITER_mhCH/b
     3 /CPARA_ITER_COND_Vfwa/Tf
     4 /CPARA_COND/delta_T,ga_soil,ga_i,ga_w,HK_s,Vf_solid,Vf_c,Vf_o,
     5  Vf_q,Vf_unsatH,Vf_unsatL,Vf_dry,ga_sat,gc_sat,gc_soil,
     6  gc_i,gc_w,no_Tstep,Vf_H2Ok,K_c,K_o,RCp_i,viscO,RCp_solid,
     7  tension_aw
      common
     1 /CPARA_COND_DTv/Vf_space
     3 /CPARA_Vfwa_mhRo/mh_OT,lambda,mh_dT,c,coe_mhi,coe_mhj,
     4  coe_alpha
```

```
     4 /CPARA_mhRo/Dc2,lambda1,mh_O2c,mh_O,mh_d,mh_i,alpha,mh_j,
     5 Vf_H2O_i,Vf_H2O_j,coef_I1,coef_I2,coef_I3,I3_exp,Vf_H2O_i_s,
     6 Vf_H2O_j_s,I3_j,I2_i,Is
     8 /para_dept/zinc,Z_1
C
C     !--------------------bounds for statements----------------------!
C
C       Read parameters from dH.prm.  Many parameters are from
C [England 1990].
C
      OPEN(unit=110,FILE='dH.prm',STATUS='OLD')
C       LAT: latitude(typical = 47. N).
      READ(110,*) RLAT
        IF ((RLAT.lt.-90.0).or.(RLAT.gt.90.0)) RLAT=47.0
C       EM: thermal IR emissivity (typical = .96 for bare soil,
C                or = .99 for prairie grassland)
      READ(110,*) EM
C       DELTMAX: convergent criterion for temperature, K
      READ(110,*) DELTMAX
C       DVfMax: convergent criterion for moisture content, %
      READ(110,*) DVfMax
C       YEAR: the year in number.
      READ (110,*) YEAR
C       NOZ: the number of soil layers, less than 100, typical = 40
      READ(110,*) NOZ
C       ZINCR: increase in depth per time step, in m.
      READ(110,*) ZINCR
C       TIME_ST:  starting time in a day, 0 - 24, hr
      READ(110,*) TIME_ST
C       NDAY_ST: the starting day number of simulation
      READ(110,*) NDAY_ST
C       NDAY_ST: the ending day number of simulation
      READ(110,*) NDAY_ED
c
c  soil parameters.
c
        read (110,*)porosity
        read (110,*)ratio_c
        read (110,*)ratio_q
        read (110,*)Tf
        read (110,*)delta_T
        read (110,*)ga_soil
        read (110,*)ga_i
        read (110,*)ga_w
        read (110,*)mh_s
        read (110,*)Vf_H2O_s
        read (110,*)HK_s
        read (110,*)b
        read (110,*)Cp_c
        read (110,*)K_c
        read (110,*)Rho_c
        read (110,*)Cp_o
        read (110,*)K_o
        read (110,*)Rho_o
        read (110,*)Cp_q
        read (110,*)Rho_q
        read (110,*)Cp_w
        read (110,*)Rho_w
        read (110,*)Cp_i
        read (110,*)Rho_i
        read (110,*)Cp_a
        read (110,*)mh_OT
        read (110,*)lambda
        read (110,*)mh_dT
        read (110,*)NSMAX
        read (110,*)tension_aw
        read (110,*)write_coe
        read (110,*)Z_1
```

```
      read (110,*)zinc
c
c vegetation variables
c       hc: vegetation height, m
      read (110,*) hc
c       zm: height of wind measurements, m
      read (110,*) zm
c       zr: depth of root, m
      read (110,*) zr
c      LAI: leaf area index, m^2/m^2
      read (110,*)LAI
c      veg: vegetation coverage
      read (110,*)veg
c      Wr: initial stored water moisture on foliage, m
      read (110,*)Wr
c      rsmin: minimum canopy surface resistance
      read (110,*)rsmin
c      rsmax: maximum canopy surface resistance
      read (110,*)rsmax
c      drydown: dry-down simulation?
      read (110,*)drydown
c      ALB: albedo of bare soil
      read (110,*)ALB
c      ALBt: albedo of thatch
      read (110,*)ALBt
c      ALBc: albedo of canopy
      read (110,*)ALBc
c      trans_ct: transmissivity of thatch / that of canopy
      read (110,*)trans_ct
c      EMc : emissivity of canopy
      read (110,*)EMc
c      EMt : emissivity of thatch
      read (110,*)EMt
      CLOSE(110)
      Cp_aw = Cp_a - Cp_w
      Cp_w_i = Cp_w / Cp_i
      rsmin_max = rsmin/rsmax
C
C  psychro = Cp_a*1.01325e5/(0.622*2.501E6), in K-Newton/m^2
C                * .01 ==> mbar-K
      psychro = Cp_a*1.01325e5/0.622
      ratio_o = 1.D0 - (ratio_c+ratio_q)
      Tstep   = delta_T * 1.e-2
      Vf_space= porosity / 100.D0
      Vf_solid= 1.D0 - Vf_space
      Vf_c    = ratio_c * Vf_solid
      Vf_o    = ratio_o  * Vf_solid
      Vf_q    = ratio_q  * Vf_solid
      Vf_sat  = Vf_space
      Vf_unsatH = 5.9574468e-1 * Vf_sat
      Vf_unsatL = 2.7659574e-1 * Vf_sat
      write(6,*)'wilting pt=',Vf_unsatL,'field capacity=',Vf_unsatH
      Vf_H2Ok = Vf_unsatL
      Vf_dry  = 0.D0
      ga_sat  = 1.D0/3.D0
      gc_sat  = 1.D0 - 2.D0 * ga_sat
      gc_soil = 1.D0 - 2.D0 * ga_soil
      gc_i    = 1.D0 - 2.D0 * ga_i
      gc_w    = 1.D0 - 2.D0 * ga_w
      no_Tstep= delta_T/Tstep +1.D0
      RCp_c = Rho_c * Cp_c
      RCp_o = Rho_o * Cp_o
      RCp_q = Rho_q * Cp_q
      RCp_w = Rho_w * Cp_w
      RCp_i = Rho_i * Cp_i
      RCp_solid = RCp_c*Vf_c + RCp_o*Vf_o + RCp_q*Vf_q
      c = lambda/2.D0 *(1.D0+lambda/2.D0)**(-1.D0-2.D0/lambda)
      coe_mhi = (lambda/2.D0+1.D0)**(1.D0/lambda)
```

```
      coe_alpha = Dexp(1.D0/lambda)
      coe_mhj = Dexp(-1.D0/lambda)
      Dc2 = 2.D0 * DSQRT(c)
      lambda1 = (lambda+1.D0)/lambda
      mh_02c  = mh_0T**2/(2.D0*c)/Vf_H2O_s
      mh_0 = mh_0T
      mh_d = mh_dT
      mh_i = mh_0* coe_mhi
      alpha = lambda*(mh_0/mh_d *coe_alpha)**lambda
      mh_j = mh_d* coe_mhj
      Vf_H2O_i = Vf_H2O_s*(1.D0-c*(mh_i/mh_0)**2)
      Vf_H2O_j = Vf_H2O_s*(mh_0/mh_j)**lambda
      coef_I1 = Dc2 / mh_0
      coef_I2 = 1./(mh_0*lambda1)
      coef_I3 = alpha/mh_d
      I3_exp = 1.D0/ (alpha*Vf_H2O_s)
      Vf_H2O_i_s = (1.D0 - Vf_H2O_i /Vf_H2O_s)**.5
      Vf_H2O_j_s = (Vf_H2O_j /Vf_H2O_s)**lambda1
      I3_j = coef_I3 * (DEXP(I3_exp*Vf_H2O_j)-1.D0)
      I2_i = I3_j + coef_I2*((Vf_H2O_i/Vf_H2O_s)**lambda1 -Vf_H2O_j_s)
      Is   = I2_i + coef_I2 * Vf_H2O_i_s
      visc0 = 1.0050e-3
      veg1 = 1.D0 -veg
      RETURN
      END
C=======================================================================
      SUBROUTINE SYEAR
C=======================================================================
C  Determine whether or not it is a leap year and the values of some
C variables, such as number of days in a month and in a year.
C
      implicit none
C--- syear
      INTEGER NDAYY,NDAYM(12),NSAMY,N1,N2,N3,LEAP,RY(12),LY(12),
     1        NDAYMS(0:12),NSAMMS(0:12),NSAMDS(0:366),NS,I
      COMMON /CYEAR/NDAYY
     1       /CYEAR_MAIN_INIT_ITER/NSAMY,NSAMDS,NSAMMS
C--- spara
      INTEGER YEAR,NSAMD
      COMMON /CPARA_MAIN_YEAR_ITER/NSAMD
     1       /CPARA_YEAR/YEAR
      DATA RY/31,28,31,30,31,30,31,31,30,31,30,31/,
     1     LY/31,29,31,30,31,30,31,31,30,31,30,31/
C
C     !---------------range of statements-----------------------------!
C
      NSAMD = 144
      N1 = MOD(YEAR,4)
      N2 = MOD(YEAR,100)
      N3 = MOD(YEAR,400)
      IF (N1.EQ.0) THEN
        IF (N2.NE.0) THEN
          LEAP = 1
        ELSEIF (N3.EQ.0) THEN
          LEAP = 1
        ELSE
          LEAP = 0
        ENDIF
      ELSE
        LEAP = 0
      ENDIF
      NS = 0
      NDAYMS(0) = 0
      NSAMMS(0) = 0
      NSAMDS(0) = 0
C
C  The number of time steps in a year is NSAMY2.
C
```

```
      IF (LEAP.EQ.1) THEN
        NDAYY = 366
        DO 20 I = 1, 12
          NDAYM(I) = LY(I)
          NS = NDAYM(I) + NS
          NDAYMS(I) = NS
          NSAMMS(I) = NDAYMS(I) * NSAMD
   20   CONTINUE
      ELSE
        NDAYY = 365
        DO 30 I = 1, 12
          NDAYM(I) = RY(I)
          NS = NDAYM(I) + NS
          NDAYMS(I) = NS
          NSAMMS(I) = NDAYMS(I) * NSAMD
   30   CONTINUE
      ENDIF
      NSAMY = NDAYY * NSAMD
      DO 40 I = 1, NDAYY
        NSAMDS(I) = NSAMDS(I-1) + NSAMD
   40 CONTINUE
      RETURN
      END
C=======================================================================
      SUBROUTINE SDECL
C=======================================================================
C Calculate average daily declination.
C
      implicit none
C--- sdecl
      integer I
      DOUBLE PRECISION DECL,GAMMA,DUM,COSDECL(366),SINDECL(366)
      COMMON /CDECL_FCL_INIT/COSDECL,SINDECL
C--- syear
      INTEGER NDAYY
      COMMON /CYEAR/NDAYY
      DUM = 2. * 3.141592654 / NDAYY
      DO 70 I = 1, NDAYY
        GAMMA = (I-1) * DUM
        DECL = .006918-.399912*COS(GAMMA)+.070257*SIN(GAMMA)
     1           -.006758*COS(2.*GAMMA)+.000907*SIN(2.*GAMMA)
     2           -.002697*COS(3.*GAMMA)+.00148*SIN(3.*GAMMA)
        COSDECL(I) = COS(DECL)
        SINDECL(I) = SIN(DECL)
   70 CONTINUE
      RETURN
      END
C=======================================================================
      SUBROUTINE SINIT
C=======================================================================
C      Derive initial conditions from the REBEX-1 and annual model.
C
      implicit none
C==== sinit
      INTEGER HR,IMAX,NOZ1,NODEP,N,I,J,NSAM,SKIP,NSAMDI,NDAY,Nr
      DOUBLE PRECISION PI,SIGMA,EM_tc,EM_t,delt_TI
      PARAMETER (NODEP=60,IMAX=16000,PI=3.1415927,SIGMA=5.6696E-8,
     1   NOZ1=40)
      DOUBLE PRECISION e_asat(IMAX),ZI1(34),TI1(34),de_TZ(34),Rn(IMAX),
     1 Rs(IMAX),RDAY(0:IMAX),TIR(IMAX),TAIR(IMAX),TSKY(IMAX),COS,PIHR,
     2 COSZ,YP1,YP2,T(0:NODEP),pp(0:IMAX),AIRF(IMAX),U10(IMAX),ALBc,
     3 Tcan(IMAX),RHa(IMAX),Vf(0:NODEP),e_ar(IMAX),S_Tc4,Qldc(IMAX),
     4 Qld(IMAX),Qsd(IMAX),Qsdc(IMAX),RHR,ZV1(10),VI1(10),de_Vz(10),
     5 q_ar(IMAX),q_asat(IMAX),r_ar,Root(NODEP),Root2(0:NODEP),zr_e,
     6 F1_f0,F1_F,F1,F3,F4,FFF(IMAX),RHR_i(IMAX),Qld_t,Rn_I,Rs_I,RDAY_I,
     7 TAIR_I,TIR_I,pp_I,U10_I,RHa_I,RNDAY_ST,Wr_max,pp_a,gc,gb,
     8 ALBc_min,ALBc_max,TB1937(4,IMAX),TB19371,TB19372,TB19373,TB19374,
     9 HG_I,HG(IMAX),DUM,DUM2,Tg(6,IMAX),Tg2_I,Tg4_I,Tg8_I,Tg16_I,
```

```
     1 Tg32_I,Tg64_I,Qsdt(IMAX),trans_c,trans_t
      COMMON /CINIT_MAIN_ITER/e_ar,pp,TAIR,AIRF,Qldc,TSKY,Qsdc,T,
     1 Qld,Qsd,Qsdt,Vf,FFF,RDAY,RHR_i,Wr_max,Wr,NSAM
     2 /CINIT_ITER/Tcan,Tg,HG,F1_f0,q_ar,q_asat,Root2
c ===c data
c
c  Soil temperatures are measured at depths of 2, 4, 8, 16, 32, and 64
c cm.  These temperatures together with deeper soil temperatures from
c the annual model are used to initialize soil temperature profile for
c the purpose of model validation.
c  For dry-down simulation, soil temperatures are from the annual model
c (see SINIT2).
c
      data ZI1/.02, .04, .08, .16, .32,  .64,
     1   6.802E-01,7.367E-01,7.973E-01,8.625E-01,9.326E-01,
     2   1.008E+00,1.089E+00,1.176E+00,1.270E+00,1.370E+00,1.478E+00,
     3   1.595E+00,1.720E+00,1.854E+00,1.999E+00,2.154E+00,2.321E+00,
     4   2.500E+00,2.693E+00,2.901E+00,3.124E+00,3.363E+00,3.621E+00,
     5   3.898E+00,4.196E+00,4.516E+00,4.860E+00,5.230E+00/
      data TI1/ 0., 0., 0., 0., 0., 0.,
     1   2.860E+02,2.860E+02,2.860E+02,2.860E+02,2.860E+02,
     2   2.860E+02,2.860E+02,2.861E+02,2.861E+02,2.861E+02,2.861E+02,
     3   2.861E+02,2.862E+02,2.862E+02,2.862E+02,2.862E+02,2.862E+02,
     4   2.862E+02,2.861E+02,2.861E+02,2.860E+02,2.859E+02,2.858E+02,
     5   2.856E+02,2.854E+02,2.852E+02,2.850E+02,2.848E+02/
c
c  Soil moisture contents are mearured at depths of (0-2), (2-4), (4-6),
c and (6-10) cm.  The average of these measured moisture content is .306.
c This moisture content plus the bound water (.035) is assigned to deep
c soils (below 1m depth).  Moisture contents at two depths (.31 and .54
c m) are linearly interpolated.  Finally, moisture profile is found
c using cubic interpolation scheme [Press et al 1989].
c
      data ZV1/.01, .03, .05, .08, .31,   .54,   1.,  2.,    3.,   5.5/
      data VI1/.400,.371,.357,.330,.335,.341,.341,.341,.341,.341/
C---- sapra
      DOUBLE PRECISION EM,hc,zm,zr,veg,veg1,TIME_ST,EMc,LAI,ALB,ALBt,
     1 trans_ct,EMt
      COMMON /CPARA_INIT/hc,zm,zr,TIME_ST,trans_ct
      INTEGER NOZ,NDAY_ST,NDAY_ED
      COMMON /CPARA_MAIN_INIT_ITER/EM,EMc,EMt,LAI,veg,veg1,NOZ,NDAY_ST,
     1 NDAY_ED
     2 /CPARA_F2_INIT_ITER/ALB,ALBt,ALBc
C***   main
      DOUBLE PRECISION COSRLAT,SINRLAT,EMSI,EMSIc,EMSIt
      COMMON /CMAIN_FCL_INIT/COSRLAT,SINRLAT
     2       /CMAIN_INIT_ITER/EMSI,EMSIc,EMSIt
C===   syear
      INTEGER NDAYY
      COMMON /CYEAR/NDAYY
C***  sdecl
      DOUBLE PRECISION COSDECL(366),SINDECL(366)
      COMMON /CDECL_FCL_INIT/COSDECL,SINDECL
C===== sdepth
      double precision Z(NODEP),Z2(0:NODEP)
      common /cdept_MAIN_INIT_ITER/Z,Z2
c===== functions
      double precision Rho_a,es
      external Rho_a,es
c
c     !--------------------bounds for statements-----------------------!
c
      YP1 = dble(1e30)
      YP2 = dble(1e30)
      PIHR = 2. * PI / 24.0
      EM_t = .95
      EM_tc = EM_t / EMc
      RNDAY_ST = dble(NDAY_ST) + TIME_ST/24.0
```

```
      SKIP = 0
      F1_f0  = (.55 * 2.) / (LAI * 100.)
      NSAM = 0
      ALBc_min = 1.
      ALBc_max = 0.
c
c      Wr_max is in meters.
c
      Wr_max = .2e-3 * LAI
c
c  Read day number, relative humidity, air temperature, net radiation,
c thermal infrared temperature, precipitation, and wind speed.  Also,
c determine
c  Qldc: downwelling longwave radiation,
c   1. Reflectance (R) models for red (B2) and near-infrared (B3) bands
c       by (Verma et al 19992)
c   2. An inversion technique by (Brest and Goward, 1987 referred by
c       Daughtry et al, 1990)
c       ALBEDO = .526 B1 + .418 B3
c       B1 = .5 to .59 microns
c       B1 = .61 to .680 microns
c       B3 = .79 to .89 microns
c       R(B1) ~ R(B2) = a few % difference (3% was chosen).
c
c     !--------------------bounds for statements----------------------!
c
      OPEN(unit=110,FILE='ini.dat',STATUS='UNKNOWN')
      OPEN(unit=111,FILE='/y/yueian/REBEX1/DATA/Day.awav',STATUS='OLD')
      OPEN(unit=112,FILE='/y/yueian/REBEX1/DATA/RH.awav',STATUS='OLD')
      OPEN(unit=113,FILE='/y/yueian/REBEX1/DATA/Ta.awav',STATUS='OLD')
      OPEN(unit=114,FILE='/y/yueian/REBEX1/DATA/RnAvg.awav',
     1    STATUS='OLD')
      OPEN(unit=115,FILE='/y/yueian/REBEX1/DATA/RsAvg.awav',
     1    STATUS='OLD')
      OPEN(unit=116,FILE='/y/yueian/REBEX1/DATA/TsEdit.awav',
     1    STATUS='OLD')
      OPEN(unit=117,FILE='/y/yueian/REBEX1/DATA/Prec.awav',STATUS='OLD')
      OPEN(unit=118,FILE='/y/yueian/REBEX1/DATA/U10Avg.awav',
     1    STATUS='OLD')
      OPEN(unit=119,FILE='/y/yueian/REBEX1/DATA/Tbs193785.awav',
     1    STATUS='OLD')
      OPEN(unit=120,FILE='/y/yueian/REBEX1/DATA/Hg.awav',STATUS='OLD')
      OPEN(UNIT=121,STATUS='OLD',FILE='/y/yueian/REBEX1/DATA/Tg2.awav')
      OPEN(UNIT=122,STATUS='OLD',FILE='/y/yueian/REBEX1/DATA/Tg4.awav')
      OPEN(UNIT=123,STATUS='OLD',FILE='/y/yueian/REBEX1/DATA/Tg8.awav')
      OPEN(UNIT=124,STATUS='OLD',FILE='/y/yueian/REBEX1/DATA/Tg16.awav')
      OPEN(UNIT=125,STATUS='OLD',FILE='/y/yueian/REBEX1/DATA/Tg32.awav')
      OPEN(UNIT=126,STATUS='OLD',FILE='/y/yueian/REBEX1/DATA/Tg64.awav')
c
c   Read unwanted data!  REBEX-1 data was stored from day 279, but
c you may start the simulation sometime after day 279.
c
      do 130 I = 1, IMAX, 1
        READ(111,*) RDAY_I
        READ(112,*) RHa_I
        READ(113,*) TAIR_I
        READ(114,*) Rn_I
        READ(115,*) Rs_I
        READ(116,*) TIR_I
        READ(117,*) pp_I
        READ(118,*) U10_I
        READ(119,*) DUM,TB19371,TB19372,DUM2,TB19373,TB19374,DUM
        READ(120,*) HG_I
        READ(121,*) Tg2_I
        READ(122,*) Tg4_I
        READ(123,*) Tg8_I
        READ(124,*) Tg16_I
        READ(125,*) Tg32_I
```

```
        READ(126,*) Tg64_I
c
c  Determine how many sets of data are disregarded.
c
        if(RDAY_I.lt.RMDAY_ST) then
          SKIP = SKIP + 1
        else
          goto 132
        endif
  130 continue
c
c  Start to read data of interest.
c
      pp_a = 0.D0
c
c   Note that you must have correct initial conditions.
c
  132 RDAY(0) = RDAY_I
      pp(0) = pp_I
      do 150 I = 1, IMAX, 1
C         RDAY : daynumber
        READ(111,*) RDAY_I
C         RH : relative humidity, %
        READ(112,*) RHa_I
C         TAIR: air temperature, Kelvin
        READ(113,*) TAIR_I
C         Rn: net radiation, W/m^2
        READ(114,*) Rn_I
C         Rs: downwelling shortwave radiation, W/m^2
        READ(115,*) Rs_I
C     TIR: thermal infrared
        READ(116,*) TIR_I
C     pp: precipitation, inches/cycle ==> m/s
        READ(117,*) pp_I
C     U10: wind speed at 10 meters
        READ(118,*) U10_I
C     TB1937: measured prairie radiobrightness and sky radiobrightness
        READ(119,*) DUM,TB19371,TB19372,DUM2,TB19373,TB19374,DUM
C     HG: heat flow at 2cm
        READ(120,*) HG_I
        READ(121,*) Tg2_I
        READ(122,*) Tg4_I
        READ(123,*) Tg8_I
        READ(124,*) Tg16_I
        READ(125,*) Tg32_I
        READ(126,*) Tg64_I
c
c      Check if any data is missing.
c
        if(pp_I.gt.0.D0)then
          pp_a = pp_a + pp_I
        endif
        if((RHa_I.lt.-1e20).or.(TAIR_I.lt.-1e20).or.(Rn_I.lt.-1e20).
     1    or.(Rs_I.lt.-1e20).or.(TIR_I.lt.-1e20).or.(pp_I.lt.-1e20).
     2    or.(U10_I.lt.-1e20)
     3   .or.(TB19371.lt.-1e20).
     4    or.(TB19372.lt.-1e20).or.(TB19373.lt.-1e20).
     5    or.(TB19374.lt.-1e20).or.(Hg_I.lt.-1e20)
     6   .or.(Tg2_I.lt.-1e20).or.(Tg4_I.lt.-1e20).or.(Tg8_I.lt.-1e20)
     7   .or.(Tg16_I.lt.-1e20).or.(Tg32_I.lt.-1e20)
     8   .or.(Tg64_I.lt.-1e20))then
          goto 150
        endif
c
c  Store data in arrays for further use in simulation.
c
        MSAM = MSAM + 1
        RDAY(MSAM) = RDAY_I
```

```
        RHa(NSAM) = RHa_I
        TAIR(NSAM) = TAIR_I
        Rn(NSAM) = Rn_I
        Rs(NSAM) = Rs_I
        TIR(NSAM) = TIR_I
        pp(NSAM) = pp_a
        U10(NSAM) = U10_I
        pp_a = 0.D0
        TB1937(1,NSAM) = TB19371
        TB1937(2,NSAM) = TB19372
        TB1937(3,NSAM) = TB19373
        TB1937(4,NSAM) = TB19374
        HG(NSAM) = HG_I
        Tg(1,NSAM) = Tg2_I
        Tg(2,NSAM) = Tg4_I
        Tg(3,NSAM) = Tg8_I
        Tg(4,NSAM) = Tg16_I
        Tg(5,NSAM) = Tg32_I
        Tg(6,NSAM) = Tg64_I
        if(NSAM.eq.1)then
          DO 136 J = 1,6
            TI1(J) = Tg(j,NSAM)
  136     CONTINUE
        endif
c
c  Write initial conditions to a file.
c
       write(110,138)NSAM,RDAY(NSAM),RHa(NSAM),TAIR(NSAM),Rn(NSAM),
     1     Rs(NSAM),TIR(NSAM),pp(NSAM),U10(NSAM)
  138  format(i5,' ',1pe13.5,5(' ',1pe12.4),6(' ',1pe9.3))
c
c     1 day = 24 * 60 * 60 = 86400 sec
c
        RHR_i(NSAM) = (RDAY(NSAM)-RDAY(NSAM-1))*86400
c
c     precipitation
c          inches ==> meters
        pp(NSAM) = pp(NSAM) * 2.54e-2 /RHR_i(NSAM)
c
c  Determine downwelling longwave radiation.
c
        Tcan(NSAM) = TIR(NSAM)
        S_Tc4 = SIGMA*Tcan(NSAM)**4
        NDAY = INT(RDAY(NSAM)-.25D0)
        RHR = (RDAY(NSAM)-.25D0)*24.D0
        COSZ=COSRLAT*COSDECL(NDAY)*(-COS(RHR*PIHR)
     1      + SINRLAT*SINDECL(NDAY))
        IF (COSZ.GT.0.0) THEN
          ALBc = 0.526*(.035 + .071 - .052  * COSZ + .0364 * COSZ**2)+
     1          0.418*(.825 - .9514 * COSZ + .4374 * COSZ**2)
          if(veg.eq.0.D0)then
            trans_c = 1.D0
            trans_t = 1.D0
          else
            trans_c = DEXP(-.4D0*LAI/COSZ)
            trans_t = DEXP(-.4D0*LAI*trans_ct/COSZ)
          endif
          DUM=Rs(NSAM)*(1.-ALBc)*veg
          DUM2=DUM*trans_c*(1.-ALBt)
          Qsdt(NSAM)=DUM2*(1.-trans_t)
          Qsdc(NSAM)=DUM*(1.-trans_c)
          Qsd(NSAM)=(Rs(NSAM)*veg1  + DUM2*trans_t)*(1.-ALB)
          if(ALBc.gt.ALBc_max)ALBc_max = ALBc
          if(ALBc.lt.ALBc_min)ALBc_min = ALBc
        ELSE
          ALBc = .4D0
          if(veg.eq.0.D0)then
            trans_c = 1.D0
```

```
            trans_t = 1.D0
          else
            trans_c = DEXP(-.4D0*LAI)
            trans_t = DEXP(-.4D0*LAI*trans_ct)
          endif
          DUM=Rs(NSAM)*(1.-ALBc)*veg
          DUM2=DUM*trans_c*(1.-ALBt)
          Qsdt(NSAM)=DUM2*(1.-trans_t)
          Qsdc(NSAM)=DUM*(1.-trans_c)
          Qsd(NSAM)=(Rs(NSAM)*veg1 + DUM2*trans_t)*(1.-ALB)
        ENDIF
c
c  Oldt = total downwelling longwave radation.  Currently, it is
c computed based upon TIR measurements of grass temp.
c
        Qld_t = (Rn(NSAM) - (1.D0-ALBc)*Rs(NSAM))/EMc+ S_Tc4
        Qldc(NSAM) = veg* EMc * Qld_t
        Qld(NSAM) = veg1 * EM * Qld_t
c
c    Find saturation vapor pressure and real vapor pressure.
c
        e_asat(NSAM) = es(TAIR(NSAM))
        e_ar(NSAM) = e_asat(NSAM)*RHa(NSAM)/100.D0
c
c    Compute specific atmospheric specific humidity.
c        r = .622 e/(p-e), mixing ratio (Iribarne and Godson, 1992)
c        q = r/ (1 + r), specific humidity
c
        r_ar = .622D0*e_ar(NSAM)/(1.01325e5 - e_ar(NSAM))
        q_ar(NSAM) = r_ar/(1.D0+ r_ar)
        r_ar = .622D0*e_asat(NSAM)/(1.01325e5 - e_asat(NSAM))
        q_asat(NSAM) = r_ar/(1.D0+ r_ar)
c
c  Noilhan and Planton, 1989, referred by Jacquemin and Noilhan,1990
c     F1_f  =  F1_f0 * Qsdc(NSAM)
c     F1 = (.01D0 + F1_f )/(1.D0+F1_f)
c     F3 = 1.D0 - .06D0*(q_asat(NSAM)-q_ar(NSAM))
c     IF(F3.LT..3D0)F3=.3D0
c      F4 = 1.D0 - 1.6E-3*(298. - TAIR(NSAM))
c      FFF(NSAM) = 50.D0/(LAI*F1*F3*F4)
c
c    aerodynamic resistance, under netural conditions
c     .4 = von Karman constant .4 **2 ==> .16
c     roughness length = .028 hc (Verma et al, 1992)
c     zero displacement = .71 hc, .71 - .028 = .682
c   resistance <==> conductance
c
c   For prairie
c        AIRF(NSAM) = veg*(U10(NSAM)*.16)/((DLOG((zm/hc-.682)/.028))**2)
c   For bar soil, roughness = .0004 m [Huang and Lyons, 1995]
c        AIRF(NSAM) = veg1*(U10(NSAM)*.16)/((DLOG((zm-.015)/.015))**2)
c
        gc = veg*(U10(NSAM)*.16)/((DLOG((zm/hc-.682)/.028))**2)
        gb = veg1*(U10(NSAM)*.16)/((DLOG((zm-.015)/.015))**2)
        AIRF(NSAM) = gb + gc
         if(RDAY(NSAM).gt.NDAY_ED) goto 152
  150 continue
  152 CLOSE(111)
      CLOSE(112)
      CLOSE(113)
      CLOSE(114)
      CLOSE(115)
      CLOSE(116)
      CLOSE(117)
      CLOSE(118)
      CLOSE(119)
      CLOSE(120)
```

```
      CLOSE(121)
      CLOSE(122)
      CLOSE(123)
      CLOSE(124)
      CLOSE(125)
      CLOSE(126)
      write(110,*)'I,RDAY  RHa  TAIR  Rn  Rs  TIR  pp  U10'
      do 154 I = 1,NSAM,1
        write(110,138)I,RDAY(I),Qsd(I),Qld(I),Qsdc(I),Qldc(I)
  154 continue
        write(110,*)'I       RDAY       Qsd      Qld     Qsdc     Qldc'
      write(110,*)'NSAM=',NSAM
C
C    Determine initial tmperature profile of the soil using the
C cubic interpolation scheme [Press et al 1989].
C
      delt_TI = TI1(7) - TI1(6)
      DO 156 J = 7,34
        TI1(J) = TI1(J) - delt_TI
  156 CONTINUE
      write(110,*)' Temperature Shift is ',delt_TI
      write(110,*)' Soil temperatures are '
      write(110,158)(TI1(J),J=1,34)
      write(110,158)(ZI1(J),J=1,34)
  158 format(6(' ',1pe12.5))
c
c   Determine root distribution.  (Feddes et al, 1974, referred by
c Verseghy et al, 1993).  Root distributions are needed when you
c calculate transpiration.
c
      zr_e = DEXP(-3.D0*zr)
      Root2(0) = 1.D0
      Nr = 0
      DO 170 N=1,NODEP
        IF(Z(N).LE.zr)THEN
          Root2(N) = (DEXP(-3.D0*Z(N)) - zr_e)/(1.D0 - zr_e)
          Nr = Nr + 1
        ELSE
          Root2(N) = 0.D0
        ENDIF
  170 CONTINUE
      Nr = Nr + 1
c
c  Interplate soil moisture content and temperature.
c
      CALL SPLINE(ZI1,TI1,34,YP1,YP2,de_TZ)
      CALL SPLINE(ZV1,VI1,9,YP1,YP2,de_VZ)
c
c  Argument, 0, represents the canopy layer.
c  Vf(0) = 1.4 mm = 1.4 kg/m^2, moisture in the canopy = average
c of the 6 canopy samples from the REBEX1.
c
      T(0) = Tcan(1)
      write(110,*)'Initial canopy temperautre is',Tcan(1)
c
c  Note Vf(0) is in meters.
c
      Vf(0) = 1.4e-3
      DO 172 N=1,NODEP
        CALL SPLINT(ZI1,TI1,de_TZ,34,Z2(N),T(N))
        CALL SPLINT(ZV1,VI1,de_VZ,9,Z2(N),Vf(N))
        Root(N) = Root2(N-1) - Root2(N)
        write(110,*)'TV',Z2(N),T(N),Vf(N)
  172 CONTINUE
      write(110,*)'Albedo max =',ALBc_max,' min=',ALBc_min
      close(110)
C
C   Initialize Z (depth), T (soil temp), and Tg (surf. temp)
```

```
C  for the first time step.
C
  189   format(i5,' ',1pe13.5,8(' ',1pe12.4))
      OPEN(UNIT=194,FILE='TbM.dat',STATUS='UNKNOWN')
      do 191 I = 1,NSAM,1
        write(194,189)I,RDAY(I),Tcan(I),(TB1937(J,I),J=1,4)
  191 continue
      close(194)
      OPEN(UNIT=195,FILE='TgM.dat',STATUS='UNKNOWN')
      do 511 I = 1,NSAM,1
        write(195,189)I,RDAY(I),(Tg(J,I),J=1,6),HG(I)
  511 continue
      close(195)
      RETURN
      END
C=======================================================================
      subroutine SITER
C=======================================================================
C  The subroutine iteratively estimates temp and moisture content/state
C profiles of soil.
C
      implicit none
      integer NODEP,NOZ,NDAY_ST,NDAY_ED,IMAX,J,NWRITE,
     1 HR,NODEPO,JO,J1,HR1,NS,Reiterate,IA,II,IIO,II1,JS,JE,
     2 I,Nice,Solution2,nT,HRO
      parameter (NODEP=60,IMAX=16000,NODEPO=NODEP-1,NWRITE=NODEP/10)
      real RHR
      double precision RCP,KWET,f_T,Vf_H2O_fr,Vf_w_fr,Vf_H2O,Tfdp,
     1 Tfpd,viscosity,DEN,FWET,DTag,Fsh,Flh,Tc,Vf_H2Oc,Phi(0:NODEP),
     2 DLv(0:NODEP),DD_T1(0:NODEP),DD_Tv(0:NODEP),P,Q,R,DUM1,psychro2,
     3 DD_H2O1(0:NODEP),DD_H2Ov(0:NODEP),DHK(0:NODEP),DKWET(0:NODEP),
     4 TD(0:NODEP),VD(0:NODEP),M(0:NODEP),N(0:NODEP),E(0:NODEP),
     5 F(0:NODEP),AT(0:NODEP),AHK(0:NODEP),AD_Tv(0:NODEP),TGrad,
     6 AKWET(0:NODEP),AD_H2Ov(0:NODEP),X(0:NODEP),Y(0:NODEP),
     7 T_NEW(0:NODEP),Vfl_NEW(0:NODEP),T_OLD(0:NODEP),Vfl_OLD(0:NODEP),
     8 Fg,Tk,Lv,dTz1(0:NODEP),dTz2(0:NODEP),dVz1(0:NODEP),RHs,
     9 dVz2(0:NODEP),ALv(0:NODEP),AD_T1(0:NODEP),AD_H2O1(0:NODEP),
     1 Qv(0:NODEP),Q1(0:NODEP),Qm(0:NODEP),Qh0(0:NODEP),Qh1(0:NODEP),
     2 Qh2(0:NODEP),dum,Qh(0:NODEP),Qh3(0:NODEP),Cp_wTk(0:NODEP),
     3 fAIRF,fe_a,fpp,FS,Qld1,fTAIR,pps,TAIRs,DNSMAX,DNS,AIRFs,e_as,
     4 FDIF,DELT60,Vfi(0:NODEP),e_ss,Vfl(0:NODEP),Vfi_OLD(0:NODEP),
     5 Vfi_NEW(0:NODEP),f_i(0:4),g_i(0:4),Ts,dV0,dT0,Vfl_OLDs,pps_max,
     6 T2_OLD(0:NODEP),Vfl2_OLD(0:NODEP),Vfi2_OLD(0:NODEP),dVi,
     7 RCp_wTk_Lv,K_Rho_Lv_T,Rho_Lv_H2O,RCp_wTk_HK,dVf_H2O,Vf_H2O2,
     8 Vfl_OLD1,ATdp(0:NODEP),Qms,dVi0,dV1,dV2,dT1,dT2,T_NEW1,T_NEW2,
     9 T_OLD0,T_OLD2,Vfl_NEW1,Vfl_NEW2,Vfl_OLD0,Vfl_OLD2,deltVf,deltT,
     1 Vf_w1,Vf_w2,Tfdp_NEW,YO(0:NODEP),Vf_NEW,AME(0:NODEP),dRT,E_eff,
     2 ANF(0:NODEP),N_M,T60_d,ANF_i,AME_i,XME,YNF,Vfi_OLD2,Vfi_NEW2,
     3 phi_max(NODEP),phi_sum,Rho_aT,RCp_aT,r_as,q_as,r_ss,q_ss,fq_a,
     4 fq_asat,q_asats,EvR,Root_phi(NODEP),Tt_OLD,Tt_NEW,Ft,DNSAM,
     5 veg_EMSI,veg_EMSIt2,veg_EMSIc,veg_EMSIt
c vegetation
      double precision FSc,ppc,e_ac,r_ac,q_ac,Etv,ppc_max,f_wet,
     1 phi_min,F1_f,F1,F2,F3,F4,r_canopy,Etr,Etrs(0:NODEP),Fshc,Qldc1,
     2 Ev,Flhc,Fc,FWETc,Etrs_t(0:NODEP),FDIFc,FDIFcs,DTas,Etr0,RCp_c,
     3 FlhEt,FlhEc,DiffT(0:6),DiffHG,DiffT2(0:6),DiffHG2,FDIFt,FDIFts,
     4 FSt,DiffHG1
      common /CITER_COND/viscosity,Lv,Vf_H2O,dVf_H2O
     1 /CITER_COND_Vfwa/Tfpd,Tfdp
c===== main
      double precision Tk_visc(11),visc(11),de_viscT(11),EMSI,Lv0,Lf0i,
     1 NF,EMSIc,EMSIt
      common /CMAIN_ITER/Tk_visc,visc,de_viscT
     1 /CMAIN_INIT_ITER/EMSI,EMSIc,EMSIt
     2 /CMAIN_ITER_COND/Lv0,Lf0i,NF
c===== spara
      integer NSMAX,NSMAX2,write_coe,NSAMD,wea_coe
      double precision Tstep,mh_s,b,Vf_H2O_s,Tf,Cp_w_i,ZINCR,RCp_w,
```

```
     1 EM,Rho_w,Cp_a,Cp_w,Cp_aw,psychro,DELTMAX,DVfMax,Vf_sat,Rho_i,
     2 DVfMaxO1,Cp_i,veg,veg1,EMc,LAI,Wr,rsmin_max,rsmin,ALB,ALBt,
     3 ALBc,EMt
      common /CPARA_MAIN_INIT_ITER/EM,EMc,EMt,LAI,veg,veg1,NOZ,NDAY_ST,
     2 NDAY_ED
     1 /CPARA_MAIN_ITER_COND/Cp_a /CPARA_MAIN_YEAR_ITER/NSAMD
     1 /CPARA_MAIN_ITER/psychro,DELTMAX,DVfMax
     2 /CPARA_ITER_COND/Tstep,RCp_w,Rho_w,Cp_w,Cp_aw,Rho_i,Cp_i
     3 /CPARA_ITER_mhCH/b
     4 /CPARA_ITER_COND_Vfwa_mhRo/Vf_H2O_s,Vf_sat
     5 /CPARA_ITER_COND_Vfwa/Tf
     6 /CPARA_ITER/Wr,rsmin_max,rsmin,Cp_w_i,ZINCR,NSMAX,
     6             write_coe,wea_coe
     6 /CPARA_ITER_mhRo/mh_s
     8 /CPARA_F2_INIT_ITER/ALB,ALBt,ALBc
C--- syear
      INTEGER NSAMY,NSAMDS(0:366),NSAMMS(0:12),NDAYY
      COMMON /CYEAR_MAIN_INIT_ITER/NSAMY,NSAMDS,NSAMMS
     1       /CYEAR/NDAYY
Cc===== sinit
      INTEGER Nr,NSAM
      DOUBLE PRECISION e_ar(IMAX),pp(0:IMAX),TAIR(IMAX),Qld(IMAX),
     1 TSKY(IMAX),Qldc(IMAX),Qsdc(IMAX),Qsd(IMAX),T(0:NODEP),Wr_max,
     2 Vf(0:NODEP),AIRF(IMAX),FFF(IMAX),RHR_i(IMAX),RDAY(0:IMAX),F1_f0,
     3 q_ar(IMAX),q_asat(IMAX),Root2(0:NODEP),HG(IMAX),Tcan(IMAX),
     4 Tg(6,IMAX),Qsdt(IMAX)
      COMMON /CINIT_MAIN_ITER/e_ar,pp,TAIR,AIRF,Qldc,TSKY,Qsdc,T,
     1 Qld,Qsd,Qsdt,Vf,FFF,RDAY,RHR_i,Wr_max,Nr,NSAM
     2 /CINIT_ITER/Tcan,Tg,HG,F1_f0,q_ar,q_asat,Root2
c===== sdepth
      double precision Z(NODEP),depth(0:NODEP),Z2(0:NODEP),
     1 depth1(NODEP),depth2(0:NODEP),alpha1(NODEP),alpha2(NODEP),
     2 beta1(NODEP),beta2(NODEP),depth3(NODEP)
      common /cdept_MAIN_INIT_ITER/Z,Z2
     1 /cdept_MAIN_ITER/depth,depth1,depth2
     2 /cdept_ITER/alpha1,alpha2,beta1,beta2,depth3
c===== scond
      double precision HK,Vf_a,Vf_w,D_T1,D_Tv,D_H2O1,D_H2Ov,M_j,N_j,
     1 E_j,F_j,Vf_i,dVf_wT,dVf_iT,Hr_T,f_T2,mh,L_cs,rdf,D_T,D_H2O,
     2 M_j0,N_j0,E_j0,F_j0,ME
      common /CCOND_ITER/D_T1,D_Tv,D_H2O1,D_H2Ov,D_T,D_H2O,M_j,N_j,
     1 E_j,F_j,Vf_i,dVf_wT,f_T2,L_cs,rdf,M_j0,N_j0,E_j0,F_j0,ME
     2 /CCOND_ITER_DT1/HK
     3 /CCOND_ITER_DTv/Vf_a,Vf_w
     4 /CCOND_ITER_Rhov_DTv/Hr_T
c===== functions
      double precision es,Vf_w_Rossi,L_v2,mh_Rossi,L_f2,phi_2,Rho_a
      external es,Vf_w_Rossi,L_v2,mh_Rossi,L_f2,phi_2,Rho_a
C
C     !-------------------bounds for statements----------------------!
C
      dVf_H2O = 0.D0
      DVfMaxO1 = DVfMax/100.D0
      DNSAM = DBLE(NSAM)
      veg_EMSI = veg * EMSI
      veg_EMSIc = veg * EMSIc
      veg_EMSIt = veg * EMSIt
      veg_EMSIt2 = veg * EMSIt * 2.
C=====================================================================!
C Compute transport coefficients vs temp/moisture and store results in !
C  Coef_T.dat and Coef_m.dat.                          --- begin      !
C=====================================================================!
      if(write_coe.eq.1)then
        open(unit=202,STATUS='UNKNOWN',FILE='Coef_T.dat')
c
c  wilting pt=  0.132765955200000     field capacity=  0.285957446400000
c
        do 206 Vf_H2Oc = .04D0,.48001D0,.11D0
```

```
          Vf_H2O2 = Vf_H2Oc
          if (Vf_H2O2.ge.Vf_H2O_s) then
            Vf_H2O = Vf_H2O_s - 0.e-12
          else
            Vf_H2O = Vf_H2O2
          endif
          dVf_H2O = Vf_H2O2 - Vf_H2O
c
c   Transport coefficients vrsus temperature.
c
        do 204 Tc = 250.0D0, 290.00001D0, .08D0
          if(Tc.lt.273.15D0)then
            if(Tc.lt.100.D0)pause 'temp is lower than 100K!'
            call RTBIS(Tfdp,Vf_H2O)
          else
            Tfdp = 273.15D0
          endif
          Tfpd = Tf - Tfdp
          CALL SPLINT(Tk_visc,visc,de_viscT,11,Tc,viscosity)
          call scond(Tc,RCP,KWET,f_T,Vf_H2O_fr,Vf_w_fr,mh)
          write(202,208)Tc,mh,Vf_H2O,Vf_w,RCP,KWET,HK,D_Tl,D_Tv,
     1                D_H2Ol,D_H2Ov
  204   continue
  206   continue
  208   format(1pd10.4,10(' ',1pd9.3))
        close(202)
        open(unit=210,STATUS='UNKNOWN',FILE='Coef_m.dat')
  212   format(1pd10.4,10(' ',1pd9.3),' ',1pd12.6)
c
c   Transport coefficients versus moisture.
c
        do 218 Tc = 265.D0, 297.D0, 8.D0
        do 216 Vf_H2Oc = .01D0,.48D0,0.00094D0
          Vf_H2O2 = Vf_H2Oc
          if (Vf_H2O2.ge.Vf_H2O_s) then
            Vf_H2O = Vf_H2O_s - 0.e-12
          else
            Vf_H2O = Vf_H2O2
          endif
          dVf_H2O = Vf_H2O2 - Vf_H2O
          if(Tc.lt.273.15D0)then
            if(Tc.lt.100.D0)pause 'temp is lower than 100K!'
            call RTBIS(Tfdp,Vf_H2O)
          else
            Tfdp = 273.15D0
          endif
          Tfpd = Tf - Tfdp
          CALL SPLINT(Tk_visc,visc,de_viscT,11,Tc,viscosity)
          call scond(Tc,RCP,KWET,f_T,Vf_H2O_fr,Vf_w_fr,mh)
          write(210,212)Tc,mh,Vf_H2O,Vf_w,RCP,KWET,HK,D_Tl,D_Tv,
     1                D_H2Ol,D_H2Ov,Tfdp
  216   continue
  218   continue
        write(210,*)'    Tc      matric_h   Vf_H2O   Vf_water    RCP     '
     1,'  KWET       HK       Themal_l Themal_v    Iso_l     Iso_v  Tfdp'
        close(210)
        pause 'All coefficients are computed!'
       endif
C=============================================================== ==========!
C Initialize soil temp and moisture state/content profiles.            !
C=====================================================================!
      Vfl(0) = Vf(0)
      Vfi(0) = 0.D0
      Tt_OLD = (T(0)+T(1))/2.D0
      DO 220 J=1,NODEP
        J0 = J - 1
        Tk = T(J) - 273.15D0
        Lv = Lv0 + Cp_aw * Tk
```

```
        Vf_H2O2 = Vf(J)
        if (Vf_H2O2.ge.Vf_H2O_s) then
          Vf_H2O = Vf_H2O_s - 0.e-12
        else
          Vf_H2O = Vf_H2O2
        endif
        dVf_H2O = Vf_H2O2 - Vf_H2O
        if(T(J).lt.273.15D0)then
          if(T(J).lt.100.D0)pause 'temp is lower than 100K!'
          call RTBIS(Tfdp,Vf_H2O)
        else
          Tfdp = 273.15D0
        endif
        Tfpd = Tf - Tfdp
        CALL SPLINT(Tk_visc,visc,de_viscT,11,T(J),viscosity)
        call scond(T(J),RCP,KWET,f_T,Vf_H2O_fr,Vf_w_fr,mh)
        Vfl(J)=Vf_w
        Vfi(J)=Vf_i
  220 CONTINUE
C=====================================================================!
C   Iterate soil temp and moisture content/state.                     !
C=====================================================================!
C
C       The file, 22.dat, stores the ground temperatres on
C     03/22(82), 06/22(174), 09/22(266), and 12/22(357).
C
      OPEN(UNIT=222,STATUS='UNKNOWN',FILE='fdEx.dat')
      OPEN(UNIT=223,STATUS='UNKNOWN',FILE='fdmo.dat')
      OPEN(UNIT=224,STATUS='UNKNOWN',FILE='fdliq.dat')
      OPEN(UNIT=225,STATUS='UNKNOWN',FILE='fdice.dat')
      OPEN (UNIT=226,STATUS='UNKNOWN',FILE='fd.dat')
      OPEN (UNIT=227,STATUS='UNKNOWN',FILE='veg.dat')
      OPEN (UNIT=228,STATUS='UNKNOWN',FILE='Tg.dat')
      OPEN (UNIT=229,STATUS='UNKNOWN',FILE='Tb.dat')
      DO 234 IA = 1, NWRITE
        II0 = (IA - 1) * 10 + 1
        II1 = IA * 10
        WRITE(222,232)(Z2(II), II=II0,II1)
        WRITE(223,232)(Z2(II), II=II0,II1)
        WRITE(224,232)(Z2(II), II=II0,II1)
        WRITE(225,232)(Z2(II), II=II0,II1)
  232   FORMAT(10(' ',1pe10.3))
  234 CONTINUE
      RHR = 0.
      DO 236 J = 0, 6
        DiffT(J) = 0.D0
        DiffT2(J) = 0.D0
  236 CONTINUE
      DiffHG = 0.D0
      DiffHG1 = 0.D0
      DiffHG2 = 0.D0
      DO 290 HR = 1, NSAM, 1
        HR0 = HR - 1
        HR1 = HR + 1
        RHR = RHR  + 1.
c
c   It is not necessary to compute veg+soil state every few seconds
c if there is no precipitation and the magnitudes of Qsdc are small,
c i.e., boundary forcing is weak.
c
        IF((Qsdc(HR).LT.10.).AND.(pp(HR).NE.0.))then
          NSMAX2 = 5
        ELSE
          NSMAX2 = NSMAX
        ENDIF
c
c    Each time step is divided into NSMAX sub-intervals.
c    The number of sub-intervals is increased by x times if
```

```
c  the time step is too big.  The basic time step is 10 minutes.
c    Note that the program might blow up if time step is not well
c  controlled.  This may occur with a strong weather forcing.
c
        DMSMAX = DBLE(MSMAX2 * INT(RHR_i(HR)/600.+1) )
        DELT60 = RHR_i(HR)/DMSMAX
        T60_d = DELT60/depth(1)
        DO 238 J=0,MODEP
          Vfl_OLD(J)=Vfl(J)
          Vfi_OLD(J)=Vfi(J)
          T_OLD(J)=T(J)
          Vfl2_OLD(J)=Vfl(J)
          T2_OLD(J)=T(J)
  238   CONTINUE
C=======================================================================!
C     Treatments of soil
C=======================================================================!
        Qld1 = Qld(HR)+Qsd(HR)
        FDIF = (Qld(HR1)+Qsd(HR1)-Qld1)/DMSMAX
        FDIFt = (Qsdt(HR1)-Qsdt(HR))/DMSMAX
        Qldc1 = Qldc(HR)+Qsdc(HR)
        FDIFc = (Qldc(HR1)+Qsdc(HR1)-Qldc1)/DMSMAX
        FDIFcs = (Qsdc(HR1)-Qsdc(HR))/DMSMAX
        fpp = (pp(HR1)-pp(HR))/DMSMAX
        fe_a  = (e_ar(HR1)-e_ar(HR))/DMSMAX
        fq_a  = (q_ar(HR1)-q_ar(HR))/DMSMAX
        fq_asat  = (q_asat(HR1)-q_asat(HR))/DMSMAX
        fTAIR = (TAIR(HR1)-TAIR(HR))/DMSMAX
        fAIRF = (AIRF(HR1)-AIRF(HR))/DMSMAX
        DO 278 MS=1,MSMAX2
          DMS  = DBLE(MS)
C=======================================================================!
C     Treatments of vegetation
C=======================================================================!
          FS   = Qld1 + DMS * FDIF
          FSc   = Qldc1 + DMS * FDIFc
          FSt   = Qsdt(HR) + DMS * FDIFt
          ppc  = (pp(HR) + DMS * fpp)*DELT60
          TAIRs= TAIR(HR) + DMS * fTAIR
          AIRFs= AIRF(HR) + DMS * fAIRF
          e_as = e_ar(HR) + DMS * fe_a
          q_asats = q_asat(HR) + DMS * fq_asat
          Rho_aT = Rho_a(TAIRs)
          RCp_aT = Rho_aT * Cp_a
          DO 240 J=1,MODEP
           JO = J - 1
           Tk = T_OLD(J) - 273.15D0
           Lv = Lv0 + Cp_aw * Tk
           Vf_H2O2 = Vfl_OLD(J) + .92D0 * Vfi_OLD(J)
           if (Vf_H2O2.ge.Vf_H2O_s) then
             Vf_H2O = Vf_H2O_s - 0.e-12
           else
             Vf_H2O = Vf_H2O2
           endif
           dVf_H2O = Vf_H2O2 - Vf_H2O
           if(T_OLD(J).lt.273.15D0)then
            if(T_OLD(J).lt.100.D0)pause 'temp is lower than 100K!'
             dum = Vf_H2O
             call RTBIS(Tfdp,dum)
           else
             Tfdp = 273.15D0
           endif
           Tfpd = Tf - Tfdp
           ATdp(J) = Tfdp
C
C SPLINT computes viscosity.
C scond computes all transport coefficients.
C
```

```
            CALL SPLINT(Tk_visc,visc,de_viscT,11,T_OLD(J),viscosity)
            call scond(T_OLD(J),RCP,KWET,f_T,Vf_H2O_fr,Vf_w_fr,mh)
            if(J.eq.1)then
              E_eff = f_T
              RHs = f_T2
            endif
            Cp_wTk(J) = Cp_w * Tk
            DLv(J) = Lv
            DD_Tl(J) = D_Tl
            DD_Tv(J) = D_Tv
            DD_H2Ol(J) = D_H2Ol
            DD_H2Ov(J) = D_H2Ov
            DKWET(J) = KWET
            DHK(J) = HK
            M(J) = M_j
            N(J) = N_j
            E(J) = E_j
            F(J) = F_j
            AME(J) = ME
            ANF(J) = NF
            Phi(J) = mh
c     Note that TD(1) and VD(1) are not used.
            TD(J) = T_OLD(J) - T_OLD(JO)
            VD(J) = Vfl_OLD(J)- Vfl_OLD(JO)
c
c    Reset transpiration = 0.
c
            Etrs(J) = 0.DO
            Etrs_t(J) = 0.DO
  240     CONTINUE
          DO 242 J=1,NODEPO
            J1 = J + 1
            dTz2(J) = TD(J1) / depth2(J)
            dVz2(J) = VD(J1) / depth2(J)
            if((DHK(J)*DHK(J1)).eq.0.DO)then
              AHK(J) = 0.DO
            else
              AHK(J) =DHK(J)*DHK(J1)/(DHK(J)+DHK(J1))
            endif
            if((DLv(J)*DLv(J1)).eq.0.DO)then
              ALv(J) = 0.DO
            else
              ALv(J) =DLv(J)*DLv(J1)/(DLv(J)+DLv(J1))
            endif
            if((DKWET(J)*DKWET(J1)).eq.0.DO)then
              AKWET(J) = 0.DO
            else
              AKWET(J) =DKWET(J)*DKWET(J1)/(DKWET(J)+DKWET(J1))
            endif
            if((DD_Tv(J)*DD_Tv(J1)).eq.0.DO)then
              AD_Tv(J) = 0.DO
            else
              AD_Tv(J) =DD_Tv(J)*DD_Tv(J1)/(DD_Tv(J)+DD_Tv(J1))
            endif
            if((DD_TL(J)*DD_TL(J1)).eq.0.DO)then
              AD_TL(J) = 0.DO
            else
              AD_TL(J) =DD_TL(J)*DD_TL(J1)/(DD_TL(J)+DD_TL(J1))
            endif
            if((DD_H2Ov(J)*DD_H2Ov(J1)).eq.0.DO)then
              AD_H2Ov(J) = 0.DO
            else
              AD_H2Ov(J) =DD_H2Ov(J)*DD_H2Ov(J1)/(DD_H2Ov(J)+DD_H2Ov(J1))
            endif
c     !-------------------bounds for statements----------------------!
            if((DD_H2OL(J)*DD_H2OL(J1)).eq.0.DO)then
              AD_H2OL(J) = 0.DO
            else
```

```
            AD_H2OL(J) =DD_H2OL(J)*DD_H2OL(J1)/(DD_H2OL(J)+DD_H2OL(J1))
           endif
           if((Cp_wTk(J)*Cp_wTk(J1)).eq.0.DO)then
            AT(J) = 0.DO
           else
            AT(J) =Cp_wTk(J)*Cp_wTk(J1)/(Cp_wTk(J)+Cp_wTk(J1))
           endif
  242     CONTINUE
          IF(veg.ne.0.DO)then
           T_OLD2 = T_OLD(0)
           Vfl_OLD2 = Wr + ppc
           Ts = T_OLD2
           DTas = TAIRs - Ts
           e_ac = es(T_OLD2)
           r_ac = .622DO*e_ac/(1.01325e5 - e_ac)
           q_ac = r_ac/(1.DO+ r_ac)
           Etv = veg*Rho_aT*(q_as-q_ac)
c
c   Drainage occurs if precipitation exceeds the maximum
c water-holding capacibility of the foliage.
c
           if(Vfl_OLD2.gt.Wr_max)then
            pps = Vfl_OLD2 - Wr_max
            Vfl_OLD2 = Wr_max
           else
            pps = 0.DO
           endif
c
c    Determine evaporation from wet fraction of the canopy.
c  Determine the fraction of the canopy covered by water.
c   by Sellers et al, 1986
           if(e_ac.gt.e_as)then
            f_wet = Vfl_OLD2/Wr_max
           else
            f_wet = 1.DO
           endif
c
c   by Deardorff, 1978.
c            f_wet = (Vfl_OLD2/Wr_max)**.66667
c   by Jacquemin and Noilhan, 1990
c           if(q_ac.ge.q_as)then
c            f_wet = Vfl_OLD2/Wr_max
c           else
c            f_wet = 1.DO
c           endif
           Ev  = f_wet * Etv * AIRFs
           Wr = Vfl_OLD2
           EvR = Ev/Rho_w *DELT60
           if((-EvR).gt.Wr)then
            Ev = Wr * Rho_w/DELT60
            Wr = 0.DO
           else
            Wr = Wr + EvR
           endif
c
c Determine transpiration if Tcanopy > 273.15K.  Otherwise, Etr = 0.
c
           If(T_OLD2.gt.273.15)then
c
c Compute matric head at root-zone layers.  There is no need to do
c this if there is no transpiration.
c  Etr = 0 if dew occurs, or wet fraction = 100% on the foliage
c
             if(q_ac.lt.q_as)then
              Etr = 0.DO
             else
              phi_sum = 0.DO
              phi_min = 1.e7
```

```
                DO 244 J=1,Nr
                  phi_max(J) = phi_2(T(J))
                  if(Phi(J).ge.phi_max(J))then
                    Root_phi(J) = 0.D0
                  else
                    Root_phi(J) = Root2(J)*(phi_max(J)-Phi(J))
                  endif
                  phi_sum = phi_sum + Root_phi(J)
                  if(Phi(J).lt.phi_min) phi_min = Phi(J)
  244           CONTINUE
                if(phi_min.lt.40.D0)then
                  F2 = 1.
                else
                  F2 = 40./phi_min
                endif
c
c Noilhan and Planton, 1989, referred by Jacquemin and Noilhan,1990
c
                F1_f  =  F1_f0 * (Qsdc(HR)+DNS * FDIFcs)
                F1 = (rsmin_max + F1_f )/(1.D0+F1_f)
                F3 = 1.D0 - .06D0*(q_asats-q_as)
                IF(F3.LT..3D0)F3=.3D0
                F4 = 1.D0 - 1.6E-3*(298. - TAIRs)
                r_canopy = rsmin/(LAI*F1*F2*F3*F4)
                Etr = (1.-f_wet)*Etv/(1./AIRFs + r_canopy)
                If(phi_sum.ne.0.)then
                  DO 246 J=1,Nr
                    Etrs(J) = Etr * Root_phi(J)/phi_sum
  246             CONTINUE
                Endif
              endif
            Else
              Etr = 0.D0
            Endif
            Fshc= veg*RCp_aT*AIRFs*(TAIRs-T_OLD2)
            DUM1 = L_v2(T_OLD2)
            FlhEt= DUM1*Etr
            FlhEc= DUM1*Ev
            Flhc= FlhEt + FlhEc
            Fc  = veg_EMSIc*Ts**4
            FNETc=FSc+Fshc+Flhc-2*Fc+veg_EMSIt*Tt_OLD**4
c
c For canopy + thatch
c   Cp_c = 2.7e3 Jj/kg-K specific heat of vegetation, Verseghy et al 1993
c   Wc   = 2.281 kg/m^2 averaged canopy wet of 6 samples [REBEX1]
c   Cp_c * Wc = 6158.7 J/K-M^2
c   RCp_c = Cp_c * Wc + Cp_w * Ww + Cp_i * Wi
c
c For thatch
c   Assume thatch weight/total canopy weith = 0.0663 ==> 0.1512303 kg/m^2
c   (The ratio is from Dahl et al 1993).
c     RCP_t = Wt*Cp_t + Ww_t * Cp_w
c             = .1512303 * 2700 + 1.4e-3*.0663*4218
c             = 408.32181  + 391.51476 = 799.83657 J/K-M^2
c For canopy
c           ==> 1.4e-3 * (1 - .0663) = 1.30718
c           ==> Wc = 2.281 - 0.1512303 = 2.1297697
c           ==> Cp_c * Wc = 2.1297697 * 2.7e3 = 5750.3782
c
            RCp_c = 5.7503782e3 + RCp_w * Vfl_OLD2
            T_NEW(0) = T_OLD(0) + FNETc*DELT60/RCp_c
            Vfl_NEW(0) = 1.30718e-3 + Wr
            Fc  = veg_EMSIc*T_NEW(0)**4
            if(veg_EMSIt2.ne.0.D0)then
              Tt_NEW = Tt_OLD + (FSt+Fc+veg_EMSI*T_OLD(1)**4
     1                  -veg_EMSIt2*Tt_OLD**4)*DELT60/799.83657
              Ft = veg_EMSIt * Tt_NEW**4
            else
```

```
              Tt_NEW = 0.DO
              Ft = 0.DO
            endif
            DO 248 J=Nr,1,-1
              Etrs_t(J-1) = Etrs(J) + Etrs_t(J)
 248        CONTINUE
          ELSE
            Tt_NEW = 0.DO
            Ft = 0.DO
          ENDIF
        DO 250 J=1,NODEPO
          J1 = J + 1
         Qv(J) = -(AD_Tv(J)*dTz2(J)+ AD_H2Ov(J)*dVz2(J))* Rho_w
         Ql(J) = -(AD_Tl(J)*dTz2(J)+ AD_H2Ol(J)*dVz2(J)-AHK(J))* Rho_w
    1            + Etrs_t(J)
         Qm(J) = Qv(J)+Ql(J)
         Qh0(J) = -AKWET(J)*dTz2(J)
         Qh1(J) =  ALv(J)*Qv(J)
         Qh2(J) =  AT(J) *Qm(J)
         Qh3(J) =  Cp_wTk(J)*Qm(J)
         Qh(J)  =  Qh0(J) + Qh1(J) + Qh2(J)
 250     CONTINUE
        Qm(NODEP)  = Qm(NODEPO)
        Qh0(NODEP) = Qh0(NODEPO)
        Qh1(NODEP) = Qh1(NODEPO)
        Qh2(NODEP) = Qh2(NODEPO)
        Qh3(NODEP) = Qh3(NODEPO)
        Qh(NODEP)  = Qh(NODEPO)
        goto 252
c
c    The following (between goto 252 and goto 264) is a test of replacing
c iterative solution of temp and moisture by a simple prognostic solution to
c heat and moisture transport.  Results turn out to be fine except that
c special choice of NSMAX is required.
c
          T_OLD2 = T_OLD(1)
          Vfl_OLD2 = Vfl_OLD(1)
c
c  Runoff occurs if the first soil layer is oversatured.
c
          if(Vfl_OLD2.ge.Vf_H2O_s)then
            pps_max = 0.
          else
            pps_max = (Vf_H2O_s - Vfl_OLD2) * depth1(1)
          endif
          if(pps.gt.pps_max)pps=pps_max
          Ts = T_OLD2
          DTag = TAIRs - Ts
          Fsh=veg1*RCp_aT*AIRFs*DTag
          e_ss = es(Ts)*RHs
          r_ss = .622D0*e_ss/(1.01325e5 - e_ss)
          q_ss = r_ss/(1.D0+ r_ss)
          Flh=veg1*L_v2(Ts)*Rho_aT*AIRFs*(q_as-q_ss)*E_eff
          Fg  = EMSI*Ts**4
          FNET=FS+Fsh+Flh-Fg+Ft
          dT1 = Ts - T_OLD(1)
          dV1 = Vfl_OLD2 - Vfl_OLD(1)
          Qv(0) =  Flh/L_cs
          Ql(0) = pps * Rho_w/DELT60 + Etrs_t(0)
          Qm(0) = Qv(0)+Ql(0)
          Qh(0) = FNET
          Qh3(0) = Cp_w*(273.15D0-Ts)*Qm(0)
          goto 264
 252      Reiterate = 0
          psychro2 = psychro/L_cs
          Solution2 = 0
          Nice = 0
          nT = 0
```

```
            T_OLD2 = T_OLD(1)
            Vfl_OLD2 = Vfl_OLD(1)
            if(Vfl_OLD2.ge.Vf_H2O_s)then
              pps_max = 0.
            else
              pps_max = (Vf_H2O_s - Vfl_OLD2) * depth1(1)/DMSMAX
            endif
            if(pps.gt.pps_max)pps=pps_max
            AME_i = - AME(1)*Vfi_OLD(1)
            AMF_i = - AMF(1)*Vfi_OLD(1)
            If(E_eff.eq.0.D0)then
              Ts = T_OLD2
              DTag = TAIRs - Ts
              Fsh=veg1*RCp_aT*AIRFs*DTag
              e_ss = es(Ts)*RHs
              r_ss = .622D0*e_ss/(1.01325e5 - e_ss)
              q_ss = r_ss/(1.D0+ r_ss)
              Flh=veg1*L_v2(Ts)*Rho_aT*AIRFs*(q_as-q_ss)*E_eff
              Fg  = EMSI*Ts**4
              FNET=FS+Fsh+Flh-Fg+Ft
              dT1 = Ts - T_OLD(1)
              dV1 = Vfl_OLD2 - Vfl_OLD(1)
              Qv(0) =  Flh/L_cs
              Ql(0) =  pps * Rho_w + Etrs_t(0)
              Qm(0) = Qv(0)+Ql(0)
              X(1) = -T60_d*(Qm(1)-Qm(0))/Rho_w
              Y(1) = -T60_d*(Qh(1)-FNET-
     1             Cp_wTk(1)*Qm(1)+Cp_w*(273.15D0-Ts)*Qm(0))
              Vf_NEW = Vf(1) + X(1)
              dum = Vf_NEW
              call RTBIS(Tfdp_NEW,dum)
              DEN = M(1)*F(1)-E(1)*M(1)
              if(DEN.NE.0.D0)THEN
                XME = X(1) - AME_i
                YMF = Y(1) - AMF_i
                dV1 = (F(1)*XME-E(1)*YMF)/DEN
                dT1 = (M(1)*YMF-M(1)*XME)/DEN
                Vfl_NEW1  = Vfl_OLD(1)+dV1
                T_NEW1  = T_OLD(1)+dT1
              else
C
C   Vfi_NEW must be determined from consersation principle of heat
C or moisture.  Here I use the latter because it is simpler than
C the former.
C
                If(J.NE.1)then
                  Vfl_NEW1 = Vfl_NEW(J0)
                  T_NEW1  = T_NEW(J0)
                Else
                  Vfl_NEW1 = 2.D0*Vfl_OLD(1)-Vfl2_OLD(1)
                  T_NEW1   = 2.D0*T_OLD(1)-T2_OLD(1)
                Endif
              endif
            Else
C-----------------------------------------------------------------------!
C Balance surface fluxes, moisture and energy                           !
C 1/4: compute f_i(j) and g_i(j), j = 1,2              === step 1 of 4 !
C-----------------------------------------------------------------------!
  254       Ts = T_OLD2
            DTag = TAIRs - Ts
            Fsh=veg1*RCp_aT*AIRFs*DTag
            e_ss = es(Ts)*RHs
            Fg  = EMSI*Ts**4
            Ql(0) = pps * Rho_w/DELT60 + Etrs_t(0)
            dT1 = Ts - T_OLD(1)
            DO 256 J = 1, 2, 1
             Vfl_OLD1 = Vfl_OLD2-1.e-10 + 2.e-10 * dble(J-1)
             if(E_eff.ne.0.D0)then
```

```
              r_ss = .622D0*e_ss/(1.01325e5 - e_ss)
              q_ss = r_ss/(1.D0+ r_ss)
              Flh=veg1*L_v2(Ts)*Rho_aT*AIRFs*(q_as-q_ss)*(E_eff+
     1             (Vfl_OLD1-Vfl_OLD(1))/Vf_sat)
             else
               Flh = 0.D0
             endif
             FNET=FS+Fsh+Flh-Fg+Ft
             dV1 = Vfl_OLD1 - Vfl_OLD(1)
             Qv(0) = Flh/L_cs
             Qm(0) = Qv(0)+Ql(0)
             X(1) = -T60_d*(Qm(1)-Qm(0))/Rho_w
             Y(1) = -T60_d*(Qh(1)-FNET-
     1              Cp_wTk(1)*Qm(1)+Cp_w*(273.15D0-Ts)*Qm(0))
             f_i(J)= M(1)*dV1+E(1)*dT1+AME_i-X(1)
             g_i(J)= N(1)*dV1+F(1)*dT1+ANF_i-Y(1)
  256       CONTINUE
C-------------------------------------------------------------------------!
C Balance surface fluxes, moisture and energy                             !
C 2/4: compute f_i(j) and g_i(j), j = 3,4              === step 2 of 4 !
C-------------------------------------------------------------------------!
            DO 258 J = 3, 4, 1
             Ts = T_OLD2-1.e-10 + 2.e-10 * dble(J-3)
             DTag = TAIRs - Ts
             Fsh=veg1*RCp_aT*AIRFs*DTag
             e_ss = es(Ts)*RHs
             r_ss = .622D0*e_ss/(1.01325e5 - e_ss)
             q_ss = r_ss/(1.D0+ r_ss)
             Flh=veg1*L_v2(Ts)*Rho_aT*AIRFs*(q_as-q_ss)*E_eff
             Fg  = EMSI*Ts**4
             FNET=FS+Fsh+Flh-Fg+Ft
             dT1 = Ts - T_OLD(1)
             dV1 = Vfl_OLD2 - Vfl_OLD(1)
             Qv(0) = Flh/L_cs
             Ql(0) = pps * Rho_w/DELT60 + Etrs_t(0)
             Qm(0) = Qv(0)+Ql(0)
             X(1) = -T60_d*(Qm(1)-Qm(0))/Rho_w
             Y(1) = -T60_d*(Qh(1)-FNET-
     1              Cp_wTk(1)*Qm(1)+Cp_w*(273.15D0-Ts)*Qm(0))
             f_i(J)= M(1)*dV1+E(1)*dT1+AME_i-X(1)
             g_i(J)= N(1)*dV1+F(1)*dT1+ANF_i-Y(1)
  258       CONTINUE
C-------------------------------------------------------------------------!
C Balance surface fluxes, moisture and energy                             !
C 3/4: compute f_i(j) and g_i(j), j = 0                === step 3 of 4 !
C-------------------------------------------------------------------------!
            Ts = T_OLD2
            DTag = TAIRs - Ts
            Fsh=veg1*RCp_aT*AIRFs*DTag
            e_ss = es(Ts)*RHs
            r_ss = .622D0*e_ss/(1.01325e5 - e_ss)
            q_ss = r_ss/(1.D0+ r_ss)
            Flh=veg1*L_v2(Ts)*Rho_aT*AIRFs*(q_as-q_ss)*E_eff
            Fg  = EMSI*Ts**4
            FNET=FS+Fsh+Flh-Fg+Ft
            dT1 = Ts - T_OLD(1)
            dV1 = Vfl_OLD2 - Vfl_OLD(1)
            Qv(0) =  Flh/L_cs
            Ql(0) =  pps * Rho_w + Etrs_t(0)
            Qm(0) = Qv(0)+Ql(0)
            X(1) = -T60_d*(Qm(1)-Qm(0))/Rho_w
            Y(1) = -T60_d*(Qh(1)-FNET-
     1             Cp_wTk(1)*Qm(1)+Cp_w*(273.15D0-Ts)*Qm(0))
            f_i(0)= M(1)*dV1+E(1)*dT1+AME_i-X(1)
            g_i(0)= N(1)*dV1+F(1)*dT1+ANF_i-Y(1)
C-------------------------------------------------------------------------!
C Balance surface fluxes, moisture and energy                             !
C 4/4: compute changes in surface temp and moisture    === step 4 of 4 !
```

```
C-----------------------------------------------------------------------!
           M(0) = (f_i(2) - f_i(1)) / 2.e-10
           N(0) = (g_i(2) - g_i(1)) / 2.e-10
           E(0) = (f_i(4) - f_i(3)) / 2.e-10
           F(0) = (g_i(4) - g_i(3)) / 2.e-10
           X(0) = - f_i(0)
           Y(0) = - g_i(0)
           DUM1 = M(0)*F(0)-E(0)*N(0)
           IF(DUM1.NE.0.D0)THEN
            deltVf = (F(0)*X(0)-E(0)*Y(0))/DUM1
            deltT = (M(0)*Y(0)-N(0)*X(0))/DUM1
           ELSE
            deltVf = 0.D0
            deltT = 0.D0
           ENDIF
           Vfl_NEW1 = Vfl_OLD2  + deltVf
           T_NEW1  = T_OLD2 + deltT
           if((Vfl_NEW1.lt.0.03D0))then
             Nice = 1
             goto 260
           else
            if((DABS(deltT).gt.DELTMAX).or.(DABS(deltVf).
     1                                    gt.DVfMax))then
              Vfl_OLD2 = Vfl_NEW1
              T_OLD2 = T_NEW1
              Solution2 = Solution2 + 1
              if(Solution2.lt.30)goto 254
            endif
           endif
         Endif
           dT1 = T_NEW1 - T_OLD(1)
           dV1 = Vfl_NEW1-Vfl_OLD(1)
           dum = Vfl_NEW1
           call RTBIS(Tfdp_NEW,dum)
           if (Tfdp_NEW.le.T_NEW1)then
             Vfl_NEW(1) = Vfl_NEW1
             Vfi_NEW(1) = 0.D0
             T_NEW(1)  = T_NEW1
             goto 264
           endif
 260       Solution2 = 0
           Nice = 1
           nT = 0
           J = 1
           T_OLD2 = T_OLD(1)
           Vfl_OLD2 = Vfl_OLD(1)
           N_M = ANF(1)/AME(1)
           P = N(1) - N_M * M(1)
           Q = F(1) - N_M * E(1)
            Ts = T_OLD2
            DTag = TAIRs - Ts
            Fsh=veg1*RCp_aT*AIRFs*DTag
            e_ss = es(Ts)*RHs
            r_ss = .622D0*e_ss/(1.01325e5 - e_ss)
            q_ss = r_ss/(1.D0+ r_ss)
            Flh=veg1*L_v2(Ts)*Rho_aT*AIRFs*(q_as-q_ss)*E_eff
            Fg  = EMSI*Ts**4
            FNET=FS+Fsh+Flh-Fg+Ft
            Qv(0) = Flh/L_cs
            Ql(0) = pps * Rho_w/DELT60 + Etrs_t(0)
            Qm(0) = Qv(0)+Ql(0)
            Qh(0) = FNET
            X(1) = -T60_d*(Qm(1)-Qm(0))/Rho_w
            Y(1) = -T60_d*(Qh(1)-FNET-Cp_wTk(1)*(Qm(1)-Qm(0)))
          R = Y(1) - N_M * X(1)
          Vf_NEW = Vf(1) + X(1)
          dum = Vf_NEW
          call RTBIS(Tfdp_NEW,dum)
```

```
  262      Vf_w2 = Vf_w_Rossi(T_OLD2-1.e-10,Vf_NEW,Tfdp_NEW)
           f_i(0) = (Vfl_OLD2-Vf_w2)/1.e-10
           dT2 = T_OLD2 - T_OLD(1)
           dV2 = Vfl_OLD2 - Vfl_OLD(1)
           g_i(1) = P*f_i(0) + Q
           g_i(0) = P*dV2 + Q*dT2 - R
           if(g_i(1).ne.0.D0)then
             deltT = - g_i(0)/g_i(1)
           else
             deltT = 0.D0
           endif
           T_NEW2 = T_OLD2 + deltT
           Vfl_NEW2= Vf_w_Rossi(T_NEW2,Vf_NEW,Tfdp_NEW)
           deltVf = Vfl_NEW2 - Vfl_OLD2
           if(DABS(deltT).ge.DELTMAX)then
             Vfl_OLD2 = Vfl_NEW2
             T_OLD2 = T_NEW2
             Solution2 = Solution2 + 1
             if(Solution2.lt.30)goto 262
           endif
           dT2 = T_NEW2 - T_OLD(1)
           dV2 = Vfl_NEW2-Vfl_OLD(1)
C
C Note that only one of (dV1,dT1) and (dV2,dT1) can satisfy the
C boundary conditions.
C
           Vfl_NEW(1) = Vfl_OLD(1)  + dV2
            T_NEW(1)  = T_OLD(1) + dT2
            if(Nice.eq.1)then
              f_i(4) = (Y(1)-N(1)*dV2-F(1)*dT2)/ANF(1)
              Vfi_NEW(1) = Vfi_OLD(1)+f_i(4)
                if(Vfi_NEW(1).lt.0.D0) Vfi_NEW(1) = 0.D0
            else
                Vfi_NEW(1) = 0.D0
            endif
C
C Balance surface fluxes, moisture and energy              === end     !
C   compute changes in surface temp and moisture                        !
C=====================================================================!
C   Upon reaching convergence criterions, recalculate surface fluxes   !
C using the newest surface temp and moisture.                          !
C=====================================================================!
  264      Qh(0) = FNET
C
C   The first soil layer is subject to weather forcing so that solutions
C of moisture and temperature are solved different from the other layers.
C
           DO 266 J=1,NODEP0
             J0 = J - 1
             dum = DELT60/depth1(J)
             X(J)=-(Qm(J)-Qm(J0))/Rho_w*dum
             Y0(J)=-(Qh(J)-Qh(J0))*dum
             Y(J)=-(Qh(J)-Qh(J0) - (Qh3(J)-Qh3(J0)))*dum
  266      CONTINUE
           DO 274 J=1,NODEP0
            J0 = J-1
C=====================================================================!
C   Since we are not sure whether the ground is partially frozen at the!
C next time step or not, we need to compute the changes in temp and    !
C moisture for both frozen and unfrozen cases, and then determine which!
C answer is true.                                                      !
C=====================================================================!
           Nice = 0
C
C Nice =0 ==> T_NEW >= Tfdp_NEW;  Nice =1 ==> T_NEW < Tfdp_NEW
C
C=====================================================================!
C   Find the first solution set by assuming T_NEW >= Tfdp_NEW.         !
```

```
C=====================================================================!
C Vf_NEW is the total water content of the next time step.
C
             AME_i = - AME(J)*Vfi_OLD(J)
             ANF_i = - ANF(J)*Vfi_OLD(J)
            Vf_NEW = Vf(J) + X(J)
            dum = Vf_NEW
            call RTBIS(Tfdp_NEW,dum)
            DEN = M(J)*F(J)-E(J)*N(J)
            IF(DEN.NE.0.D0)THEN
              XME = X(J) - AME_i
              YNF = Y(J) - ANF_i
              dV1 = (F(J)*XME-E(J)*YNF)/DEN
              dT1 = (M(J)*YNF-N(J)*XME)/DEN
              Vf1_NEW1  = Vf1_OLD(J)+dV1
              T_NEW1  = T_OLD(J)+dT1
             ELSE
              if(J.NE.1)then
                Vf1_NEW1 = Vf1_NEW(J0)
                T_NEW1  = T_NEW(J0)
              else
                Vf1_NEW1 = 2.D0*Vf1_OLD(J)-Vf12_OLD(J)
                T_NEW1   = 2.D0*T_OLD(J)-T2_OLD(J)
              endif
             ENDIF
             if(T_NEW1.gt.Tfdp_NEW)then
              dV0 = dV1
              dT0 = dT1
              goto 270
             endif
C=====================================================================!
C   Find the second solution set by assuming T_NEW < Tfdp_NEW.        !
C=====================================================================!
C In genral, Solution2 <= 2, unless solutions do not converge.
C
           Solution2 = 0
           nT = 0
           T_OLD2 = T_OLD(J)
           Vf1_OLD2 = Vf1_OLD(J)
           N_M = ANF(J)/AME(J)
           P = N(J) - N_M * M(J)
           Q = F(J) - N_M * E(J)
           R = Y(J) - N_M * X(J)
  268      Vf_w2 = Vf_w_Rossi(T_OLD2-1.e-8,Vf_NEW,Tfdp_NEW)
           f_i(1) = (Vf_w_Rossi(T_OLD2+1.e-8,Vf_NEW,Tfdp_NEW)
     1               -Vf_w2)/2.e-8
           dT2 = T_OLD2 - T_OLD(J)
           dV2 = Vf1_OLD2 - Vf1_OLD(J)
           g_i(1) = P*f_i(1) + Q
           g_i(0) = P*dV2 + Q*dT2 - R
           if(g_i(1).ne.0.D0)then
             deltT = - g_i(0)/g_i(1)
           else
             deltT = 0.D0
           endif
           T_NEW2 = T_OLD2 + deltT
           Vf1_NEW2= Vf_w_Rossi(T_NEW2,Vf_NEW,Tfdp_NEW)
           deltVf = Vf1_NEW2 - Vf1_OLD2
           if(DABS(deltT).ge.DELTMAX)then
             Vf1_OLD2 = Vf1_NEW2
             T_OLD2 = T_NEW2
             Solution2 = Solution2 + 1
             if(Solution2.lt.30)goto 268
          endif
          dT2 = T_NEW2 - T_OLD(J)
          dV2 = Vf1_NEW2-Vf1_OLD(J)
          dV0 = dV2
          dT0 = dT2
```

```
          Nice = 1
          goto 270
C
C   X(J) represents the change in total water content.
C   YO(J) represents the change in total heat content.
C  i.e.
C   X(J) > 0 ==> water content increases.
C   YO(J) > 0 ==> heat content increases.
C
C=====================================================================!
C  Compute the change in ice content.                                 !
C=====================================================================!
c Nice = 1 (T_NEW < Tfdp_NEW) ==> a change in ice content
c
  270       Vfl_NEW(J) = Vfl_OLD(J)  + dVO
            T_NEW(J)  = T_OLD(J) + dTO
            if(T_NEW(J).lt.Tfdp_NEW)then
              Nice=1
            endif
            if(Nice.eq.1)then
              f_i(0) = (X(J)-dVO)/.92D0
              Vfi_NEW(J) = Vfi_OLD(J)+f_i(0)
              if(Vfi_NEW(J).lt.DVfMax) Vfi_NEW(J) = 0.D0
            else
              Vfi_NEW(J) = 0.D0
            endif
  274     CONTINUE
          Tt_OLD = Tt_NEW
          DO 276 J=0,NODEPO
            Vfl2_OLD(J) = Vfl_OLD(J)
            Vfi2_OLD(J) = Vfi_OLD(J)
            T2_OLD(J)  = T_OLD(J)
            Vfl_OLD(J) = Vfl_NEW(J)
            Vfi_OLD(J) = Vfi_NEW(J)
            Vf(J) = Vfl_NEW(J) + .92D0 * Vfi_NEW(J)
            T_OLD(J)  = T_NEW(J)
  276     CONTINUE
  278     CONTINUE
          DO 280 J=0,NODEPO
            Vfl(J)=Vfl_NEW(J)
            Vfi(J)= Vfi_NEW(J)
            Vf(J) = Vfl(J) + .92D0 * Vfi(J)
            T(J)=T_NEW(J)
  280     CONTINUE
C
C     !--------------------bounds for statements----------------------!
C
          DO 284 IA = 1, NWRITE
            II0 = (IA - 1) * 10 + 1
            II1 = IA * 10
            WRITE(222,282)(T(II), II=II0,II1)
            WRITE(223,282)(Vf(II), II=II0,II1)
            WRITE(224,282)(Vfl(II), II=II0,II1)
            WRITE(225,282)(Vfi(II), II=II0,II1)
  282       FORMAT(10(' ',1pe10.3))
  284     CONTINUE
        TGrad=(T(2)-T(1))/depth2(1)
        WRITE(226,286)RDAY(HR),T(1),TGrad,TAIR(HR),Flh,
     1              Fsh,Qsd(HR),Vfi(1),Vfl(1)
  286     FORMAT(f7.3,' ',1(' ',1pe11.4),7(' ',1pe10.3))
        WRITE(227,286)RDAY(HR),T(0),Vf(0),Tt_NEW,FlhEt,FlhEc,Fshc,
     1              Qsdc(HR)
        WRITE(228,286)RDAY(HR),T(4),T(7),T(11),T(17),T(24),T(32),
     1              (Qh(4)-Qh3(4))
        WRITE(229,286)RDAY(HR),T(0),Vf(0),Tt_NEW,T(1),Vfi(1),Vfl(1)
        DiffT(0) = DiffT(0) + (T(0)-Tcan(HR))
        DiffT(1) = DiffT(1) + (T(4)-Tg(1,HR))
        DiffT(2) = DiffT(2) + (T(7)-Tg(2,HR))
```

```
          DiffT(3) = DiffT(3) + (T(11)-Tg(3,HR))
          DiffT(4) = DiffT(4) + (T(17)-Tg(4,HR))
          DiffT(5) = DiffT(5) + (T(24)-Tg(5,HR))
          DiffT(6) = DiffT(6) + (T(32)-Tg(6,HR))
          DiffHG = DiffHG + DABS((Qh(4)-Qh3(4))-HG(HR))
          DiffHG1 = DiffHG1 + ((Qh(4)-Qh3(4))-HG(HR))
          DiffT2(0) = DiffT2(0) + DABS(T(0)-Tcan(HR))**2
          DiffT2(1) = DiffT2(1) + DABS(T(4)-Tg(1,HR))**2
          DiffT2(2) = DiffT2(2) + DABS(T(7)-Tg(2,HR))**2
          DiffT2(3) = DiffT2(3) + DABS(T(11)-Tg(3,HR))**2
          DiffT2(4) = DiffT2(4) + DABS(T(17)-Tg(4,HR))**2
          DiffT2(5) = DiffT2(5) + DABS(T(24)-Tg(5,HR))**2
          DiffT2(6) = DiffT2(6) + DABS(T(32)-Tg(6,HR))**2
          DiffHG2 = DiffHG2 + DABS((Qh(4)-Qh3(4))-HG(HR))**2
  290   CONTINUE
        WRITE(226,*)'Day#     Tgnd    Tgrad(K/m)      Tair       Flh      '
       1' Fsh        Fsun    Vf_ice  Vf_water'
        WRITE(226,*)' '
  292   format(12(' ',1pe11.4))
        WRITE(226,*)'The average of the difference between measured and'
       1' pred. canopy temp and soil temp at 2, 4, 8, 16, 32, and 64 cm'
        WRITE(226,292)(DiffT(J)/DMSAM,J=0,6)
        WRITE(226,*)'Corresponding standard deviation'
        WRITE(226,292)((DiffT2(J)/DMSAM)**.5,J=0,6)
        WRITE(226,*)'The ave. of the diff., the ave. of the abs. value '
       1'of the diff, & the stan. dev. for 2cm heat flux'
        WRITE(226,292)DiffHG1/DMSAM,DiffHG/DMSAM,(DiffHG2/DMSAM)**.5
        close(222)
        close(223)
        close(224)
        close(225)
        close(226)
        close(227)
        close(228)
        close(229)
        return
        end
C=======================================================================
        subroutine scond(T,RCP,K_soil,f_T,Vf_H2O_fr,Vf_w_fr,mh)
C=======================================================================
C   The subroutine finds soil properties such as thermal conductivity,
C and transport coefficients. of moist soils.  All units are in MKS.
C
C     K = conductivity, cal/cm-K ==> J/m-K
C     Cp = specific heat, cal/g-K
C     H2O       = liquid water + water ice (+ water vapor)
C     Rho = density, g/cm^3 ==> kg/m^3
C     RCp = heat capacity, cal/cm^3-K ==> J/m^3-K
C     scale = a weighting factor used to compute thermal conductivity
C     Vf = volume fraction
C     Wu = unfrozen water content, kg H2O/ kg bulksoil
C     Tstep = temperature step to compute heat capacity, 0.01 K
C     Tf = freezing point of pure water, 273.15 K
C     Tfpd = freezing pt depression of water within soil, < 273.15K
C     b_dry,c_dry,denom_dry,kw_dry,K_dry,r_dry
C     b_sat,c_sat,denom_sat,kw_sat,K_sat,r_sat
C               = parameters used to compute ga, shape factors of soil
C                 constitutents
C     unsatH    = field capacity
C     unsatL    = wilting point
C     f  = evaporation efficiency
C
        implicit none
c===== main
        double precision Lv0,Lf0i,MF
        common /CMAIN_ITER_COND/Lv0,Lf0i,MF
c===== iter
        double precision Tfpd,Vf_H2O,Tfdp,viscosity,Lv,dVf_H2O
```

```
      common /CITER_COMD/viscosity,Lv,Vf_H2O,dVf_H2O
     1 /CITER_COMD_Vfwa/Tfpd,Tfdp
C===== spara
      double precision Tf,delta_T,ga_soil,ga_i,ga_w,HK_s,Tstep,Vf_space,
     1 Vf_solid,Vf_c,Vf_o,Vf_q,Vf_sat,Vf_unsatH,Vf_unsatL,Vf_dry,ga_sat,
     2 gc_sat,gc_soil,gc_i,gc_w,no_Tstep,Vf_H2Ok,K_c,K_o,tension_aw,
     3 Rho_w,Rho_i,Cp_a,visc0,Vf_H2O_s,Cp_w,Cp_aw,RCp_solid,Cp_i
      common /CPARA_MAIN_ITER_COMD/Cp_a
     1 /CPARA_ITER_COMD/Tstep,RCp_w,Rho_w,Cp_w,Cp_aw,Rho_i,Cp_i
     2 /CPARA_ITER_COMD_Vfwa_mhRo/Vf_H2O_s,Vf_sat
     3 /CPARA_ITER_COMD_Vfwa/Tf
     4 /CPARA_COMD/delta_T,ga_soil,ga_i,ga_w,HK_s,Vf_solid,Vf_c,Vf_o,
     5  Vf_q,Vf_unsatH,Vf_unsatL,Vf_dry,ga_sat,gc_sat,gc_soil,
     6  gc_i,gc_w,no_Tstep,Vf_H2Ok,K_c,K_o,RCp_i,visc0,RCp_solid,
     7  tension_aw
     8 /CPARA_COMD_DTv/Vf_space
c===== scond
      double precision RCP,f_T,Tl,Th,RCp_Le,RCp_soil_sum,RCp_soil_ave,
     1 T,RH,scale_total,Wt_H2O,Wt_w,K_vT,T2,Wt_w2,ga,ga_dry,ga_unsatH,
     2 gc,ga_dry_sat,RCp_soil,KO,K_soildry,K_soil,K_unsatL,b_dry,c_dry,
     3 denom_dry,kw_dry,K_dry,r_dry,b_sat,c_sat,denom_sat,kw_sat,K_sat,
     4 r_sat,etta,TO,Vf_w2,dummy,Lf,scale_i,scale_c,scale_o,Vf_w,
     5 scale_a,scale_q,Vf_i,Vf_a,HK,D_Tv,D_Tl,D_H2Ol,D_H2Ov,K_iT,K_wT,
     6 K_aT,K_qT,ki,ka,kc,kq,ko,RCp_i,RCp_w,RCp_a,Vf_i2,Vf_a2,dVf_iT,
     7 Rho_aT,D_vT,Rho_vT,dum,K_aTO,Vf_aL,Vf_i3,Vf_a3,Vf_w3,
     8 Vf_iL,Vf_wL,gaL,gcL,RHL,K_aTL,etta_soildry,etta_unsatL,Beta_T,
     9 Hr_T,dVf_wT,dmh_T,f_T2,L_sT,L_vT,L_fT,L_cs,rdf,D_T,D_H2O
      double precision gR,gRT,gRT2,Rho_OT,S_Vf,SgRT,S_Vf_hr,M_j,M_j,
     1  E_j,F_j,M_j0,M_j0,E_j0,F_j0,ME,dVf_iw
      common /CCOMD_ITER/D_Tl,D_Tv,D_H2Ol,D_H2Ov,D_T,D_H2O,M_j,M_j,
     1 E_j,F_j,Vf_i,dVf_wT,f_T2,L_cs,rdf,M_j0,M_j0,E_j0,F_j0,ME
     2 /CCOMD_ITER_DTv/Vf_a,Vf_w
     3 /CCOMD_ITER_DTl/HK       /CCOMD_Kvap_DTv/D_vT
     4 /CCOMD_ITER_Rhov_DTv/Hr_T     /CCOMD_DTv/etta,Rho_vT,Beta_T
c===== functions
      double precision Vf_H2O_free,Vf_H2O_fr,Vf_w_free,Vf_w_fr,mh,
     1 dmh_Rossi,mh_Rossi
      double precision K_w,K_i,K_a,K_q,K_v,Rho_a,D_v,es,Vf_w_Rossi,
     1 HKr_Rossi,D_T_v,Rho_v,L_v2,L_f2,Rho_O
      external K_w,K_i,K_a,K_q,K_v,Rho_a,D_v,es,Vf_w_Rossi,
     1 D_T_v,Rho_v,L_v2,L_f2,Rho_O,mh_Rossi
      common /cmhRo_COMD/dmh_Rossi,HKr_Rossi
C
C     !--------------------bounds for statements----------------------!
C
      Tl =T
      Th = Tl + delta_T
      Wt_H2O    = Vf_H2O * Rho_w
      S_Vf = Vf_space - Vf_H2O
      Rho_OT= Rho_O(T)
C
C       Hr = DEXP(mh*g/(R_v*T)) & 9.81/461.51 = 2.125631e-2
C
      gR = 0.02125631D0
      gRT   = gR / T
      Beta_T = 2.057188e+09 * DEXP(-4975.9D0/T) / T**2.
      L_vT  = L_v2(T)
      L_fT  = L_f2(T)
      L_sT  = L_fT + L_vT
      K_qT  = K_q(T)
      K_wT  = K_w(T)
      K_aTO = K_a(T)
c
c  K_v must be run after D_v because it is a fn of D_v.
c
      D_vT  = D_v(T)
      K_vT  = K_v(T)
      KO    = K_wT
```

```
      RCp_soil_ave= 0.D0
      RCp_soil_sum= 0.D0
      if (Tl.ge.Tfdp) then
        L_cs = L_vT
        Rho_aT = Rho_a(Tl)
        RCp_a  = Rho_aT * Cp_a
        Vf_w   = Vf_H2O
        Vf_a   = Vf_space - Vf_w
        RCP = RCp_solid + RCp_w*Vf_w+RCp_a*Vf_a
      else
        L_cs = L_vT
        do 310 T0 = Tl,Th, Tstep
          Rho_aT    = Rho_a(T0)
          RCp_a     = Rho_aT * Cp_a
          if (T0.ge.Tfdp) then
            Vf_w = Vf_H2O
            Vf_a   = Vf_space - Vf_w
            RCp_soil = RCp_solid+RCp_w*Vf_w+RCp_a*Vf_a
            RCp_soil_sum = RCp_soil_sum + RCp_soil
          else
            Vf_w = Vf_w_Rossi(T0,Vf_H2O,Tfdp)
            Lf = L_f2(T0)
            T2 = T0+Tstep
            Vf_w2 = Vf_w_Rossi(T2,Vf_H2O,Tfdp)
            Wt_w  = Vf_w * Rho_w
            Wt_w2 = Vf_w2 * Rho_w

            Vf_i  = (Wt_H2O - Wt_w)/Rho_i
            Vf_a  = Vf_space - (Vf_w+Vf_i)
            if (Vf_a.le.0.D0) then
              Vf_a = 0.D0
              Vf_i = Vf_space - Vf_w
            endif
            RCp_soil = RCp_solid+RCp_w*Vf_w+RCp_a*Vf_a+RCp_i*Vf_i
            RCp_Le = Lf*(Wt_w2-Wt_w)
            RCp_soil_ave = RCp_soil_ave + RCp_Le
            RCp_soil_sum = RCp_soil_sum + RCp_soil
          endif
  310   continue
C
C f = evaporation efficiency, a ratio between real evaporation and
C   potential evaporation, is assumed to be a linear function of
C   moisture content with maximum 1.D0 and minium 0.D0 corresponding
C   to field capacity and wilting point, respestively.
C
        RCP = RCp_soil_sum/no_Tstep +RCp_soil_ave /delta_T
      endif
C
C   Find mh_Rossi before HKr_Rossi since some parameters in
C mh_Rossi are required for estimates of HKr_Rossi.
C
      if (T.ge.Tfdp) then
        Vf_w = Vf_H2O
        Vf_i = 0.D0
        Vf_a = Vf_space - Vf_w
      else
        Vf_w3 = Vf_w_Rossi(T-1.e-12, Vf_H2O,Tfdp)
        Vf_i3  = (Vf_H2O - Vf_w3)/.92D0
        Vf_a3  = Vf_space - (Vf_w3+Vf_i3)
        if (Vf_a3.le.0.D0) then
          Vf_a3 = 0.D0
          Vf_i3 = Vf_space - Vf_w3
        endif
        K_iT = K_i(T)
        Vf_w = Vf_w_Rossi(T,Vf_H2O,Tfdp)
C
C Conserve water mass.
C
```

```
        Vf_i = (Vf_H2O - Vf_w)/.92D0
        Vf_a = Vf_space - (Vf_w+Vf_i)
        if (Vf_a.le.0.D0) then
          Vf_a = 0.D0
          Vf_i = Vf_space - Vf_w
        endif
      endif
C
C  Continuious medium in moist soil is water if Vf_w >= Vf_unsatL.
C  The apparent thermal conductivity of a gas-filled pore is due to
C both heat conduction K_a and vapor movement K_v.  Hence
C           K_a = K_a + K_v.
C     K_v = K_v for saturated vapor as Vf_w >= Vf_wH
C     K_v = RH * K_v for saturated vapor as Vf_w < Vf_wH
C  Note RH is not the relative humidity, but a linear function of
C water content between Vf_w=Vf_dry and Vf_w=Vf_unsatH.
C
      K_sat = K_aT0 + K_vT
      r_sat  = K_sat/K_wT -1.D0
      kw_sat =(2.D0/(1.D0+ (K_wT/K_sat -1.D0)*ga_w)+1.D0/
     1        (1.D0+ (K_wT/K_sat -1.D0)*gc_w))/3.D0
      denom_sat = -6.D0*r_sat**2 / kw_sat
      b_sat =(3.D0*(r_sat-1)/kw_sat+3.D0)*r_sat/denom_sat
      c_sat =(3.D0*(1+r_sat)/kw_sat-(3.D0+2.D0*r_sat))/denom_sat
      ga_dry_sat = (-b_sat-DSQRT(b_sat**2 - 4.D0*c_sat))/2.D0
      if(Vf_H2O.ge.Vf_unsatH)then
        ga = ga_sat -(Vf_a/Vf_sat) * (ga_sat-ga_dry_sat)
        gc = 1.D0 - 2.D0 * ga
        K_aT = K_aT0 + K_vT
      else
        K_dry = K_aT0
        r_dry = K_dry/K_wT -1.D0
        kw_dry=(2.D0/(1.D0+(K_wT/K_dry -1.D0)*ga_w) + 1.D0/
     1         (1.D0+(K_wT/K_dry -1.D0)*gc_w))/3.D0
        denom_dry = -6.D0*r_dry**2 / kw_dry
        b_dry =(3.D0*(r_dry-1)/kw_dry+3.D0)*r_dry/denom_dry
        c_dry =(3.D0*(1+r_dry)/kw_dry-(3.D0+2.D0*r_dry))/denom_dry
        ga_dry = (-b_dry-DSQRT(b_dry**2 - 4.D0*c_dry))/2.D0
        ga_unsatH=ga_sat-(1.D0-Vf_unsatH/Vf_sat)*(ga_sat-ga_dry_sat)
        ga =ga_dry+Vf_H2O/Vf_unsatH *(ga_unsatH-ga_dry)
        gc = 1.D0 - 2.D0 * ga
        RH = Vf_H2O/Vf_unsatH
        K_aT = K_aT0 + RH * K_vT
C
C  Continuious medium is air if Vf_w = 0.D0
C  K_soildry is soil conductivity at Vf_w = 0.D0
C  K_soil is linearly interpolated if  0 < Vf_w < Vf_unsatL.
C
        if(Vf_H2O.lt.Vf_unsatL) then
          dummy=K_c/K_dry -1.
          kc  =ga_sat*(2./(1.+dummy*ga_soil)+1./(1.+dummy*gc_soil))
          dummy=K_o/K_dry -1.
          ko   =ga_sat*(2./(1.+dummy*ga_soil)+1./(1.+dummy*gc_soil))
          dummy=K_qT/K_dry -1.
          kq =ga_sat*(2./(1.+dummy*ga_soil)+1./(1.+ dummy*gc_soil))
          scale_c = kc*Vf_c
          scale_o = ko*Vf_o
          scale_q = kq*Vf_q
          scale_total=scale_c+scale_o+scale_q+Vf_sat
          K_soildry=1.25*(scale_c*K_c+scale_o*K_o+scale_q*K_qT+
     1              Vf_sat*K_dry)/scale_total
          etta_soildry =  1./scale_total
C
C  Note Vf_a = Vf_space = Vf_sat above.
C
          gaL =ga_dry+Vf_unsatL/Vf_unsatH *(ga_unsatH-ga_dry)
          gcL = 1.D0 - 2.D0 * gaL
          RHL = Vf_unsatL/Vf_unsatH
```

```
          K_aTL = K_aT0 + RHL * K_vT
           if (T.ge.Tfdp) then
             Vf_wL = Vf_unsatL
             Vf_iL = 0.D0
             Vf_aL = Vf_space - Vf_wL
           else
             Vf_wL = Vf_w_Rossi(T,Vf_H2O,Tfdp)
             Vf_iL = (Vf_unsatL-Vf_wL)*Rho_w/Rho_i
             Vf_aL = Vf_space - (Vf_wL +Vf_iL )
             if (Vf_aL .le.0.D0) then
               Vf_aL  = 0.D0
               Vf_iL  = Vf_space - Vf_wL
             endif
           endif

          dummy=K_c/K0 -1.
          kc   =ga_sat*(2./(1.+dummy*ga_soil)+1./(1.+dummy*gc_soil))
          dummy=K_o/K0 -1.
          ko   =ga_sat*(2./(1.+dummy*ga_soil)+1./(1.+dummy*gc_soil))
          dummy=K_qT/K0 -1.
          kq   =ga_sat*(2./(1.+dummy*ga_soil)+1./(1.+ dummy*gc_soil))
          dummy=K_aTL/K0 -1.
          ka   =ga_sat*(2./(1.+dummy*gaL)+1./(1.+dummy*gcL))
          dummy=K_iT/K0 -1.
          ki   =ga_sat*(2./(1.+dummy*ga_i)+1./(1.+dummy*gc_i))
          scale_c = kc *Vf_c
          scale_o = ko *Vf_o
          scale_q = kq *Vf_q
          scale_i = ki *Vf_iL
          scale_a = ka *Vf_aL
          scale_total = (scale_c+scale_o+scale_q+scale_a+Vf_wL+scale_i)
          K_unsatL=(scale_c*K_c+scale_o*K_o+scale_a*K_aTL+scale_q*K_qT+
     1              scale_i*K_iT+Vf_wL*K_wT)/scale_total
          etta_unsatL =  ka/scale_total
C
C     !--------------------bounds for statements-----------------------!
C  Note Vf_w = Vf_unsatL above when calculate K_unsatL.
C
          K_soil=K_soildry+Vf_H2O*((K_unsatL-K_soildry)
     1     /(Vf_unsatL-Vf_dry))
          etta=etta_soildry+Vf_H2O*((etta_unsatL-etta_soildry)
     1     /(Vf_unsatL-Vf_dry))
          goto 320
        endif
       endif
       dummy=K_c/K0 -1.
       kc  =ga_sat*(2./(1.+dummy*ga_soil)+1./(1.+dummy*gc_soil))
       dummy=K_o/K0 -1.
       ko   =ga_sat*(2./(1.+dummy*ga_soil)+1./(1.+dummy*gc_soil))
       dummy=K_qT/K0 -1.
       kq=ga_sat*(2./(1.+dummy*ga_soil)+1./(1.+ dummy*gc_soil))
       dummy=K_aT/K0 -1.
       ka   =ga_sat*(2./(1.+dummy*ga)+1./(1.+dummy*gc))
       dummy=K_iT/K0 -1.
       ki   =ga_sat*(2./(1.+dummy*ga_i)+1./(1.+dummy*gc_i))
       scale_c = kc*Vf_c
       scale_o = ko*Vf_o
       scale_q = kq*Vf_q
       scale_i = ki*Vf_i
       scale_a = ka*Vf_a
       scale_total =(scale_c+scale_o+scale_q+scale_a+Vf_w+scale_i)
       K_soil=(scale_c*K_c+scale_o* K_o+scale_q*K_qT+scale_a*K_aT+
     1         scale_i*K_iT +Vf_w*K_wT)/scale_total
C
C Note Vf_w = Vf_sat if soil is saturated.
C
       etta =  ka/scale_total
  320 if (Vf_H2O.gt.Vf_unsatL) then
```

```
        if (Vf_i.le.0.D0) then
          Vf_H2O_free = Vf_H2O - Vf_unsatL
          Vf_w_free = Vf_H2O_free
        else
          Vf_H2O_free = Vf_w + Vf_i - Vf_unsatL
          Vf_w_free = Vf_w
        endif
      else
        Vf_H2O_free = 0.D0
        Vf_w_free = 0.D0
      endif
      Vf_H2O_fr  = Vf_H2O_free
      if(Vf_H2O_fr.eq.0.D0) then
        Vf_w_fr = 0.D0
      else
        Vf_w_fr=Vf_w_free /Vf_H2O_fr
      endif
      f_T       = Vf_w_free /Vf_sat
c      if (Vf_H2O.ge.Vf_unsatH) then
c        f_T2 = 1.D0
c      else
c        f_T2 = 1.D0 - ((Vf_unsatH-Vf_H2O)/Vf_unsatH)**3.
c      endif
c
c  D_H2Ol, D_H2Ov and dmh_Rossi must follow mh_Rossi
c  D_H2Ov = alpha*Vf_a*D_v*g*Rho_v/(Rho_w*R_v*T)
c  dmh_Rossi is also computed in mh_Rossi. Hence, you need to run
c
      mh = mh_Rossi(Vf_w,T)
c      f_T2 = EXP(-mh*9.81/R/T)
      dmh_T = - tension_aw * mh
      gRT2  = gRT * mh * Rho_0T / T
      SgRT  = S_Vf *gRT * dmh_Rossi - 1.D0
      Hr_T  = DEXP(-gRT*mh)
      f_T2 = Hr_T
      Rho_vT= Rho_v(T,mh)
      HK    = HKr_Rossi * HK_s * visc0/viscosity
      S_Vf_hr = S_Vf * Hr_T * (Beta_T - gRT2)
      if (T.ge.Tfdp) then
        rdf = 1.D0
        D_H2Ol=HK * dmh_Rossi
        D_H2Ov=2.125631e-05*(Vf_a**1.67)* dmh_Rossi *D_vT*Rho_vT/T
        D_Tl  =  HK*dmh_T
        D_Tv  = D_T_v(T,mh,Vf_H2O)
      else
C
C  A reduction factor for D_H2Ol, D_H2Ov, D_Tl, D_Tv, and HK is introduced
C at T < Tf.  The reductions factor is 10**(10Vf_i) [Taylor et al 1978].
c
c        rdf   =(Vf_w/Vf_space)**(-5.D0)
c
        rdf   =10.D0 **(10.D0 *Vf_i)
        HK = HK / rdf
        D_H2Ol=HK * dmh_Rossi
        D_H2Ov=2.125631e-05*(Vf_a**1.67)* dmh_Rossi *D_vT*Rho_vT/T/rdf
        D_Tl  = HK*dmh_T
        D_Tv  = D_T_v(T,mh,Vf_H2O)/rdf
      endif
      D_T = D_Tl +  D_Tv
      D_H2O = D_H2Ol + D_H2Ov
      if(T.ge.Tfdp)then
        M_j=1.D0 + Rho_vT * SgRT / Rho_w
        H_j=Lv*Rho_vT*SgRT+Rho_w*2.343526D0*(mh-T*dmh_T)
        E_j=S_Vf_hr / Rho_w
        F_j=RCP + Lv * S_Vf_hr
        Vf_w = Vf_w + dVf_H2O
      else
        dVf_iw = -(Vf_w-Vf_w_Rossi(T-1.e-12,Vf_H2O,Tfdp))/.92e-12
```

```
        M_j0 = 1.D0 + Rho_vT * SgRT / Rho_w
        E_j0 = S_Vf_hr / Rho_w
        H_j0 = Lv*Rho_vT*SgRT+Rho_w*2.343526D0*(mh-T*dmh_T)
        F_j0 = RCP + Lv * S_Vf_hr
        M_j = M_j0
        E_j = E_j0
c
c  reference state is liquid water Lf < 0!!
c
        H_j = H_j0
        F_j = F_j0
        Vf_i = Vf_i + dVf_H2O/.92D0
      endif
      MF = (-Lf0i + (Cp_i-Cp_w)*(T-273.15D0)*Rho_i)-Lv*Rho_vT
      ME = (Rho_i-Rho_vT)/Rho_w
      return
      end
C=======================================================================
      double precision function D_T_v(T,mh,Vf_H2O)
C=======================================================================
C  Compute diffision coefficient.
C
      implicit none
      double precision f,T,Vf_space,Vf_H2Ok,Vf_w,Vf_a,etta,mh,D_vT,
     1       Rho_vT,Beta_T,Hr_T,Vf_H2O
      common /CPARA_COMD_DTv/Vf_space
     1 /CPARA_DTv/Vf_H2Ok
     2 /CCOMD_ITER_DTv/Vf_a,Vf_w
     3 /CCOMD_Kvap_DTv/D_vT
     4 /CCOMD_ITER_Rhov_DTv/Hr_T /CCOMD_DTv/etta,Rho_vT,Beta_T

      if(Vf_H2O.le.Vf_H2Ok)then
        f = Vf_space
      else
        f = Vf_a*(1.D0 + Vf_H2O/(Vf_space-Vf_H2Ok))
      endif
      D_T_v= 1.e-3*f*D_vT*etta*(Beta_T*Hr_T-2.1256311e-2
     1       *Rho_vT*mh/T**2)
      return
      end
C=======================================================================
      double precision function D_v(T)
C=======================================================================
C The diffusion coefficient of water vaper in air, m^2/sec.
C
      implicit none
      double precision T
        D_v = 1.247766e-09 * (T**1.75)
      return
      end
C=======================================================================
      double precision function es(T)
C=======================================================================
c   es estimates saturation vapor pressure, Pa
c
      implicit none
      double precision T
        es = 2.535712e+11 * 10.**(-2354.D0/T)
      return
      end
C=======================================================================
      double precision function K_a(T)
C=======================================================================
      double precision T
        K_a = 4.9756549e-3 + 7.046433e-5 * T
      return
      end
C=======================================================================
```

```
      double precision function K_i(T)
C=======================================================================
      implicit none
      double precision T
        K_i = (T**2) * (1.6744e-4) + T*(-9.7754821e-2) + 16.448468
      return
      end
C=======================================================================
      double precision function K_q(T)
C=======================================================================
      double precision T
        K_q= -1.9027254e-6 * T**3 + 1.8922227e-3* T**2
     1            -6.517895e-1 * T      + 8.493394 e1
      return
      end
C=======================================================================
      double precision function K_v(T)
C=======================================================================
c  p/ R_v **2 = 1.101325e5/4.6151e3**2 = 0.5170746734D0
c  K_v=L_v(T)**2*D_v(T)*p*es2/((R_v**2)*(T**3)*(p-es2))
c
      implicit none
      double precision T,L_v2,D_vT,es2,es
      common /CCOMD_Kvap_DTv/D_vT
      external L_v2,es
        es2 = es(T)
        K_v = 0.5170746734D0 *L_v2(T)**2 *D_vT* es2
     1          /((T**3)*(1.101325e5-es2))
      return
      end
C=======================================================================
      double precision function K_w(T)
C=======================================================================
      implicit none
      double precision T
        K_w= 0.58604D0 + 1.15115e-3 *(T - 283.16)
      return
      end
C=======================================================================
      double precision function L_f2(T)
C=======================================================================
C  Latent heat of fusion, cal/g *4.186e3 = J/kg
c ==== main
      double precision Tk_Lf(6),L_f(6),de_Lf_T(6),T
      common /CMAIN_Lf2/Tk_Lf,L_f,de_Lf_T
        call SPLINT(Tk_Lf,L_f,de_Lf_T,6,T,L_f2)
      return
      end
C=======================================================================
      double precision function L_v2(T)
C=======================================================================
C Latent heat of vaporation, cal/g *4.186*1e3 =J/kg
C
      implicit none
      double precision Tk_Lv(16),L_v(16),de_Lv_T(16),T
      common /CMAIN_Lv2/Tk_Lv,L_v,de_Lv_T
        call SPLINT(Tk_Lv,L_v,de_Lv_T,16,T,L_v2)
      return
      end
C=======================================================================
      double precision function L_s2(T)
C=======================================================================
C Latent heat of sublimation
      implicit none
      double precision Tk_Ls(9),L_s(9),de_Ls_T(9),T
      common /CMAIN_Ls2/Tk_Ls,L_s,de_Ls_T
        call SPLINT(Tk_Ls,L_s,de_Ls_T,9,T,L_s2)
      return
```

```
      end
C=======================================================================
      double precision function phi_2(T)
C=======================================================================
      implicit none
      double precision Tk_phi(27),phi_d(27),de_phi(27),T
      common /CMAIN_phi2/Tk_phi,phi_d,de_phi
        call SPLINT(Tk_phi,phi_d,de_phi,27,T,phi_2)
      return
      end
C=======================================================================
      double precision function mh_Rossi(Vf_H2O,T)
C=======================================================================
C
C  Find matric head following Rossi and Nimmo 1994.
C
c===== para
      double precision Vf_H2O_s,Vf_H2O_i,Vf_H2O_j,mh_OT,mh_dT,c,alpha,
     1 lambda,Vf_H2O,lambda1,I2_i,I3_j,coef_I1,coef_I2,Vf_H2O_i_s,
     2 Vf_H2O_j_s,I3_exp,Is,coef_I3,mh_i,mh_j,Dc2,coe_mhi,coe_mhj,
     3 coe_alpha,mh_02c,mh_s,Vf_sat
      common /CPARA_ITER_COND_Vfwa_mhRo/Vf_H2O_s,Vf_sat
     2 /CPARA_Vfwa_mhRo/mh_OT,lambda,mh_dT,c,coe_mhi,coe_mhj,
     3 coe_alpha
     4 /CPARA_mhRo/Dc2,lambda1,mh_02c,mh_0,mh_d,mh_i,alpha,mh_j,
     5 Vf_H2O_i,Vf_H2O_j,coef_I1,coef_I2,coef_I3,I3_exp,Vf_H2O_i_s,
     6 Vf_H2O_j_s,I3_j,I2_i,Is
     7 /CPARA_ITER_mhRo/mh_s
c===== mhRo
      double precision Vf_H2O_ds,dmh_Rossi,const,HKr_Rossi,In,T,mh_0,
     1 mh_d
      common /cmhRo_COND/dmh_Rossi,HKr_Rossi
      if (Vf_H2O.ge.Vf_H2O_s) Vf_H2O = Vf_H2O_s-1.e-12
c
c Note: dmh_Rossi = - D(mh_Rossi)/D(Vf_H2O), where D is the derivative.
c       matric potential = - matric head
c Milly suggested a value of 6.38e-3, while Philip and de Vries 1957-8
C suggested a value of 2.09e-3.  I follow Philip and de Vries.
C
      Vf_H2O_ds = Vf_H2O / Vf_H2O_s
      if(Vf_H2O.ge.Vf_H2O_j)then
        if(Vf_H2O.le.Vf_H2O_i)then
          In = I3_j+ coef_I2*(Vf_H2O_ds**lambda1 - Vf_H2O_j_s)
          mh_Rossi = mh_0/Vf_H2O_ds**(1.D0/lambda)
     1               * Dexp(-2.09e-3*(T-293.15))
          dmh_Rossi = mh_Rossi /(Vf_H2O * lambda)
        else
          In = I2_i+ coef_I1*(Vf_H2O_i_s - DSQRT(1.D0-Vf_H2O_ds))
          const = DSQRT((1.D0-Vf_H2O_ds)/c)
          mh_Rossi = mh_0*const * Dexp(-2.09e-3*(T-293.15))
          if(mh_Rossi.lt.mh_s) mh_Rossi = mh_s
          dmh_Rossi = mh_02c/mh_Rossi
        endif
      else
        In = coef_I3*(DEXP(I3_exp * Vf_H2O) - 1.D0)
        mh_Rossi = mh_d / Exp(Vf_H2O_ds/alpha)
     1               * Dexp(-2.09e-3*(T-293.15))
        dmh_Rossi = mh_Rossi/(Vf_H2O_s * alpha)
      endif
      HKr_Rossi = DSQRT(Vf_H2O_ds) * (In / Is)**2
      return
      end
C=======================================================================
      double precision function Rho_a(T)
C=======================================================================
      implicit none
      double precision T
        Rho_a = 3.4855216e2/T
```

```
      return
      end
C=======================================================================
      double precision function Rho_0(T)
C=======================================================================
      implicit none
      double precision T
        Rho_0 = 413430.51D0 * DEXP(-4975.9/T)
      return
      end
C=======================================================================
      double precision function Rho_v(T,mh)
C=======================================================================
      implicit none
      double precision T,mh,Rho_0,Hr_T
      external Rho_0
      common /CCOMD_ITER_Rhov_DTv/Hr_T
        Rho_v = Rho_0(T) * Hr_T
      return
      end
C=======================================================================
      subroutine RTBIS(Tr,Vf_H20)
C=======================================================================
C  Determine the freezing depression point.
C
      implicit none
C
C      matric head = Latent heat * Tfpd / (gravity * Temp)
C
      double precision Tr,Vf_H20,X1,X2,TACC,F,FMID,DT,TMID,Lf,L_f2,
     1 mh_Rossi
      integer J,JMAX
c===== main
      common/CMAIN_RTBI/X1,X2,TACC
      external L_f2,mh_Rossi
      parameter(JMAX=40)

      if(Vf_H20.gt..48D0)Vf_H20 = .48D0
      Lf = L_f2(X1)
      FMID= 9.81D0*mh_Rossi(Vf_H20,X1) * X1 - Lf * (273.15D0 - X1)
      Lf = L_f2(X2)
      F= 9.81D0*mh_Rossi(Vf_H20,X1)* X2 - Lf * (273.15D0 - X2)
      IF(F.LT.0.D0) THEN
        Tr = X1
        DT = X2 - X1
      ELSE
        Tr=X2
        DT = X1 - X2
      ENDIF
      DO 330 J = 1, JMAX
        DT = DT/2.
        TMID= Tr+DT
        Lf = L_f2(TMID)
        FMID=9.81D0*mh_Rossi(Vf_H20,TMID)*TMID -Lf*(273.15D0-TMID)
        IF(FMID.EQ.0.D0)THEN
          Tr=TMID
          RETURN
        ELSEIF(FMID.GT.0.D0)THEN
          Tr=TMID
        ENDIF
        IF(DABS(DT).LT.TACC)RETURN
  330 CONTINUE
      PAUSE 'too many bisections'
      RETURN
      end
C=======================================================================
      subroutine sdepth
C=======================================================================
```

```
C  Determine thicknesses of soil layers.
C
      implicit none
      integer NODEP,NODEPO,i
      parameter (NODEP=60,NODEPO=NODEP-1)
      double precision Z(NODEP),depth(0:NODEP),depth1(NODEP),
     1 Z2(0:NODEP),depth2(0:NODEP),alpha1(NODEP),alpha2(NODEP),
     2 beta1(NODEP),beta2(NODEP),a,b,c,depth3(NODEP)
      common /cdept_MAIN_INIT_ITER/Z,Z2
     1 /cdept_MAIN_ITER/depth,depth1,depth2
     2 /cdept_ITER/alpha1,alpha2,beta1,beta2,depth3
c==== para
      double precision zinc,Z_1
      common /para_dept/zinc,Z_1
      Z(1) = Z_1
      write(6,*)Z(1),zinc
      do 350 i = 2, NODEP
        Z(i) = Z(i-1) + Z(1) * zinc**i
  350 continue
      depth1(1) = Z(1)
      depth(1)  = depth1(1) * .5D0
      depth(0)  = 0.D0
      do 352 i = 2, NODEP
        depth1(i) = Z(i) - Z(i-1)
        depth(i)  = depth1(i) * .5D0
  352 continue
      depth2(0) = depth(1)-depth(0)
      Z2(0)     = 0.D0
      do 354 i = 1, NODEPO
        depth2(i)  = depth(i) + depth(i+1)
        Z2(i)      = Z(i) - depth(i)
  354 continue
      Z2(NODEP) = Z(NODEP) - depth(NODEP)
      do 356 i = 1, NODEPO
        a = depth2(i-1)/depth2(i)
        b = depth2(i-1) + depth2(i)
        c = depth1(i) + depth1(i+1)
        depth3(i) = b/2.D0
        alpha1(i) = a/b
        beta1(i) = 1.D0/a/b
        alpha2(i) = depth1(i+1)/c
        beta2(i) = depth1(i)/c
  356 continue
      depth3(NODEP) = (depth2(NODEP-1)+depth2(NODEP))/2.D0
      OPEN(UNIT=370,STATUS='UNKNOWN',FILE='fd_depth.dat')
       write(370,*)'Z2(0),depth2(0)'
        write(370,358)Z2(0),depth2(0)
  358   format('          ',1pe9.2,'                  ',1pe9.2)
        write(370,*)' i    Z(i)   Z2(i)  depth(i)  depth1(i)  depth2(i)'
       do 362 i =1, NODEPO
       write(370,360)i,Z(i),Z2(i),depth(i),depth1(i),depth2(i),
     1 iepth3(i)
  360  format(I3,6(' ',1pe9.2))
  362  continue

       write(370,*)' i  alpha1(i)  beta1(i)  alpha2(i)  beta2(i)'
       do 366 i =1, NODEPO
       write(370,364)i,alpha1(i),beta1(i),alpha2(i),beta2(i)
  364  format(I3,6(' ',1pe9.2))
  366  continue
      close(370)
      return
      end
C=======================================================================
      SUBROUTINE SPLINE(X,Y,N,YP1,YPN,Y2)
C=======================================================================
C       Subroutines SPLINE and SPLINT are from Numerical Recipes
C   [Press et al 1989].
```

```
      implicit none
      integer NMAX,I,N,K
      PARAMETER (NMAX=500)
      double precision X(N),Y(N),Y2(N),U(NMAX),YP1,YPN,SIG,P,QN,UN
      IF (YP1.GT..99E30) THEN
        Y2(1)=0.D0
        U(1)=0.D0
      ELSE
        Y2(1)=-dble(0.5)
        U(1)=(dble(3.)/(X(2)-X(1)))*((Y(2)-Y(1))/(X(2)-X(1))-YP1)
      ENDIF
      DO 380 I=2,N-1
        SIG=(X(I)-X(I-1))/(X(I+1)-X(I-1))
        P=SIG*Y2(I-1)+2.D0
        Y2(I)=(SIG-1.)/P
        U(I)=(dble(6.)*((Y(I+1)-Y(I))/(X(I+1)-X(I))-(Y(I)-Y(I-1))
     1       /(X(I)-X(I-1)))/(X(I+1)-X(I-1))-SIG*U(I-1))/P
  380 CONTINUE
      IF (YPN.GT..99E30) THEN
        QN=0.D0
        UN=0.D0
      ELSE
        QN=5D0
        UN=(3.D0/(X(N)-X(N-1)))*(YPN-(Y(N)-Y(N-1))/(X(N)-X(N-1)))
      ENDIF
      Y2(N)=(UN-QN*U(N-1))/(QN*Y2(N-1)+1.D0)
      DO 382 K=N-1,1,-1
        Y2(K)=Y2(K)*Y2(K+1)+U(K)
  382 CONTINUE
      RETURN
      END
C=======================================================================
      SUBROUTINE SPLINT(XA,YA,Y2A,N,X,Y)
C=======================================================================
      implicit none
      integer N
      double precision XA(N),YA(N),Y2A(N),X,Y,H,A,B
      integer KLO,KHI,K
      KLO=1
      KHI=N
1     IF (KHI-KLO.GT.1) THEN
        K=(KHI+KLO)/2
        IF(XA(K).GT.X)THEN
          KHI=K
        ELSE
          KLO=K
        ENDIF
      GOTO 1
      ENDIF
      H=XA(KHI)-XA(KLO)
      IF (H.EQ.0.) PAUSE 'Bad XA input.'
      A=(XA(KHI)-X)/H
      B=(X-XA(KLO))/H
      Y=A*YA(KLO)+B*YA(KHI)+
     1       ((A**3-A)*Y2A(KLO)+(B**3-B)*Y2A(KHI))*(H**2)/6.D0
      RETURN
      END
C=======================================================================
      double precision function Vf_w_Rossi(T,Vf_H2O,Tfdp)
C=======================================================================
C  A function used to determine freezing depression point.
C
C===== para
      double precision Vf_H2O_s,mh_OT,lambda,mh_dT,c,alpha,mh_i,mh_j,Tf,
     1  coe_mhi,coe_mhj,coe_alpha,Tfdp,Vf_H2O,Vf_sat
      common /CPARA_ITER_COND_Vfwa_mhRo/Vf_H2O_s,Vf_sat
     1 /CPARA_ITER_COND_Vfwa/Tf
     2 /CPARA_Vfwa_mhRo/mh_OT,lambda,mh_dT,c,coe_mhi,coe_mhj,
```

```
     3  coe_alpha
c===== Vf_w
      double precision mh,T,L_f2,mh_0,mh_d
      external L_f2

      mh_0 = mh_0T * Dexp(-2.09e-3*(T-293.15))
      mh_d = mh_dT * Dexp(-2.09e-3*(T-293.15))
      mh_i = mh_0 * coe_mhi
      alpha = lambda*(mh_0/mh_d *coe_alpha)**lambda
      mh_j = mh_d * coe_mhj
      if(T.ge.Tfdp) then
        Vf_w_Rossi = Vf_H20
      else
        mh = L_f2(T)*(273.15D0-T)/(9.81D0*T)
        if(mh.ge.mh_i)then
          if(mh.le.mh_j)then
            Vf_w_Rossi = (mh_0/mh)**lambda*Vf_H20_s
          else
            Vf_w_Rossi = alpha * DLOG(mh_d/mh)*Vf_H20_s
          endif
        else
          Vf_w_Rossi = (1.D0-c*(mh/mh_0)**2)*Vf_H20_s
        endif
      endif
      return
      end
C=======================================================================
      SUBROUTINE SINIT2
C=======================================================================
C  The subroutine is written to provide climatological and sky radiance
C information.  It primarily follows the AT code [Chapter 2].
C
      implicit none
C==== sinit
      INTEGER HR,IMAX,NOZ1,NOZ11,NODEP,N,I,JS,JE,NR5,NSAM_ST1,Im,
     1  NSAMDI,II,II0,II1,IA,HR1,NSAM_ST,N1,NSAMD2,NSAM1,
     2  J,NSAM,SKIP,NDAY,Nr
      DOUBLE PRECISION PI,SIGMA,EM_tc,EM_t,delt_TI,DUMMY,SOLAR,e_max
      PARAMETER (NODEP=60,IMAX=16000,PI=3.1415927,SIGMA=5.6696E-8,
     1   NOZ1=40,NOZ11=NOZ1+1,NR5=NOZ1/10,NSAMDI=144)
      CHARACTER INITIAL*46,INITIAL1*45
      DOUBLE PRECISION e_asat(IMAX),ZI1(NOZ1),MOIS,TgI(NSAMDI),
     1 TI1(NOZ1),de_TZ(NOZ1),Rn(IMAX),
     2 Rs(IMAX),RDAY(0:IMAX),TIR(IMAX),TAIR(IMAX),TSKY(IMAX),COS,PIHR,
     3 COSZ,YP1,YP2,T(0:NODEP),pp(0:IMAX),AIRF(IMAX),U10(IMAX),ALBc,
     4 Tcan(IMAX),RHa(IMAX),Vf(0:NODEP),e_ar(IMAX),S_Tc4,Qldc(IMAX),
     5 Qld(IMAX),Qsd(IMAX),Qsdc(IMAX),RHR,Qsdt(IMAX),
     6 q_ar(IMAX),q_asat(IMAX),r_ar,Root(NODEP),Root2(0:NODEP),zr_e,
     7 F1_f0,F1_F,F1,F3,F4,FFF(IMAX),RHR_i(IMAX),Qld_t,Rn_I,Rs_I,RDAY_I,
     8 TAIR_I,TIR_I,pp_I,U10_I,RHa_I,NDAY_ST,Wr_max,pp_a,gc,gb,
     9 ALBc_min,ALBc_max,TB1937(4,IMAX),TB19371,TB19372,TB19373,TB19374,
     1 HG_I,HG(IMAX),DUM,DUM2,Tg(6,IMAX),Tg2_I,Tg4_I,Tg8_I,Tg16_I,
     2 Tg32_I,Tg64_I,ZI(0:NOZ1,0:NSAMDI),TI(0:NOZ1,0:NSAMDI),SOLARCL,
     3 trans_c,trans_t
      COMMON /CINIT_MAIN_ITER/e_ar,pp,TAIR,AIRF,Qldc,TSKY,Qsdc,T,
     1 Qld,Qsd,Qsdt,Vf,FFF,RDAY,RHR_i,Wr_max,Nr,NSAM
     2 /CINIT_ITER/Tcan,Tg,HG,F1_f0,q_ar,q_asat,Root2
C---- sapra
      DOUBLE PRECISION EM,hc,zm,zr,veg,veg1,TIME_ST,EMc,LAI,
     1 ALB,ALBt,trans_ct,EMt
      COMMON /CPARA_INIT/hc,zm,zr,TIME_ST,trans_ct
      INTEGER NOZ,NDAY_ST,NDAY_ED
      COMMON /CPARA_MAIN_INIT_ITER/EM,EMc,EMt,LAI,veg,veg1,NOZ,NDAY_ST,
     1 NDAY_ED
     8 /CPARA_F2_INIT_ITER/ALB,ALBt,ALBc
C***   main
      DOUBLE PRECISION COSRLAT,SINRLAT,EMSI,EMSIc,EMSIt
      COMMON /CMAIN_FCL_INIT/COSRLAT,SINRLAT
```

```
     2       /CMAIN_INIT_ITER/EMSI,EMSIc,EMSIt
C===   syear
       INTEGER NDAYY,NSAMY,NSAMDS(0:366),NSAMMS(0:12)
       COMMON /CYEAR/NDAYY
      1       /CYEAR_MAIN_INIT_ITER/NSAMY,NSAMDS,NSAMMS
C***  sdecl
       DOUBLE PRECISION COSDECL(366),SINDECL(366)
       COMMON /CDECL_FCL_INIT/COSDECL,SINDECL
C--- subroutine sf2
       DOUBLE PRECISION F2(366)
       EXTERNAL FCLOUD
       COMMON /CF2_INIT/F2
C=== subroutine stoair
       DOUBLE PRECISION TOAIR(0:366)
       COMMON /CTOAIR_INIT_ITER/TOAIR
C===== sdepth
       double precision Z(NODEP),Z2(0:NODEP)
       common /cdept_MAIN_INIT_ITER/Z,Z2
c===== functions
       double precision Rho_a,es
       external Rho_a,es

       YP1 = dble(1e30)
       YP2 = dble(1e30)
       PIHR =  PI / 72.0
       EM_t = .95
       EM_tc = EM_t / EMc
       SKIP = 0
       F1_f0  = (.55 * 2.) / (LAI * 100.)
       NSAM = 0
       Wr_max = .2e-3 * LAI
       OPEN(unit=410,FILE='ini.dat',STATUS='UNKNOWN')
C
C       Find SOLAR, TAIR(I), TSKY(I), Qld(I), Rs and FWIND(I).
C
       DO 430 I = NDAY_ST,NDAY_ED
         JS = NSAMDS(I-1) + 1
         JE = NSAMDS(I)
         DO 420 HR = JS, JE
           NSAM = NSAM + 1
           COSZ=COSRLAT*COSDECL(I)*(-COS(DBLE(HR)*PIHR)
     1        + SINRLAT*SINDECL(I))
           IF (COSZ.GT.0.0) THEN
             SOLAR = COSZ - .2 * COSZ ** .5
             IF (SOLAR.LT.0.0) SOLAR = 0.0
           ELSEIF (COSZ.LE.0.) THEN
             SOLAR = 0.0
           ENDIF
           if(MOD(HR,NSAMDI).eq.0.)then
             RDAY(NSAM)=DBLE(I+1)
           else
             RDAY(NSAM)=DBLE(I)+DBLE(MOD(HR,NSAMDI))/DBLE(NSAMDI)
           endif
           TAIR(NSAM)= TOAIR(I)-5.*COS((HR-12.)*PIHR)
           TSKY(NSAM)= TAIR(NSAM)*0.89913765
           Qld_t= SIGMA*TSKY(NSAM) ** 4.+F2(I)
           SOLARCL = 1191.1
           Rs(NSAM) = SOLAR * SOLARCL
           RHa(NSAM) = 0.80D0
           U10(NSAM) = 5.D0
           TB1937(3,NSAM) = 0.D0
           TB1937(4,NSAM) = 0.D0
           NDAY = INT(RDAY(NSAM))
           RHR = RDAY(NSAM)*24.D0
           IF (COSZ.GT.0.0) THEN
             ALBc = 0.526*(.035 + .071 - .052  * COSZ + .0364 * COSZ**2)+
     1              0.418*(.825 - .9514 * COSZ + .4374 * COSZ**2)
             if(veg.eq.0.D0)then
```

```
              trans_c = 1.D0
              trans_t = 1.D0
            else
              trans_c = DEXP(-.4D0*LAI/COSZ)
              trans_t = DEXP(-.4D0*LAI*trans_ct/COSZ)
            endif
            DUM=Rs(NSAM)*(1.-ALBc)*veg
            DUM2=DUM*trans_c*(1.-ALBt)
            Qsdt(NSAM)=DUM2*(1.-trans_t)
            Qsdc(NSAM)=DUM*(1.-trans_c)
            Qsd(NSAM)=(Rs(NSAM)*veg1  + DUM2*trans_t)*(1.-ALB)
          else
            Qsd(NSAM) = 0.D0
            Qsdc(NSAM) = 0.D0
            Qsdt(NSAM) = 0.D0
          endif
          Qldc(NSAM) = veg * EMc * Qld_t
          Qld(NSAM) = veg1 * EM * Qld_t
          RHR_i(NSAM) = 600
  420   CONTINUE
  430 CONTINUE
      NSAM1 = NSAM +1
      TAIR(NSAM1) = TAIR(NSAM)
      Qld(NSAM1) = Qld(NSAM)
      Qldc(NSAM1) = Qldc(NSAM)
      Qsd(NSAM1) = Qsd(NSAM)
      Qsdc(NSAM1) = Qsdc(NSAM)
      Qsdt(NSAM1) = Qsdt(NSAM)
      Rs(NSAM1) = Rs(NSAM)
      NSAM = 0
      DO 434 I = NDAY_ST,NDAY_ED
        JS = NSAMDS(I-1) + 1
        JE = NSAMDS(I)
        e_max = dble(es(TAIR(NSAM+NSAMDS(1)/2))) * .8D0
        DO 432 HR = JS, JE
          NSAM = NSAM + 1
c
c    Find saturation vapor pressure and real vapor pressure.
c
          e_asat(NSAM) = es(TAIR(NSAM))
          e_ar(NSAM) = e_asat(NSAM)
          if (e_ar(NSAM).gt.e_max) e_ar(NSAM) = e_max
c
c    Compute specific atmospheric specific humidity.
c        r = .622 e/(p-e), mixing ratio (Iribarne and Godson, 1992)
c        q = r/ (1 + r), specific humidity
c
          r_ar = .622D0*e_ar(NSAM)/(1.01325e5 - e_ar(NSAM))
          q_ar(NSAM) = r_ar/(1.D0+ r_ar)

          r_ar = .622D0*e_asat(NSAM)/(1.01325e5 - e_asat(NSAM))
          q_asat(NSAM) = r_ar/(1.D0+ r_ar)
          gc = veg*(U10(NSAM)*.16)/((DLOG((zm/hc-.682)/.028))**2)
          gb = veg1*(U10(NSAM)*.16)/((DLOG((zm-.015)/.015))**2)
          AIRF(NSAM) = gb + gc
          if(NSAM.eq.1) then
            write(410,490)NSAM,RDAY(NSAM),gc,gb,U10(NSAM)
          endif
  432   CONTINUE
  434 CONTINUE
      NSAM1 = NSAM + 1
      e_ar(NSAM1) = e_ar(NSAM)
      e_asat(NSAM1) = e_asat(NSAM)
      q_ar(NSAM1) = q_ar(NSAM)
      q_asat(NSAM1) = q_asat(NSAM)
      SKIP = NDAY_ST-1
C
C  Determine the input file for initial conditions.  These files
```

```
C are from the AT model [Chapter 2].
C
      MOIS = .3802
      IF(MOIS.eq..1728)THEN
        INITIAL = '/y/yueian/BARE/ANN/TH/M12/TZ.dat'
        INITIAL1 = '/y/yueian/BARE/ANN/TH/M12/T.dat'
      ELSEIF(MOIS.eq..242)THEN
        INITIAL = '/y/yueian/BARE/ANN/TH/M17/TZ.dat'
        INITIAL1 = '/y/yueian/BARE/ANN/TH/M17/T.dat'
      ELSEIF(MOIS.eq..3802)THEN
        INITIAL = '/y/yueian/BARE/ANN/TH/M27/TZ.dat'
        INITIAL1 = '/y/yueian/BARE/ANN/TH/M27/T.dat'
      ELSE
        WRITE(6,*)'YOUR INITIAL MOISTURE IS INAPPROPRIATE'
      ENDIF
      OPEN(UNIT=480,STATUS='OLD',FILE=INITIAL)
      OPEN(UNIT=481,STATUS='OLD',FILE=INITIAL1)
        DO 450 I = 1, SKIP, 1
          READ(481,*)DUMMY
          DO 442 IA = 1, NR5
            READ(480,*)DUMMY
            READ(480,*)DUMMY
  442     CONTINUE
  450   CONTINUE
        HR = 1
        READ(481,*)DUMMY,DUMMY,TgI(HR)
        TI(0,HR) = TgI(HR)
        ZI(0,HR) = 0.D0
        DO 464 IA = 1, NR5
          II0 = (IA - 1) * 10 + 1
          II1 = IA * 10
          READ(480,*)(TI(II,HR), II=II0,II1)
  464   CONTINUE
        DO 468 IA = 1, NR5
          II0 = (IA - 1) * 10 + 1
          II1 = IA * 10
          READ(480,*)(ZI(II,HR), II=II0,II1)
  468   CONTINUE
      CLOSE(480)
        DO 470 N = 0,NOZ-1
          N1 = N + 1
          TI1(N1) = TI(N,HR)
          ZI1(N1) = ZI(N,HR)
          ZI1(N1)=ZI1(N1)+dble(N1)*(1.e-8)
  470   CONTINUE
        CALL SPLINE(ZI1,TI1,NOZ1,YP1,YP2,de_TZ)
C
C     !--------------------bounds for statements----------------------!
C
        write(410,*)'    I      RDAY         Qsd          Qsdt         '
     1' Qsdc Qldc TSKY TAIR Qld e_ar'
      do 472 I = 1, NSAM
        write(410,490)I,RDAY(I),Qsd(I),Qsdt(I),Qsdc(I),Qldc(I),TSKY(I),
     1 TAIR(I),Qld(I),e_ar(I)
  472 continue
      write(410,*)'I       RDAY       Qsd      Qld     Qsdc     Qldc  '
      write(410,*)'NSAM=',NSAM
C
C  Determine initial tmperature profile of the soil.
C
      delt_TI = TI1(7) - TI1(6)
      write(410,*)' Soil temperatures are '
      write(410,474)(TI1(J),J=1,NOZ1)
      write(410,474)(ZI1(J),J=1,NOZ1)
  474 format(6(' ',1pe12.5))
c
c     Determine root distribution.  (Feddes et al, 1974, referred by
c   Verseghy et al, 1993).  Root distributions are needed for estimates
```

```
c   of transpiration.
c
      zr_e = DEXP(-3.D0*zr)
      Root2(0) = 1.D0
      Nr = 0
      DO 476 N=1,NODEP
        IF(Z(N).LE.zr)THEN
          Root2(N) = (DEXP(-3.D0*Z(N)) - zr_e)/(1.D0 - zr_e)
          Nr = Nr + 1
        ELSE
          Root2(N) = 0.D0
        ENDIF
  476 CONTINUE
      Nr = Nr + 1
      write(6,*)'Nr=',Nr
c
c     Interplate soil temperature.
c
      CALL SPLINE(ZI1,TI1,NOZ1,YP1,YP2,de_TZ)
      Vf(0) = 1.4e-3
      DO 478 N=1,NODEP
        CALL SPLINT(ZI1,TI1,de_TZ,NOZ1,Z2(N),T(N))
        Vf(N) = .3802
        Root(N) = Root2(N-1) - Root2(N)
        write(410,*)'TV',Z2(N),T(N),Vf(N)
  478 CONTINUE
      T(0) = TAIR(1)
      Tcan(1) = T(0)
      write(410,*)'Initial canopy temperautre is',Tcan(1),T(1),TAIR(1)
      write(410,*)'Albedo max =',ALBc_max,' min=',ALBc_min
      close(410)
C
C     Initialize Z (depth), T (soil temp), and Tg (surf. temp)
C     for the first time step.
C
  490   format(i5,1pe13.5,10(' ',1pe12.4))
      RETURN
      END
C=======================================================================
      SUBROUTINE SF2
C=======================================================================
C       Find irradiance from clouds.
C
      implicit none
C--- sf2
      integer I,NDAY
      DOUBLE PRECISION F2(366)
      COMMON /CF2_INIT/F2
     1       /CF2_FCL/NDAY
C--- PARA
      DOUBLE PRECISION ALB,ALBt,ALBc
      COMMON /CPARA_F2_INIT_ITER/ALB,ALBt,ALBc
C=== subroutine syear
      INTEGER NDAYY
      COMMON /CYEAR/NDAYY
      DOUBLE PRECISION F20,FC
C--- function
      DOUBLE PRECISION FCLOUD
      EXTERNAL FCLOUD

      F20 = (.2/2.)*1385./24.
      DO 500 I = 1, NDAYY
        NDAY = I
        FC = 0.
        CALL QTRAP(FCLOUD,0.D0,24.D0,FC)
        F2(I) = F20 * FC
  500 CONTINUE
      RETURN
```

```
      END
C=======================================================================
      FUNCTION FCLOUD(HOUR)
C=======================================================================
C       FCLOUD is a function for estimates of irradiance from clouds.
C
      implicit none
      DOUBLE PRECISION DUM1,FCLOUD

      INTEGER NDAY
      DOUBLE PRECISION COSRLAT,SINRLAT,COSDECL(366),SINDECL(366),
     1 PERIODD,HOUR,PI2PER
      COMMON /CMAIN_FCL_INIT/COSRLAT,SINRLAT
     1 /CMAIN_FCL/PERIODD,PI2PER
     2 /CF2_FCL/NDAY
     3 /CDECL_FCL_INIT/COSDECL,SINDECL
      DUM1 = COSRLAT*COSDECL(NDAY)*(-COS(PI2PER*HOUR)+
     1       SINRLAT*SINDECL(NDAY))
      IF (DUM1.GT.0.) THEN
        FCLOUD = DUM1 - 0.2 * DUM1 ** 0.5
        IF (FCLOUD.LE.0.) FCLOUD = 0.
      ELSE
        FCLOUD = 0.
      ENDIF
      RETURN
      END
C=======================================================================
      SUBROUTINE QTRAP(FCLOUD,A,B,S)
C=======================================================================
C  Returns as S the integral of the function FUNC from A to B.  The
C parameters EPS can be set to the desired fractional accuracy and
C JMAX so that 2 to the (JMAX-1)th power is the maximum allowed number
C of steps.  Integration is performed by the trapezoidal rule.
C  Subroutines QTRAP and TRAPZD are from Numerical Recipes
C [Press et al 1989].
C
      implicit none
      DOUBLE PRECISION EPS,A,B,OLDS,ABS,S,FCLOUD
      integer JMAX,J
      EXTERNAL FCLOUD
      PARAMETER (EPS=1.E-5, JMAX=18)
C
C       OLDS is any number that is unlikely to be the average of the
C     function at its endpoints will do here.
C
      OLDS=-1.E30
      DO 510 J=1,JMAX
        CALL TRAPZD(FCLOUD,A,B,S,J)
        IF (ABS(S-OLDS).LT.EPS*ABS(OLDS)) RETURN
        OLDS=S
  510 CONTINUE
      RETURN
      END
C=======================================================================
      SUBROUTINE TRAPZD(FCLOUD,A,B,S,N)
C=======================================================================
C  This routine computes the N'th stage of refinement of an extended
C trapezoidal rule.  FUNC is input as the name of the function to be
C integrated between limits A and B, also input.  When called with
C N = 1, the routine returns as S the crudest estimate of the integral.
C Subsequent calls with N = 2, 3, ... (in that sequential order) will
C improve the accuracy of S by adding 2 to the (N-1)th power additional
C interior points. S should not be modified between sequential calls.
C
      implicit none
      DOUBLE PRECISION FCLOUD,S,B,A,DEL,X,SUM,TNM
      integer IT,J,N
      EXTERNAL FCLOUD
```

```
      SAVE IT

      IF (N.EQ.1) THEN
        S=0.5*(B-A)*(FCLOUD(A)+FCLOUD(B))
C
C       IT is the number of points to be added on the next call.
C
        IT=1
      ELSE
        TNM=DBLE(IT)
C
C       DEL is the spacing of the points to be added.
C
        DEL=(B-A)/TNM
        X=A+0.5*DEL
        SUM=0.
        DO 520 J=1,IT
          SUM=SUM+FCLOUD(X)
          X=X+DEL
  520   CONTINUE
C
C       This replaces S by its refined value.
C
        S=0.5*(S+(B-A)*SUM/TNM)
        IT=2*IT
      ENDIF
      RETURN
      END
C=======================================================================
      SUBROUTINE STOAIR
C=======================================================================
C Calculate average daily air temperature.
C
      implicit none
      DOUBLE PRECISION TAIRO,TAIR1,PLAG2,P2,COS,THETALAG,NDAY2
      integer I
      INTEGER NDAYY,NDUM
      COMMON /CYEAR/NDAYY
      DOUBLE PRECISION TOAIR(0:366)
      COMMON /CTOAIR_INIT_ITER/TOAIR
      TAIRO = 278.3
      TAIR1 = 16.9
      THETALAG = 1.12
      PLAG2 = 0.58643063
      P2 = 2. * 3.141592654 / NDAYY
      IF(NDAYY.EQ.366) THEN
        NDUM = 10
      ELSE
        NDUM = 9
      ENDIF
      DO 530 I = 1, NDAYY
        NDAY2 = I + NDUM
        TOAIR(I)=TAIRO-TAIR1*COS(P2 * DBLE(NDAY2) - PLAG2)
  530 CONTINUE
      TOAIR(0) = TOAIR(NDAYY)
      RETURN
      END

C=======================================================================
C=======================================================================
C  Input file of parameters, dH.prm.
C=======================================================================
C
 43.5     { LAT: latitude(typical = 47. N).
 .96      { EM: thermal IR emissivity(typical = .95)
 1.e-2    { DELTMAX: convergent criterion for temperature, K
 1.e-4    {  DVfMax: convergent criterion for moisture content, %
 1992     { YEAR: the year in number.
```

```
 40       { NOZ: the number of soil layers, less than 100, typical = 40
 .01D0    { ZINCR: increase depth per step, in m.
  21D0    { TIME_ST: the starting time on the first day of simulation, hr
 287      { NDAY_ST: the starting day number of simulation
 301      { NDAY_ED: the ending day number of simulation
48.D0     { porosity
.225D0   { ratio_c
.775D0   { ratio_q
273.15D0 { Tf
1.e-5     { delta_T
.144D0   { ga_soil
.144D0   { ga_i
.144D0    { ga_w
.01D0     { mh_s
.48D0     { Vf_H2O_s
1.23e-7   { HK_s
5.39D0    { b
701.96    { Cp_c
2.9302    { K_c
2.65e3    { Rho_c
1.932e3   { Cp_o
2.5116e-1{ K_o
1.3e3     { Rho_o
7.5536843e2  { Cp_q
2.66e3    { Rho_q
4218.     { Cp_w
1.e3      { Rho_w
2106.     { Cp_i
.92e3     { Rho_i
1004.64   { Cp_a
1.312D0   { mh_OT
.29D0     { lambda
1.e5      { mh_dT
60        { NSMAX
-2.09e-3 { tension_aw
0         { write_coe
 .005D0   { Z_1
 1.075D0 { zinc
 .6D0     { hc: vegetation height, m
 10.D0    { zm: height of wind measurements, m
  .30     { zr: depth of root, m
  3.D0    { LAI: leaf area index, m^2/m^2
  1.D0    { veg: vegetation coverage
  1.5e-4 { Wr: initial stored water on foliage, m
  400.    { rsmin: minimum canopy surface resistance, s/m
 5000.    { rsmax: maximum canopy surface resistance, s/m
  0       { drydown: 1 = dry-down simulation; 0 otherwise
 .3       { ALB: albedo of bare soil
 .4       { ALBt: albedo of thatch
 .2       { ALBc: albedo of canopy, used for the dry-down simulation
 .0663    { trans_ct: weight of thatct / weight of canopy
 .98      { EMc: emissivity of canopy
 .97      { EMt: emissivity of thatch
```

B.2 The Radiobrightness Module

```
C ================================================================
      PROGRAM TB
C ================================================================
C  This code is written to compute terrain radiobrightness for model
C validation.  The wet permittivity of wet canopy follows the
C dual-dispersion model by Ulaby and El-Rayes 1987.  Optical thickness
C of the canopy is after England and Galantowicz 1995.
C
C       Written by Yuei-An Liou, 1996.
C
C     FF : fraction of free water in liquid,
C     TK    : ground temperature, K
C     TC : ground temperature, C (Centigrade)
C     TG         : temperature gradient w.r.t. depth at the surface
C  Vf_H2O_fr     : volume fraction of free water
c     Wc         : averaged dry canopy weight, 10^-3 kg/m^2 [REBEX-1]
c     Ww         : canopy moisture weight, 10^-3 kg/m^2
c     Mg         : gravimetric moisture content = Ww/Wc
C
      implicit none
      INTEGER IMAX
      double precision C0,PIR,PID
      PARAMETER(C0=3.E8,PIR=3.14159,PID=180.,IMAX=1500)
CCC soil
      double precision zefftemp,zefftemp1,THETAR,Tair,Flh,Fsh,Fsun,
     1 Vf_w,Vf_i,Vf_a,hc
      INTEGER ifreq,I,NDAYY,DAY2,II
      COMPLEX COSRO,Es,EGND(3),NGND(3),j
     1     ,COSTO(3),NCOS1(3), NCOS2(3),AMPV(3),AMPH(3)
      CHARACTER MO*2,LATENT*1
      double precision PIRD,COSR,SINR,ANGF(3),ZEFFO(3),TIME,TG,FF,TK,
     1 COST(3),TEFF(3),ZEFFCM(3),ZEFFMIN(3),ZEFFMAX(3),TGMIN,TGMAX,TC,
     2 ZEFF(3),RV(3),RH(3),EH(3),EV(3),TBV(3,IMAX),TBH(3,IMAX),FREQ,
     3 TbV6a(366,3),TbV6p(366,3),TbH6a(366,3),TbH6p(366,3),Vf_H2O_fr,
     4 Tg6am(366),Tg6pm(366),Vf_H2O_fr_6am(366),FF_6am(366),TBVO(3),
     5 TBHO(3),DAY,THETAT(3),Tcanopy,Tb_sumH(3),ADiffTb(2),Tt
ccc vegetation
      double precision TAU
      complex Ecanopy(3),Ncanopy(3)
      double precision Mg,Ww,Wc,Vfw,Vb,Eresidual,KO(3),Tb19HM(IMAX),
     1 Tb37HM(IMAX),DiffTb2(3),
     1 DUM,EXP_TAU,Tb_skyV(3),Tb_skyH(3),Tb_cdV(3),Tb_cdH(3),Tb_gV(3),
     2 Tb_gH(3),Tb_cuV(3),Tb_cuH(3),DiffTb(3),Devi(2),Var(2),Tsky(3)
      COMMON /CMAIN_WATER_ICE/FREQ
     1       /CMAIN_WATER/TC
     2       /CMAIN_ICE/TK
c==== spara
      double precision EsR,LTAN,THETA,FREQ2(3),Vf_s,Vf_bw,alpha,RELAXT
      INTEGER NDAY_ST,NDAY_ED,NSAM
      CHARACTER DATAI*32,DATAI2*33,DATAI3*29
      COMMON /CPARA_MAIN/EsR,LTAN,THETA,Vf_s,Vf_bw,alpha,hc,
     1       FREQ2,NSAM,NDAY_ST,NDAY_ED,DATAI,DATAI2,DATAI3
c==== ewater,eice
      COMPLEX Ew,Ei,Ebw,Ea
      COMMON/CEWATER_MAIN/Ew,RELAXT
      COMMON/CEICE_MAIN/Ei
c==== functions
      complex Nc
      DOUBLE PRECISION TAUO
      EXTERNAL TAUO
      DOUBLE PRECISION z,KOO
      COMMON /CMAIN_TAU/Nc,KOO
C
C     !-------------------bounds for statements----------------------!
C
```

```
      CALL SPARA
      j = cmplx(0.,1.)
      TGMIN = 1.
      TGMAX = 0.
      PIRD = PIR / PID
      THETAR = THETA * PIRD
      COSR = COS(THETAR)
      COSRO = CMPLX(COSR,0.DO)
      SINR = SIN(THETAR)
      Wc = 2.281e-3
      do 11 ifreq = 1,3
        FREQ = FREQ2(ifreq)
        ZEFFMIN(ifreq)= 1.
        ZEFFMAX(ifreq) = 0.
        ANGF(ifreq) = 2. * PIR * FREQ
        ZEFFO(ifreq) = CO / (2. * ANGF(ifreq))
        KO(ifreq) = ANGF(ifreq)/CO
        Tb_sumH(ifreq) = 0.DO
   11 continue
      Es = CMPLX(EsR,-EsR*LTAN)
      Es = CMPLX(4.7, 0.)
      Ebw   = cmplx(35., -15.)
      Ea  = cmplx(1., 0.)
      OPEN(UNIT=50,FILE=DATAI,STATUS='OLD')
      OPEN(UNIT=52,FILE=DATAI2,STATUS='OLD')
      OPEN(UNIT=53,FILE=DATAI3,STATUS='OLD')
      OPEN(UNIT=70,FILE='Tb.dat',STATUS= 'UNKNOWN')
      OPEN(UNIT=74,FILE='Tb_d.dat',STATUS= 'UNKNOWN')
      OPEN(UNIT=76,FILE='Tb_i.dat',STATUS= 'UNKNOWN')
   21 FORMAT(F7.3,12(' ',1pe11.5))
c
c  Tsky at 85 GHz and L-band are not available before day 301.
c  UNITs 50 and 52 store temperatures and moisture contents for
c soil and vegetation, respectively.
c  UNIT 53 stores measured sky brightness at SSM/I frequencies.
c
      Tsky(3) = 0.DO
      DO 30 I = 1, NSAM
        read(50,*)DAY,TK,TG,Tair,Flh,Fsh,Fsun,Vf_i,Vf_H2O_fr
        read(52,*)DUM,Tcanopy,Ww,Tt
        Tcanopy = (Tcanopy + Tt)/2.
        read(53,*)DUM,DUM,DUM,Tb19HM(I),Tb37HM(I),Tsky(1),Tsky(2)
c
c  Bound water is determined using the [Dobson et al 1985] approach.
c
        if(Vf_H2O_fr.ge.Vf_bw)then
          Vf_w = Vf_H2O_fr - Vf_bw
        else
          Vf_w = 0.
        endif
        Vf_a = 1. - Vf_w - Vf_bw - Vf_i - Vf_s
        FF = (Vf_w+Vf_bw)/(Vf_w+Vf_bw+Vf_i)
        IF (TG.GT.TGMAX) THEN
          TGMAX = TG
        ELSEIF (TG.LT.TGMIN) THEN
          TGMIN = TG
        ENDIF
        TC = TK - 273.15
        Mg = Ww/Wc
c
c  Ulaby and El Rayes's 1987
c
        Vfw = Mg*(.55*Mg-.076)
        Vb = 4.64*Mg**2/(1.+7.36*Mg**2)
        Eresidual = 1.7 -.74 * Mg + 6.16*Mg**2
c
c  England 1995
c       DUM = (1.+Mg)**2
```

```
c       Vfw = (.474*Mg**2 - .076*Mg)/DUM
c       Vb  = 4.64*Mg**2/(1.+2.*Mg+8.36*Mg**2)
c       Eresidual = (1.7 - 4.14 * Mg + 7.12*Mg**2)/DUM
c
        do 25 ifreq = 1,3,1
         FREQ = FREQ2(ifreq)
         CALL SEWATER
         CALL SEICE
         EGMD(ifreq)=(Vf_s*Es**alpha+Vf_a*Ea**alpha+Vf_w*Ew**alpha+
     1               Vf_i*Ei**alpha+Vf_bw*Ebw**alpha)**(1./alpha)
         MGMD(ifreq) = CSQRT(EGMD(ifreq))
         THETAT(ifreq) = ASIN(SINR/DBLE(MGMD(ifreq)))
C
C  Compute reflectivity.
C
         COST(ifreq) =  COS(THETAT(ifreq))
         COSTO(ifreq) = CMPLX(COST(ifreq),0.DO)
         MCOS1(ifreq) = MGMD(ifreq)*COSR
         MCOS2(ifreq) = MGMD(ifreq)*COST(ifreq)
         AMPV(ifreq) = (MCOS1(ifreq)-COSTO(ifreq)) /
     1                 (MCOS1(ifreq)+COSTO(ifreq))
         AMPH(ifreq) = (COSRO-MCOS2(ifreq)) /
     1                 (COSRO+MCOS2(ifreq))
C
C  Compute emissivity.
C
         RV(ifreq) = CABS(AMPV(ifreq)) ** 2
         RH(ifreq) = CABS(AMPH(ifreq)) ** 2
         EV(ifreq) = 1. - RV(ifreq)
         EH(ifreq) = 1. - RH(ifreq)
         zefftemp = ABS(AIMAG(MGMD(ifreq)))
         zefftemp1 = ZEFFO(ifreq)/zefftemp
         ZEFF(ifreq)=COST(ifreq)*zefftemp1
         ZEFFCM(ifreq) = ZEFF(ifreq) * 100.0
         IF (ZEFFCM(ifreq).GT.ZEFFMAX(ifreq)) THEN
           ZEFFMAX(ifreq) = ZEFFCM(ifreq)
         ELSEIF (ZEFFCM(ifreq).LT.ZEFFMIN(ifreq)) THEN
           ZEFFMIN(ifreq) = ZEFFCM(ifreq)
         ENDIF
         TEFF(ifreq) = TK + ZEFF(ifreq) * TG
         Ecanopy(ifreq) = Eresidual +
     1   Vfw*(4.9+75./(1.+j*FREQ/18.e9)-j*22.86e9/FREQ)+
     2   Vb*(2.9+55.0/(1.+(j*FREQ/.18e9)**.5))
         Mcanopy(ifreq)=csqrt(Ecanopy(ifreq))
         Mc  = Mcanopy(ifreq)
         KOO = KO(ifreq)
         TAU = KOO*AIMAG(Mc)*(DEXP(-hc/.1149)-1.)
     1         * 2.128e-3
         EXP_TAU = EXP(-TAU/COSR)
         Tb_skyV(ifreq) = Tsky(ifreq)*RV(ifreq)*EXP_TAU**2
         Tb_skyH(ifreq) = Tsky(ifreq)*RH(ifreq)*EXP_TAU**2
         Tb_cdV(ifreq) = Tcanopy*RV(ifreq)*(1.-EXP_TAU)*EXP_TAU
         Tb_cdH(ifreq) = Tcanopy*RH(ifreq)*(1.-EXP_TAU)*EXP_TAU
         Tb_gV(ifreq) = TEFF(ifreq) * EV(ifreq) * EXP_TAU
         Tb_gH(ifreq) = TEFF(ifreq) * EH(ifreq) * EXP_TAU
         Tb_cuV(ifreq) = Tcanopy*(1.-EXP_TAU)
         Tb_cuH(ifreq) = Tb_cuV(ifreq)
         TBV(ifreq,I) = Tb_skyV(ifreq)+Tb_cdV(ifreq)+Tb_gV(ifreq)+
     1                  Tb_cuV(ifreq)
         TBH(ifreq,I) = Tb_skyH(ifreq)+Tb_cdH(ifreq)+Tb_gH(ifreq)+
     1                  Tb_cuH(ifreq)
   25   continue
        Tb_sumH(1) = Tb_sumH(1) + Tb19HM(I)
        Tb_sumH(2) = Tb_sumH(2) + Tb37HM(I)
        WRITE(70,21)DAY,TK,TBV(1,I),TBH(1,I),TBV(2,I),TBH(2,I),
     1            TBV(3,I),TBH(3,I)
       WRITE(74,21)DAY,TK,TBH(1,I)-Tb19HM(I),TBH(2,I)-Tb37HM(I)
       WRITE(76,21)DAY,Tb_skyH(1),Tb_cdH(1),Tb_gH(1),Tb_cuH(1),
```

```
     1                Tb_skyH(2),Tb_cdH(2),Tb_gH(2),Tb_cuH(2),
     2                Tb_skyH(3),Tb_cdH(3),Tb_gH(3),Tb_cuH(3)
  30 CONTINUE
     DO 40 ifreq = 1, 2, 1
       Tb_sumH(ifreq) = Tb_sumH(ifreq)/DBLE(NSAM)
       ADiffTb(ifreq) = 0.DO
       DiffTb(ifreq) = 0.DO
       DiffTb2(ifreq) = 0.DO
  40 CONTINUE
     DO 50 I = 1, NSAM, 1
       DiffTb(1) = DiffTb(1) + DABS((TBH(1,I)-Tb19HM(I)))
       DiffTb(2) = DiffTb(2) + DABS((TBH(2,I)-Tb37HM(I)))
       ADiffTb(1) = ADiffTb(1) + (TBH(1,I)-Tb19HM(I))
       ADiffTb(2) = ADiffTb(2) + (TBH(2,I)-Tb37HM(I))
       DiffTb2(1) = DiffTb(1) + (TBH(1,I)-Tb19HM(I))**2
       DiffTb2(2) = DiffTb(2) + (TBH(2,I)-Tb37HM(I))**2
  50 CONTINUE
     DO 60 I = 1, 2, 1
     DiffTb(I) = DiffTb(I)/DBLE(NSAM)
     ADiffTb(I) = ADiffTb(I)/DBLE(NSAM)
     Var(I) = DiffTb2(I)/DBLE(NSAM)
     Devi(I)= Var(I)**.5
  60 CONTINUE
C    !--------------------bounds for statements----------------------!
     WRITE(70,*)'DAY     Tgnd TBV(1),TBH(1),TBV(2),TBH(2) 3 3 '
     WRITE(70,*)'The temperature gradient maximum and minimum  are   ',
    1  TGMIN,' to ',TGMAX,' K/meter.'
     WRITE(70,*)'The ave. of the abs. value of the difference between',
    1' meas and pred Tb'
     WRITE(70,*)' at 19, 37= ',DiffTb(1),DiffTb(2)
     WRITE(70,*)'The ave. of the diff b/t meas & pred Tb'
     WRITE(70,*)' at 19, 37= ',ADiffTb(1),ADiffTb(2)
     WRITE(70,*)'The variance 19, 37= ',Var(1),Var(2)
     WRITE(70,*)'The standard deviation is (19,37)',Devi(1),Devi(2)
     CLOSE(50)
     CLOSE(52)
     CLOSE(53)
     CLOSE(70)
     CLOSE(72)
     CLOSE(74)
     STOP
     END
C
C =====================================================================
     SUBROUTINE  SPARA
C =====================================================================
C  Read some parameters.  All units are in SI.
C
     implicit none
     double precision EsR,LTAN,THETA,FREQ2(3),Vf_s,Vf_bw,alpha,hc
     INTEGER NSAM,NDAY_ST,NDAY_ED
     CHARACTER DATAI*32,DATAI2*33,DATAI3*29
     COMMON /CPARA_MAIN/EsR,LTAN,THETA,Vf_s,Vf_bw,alpha,hc,
    1        FREQ2,NSAM,NDAY_ST,NDAY_ED,DATAI,DATAI2,DATAI3
C
C    !--------------------bounds for statements----------------------!
C
C  Read parameters.
C
     OPEN(110,FILE='Tb.prm',STATUS='OLD')
C      EsR: 3.5% moist soil dielectric constant(typical = 3.3).
     READ(110,*) EsR
C      LTAN: 3.5% moist soil loss tangent(typical = .23).
     READ(110,*) LTAN
C      NSAM: number of observations
     READ (110,*) NSAM
C      NDAY_ST: the starting day number of simulation
     READ(110,*) NDAY_ST
```

```
C       NDAY_ST: the ending day number of simulation
        READ(110,*) NDAY_ED
C       FREQ: frequency, Hz(typical=SSM/I frequencies)
        READ(110,*) FREQ2(1)
        READ(110,*) FREQ2(2)
        READ(110,*) FREQ2(3)
C       THETA(1): incident angle, degrees(typical=53.1 for the SSM/I)
        READ(110,*) THETA
C         Vf_s = volumetric content of soil solids
        READ(110,*) Vf_s
C         Vf_bw = vloumetric content of bound water
        READ(110,*) Vf_bw
C         alpha = a constant shape factor to determine dielect costant
C                 of moist soils
        READ(110,*) alpha
C         hc = height of canopy
        READ(110,*) hc
C       DATAI: input file name, fd.dat
        READ(110,*) DATAI
C       DATAI2: input file name, veg.dat
        READ(110,*) DATAI2
C       DATAI3: input file name for the measured Tcanopy, Tb, and
C                Tsky, TbM.dat
        READ(110,*) DATAI3
        CLOSE(110)
        RETURN
        END
C ===============================================================
      SUBROUTINE SEWATER
C ===============================================================
C  This subroutine computes the complex dielectric constant
C of water, which is described by the Debye equation.
C *** Reference: [Ulaby et al 1986] Volume III.
C
C  TC : ground temperature, C
C  FREQ : frequency, Hz
C
      implicit none
      double precision EWAT0,EWAT9,DELTAEW,RELAXT,RELAXTF,PORTEW,
     1     EREAL,EIMAG
      COMPLEX Ew
      COMMON/CEWATER_MAIN/Ew,RELAXT
c main ======
      double precision FREQ,TC
      COMMON /CMAIN_WATER_ICE/FREQ
     1       /CMAIN_WATER/TC

      EWAT9=4.9
C Eq. E.19 in [Ulaby et al 1986] Volume III.
      EWAT0=88.045-(0.4147*TC)+(6.295E-4)*(TC**2)+(1.075E-5)*
     1      (TC**3)
C Eq. E.16
      DELTAEW = EWAT0 - EWAT9
C The relaxation time of pure water -- Eq. E.17
      RELAXT=1.1109E-10 -3.824E-12 * TC+6.938E-14 * TC**2
     1        - 5.096E-16 * TC**3
      RELAXTF=RELAXT * FREQ
      PORTEW=DELTAEW/(1.+RELAXTF**2)
C Eq. E.15a
      EREAL=EWAT9 + PORTEW
C Eq. E.15b
      EIMAG = - RELAXTF * PORTEW
      Ew= CMPLX(EREAL,EIMAG)
      RETURN
      END
C ===============================================================
      SUBROUTINE SEICE
C ===============================================================
```

```
C  This subroutine computes the complex dielectric constant of ice
C [England 1990].
C
C TK       : ground temperature, K **
C FREQ     : operating frequency, Hz
C BOLTZMAN: Boltzmann's constant, J/K
C
      implicit none
C eice ======
      double precision PIR,RELAXO,BOLTZMAN,BOLC,Ei9,Ei0,RELAXT,
     1     PORTEI,EREAL,EIMAG
      COMPLEX Ei
      COMMON /CEICE_MAIN/Ei
c main ======
      double precision FREQ,TK
      COMMON /CMAIN_WATER_ICE/FREQ
     1       /CMAIN_ICE/TK
      PIR = 3.141592654
      RELAXO = 2. * PIR * FREQ * 4.76E-16
      BOLTZMAN = 1.3806 E -23
      BOLC = 9.24E-20/BOLTZMAN
      Ei9 = 3.2
      Ei0 = 20715. / (TK-38.)
      RELAXT = RELAXO * EXP(BOLC/TK)
      PORTEI = Ei0/(1.+RELAXT**2)
      EREAL = Ei9 + PORTEI
      EIMAG = - RELAXT * PORTEI
      Ei = CMPLX(EREAL,EIMAG)
      RETURN
      END
C=======================================================================
      FUNCTION TAUO(z)
C=======================================================================
C  Find optical thickness of the canopy [England and Galantowicz 1995].
C
      implicit none
      complex Nc
      DOUBLE PRECISION TAUO
      DOUBLE PRECISION z,KOO
      COMMON /CMAIN_TAU/Nc,KOO
      TAUO = - 2.DO*KOO*DIMAG(1.+9.26e-3*Nc*exp(-z/.1149))
      RETURN
      END

C=======================================================================
C=======================================================================
C  Input file of parameters, Tb.prm.
C=======================================================================
3.3    {ESOILR: 3.5% moist soil dielectric constant(typical = 3.3).
.23    {LTAN: 3.5% moist soil loss tangent(typical = .23).
995    {NSAM: the number of observations
 287   {NDAY_ST: the starting day number of simulation
 301   {NDAY_ED: the ending day number of simulation
19.35e9{FREQ2: frequency, Hz
37.00e9{FREQ2: frequency, Hz
1.4e9  {FREQ2: frequency, Hz
53.1   {THETA: SSM/I incident angle, degrees(typical=53.1)
.48    {Vf_s : volumetric content of soil solids
.035   {Vf_bw: volumetric content of bound water
.65    {alpha = a constant shape factor to determine dielect costant
                of moist soils
.60    {hc: height of canopy, m
'/y/yueian/REBEX1/FTN/LAI6/fd.dat'
'/y/yueian/REBEX1/FTN/LAI6/veg.dat'
'/y/yueian/REBEX1/DATA/TbM.dat'
```

BIBLIOGRAPHY

[1] Abdel-Hadi, O. N., and J. K. Mitchell, "Coupled heat and water flows around buried cables," *J. Geotechnical Engin. Division*, **107**, 1461–1487, 1981.

[2] Ahmad, S. P., and D. W. Deering, "A simple analytical function for bidirectional reflectance," *J. Geophys. Res.*, **97**, 18867-18886.

[3] Ahmed, N. U., "Estimating soil moisture from 6.6 GHz dual polarization, and/or satellite derived vegetation index," *Int. J. Remote Sensing*, **16**, 687–708, 1995.

[4] Anderson, D. M., A. R. Tice, and H. L. McKim, "The unfrozen water and the apparent specific heat capacity of frozen soils," *Second International Permafrost Conference*, 289-294, 1973.

[5] Anderson, D. M., and N. R. Morgenstern, "Physics, chemistry, and mechanics of frozen ground: A review," *Proc. 2nd Int. Conf. Permafrost*, 289-294, National Academy of Sciences, Washington, DC, USA, 1973.

[6] Andersland, O. B., and D. M. Anderson, *Geotechnical Engineering for Cold Regions*, McGraw Hill, New York, 1978.

[7] Bach, L. B., "Soil water movement in response to temperature gradients: experimental measurements and model evaluation," *Soil Sci. Soc. Am. Proc.*, **56**, 37–46, 1992.

[8] Bouttier, F., J.-F., Mahfouf, and J. Noilhan, "Sequential assimilation of soil moisture from atmospheric low–level parameters. Part I: Sensitivity and calibration studies," *J. Appl. Meteor.*, **32**, 1335–1351, Aug. 1993.

[9] Bouttier, F., J.-F., Mahfouf, and J. Noilhan, "Sequential assimilation of soil moisture from atmospheric low–level parameters. Part II: Implementation in a mesoscale model," *J. Appl. Meteor.*, **32**, 1352–1364, Aug. 1993.

[10] Brest, C. L., and S. N. Goward, "Deriving surface albedo measurements from narrow band satellite data," *Int. J. Remote Sens.*, **8**, 351–367, 1987.

[11] Brooks, R. H., and A. T. Corey, "Properties of porous media affecting fluid flow," *J. Irrig. Drain. Div. Am. Soc. Civ. Eng.*, **92**, 61-87, 1966.

[12] Brown, S. C., and D. Payne, "Frost action in clay soils. I. A temperature-step and equilibrate differential scanning calorimeter technique for unfrozen water content determinations below 0°C," *J. Soil Sci.*, **40**, 535-546, 1990.

[13] Brutsaert, W., "On a derivable formula for long-wave radiation from clear skies," *Water Resour. Res.*, **11**, 742–744, 1975.

[14] Brutsaert, W., and M. Sugita, "Regional surface fluxes from satellite-derived surface temperatures (AVHRR) and radiosonde profiles," *Boundary-Layer Meteorol.*, **58**, 355–366, 1992.

[15] Camillo, P. J., R. J. Gurney, and T. J. Schmugge, "A soil and atmospheric boundary layer model for evapotranspiration and soil moisture studies," *Water Resour. Res.*, **19**, 371–380, 1983.

[16] Cary, J. W., "A new method for calculating frost heave including solute effects," *Water Resour. Res.*, **23**, 1620-1624, 1987.

[17] Cassel, D. K., D. R. Nielsen, and J. W. Biggar, "Soil-water movement in response to imposed temperature gradients," *Soil Sci. Soc. Am. Proc.*, **33**, 493–500, 1969.

[18] Chehbouni, A., E. G. Njoku, J.-P. Lhomme, and Y. H. Kerr, "Approaches for averaging surface parameters and fluxes over heterogeneous terrain," *J. Climate*, **8**, 1386-1393, 1995.

[19] Choudhury, B. J., and J. L. Monteith, "A four-layer model for the heat budget of homogeneous land surfaces," *Quart. J. Roy. Meteor. Soc.*, **114**, 373–398, 1988.

[20] Cunnington, W. M., and P. R. Rowntree, "Simulation of the Saharan atmosphere–dependence on moisture and albedo," *Quart. J. R. Met. Soc.*, **112**, 971–999, 1986.

[21] Dahl, P., J. Judge, J. Gallo, and A. W. England, "Vertical distribution of biomass and moisture in a prairie grass canopy," UM Radiation Laboratory Technical Report RL-902, November 1993.

[22] Daughtry, C. S. T., K. P. Gallo, S. N. Goward, S. D. Prince, and W. P. Kustas, "Spectral estimates of absorbed radiation and phytomass production in corn and soybean canopies," *Remote Sens. Environ.*, **39**, 141-152, 1992.

[23] de Vries, D. A., "Simultaneous transfer of heat and moisture in porous media," *Trans. Am. Geophys. Union*, **39**, 909–916, Oct. 1958.

[24] de Vries, D. A., "Thermal Properties of Soils," 210–235. In W. R. van Wijk (ed.), *Physics of Plant Environment.* North–Holland Publishing Co., Amsterdam, 1963

[25] Dickinson, R. E., Ann Henderson-Sellers, P. J. Kennedy, and W. F. Wilson, "Biosphere-atmosphere transfer scheme (BATS) for the NCAR Community Climate Model," *Tech. Note NCAR/TN-275+STR*, Natl. Cent. for Atm. Res., Boulder, Colo., 1986.

[26] Dickinson, R. E.,and Ann Henderson-Sellers, "Modeling tropical deforestation: A study of GCM land-surface parameterizations," *Q. J. R. Meteor. Soc.*, **114**, 439–462, 1988.

[27] Dobson, M. C., F. T. Ulaby, M. T. Hallikainen, and M. A. El-Rayes, "Microwave dielectric behavior of wet soil – Part II: Dielectric mixing models," *IEEE Trans. Geosci. Rem. Sens.*, **GE-23**, 35–46, Jan. 1985.

[28] Dorman, J. L., and P. J. Sellers, "A global climatology of albedo, roughness length and stomatal resistance for atmospheric general circulation models as represented by the Simple Biosphere Model (SiB)," *J. Appl. Meteor.*, **28**, 833–855, Sep. 1989.

[29] England, A. W., "Radiobrightness of diurnally heated, freezing soil," *IEEE Trans. Geosci. Rem. Sens.*, **28**, 464–476, Jul. 1990.

[30] England, A. W., J. F. Galantowicz, and B. W. Zuerndorfer, "A volume scattering explanation for the negative spectral gradient of frozen soil," *Proc. IGARSS'91*, Espoo, Finland, June 3–6, 1991.

[31] England, A. W., J. F. Galantowicz, and M. S. Schretter, "The Radiobrightness thermal Inertia measure of soil moisture," *IEEE Trans. Geosci. Rem. Sens.*, **30**, 132-139, Jan. 1992.

[32] England, A. W., and J. F. Galantowicz, "Observed and modeled radiobrightness of prairie grass in early fall," *Proc. IGARSS'95 Symp.*, Florence, July 10-12, 1995.

[33] Entekhabi, D., H. Nakamura, and Eni G. Njoku, "Solving the inverse problem for soil moisture and temperature profiles by sequential assimilation of multi-frequency remotely sensed observations," *IEEE Trans. Geosci. Rem. Sens.*, **32**, 438–448, Mar. 1994.

[34] Ewen, J., and H. R. Thomas, "Heating unsaturated medium sand," *Geotechnique*, **39**, 455–470, 1989.

[35] Flerchinger, G. N., and K. E. Saxton, "Simultaneous heat and water model of a freezing snow-residue-soil system I. theory and Development," *Trans. ASAE*, **32**, 565-571, 1989.

[36] Fuchs, M., G. S. Campbell, and R. I. Papendick, "An analysis of sensible and latent heat in a partially frozen unsaturated soil," *Soil Sci. Soci. Am. J.*, **42**, 379–385, 1978.

[37] Galantowicz, J. F., and A. W. England, "Radiobrightness signatures of energy balance processes: Melt/freeze cycles in snow and prairie grass covered ground," *Proc. IGARSS'95 Symp.*, Florence, Italy, July 10–14, 1995 .

[38] Galantowicz, J. F., *Microwave Radiometry of Snow-Covered Grasslands for the Estimation of Land-Atmosphere Energy and Moisture Fluxes*, Ph.D. dissertation, pp 196, 1995.

[39] Galantowicz, J. F., (A. W. England, Principal Investigator), "Field data report for the First Radiobrightness Energy Balance Experiment (REBEX–1), October 1992 – April 1993, Sioux Falls, South Dakota," UM Radiation Laboratory Technical Report RL–913, February, 1995.

[40] Gee, G. W., "Water movement in soils as influenced by temperature gradients," Ph.D. dissertation, Washington State University, Pullman, Washington, 1966. (Diss. Abstr. 66-13560)

[41] Gillies, R. R., and Carlson, T. N., "Thermal remote sensing of surface soil water content with partial vegetation cover for incorporation into climate models," *J. Appl. Meteor.*, **34**, 745–756, 1995.

[42] Gilpin, R. R., "A model for the prediction of ice lensing and frost heave in soils," *Water Resour. Res.*, **16**, 918-930, October 1980.

[43] Guymon, G. L., and J. N. Luthin, "A coupled heat and moisture transport model for arctic soils," *Water Resour. Res.* , **10**, 995-1001, 1974.

[44] Hallikainen, M., F. T. Ulaby, M. C. Dobson, M. El-Rayes, and L.-K. Wu, "Microwave dielectric behavior of wet soil – Part I: Empirical models and experimental observations," *IEEE Trans. Geosci. Rem. Sens.*, **GE-23**, 25–34, Jan. 1985.

[45] Harlan, R. L., "Analysis of coupled heat-fluid transport in partially frozen soil," *Water Resour. Res.* , **9**, 1314–1323, 1973.

[46] Hasson, A. M., "Radiation components over bare and planted soils in a greenhouse," *Solar Energy*, **44**, 1–6, 1990.

[47] Heilman, J. L., and D. G. Moore, "HCMM detection of high soil moisture areas," *Rem. Sens. of Environment*, **11**, 73–76, 1981.

[48] Heilman, J. L., and D. G. Moore, "Evaluating near-surface soil moisture using Heat Capacity Mapping Mission data," *Rem. Sens. of Environment*, **12**, 117–121, 1982.

[49] Hollinger, J., R. Lo, G. Poe, R. Savage, and J. Pierce, *Special Sensor Microwave/Imager User's Guide*, Naval Research Laboratory, Washington, D. C., 1987.

[50] Horiguchi, K., and R. D. Miller, "Hydraulic conductivity functions of frozen materials," *Proc. 4th Int. Conf. on Permafrost*, 289-294, National Academy of Sciences, Washington, DC, USA, 1983.

[51] Huang, X., T. J. Lyons, R. C. G. Smith, J. M. Hacker, and P. Schwerdtfeger, "Estimation of surface energy balance from radiant surface temperature and NOAA AVHRR sensor reflectances over agricultural and native vegetation," *J. Appl. Meteor.*, **32**, 1441–1449, Aug. 1993.

[52] Idso, S. B., R. D. Jackson, R. J. Reginato, B. A. Kimball, and F. S. Nakayama, "The dependence of bare soil on soil water content," *J. Appl. Met.*, **14**, 109–113, 1975.

[53] Iribarne, J. V., and W. L. Godson, *Atmospheric Thermodynamics*, 2nd ed, Kluwer Academic Publishers, 1981.

[54] Jacquemin, B., and J. Noilhan, "Sensitivity study and validation of land surface parameterization using the HAPEX-MOBILHY data set," *Bound.-Layer Meteor.*, **52**, 93–134, 1990.

[55] Jackson, T. J., and R. E. O'Neill, "Attenuation of soil microwave emission by corn and soybeans at 1.4 and 5 GHz," *IEEE Trans. Geosci. Rem. Sen.*, **GE-28**, 978–980, 1990.

[56] Jackson, R. D., R. J. Reginato, B. A. Kimball, and F. S. Nakayama, "Diurnal soil-water evaporation: comparison of measured and calculated soil water fluxes," *Soil Sci. Soc. Am. Proc.*, **38**, 861-866, 1974.

[57] Jame, Y. W., and D. I. Norum, "Heat and mass transfer in a freezing unsaturated porous medium," *Water Resour. Res.*, **16**, 811-819, 1980.

[58] Judge, Jasmeet, Y.-A. Liou, and A. W. England, "An LSP/Radiobrightness model for Northern Prairie in Summer," submitted to *Third International Workshop on Application of Remote Sensing in Hydrology*, October 16-18, 1996.

[59] Kahle, A. B., "A simple thermal model of the earth's surface for geologic mapping by remote sensing," *J. Geophys. Res.*, 380–387, **11**, Apr. 10, 1977.

[60] Kim, E. J., (A. W. England, Principal Investigator), "Field data report for the Third Radiobrightness Energy Balance Experiment (REBEX–3), September 1994 - September 1995, wet acidic tundra on the Alaskan North Slope," UM Radiation Laboratory Technical Report RL-918, July, 1996.

[61] Kimball, B. A., R. D. Jackson, R. J. Reginato, F. S. Nakayama, and S. B. Idso, "Comparison of field-measured and calculated soil-heat fluxes," *Soil Sci. Soc. Am. Proc.*, **40**, 18–25, 1976.

[62] Kimura, F., and Y. Shimizu, "Estimation of sensible and latent heat fluxes from soil surface temperature using a linear air-land transfer model," *J. Appl. Meteor.*, **33**, 477–489, 1994.

[63] Konrad, J. -M., and C. Duquennoi, "A model for water transport and ice lensing in freezing soils," *Water Resour. Res.*, **29**, 3109–3124, 1993.

[64] Koopmans, R. W. R., and R. D. Miller, "Soil freezing and soil water characteristic curves," *Soil Sci. Soc. Amer. Proc.*, **30**, 680-685, 1966.

[65] Kubota, A., and M. Sugita, "Radiometrically determined skin temperature and scalar roughness to estimate surface heat flux. Part I: Parameterization of radiometric scalar roughness," *Boundary-Layer Meteorol.*, **69**, 397–416, 1994.

[66] Lai, S., J. M. Tiedje, and A. E. Erickson, "In situ measurement of gas diffusion coefficients in soils," *Soil Sci. Soc. Am. Proc.*, **40**, 3–6, 1976.

[67] Li, Y., T. H. Demetriades-Shah, e. T. Kanemasu, J. K. Shultis, and M. B. Kirkham, "Use of second derivatives of canopy reflectance for monitoring prairie vegetation over different soil backgrounds," *Remote Sens. Environ.*, **44**, 81–87, 1993.

[68] Liang, X., D. P. Lettenmaier, E. F. Wood, and S. J. Burges, "A simple hydrologically based model of land surface water and energy fluxes for general circulation models," *J. Geophys. Res.*, **99**, 14415-14428, 1994.

[69] Liou, Y.-A., and A. W. England, "An annual model of SSM/I radiobrightness for dry soil," *Proc. IGARSS'92 Symp.*, Houston, Texas, May 16–20, 1992.

[70] Liou, Y.-A., and A. W. England, "Annual temperature and radiobrightness signatures for bare soils," to appear in *IEEE Trans. Geosci. Remote Sensing*, July 1996.

[71] Liou, Y.-A., and A. W. England, "A land surface process/radiobrightness model with coupled heat and moisture transport in soil," Submitted to *IEEE Trans. Geosci. Remote Sensing.*

[72] Liou, Yuei-An, and A. W. England, "A land surface process/radiobrightness model with coupled heat and moisture transport for freezing soils," in preparation for *IEEE Trans. Geosci. Remote Sensing*, 1996.

[73] Mahfouf, J.-F., E. Richard, and P. Mascart, "The influence of soil and vegetation on the development of mesoscale circulations," *J. Appl. Meteor.*, **26**, 1483–1495, 1987.

[74] Mahfouf, J.-F., " Analysis of soil moisture from near-surface parameters: A feasibility study," *J. Appl. Meteor.*, **30**, 1534–1547, 1991.

[75] Manabe, S., "The atmospheric circulation and hydrology of the earth's surface," *Mon. Wea. Rev.*, **97**, 739–774, 1969.

[76] Middleton, E. M., "Solar zenith angle effects on vegetation indices in tallgrass prairie," *Remote Sens. Environ.*, **38**, 45-62, 1991.

[77] Milly, P. C. D. "Moisture and heat transport in hysteretic, inhomogeneous porous media: A matric head based formulation and a numerical model," *Water Resour. Res.*, **18**, 489-498, Jun. 1982.

[78] Milly, P. C. D. "A simulation analysis of thermal effects on evaporation from soil," *Water Resour. Res.* , **20**, 1087–1098, Aug. 1984.

[79] Milly, P. C. D., and P. S. Eagleson, "The coupled transport of water and heat in a vertical soil column under atmospheric excitation," *Technical Report 258*, R. M. Parsons Lab., Dep. of Civil Engineering, Mass. Inst. of Technology, Cambridge, 1980.

[80] Milly, P. C. D., and P. S. Eagleson, "Parameterization of moisture and heat fluxes across the land surface for use in atmospheric general circulation models," *Technical Report 279*, R. M. Parsons Lab., Dep. of Civil Engineering, Mass. Inst. of Technology, Cambridge, 1982.

[81] Mintz, Y., and G. K. Walker, "Global fields of soil moisture and land surface evapotranspiration derived from observed precipitation and surface air temperature," *J. Appl. Meteor.*, **32**, 1305–1334, Aug 1993.

[82] Mualem, Y, "A new model for predicting the hydraulic conductivity of unsaturated porous media," *Water Resour. Res.* , **12**, 513-522, Jun. 1976.

[83] Namias, J., "Persistence of mid-tropospheric circulations between adjacent months and seasons," *The Atmosphere and Sea in Motion* (Rossby Memorial Volume), P. Polin, Ed., Rockefeller Institute Press and Oxford University Press, 240–248, 1958.

[84] Nassar, I. N., and R. Horton, "Water transport in unsaturated nonisothermal salty soil: II. theoretical development," *Soil Sci. Soc. Am. Proc.*, **53**, 1330–1337, 1989.

[85] Nimmo, J. R., Comment on the treatment of residual water content in "A consistent set of parametric models for the two-phase flow of immiscible fluids in the subsurface" by L. Luckner et al., *Water Resour. Res.*, **27**, 661-662, 1991.

[86] Noilhan, J., and S. Planton, "A simple parameterization of land surface processes in meteorological models," *Mon. Wea. Rev.*, **117**, 536–549, 1989.

[87] Owe, M., A. T. C. Chang, and R. E. Golus, "Estimating surface soil moisture from satellite microwave measurements and a satellite derived vegetation index," *Remote Sensing of Environment, 24*, 331–345, 1988.

[88] Owe, M., A. A. Van De Griend, and A. T. C. Chang, "Surface moisture and satellite microwave observations in semiarid southern Africa," *Water Resources Research*, **28**, 829-839, 1992.

[89] Paloscia, S., and P. Pampaloni, "Microwave vegetation indexes for detecting biomass and water conditions of agricultural crops," *Remote Sens. Environ.*, **40**, 15-26, 1992.

[90] Patterson, D. E., and M. W. Smith, "Measurement of unfrozen water content in saline permafrost using time domain reflectometry," *Proc. 4th Int. Conf. on Permafrost*, 968-972, National Academy of Sciences, Washington, DC, USA, 1983.

[91] Peixoto, J. P., and A. H. Oort, *Physics of Climate*, 235–239, American Institute of Physics, New York, 520 pp, 1992.

[92] Philip, J. R., and D. A. de Vries, "Moisture movement in porous materials under temperature gradients," *Trans. Am. Geophys. Union*, **38**, 222–232, Apr. 1957.

[93] Pikul, J. L. Jr., L. Boersma, and R. W. Rickman, "Temperature and water profiles during diurnal soil freezing and thawing: field measurements and simulation," *Soil Sci. Soc. Am. J.*, **53**, 3-10, 1989.

[94] Press, W. H., B. P. Flannery, S. A. Teukolsky, W. T. Vetterling, *Numerical Recipes (FORTRAN)*, pp. 702, Cambridge University Press, 1989.

[95] Price, J. C., "Thermal inertia mapping: A new view of the Earth," *J. Geophys. Res.*, **82**, pp. 2582–2590, 1977.

[96] Price, J. C., "The potential of remotely sensed thermal infrared data to infer surface moisture and evaporation," *Water Resources Res.*, **16**, pp. 787–795, 1980.

[97] Ranson, K. J., J. R. Irons, and C. S. T. Daughtry, "Surface albedo from bidirectional reflectance," *Remote Sens. Environ.*, **35**, 201-211, 1991.

[98] Richardson, A. J., and C. L. Wiegand, "Canopy leaf display effects on absorbed, transmitted, and reflected solar radiation," *Remote Sens. Environ.*, **29**, 15-24, 1989.

[99] Rowell, D. P., and C. Blondin, "The influence of soil wetness distribution on short-range rainfall forecasting in the West African Sahel," *Q. J. R. Meteorol. Soc.*, **116**, 1471-1485, 1990.

[100] Rowntree, P. R., and J. R. Bolton, "Simulation of the atmospheric response to soil moisture anomalies over Europe," *Quart. J. Roy. Meteor. Soc.*, **109**, 501–526, 1983.

[101] Ross, P. J., J. Williams, and K. L. Bristow, "Equation for extending water-retention curves to dryness," *Soil Sci. Soc. Am. Proc.*, **55**, 923-927, 1991.

[102] Rossi, C., and J. R. Nimmo, "Modeling of soil water retention from saturation to oven dryness," *Water Resour. Res.* , **30**, 701-708, Mar. 1994.

[103] Sato, N., P. J. Sellers, D. A. Randall, E. K. Schneider, J. L. Kinter III, Y.-T. Hou, and E. Alvertazzi, "Effects of implementing the simple biosphere model in a general model in a general circulation model," *J. Atm. Sci.*, **46**, 2757–2782, Sep. 15, 1989.

[104] Satterlund, D. R., "An improvbed equation for estimating long-wave radiation from the atmosphere," *Water Resour. Res.*, **15**, 1649–1650, 1979.

[105] Schmugge, T. J., P. E. O'Neill, and J. R. Wang, "Passive microwave soil moisture research," *IEEE Trans. Geosci. Rem. Sen.*, **GE-24**, 12–22, Jan. 1986.

[106] Sellers, P J., Y. Mintz, Y. C. Sud, and A. Dalcher, "A simple biosphere model (SiB) for use within general circulation models," *J. Atm. Sci.*, **43**, 505-31, Mar. 1986.

[107] Shah, D. J., J. W. Ramsey, and M. Wang, "An experimental determination of the heat and mass transfer coefficients in moist, unsaturated soils," *Int. J. Heat Mass Transfer*, **27**, 1075–1085, 1984.

[108] Shibayama, M., and T. Akiyama, "Seasonal visible, near-infrared and mid-infrared spectra of rice canopies in relation to LAI and above-ground dry phytomass," *Remote Sens. Environ.*, **27**, 119-127, 1989.

[109] Shibayama, M., W. Takahashi, S. Morinaga, and T. Akiyama, "Canopy water deficit detection in paddy rice using a high resolution field spectroradiometer," *Remote Sens. Environ.*, **45**, 117-126, 1993.

[110] Smith, C. B., M. N., Lakhtakia, W. J. Capehart, and T. N. Carlson, "Initialization of soil-water content in regional-scale atmospheric prediction models," *Bull. Amer. Meteor. Soc.*, **75**, 585–593, 1994.

[111] Sugita, M., and W. Brutsaert, "Landsat surface temperatures and radio soundings to obtain regional surface fluxes," *Water Resour. Res.*, **28**, 1675–1679, 1992.

[112] Sugita, M., and Brutsaert, W., "Comparison of land surface temperatures derived from satellite observations with ground truth during FIFE," *Int. J. Remote Sensing*, **14**, 1659–1676, 1993.

[113] Taylor, G. S., and J. N. Luthin, "A model for coupled heat and moisture transfer during soil freezing," *Can. Geotech. J.*, **15**, 548-555, 1978.

[114] Thomas, H. R., "Nonlinear analysis of heat and moisture transfer in unsaturated soil," *J. Engin. Mechanics*, **113**, 1163–1180, 1987.

[115] Thomas, H. R., and S. d. King, "Coupled heat and mass heat transfer in unsaturated soil — A potential-based solution," *Int. J. for Numerical and Analytical Methods in Geomechanics*, **16**, 757–773, 1992.

[116] Tice, A. R., C. M. Burrous, and D. M. Anderson, "Determination of unfrozen water in frozen soil by pulsed nuclear magnetic resonance," *Proc. 3rd Int. Conf. Permafrost*, 150-155, National Academy of Sciences, Washington, DC, USA, 1978.

[117] Trenberth, K. E. (ed), *Climate System Modeling*, 454–457, Cambridge University Press, 788 pp, 1992.

[118] Ulaby, F. T., M. Razani, and M. C. Dobson, "Effects of vegetation cover on the microwave radiometric sensitivity to soil moisture," *IEEE Trans. Geosci. Rem. Sens.*, **GE-21**, 51–61, 1983.

[119] Ulaby, F. T., R. K. Moore and A. K. Fung, *Microwave Remote Sensing, Active and Passive*, Vol. III, Norwood, MA, 1986.

[120] Ulaby, F. T., and M. A. El-Rayes, "Microwave dielectric spectrum of vegetation–Part II: Dual-dispersion model," *IEEE Trans. Geosci. Rem. Sens.*, **GE-25**, 550–557, Sep. 1987.

[121] van Genuchten, M. T., "A closed-form equation for predicting the hydraulic conductivity of unsaturated flow," *Soil Sci. Soc. Am. Proc.*, **44**, 892–898, 1980.

[122] Verma, S. B., J. Kim, and R. J. Clement, "Momentum, water vapor, and Carbon Dioxide exchange at a centrally located prairie site during FIFE," *J. Geo. Res.*, **97**, 18629-18639, Nov. 30, 1992.

[123] Verseghy, D. L., N. A. McFarlane, and M. Lazare, "CLASS — A Canadian land surface scheme for GCMs. II. Vegetation model and coupled runs," *Int. J. Climatology*, **13**, 347–370, 1993.

[124] Wang, J. R., and T. J. Schmugge, "An empirical model for the complex dielectric permittivity of soils as a function of water content," *IEEE Trans. Geosci. Rem. Sens.*, **GE-18**, 288–295, Oct. 1980.

[125] Watson, K., "Geologic applications of thermal infrared images," *Proc. IEEE*, 370–379, 1975.

[126] Wegmuller, U., C. Matzler, and E. Schanda, "Microwave signatures of bare soil," *Adv. Space Res.*, **9**, 307–316, 1989.

[127] Williams, P. J., "Experimental determination of apparent specific heats of frozen soils," *Geotechnique*, **14**. 133-142, 1964.

[128] World Meteorological Organization, *Scientific Plan for the Global Energy and Water Cycle Experiment*, WCRP-40, WMO-TD-No. 376, 83 pp, 1990.

[129] World Meteorological Organization, *Scientific Plan for the GEWEX Continental-Scale International Project (GCIP)*, WCRP-67, WMO-TD-No. 61, 65 pp, 1992.

[130] Xue, Y., P. J. Sellers, J. L. Kinter, and J. Shukla, "A simplified biosphere model for global climate studies," *J. Climate*, **4**, 345–364, Mar. 1991.

[131] Zuerndorfer, B. W., A. W. England, C. M. Dobson, and F. T. Ulaby, "Mapping freeze/thaw boundaries with SMMR data," *J. Agriculture and Forest Meteorology*, **52**, 199-225, 1990.

[132] Zuerndorfer, B. W., and A. W. England, "Radiobrightness decision criteria for freeze/thaw boundaries," *IEEE Trans. Geosc. Rem. Sens.*, **30**, 89-101, 1992.